Photochromic Properties of Spiropyran Derivatives and their Potential Influence on the *cis/trans*-Equilibrium of Proline

Inaugural-Dissertation

zur

Erlangung des Doktorgrades

der Mathematisch-Naturwissenschaftlichen Fakultät der Universität zu Köln

vorgelegt von

Niklas Hermes

aus Bonn

Köln, 2024

Berichterstatter: Prof. Dr. Ralf Giernoth

Prof. Dr. Axel Griesbeck

Dedicated to my family

Acknowledgement

The work portrayed in this thesis was carried out from October 2019 to June 2024 in the Department of Chemistry of the University of Cologne under the supervision of Prof. Dr. Ralf Giernoth. I want to express my gratitude to him for giving me the opportunity to work on this thesis. I am also thankful for his support I'm also grateful for the help outside of work, especially during the COVID-19 pandemic.

I want to thank Prof. Dr. Axel Griesbeck for several helpful and inspiring conversations during the second supervision. I am also thankful to him for being the second reviewer of this thesis.

I thank Prof. Dr. Klas Lindfors for being the chair of my thesis committee.

I also want to thank Dr. Jörg-Martin Neudörfl for writing the protocol during my disputation but also for numerous inspiring discussions throughout my whole academic career.

My special thanks go to Luca Denkler, Dr. Christina Wartmann, Sebastian Barutzki, Mira Scheithe and Alicia Köcher for proofreading this thesis.

I also want to express my thanks to the whole blue floor for the welcoming and inspiring work atmosphere. This not only includes working group of Prof. Dr. Stephanie Kath-Schorr, but also the former working groups of Prof. Dr. Albrecht Berkessel and Prof. Dr. Martin Breugst. My special thanks go to the “coffee-group” which was always open to lively discussions on various scientific topics that could occasionally digress.

I also want to thank my friend and colleagues who made the time during my PhD to the unforgettable and great time it was. Particularly noteworthy are Luca Denkler, Dr. Lars Hemmersbach, Dr. Christina Wartmann, Robert Dörrenhaus, Lukas Neu, Mira Scheithe, Alicia Köcher, Philip Wagner, Hui-Chung Wen, Thiemo Arntd, Fabian Severin and Sabine Voell.

Special thanks go to the people who enabled all the research. I thank all members of the NMR-facility namely Dr. Daniel Friedrich, Dr Daniel Hegemann, Daniela Naumann and Kathrin König. I want to especially thank Kathrin König for teaching me the use of the spectrometer that exceed the routine measurements. I thank Michael Neihs and Hui-Chung Wen from the facility for mass spectrometry under the

guidance of Prof. Dr. Mathias Schäfer. I also thank Christoph Schmitz for conducting the elemental analysis and his help concerning IR-spectroscopy. I am grateful to Sawar Azis and Christoph Schmitz for maintaining all the analytic machines on the blue floor. I also want to thank the RRZK and the CHEOPS HPC-cluster for enabling the DFT calculations presented within this thesis.

For the help with contracts, holiday applications and several other administrative issues I want to thank Susanne Geuer and Sarah Hensel. All the maintenance work in the department I am grateful to Andreas Wallraff and Ditmar Rutsch. I am also thankful to Thomas Dautert for his help with many technical and software issues.

Of course, I also thank my parents Astrid and Frank and my brother Jannick and Maik for the support throughout my whole academic career. Special thanks go to my grandparents Margareta and Norbert for their support especially during my bachelor and master studies. Without my family, I wound not have made it this far.

I am most thankful to my girlfriend Luca Denkler for all her support during the last years. She was always there to help me with personal but also scientific issues and also told me to work a little less when it was necessary. I am especially thankful for her help during stressful times. Thank you!

Contents

1 Introduction

In today's society, we experience a variety of light-induced structural changes in our daily lives. One of the most important of these photo-isomerisations is the conversion of 11-*cis*-retinal to all-*trans*-retinal, as this process is an essential part of our vision (Scheme 1).[1] Retinal is bound to the protein opsin via a lysine. The isomerisation triggers a cascade of reactions leading to a conformational change of the whole protein and finally to a cleavage of all-*trans*-retinal. In the human body, this process can only be reversed by the action of several different enzymes.

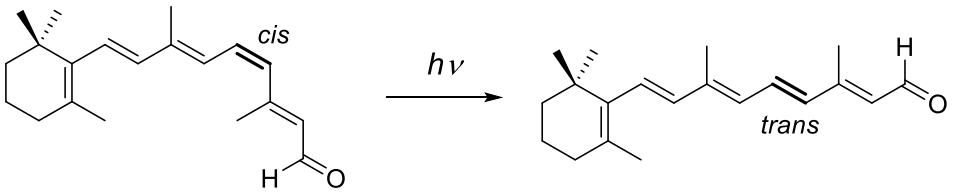

***Scheme 1*:** Light-induced isomerisation of 11-*cis*-retinal to all-*trans*-retinal.

Under laboratory conditions the re-isomerisation to the 11-*cis*-retinal is possible by irradiation with UV-light.[2] This phenomenon is known under the term photochromism. The IUPAC defines photochromism as follows:

"*Photochromism is a reversible transformation of a chemical species induced in one or both directions by absorption of electromagnetic radiation between two forms, A and B, having different absorption spectra*."[3]

Today, photochromic systems are utilised and researched for a wide range of applications.

2 State of the Art

2.1 Photochromism

The first examples of photochromism were reported as early as 1867, when J. Fritzsche observed a decolouration of an orange tetracene solution in sunlight.[4] The term photochromism was first established in 1950 by Y. Hirshberg when he investigated this phenomenon for dianthrone systems.[5] The word is derived from the Greek words for light (phos) and colour (chroma). In the 1950s and 1960s, Y. Hirshberg and E. Fisher further aroused interest in the field of photochromic molecules with their research on so-called spiropyrans,[6, 7] which remains a broad field of research to this day (Scheme 2).

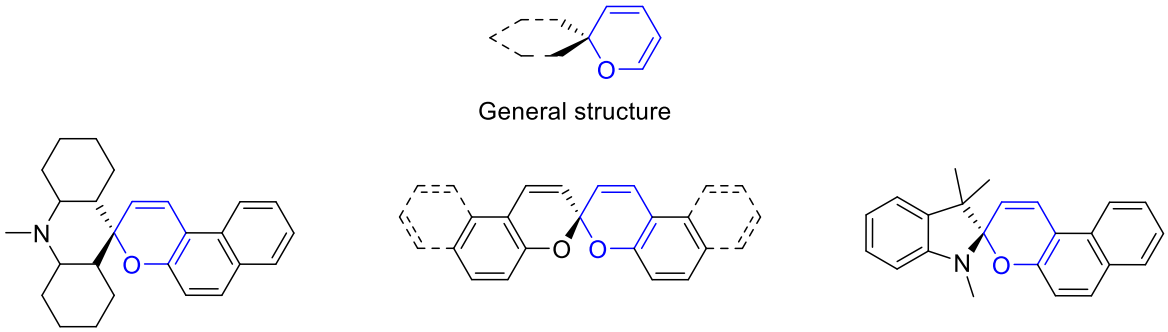

Scheme 2: General structure of spiropyrans (top) and three of the photochromic spiropyrans investigated by Y. Hirshberg and E. Fisher in the 1950s and 1960s.[6, 7]

Based on the photochemical properties of the system, photochromism can be dvided into P-type or T-type, as well as negative or positive photochromism.

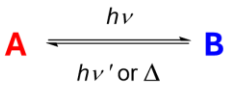

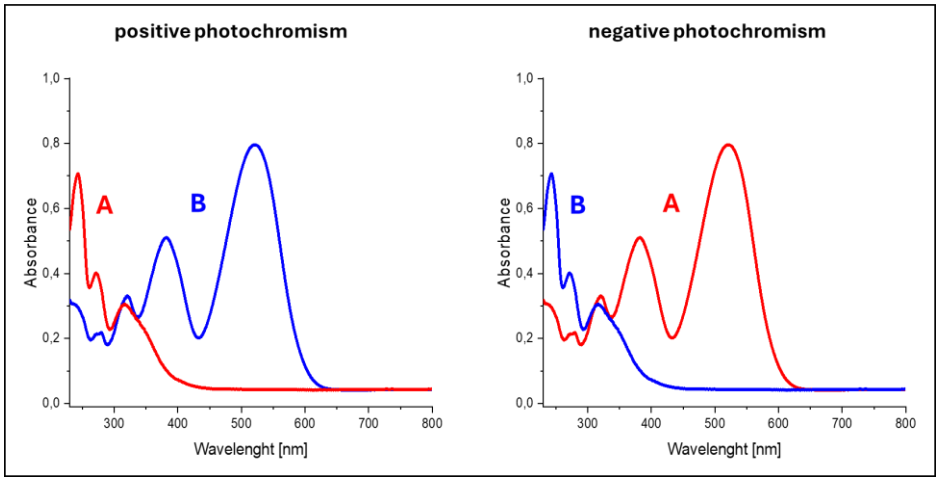

Scheme 3: Illustration of a positive photochromic system (left) and a negative photochromic system (right).

The classification between positive and negative photochromism is based on the absorption maxima of the observed species. An example of a photochromic system is shown in Scheme 3. A photochromic system with a stable form **A** and a metastable form **B** is considered. If **A** has its absorption maximum (λ_{max}) at a lower wavelength than the **B**, this is called positive photochromism (λ_{max} **A** < λ_{max} **B**) (Scheme 3, left). If on the other hand, **A** has an absorption maximum at a higher wavelength than **B**, this is called negative or inversed photochromism (λ_{max} **A** > λ_{max} **B**) (Scheme 3, right).[3, 8–10]

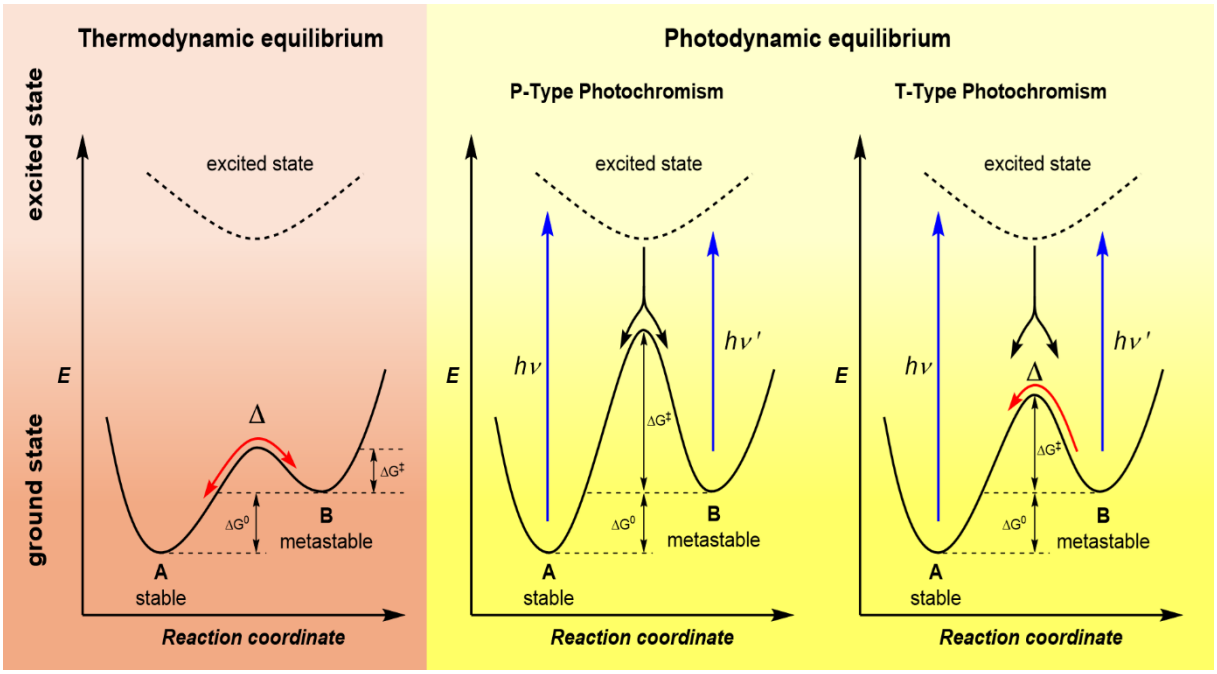

Scheme 4: Overview for thermodynamic (red) and photochemical equilibria (yellow) between a stable form **A** and a metastable form **B**. For the thermodynamic equilibrium the free Gibbs energy (ΔG^0) and the energy barrier $\Delta G^‡$ are indicated. For the photodynamic equilibrium the model of a P-type (middle) and a T-type (right) photochromic system are shown. The photoexcitation processes are indicated by blue arrows, thermal processes by red arrows. The wavelengths for the excitations are stated as hν (forward) and hν' (backwards).[11]

The classification between P-type and T-type photochromism is based on the characteristics of the backwards reaction from **B** to form **A**. In case of P-type photochromic molecules this reaction can only occur photochemically while for T-type molecules this is also possible thermally. In classic thermodynamic the energy barrier between a stable state **A** and a metastable state **B** can be overcome by thermal energy.[11] The energy difference between the two states is the Gibbs free energy (ΔG^0) while the energy barrier can be described as $\Delta G^‡$ (Scheme 4. left). If this energy barrier is too high, the population of the metastable state **B** is thermally not possible. In the case of photodynamic systems, this barrier can be bypassed. The

stable form **A** can be elevated to the excited state via light of a suitable wavelength hν (photoexcitation). Upon relaxation from the excited state to the ground state, the metastable form **B** can be obtained (Scheme 4, middle and right). For P-type photochromic systems the backward reaction to the stable form **A** can only be achieved via photoexcitation with a wavelength hν', since the energy barrier is too high for a thermodynamic transition (Scheme 4, middle). In case of T-type photochromism, the energy barrier of the backward reaction from **B** to **A** is lower, which enables an additional thermal pathway (Scheme 4, right).[3, 8, 11]

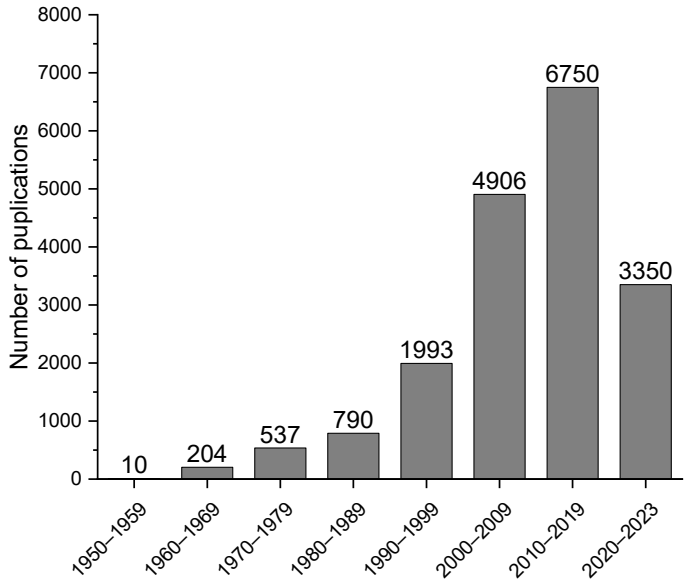

***Graph 1*:** Publications with the keywords "photochromism", "photochrom" and "photochromic" found on Web of science in May 2024.[12]

Over the past decades, the field of photochromic systems has continuously evolved and become increasingly significant (Graph 1).[12] Today, numerous photochromic compounds are known. Since the photochromic compounds often vary greatly in their physical properties, the different systems can be used for various applications. These range from optical memories,[13–15] chemo- and biosensing,[16, 17] switchable biomolecules,[18, 19] light responsive sunglasses,[20] switches for electrical circuits[21] and many more.[3, 22, 23]

Four examples of different photochromic systems are shown in Scheme 5. For all those examples, the photochromic character is based on a photoinduced isomerisation of one or more double bonds or/and a cyclisation reaction. Upon irradiation with UV-light, azobenzenes undergo an *E*/*Z*-isomerisation which leads to a

significant change in the structure of the molecule. The re-isomerisation to the stable *E*-isomer can be obtained photochemically and thermally (T-type).[24]

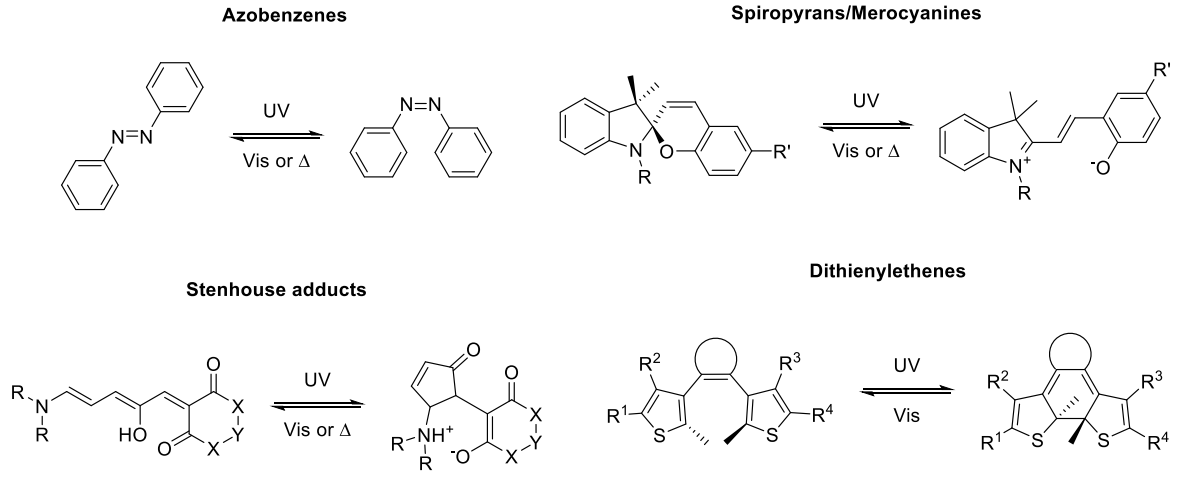

***Scheme 5*:** Photochromic properties and structural changes of selected photochromic systems. Shown are the popular systems of azobenzenes (top, left), spiropyrans/merocyanines (top, right), Stenhouse adducts (bottom, left) and dithienylethenes (bottom, right).

Spiropyrans and Stenhouse adducts are considered T-type photochromic systems as well. While for spiropyrans the irradiation with UV-light leads to a ring opening followed by a *Z/E*-isomerisation, the Stenhouse adducts experience several *E/Z*-isomerisations followed by a cyclisation. In both cases, large changes in the molecular geometry are observed while also changing from an uncharged to a zwitterionic structure. Stenhouse adducts are an example for negative photochromism[9, 10], while spiropyrans can be positive or negative photochromic based on the substituents.[25] The photochromism of the dithienylethenes is also based on a cyclisation reaction, but in this case the structural changes of the molecule are significantly smaller. Based on the substituents, dithienylethenes can be T-type or P-type photochromic.[26] In this thesis, only the class of spiropyrans will be discussed in detail.

2.2 Photochromic Properties of Spiropyrans and Merocyanines

As previously mentioned, the spiropyran/merocyanine (SP/MC) system acts as T-type photoswitch. In 2014, R. Klajn[22] formulated both a photochemical and a thermal mechanism for the transition between the spiropyran (SP) and merocyanine (MC) (Scheme 6). Beside several other publications, the studies by S. Swansburg et al.[27] on the racemisation of spiropyrans contributed a mayor part towards the mechanisms.

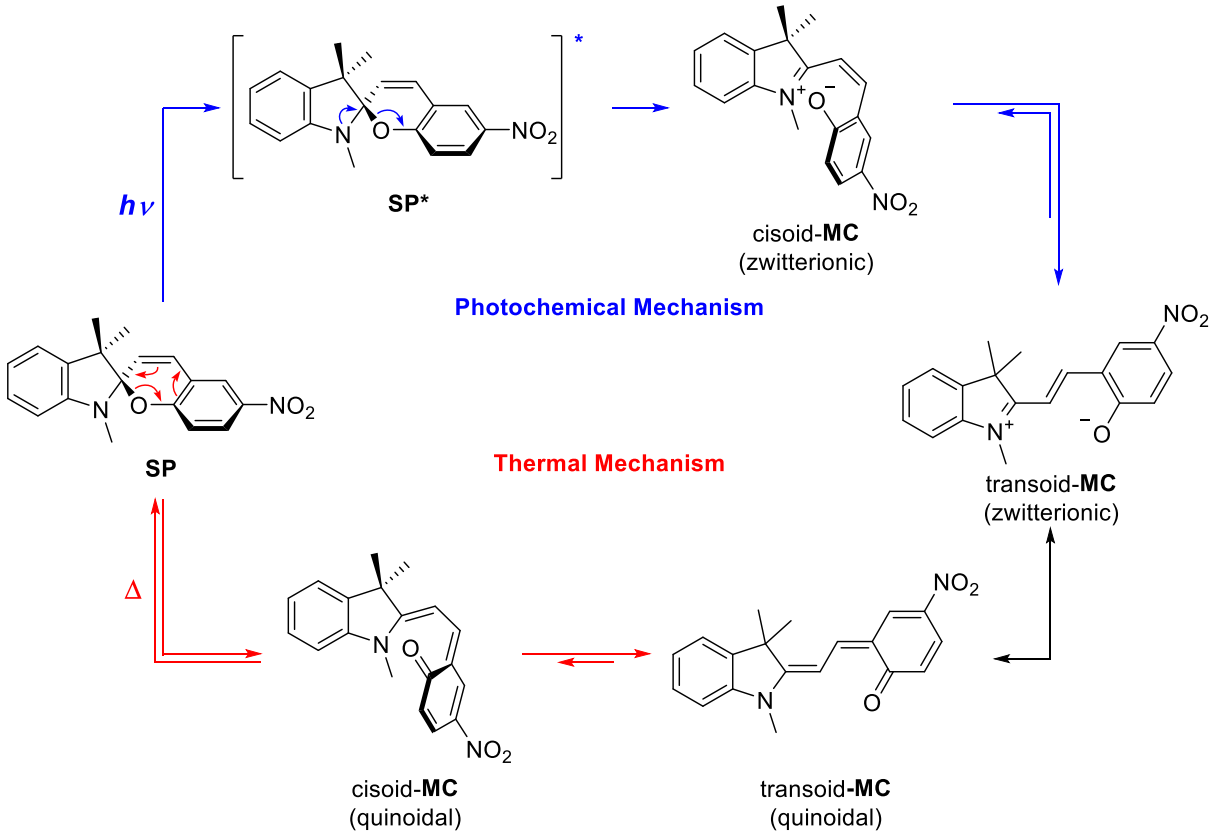

Scheme 6: Reaction mechanism for the photochromic (top) and thermal (bottom) transformation between spiropyran and merocyanine.

Starting from the SP-form, a thermal 6p-electroncyclic ring opening of the pyran leads to the formation of a *cisoid*-MC in its quinoidal from. Due to the steric hindrance the rearrangement to the more stable *transoid*-MC is favoured. This is a mesomeric form of the *transoid*-MC in its zwitterionic from. The photochemical mechanism begins with the excitation of the spiropyran to SP*. The excitation of the molecule initialises a C-O-bond cleavage which results in the *cisoid*-MC in its zwitterionic form. After isomerisation to the more stable *transoid*-form, the same mesomeric forms can be obtained as for the thermal mechanism. If the zwitterionic or the quinoidal-

mesomeric form is favoured is highly depending on several factors as solvent polarity or substituents.[22, 27] The photochromic properties (e.g. rate constant, positive or negative photochromism) of the system are highly influenced by the substituents as well. For this, not only the electronic and mesomeric effects of the functional groups but also their positions are extremely important.

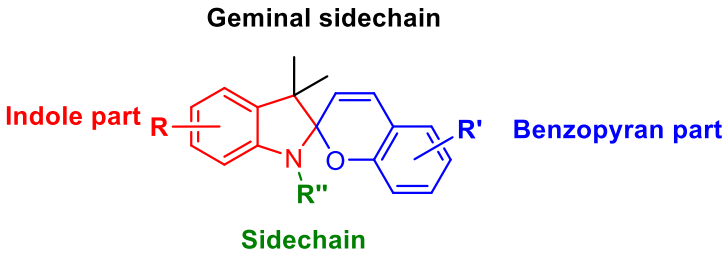

***Scheme 7*:** Division of the spiropyran structure into the four moieties, indole (red), sidechain (green), benzopyran (blue) and the geminal sidechains (black).

In order to have a more nuanced discussion about the influence of different substituents the molecule is divided in four moieties, depicted in Scheme 7. In the following, only the influence of substituents at these positions regarding the photochromic properties are described. Other stimuli which can affect the SP/MC system like pH (acidochromism),[23, 28–31] redox potential (electrochromism),[23, 32] mechanical force (mechanochromism),[33] or metal Ions[16, 34–36] are not described here, as this would exceed the scope of this paper.

2.2.1 Influence of Substituents on the Photochromic System: The *N*-Substituent

Substituents at the indole nitrogen (Scheme 7, red) are often used to bind the spiropyrans to polymers, biomolecules, nanoparticles, surfaces, fluorophores and many more.[22, 28, 32–34, 36–38] However, substituents at this position also highly impact on the photochromic properties of the SP/MC-system.

In their DFT studies on the Hammett constants of the SP/MC transition, O. Brügner et. al.[39] also considered different substituents at the indole nitrogen. They concluded that electron donating groups (EDG) with a negative Hammett-constants ($-\sigma$) like NH_2 lead to the stabilisation of the merocyanine-form. On the other hand, electron withdrawing groups with a positive Hammett-constants ($+\sigma$) like NO_2 or SO_3H

stabilises the spiropyran. This stabilisation is based on the effect of the substituents on the electrons in the free electron pair at the nitrogen (n_N-orbital) which is crucial for the ring opening (Scheme 6). If electrons are drawn from the nitrogen, the ring opening is disfavoured therefore stabilising the spiropyran. However, from a synthetic viewpoint the *N*-substituents considered by Brügner et al. are not feasible.

Experimental insight was provided by E. Beves and coworkers[40] and C. Berton et al..[41] Besides the impact onto the photo acidic character of the SP/MC system, the groups investigated the photochromic properties as well. For this purpose, alkyl chains of different lengths with terminal ammonium and sulphonate groups were considered as substituents (Scheme 8). The photochromic behaviour was investigated in aqueous solutions and the equilibrium constants for the ring closure to the corresponding spiropyrans (K_c) were calculated.

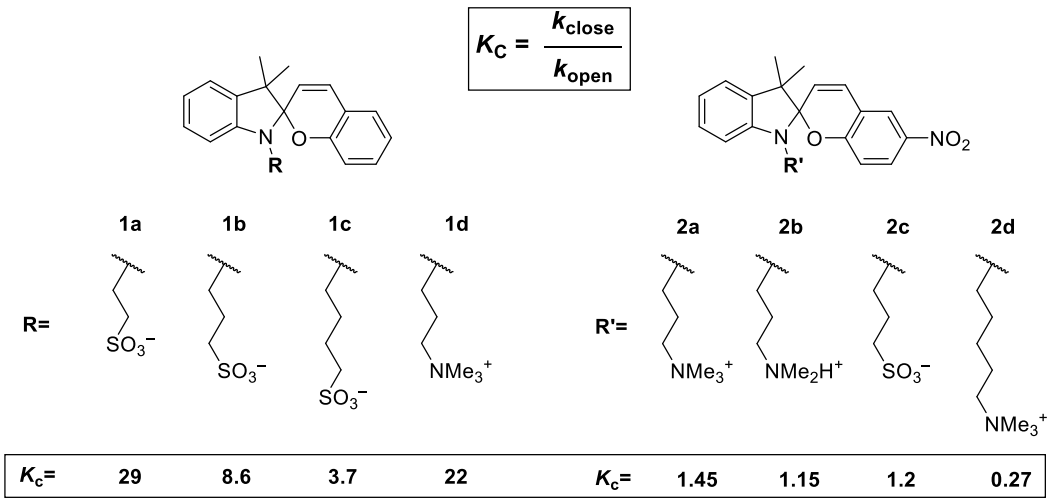

Scheme 8: Influence of the *N*-substituents onto the photochemical equilibrium of SP/MC-systems. The equilibrium constants for the ring closing reaction (K_c) from MC to SP in aqueous solutions are given underneath the substituents.[40]

Comparing the equilibrium constants for the ethyl-, propyl- and butyl sulfonate **1a-c** (Scheme 8, left), all three substituents stabilise the spiropyran.[40] This stabilisation is rapidly weakened with the increasing length of the alkyl chain. Since the Hammett constants for the sulfonates with different alkyl chain lengths are not available, trimethylammonium substituents with varying chain lengths are used to explain this trend. For the ammonium substituents the Hammett constants decrease with increasing length of the alkyl chain from NMe_3^+ (σ_p = 0.82) through $CH_2NMe_3^+$ (σ_p = 0.44) to $CH_2CH_2NMe_3^+$ (σ_p = 0.13).[42] This trend is therefore in line with the results observed by Beves and coworkers. Comparing the influence of the sulfonate **1b** (K_c =

8.6) with the ammonium **1d** (K_c = 22), the impact of the latter is significantly higher. These results are again in line with the Hammett values as well, since the sigma value of 0.82 for ammonium substituent **1d** is noticeably higher than the sigma value for sulfonate **1b** with 0.35.[42] The second system investigated by Beves and coworkers contained an additional nitro group at the benzopyran moiety (Scheme 8, right). While the same trends concerning the *N*-substituent can be observed for this system, due to the electron withdrawing character of the nitro group, the equilibrium constants are in general significantly lower. The effects of benzopyran substituents are discussed in the next chapter. However, the influence of the *N*-substituents is higher than those of the nitro group. These experimental results are all in line with the previously mentioned calculations by Brügner et al.[40]

2.2.2 Influence of Substituents on the Photochromic System: The Benzopyran Moiety

As already briefly mentioned in the previous chapter, DFT calculations by Brügner et al.[39] indicated that substituents at the benzopyran moiety of the SP/MC-system with electron donating groups stabiles the closed form while those with electron withdrawing groups stabiles the open form. The same trend was experimentally proven by Beves and coworkers[40] when they compared the equilibrium constants for spiropyrans with different substituents in *para*-position regarding the oxygen (Figure 1).

A

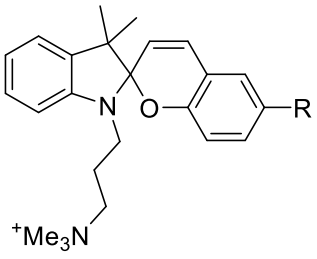

B

$$K_c = \frac{k_{close}}{k_{open}}$$

SP	2a	3	4	5	6
R	NO_2	CHO	CN	H	*t*Bu
K_c	1.45	2.38	6.25	123	183

Figure 1: **A** General structure of the spiropyrans investigated by Beves and coworkers. **B** Equilibrium constants for the cyclisation of different *para*-substituted merocyanines towards the respective spiropyrans. Substituent description is based on the position regarding the pyran oxygen. The constants were calculated based on kinetic measurements conducted in aqueous solution.[40]

The ring closing reaction from MC to SP is, with a $K_C = 1.45$, only slightly favoured for the nitro substituted spiropyran **2a**.[40] For the systems **3** and 4 with an aldehyde and a nitrile substituent respectively, the equilibrium constants are slightly higher since both groups are also weaker EWG with smaller Hammett constants (σ_p: $NO_2 = 0.78$; CN = 0.66, CHO = 0.42).[42] Comparing the equilibrium constants of the nitro substituted spiropyran **2a** and the unsubstituted spiropyran **5** the later one is greater by two orders of magnitudes. By adding an electron donating substituent like *t*Bu ($\sigma_p = -0.20$),[42] the equilibrium is even stronger shifted towards the spiropyran form.[40]

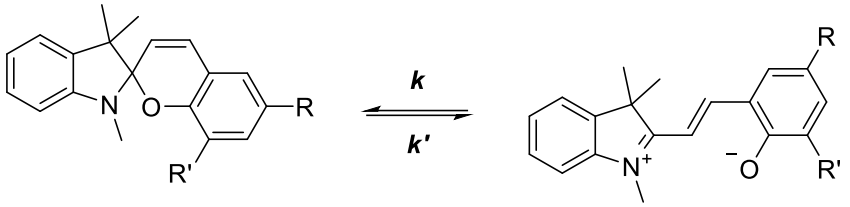

SP **MC**

***Scheme 9**:* General structure of the system investigated by Thomson and coworkers. The rate constant *k* for the cyclisation of the merocyanines to the corresponding spiropyrans were determined.

F. D. Thomson and coworkers[43] investigated the combination of *para*- and *ortho*-substituents regarding the oxygen of the benzopyran (Scheme 9). Since they conducted their measurements in ethanolic solutions and at 7 °C, the data cannot be directly compared with those presented by Beves and coworkers.[40]

***Table 1*:** Influence of different substituents in *para*- and *ortho*-position regarding the pyran oxygen. The rate constants (Σσ) for the thermal cyclisation from MC to SP measured in ethanol at 7 °C are given. The shown sum of the sigma constants is obtained by using Hammett's sigma constants for *para*-substituents and Taft's sigma constants for *ortho*-substituents which also include steric factors.[43]

SP	**7**	**8**	**9**	**10**	**11**	**12**
R	NO_2	Br	NO_2	Br	NO_2	OMe
R'	H	Br	Br	NO_2	OMe	NO_2
***k* [sec^{-1}]**	4.28×10^{-5}	3.97×10^{-3}	3.67×10^{-6}	1.70×10^{-5}	5.53×10^{-4}	1.32×10^{-2}
Σσ	0.79	0.38	1.00	0.95	0.28	0.01

For spiropyran **7** with only a nitro group in *para*-position a rate constant (*k*) for the thermal ring closure of 4.28×10^{-5} was obtained (Table 1). Even though spiropyran **8** contains two bromine substituents, the rate constant is higher by two orders of magnitude ($k = 3.7\times10^{-3}$) since bromine has a relatively small Hammett constants ($\sigma_p = 0.23$). This means that for system **8** the merocyanine form is less stabilised than for

system **7**. However, if the system with a nitro substituent in *para*-position is enhanced by an additional bromide in *ortho*-position **9**, the rate constant of the cyclisation is decreased by one order of magnitude (k = 3.67x10^{-6}) which therefore better stabilises the merocyanine. When comparing **9** and **10**, the importance of the substituent position is highlighted. Both systems contain one nitro- and one bromine-substituent but the positions are inverted. The rate constant for **10** with the nitro group in *ortho*-position is significantly higher (1.70x10^{-5}) than for **9** with the nitro group in *para*-position (3.67x10^{-6}). When the nitro group is combined with a EDG like OMe the merocyanine is destabilised which can be seen for **11** and **12**. Again, the positions of the substituents have a significant impact on the rate constants. If the nitro group is in *para*- and the methoxy group in *ortho*-position **11**, the merocyanine is better stabilised (k = 5.53x10^{-5}) compared to system **12** where the substituents are inverted (k = 1.32x10^{-2}).

The results presented by Beves and coworkers[40] indicate that the substituents in *para*-position have stronger impact on the SP/MC equilibrium than those in *ortho*-position. It is well known that constants provided by Hammett are not suitable for substituents in *ortho*-position since steric effects are not taken into account. Therefore, R. W. Taft modified the Hammett equation by adding a steric substituent constant E_s.[44] In case of the results obtained by Beves and coworkers linear correlation between the substituents and the Hammett constants could be obtained. Similar substituent effects were reported be Zaichenko et al.[45] in their studies on the free energy of activation for the inversion of the spiropyran which will be further discussed in the next chapter.

In summary, theoretical and experimental results showed stabilisation of the merocyanine when EWG were added at the benzopyran while EDG lead to destabilisation.

2.2.3 Influence of Substituents on the Photochromic System: The Indole Moiety

Compared with the data on the influence of the benzopyran substituents, only relatively few data are available on the influence of the substituents on the indole. In 1987, Zaichenko et al.[45] investigated the free energy of activation for the thermally

induced inversion of the spiro centre of substituted spiropyrans. Therefore, NMR-studies in DMSO at 185 °C were conducted.

Since the C–O-bond of the spiropyran needs to be cleaved for this inversion, the energy can also be used to get information about the stability of the SP or MC form (Scheme 4, Chapter 2.1). For spiropyran **7** with no substituent at the indole a $\Delta G^{\ddagger}$ of 21.9 kcal/mol was determined (Scheme 10). When electron withdrawing groups like CF_3 and NO_2 were added, the energy was increased to 24.9 kcal/mol and 25.0 kcal/mol respectively. This means that these substituents stabilise the spiropyran. On the other hand, electron donating groups like OMe decrease the energy difference (20.0 kcal/mol) and therefore destabilise the spiropyran.

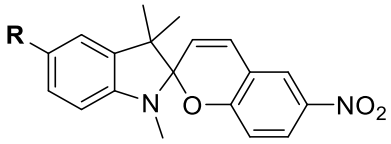

7, 13–15

13, R = OMe; $\Delta G^{\ddagger}$ = 20.0 kcal/mol
7, R = H; $\Delta G^{\ddagger}$ = 21.9 kcal/mol
14, R = CF_3; $\Delta G^{\ddagger}$ = 24.1 kcal/mol
15, R = NO_2; $\Delta G^{\ddagger}$ = 25.0 kcal/mol

***Scheme 10*:** Structure of different indole substituents (left) investigated by Zaichenko et al.[47] and the free activation energy needed for the inversion of the spiro centre (right). The energies were calculated by ^{1}H-NMR studies in DMSO-d_6 at 185 °C,

The reason for this stabilisation/destabilisation is, as already mentioned in Chapter 2.2.1, the impact on the lone pair at the indole nitrogen. EWG like NO_2 or CF_3 lower the electron density of the indole. Since the lone pair of the nitrogen is crucial for the ring opening, lowering the electron density at the indole disfavours the formation of the merocyanine. On the other hand, electron donating groups like OMe have the opposite effect.[45] Similar substituent effects were reported by Beves and coworkers[40] and Balmond et al.[46] Recently K. Palasis and A. Abell[47] investigated the ratio between the spiropyran and the protonated merocyanine (MCH^+) in acidic DMSO by ^{1}H-NMR. They reported that for systems with EDG like OMe at the indole, the MCH^+ was favoured while for those with electron withdrawing groups like NO_2 and COOH the spiropyran was predominantly. In contrast, Metelisa and coworkers[48] could not find a correlation between the indole substituent and the kinetics. They also reported that the influence of the substituents at the benzopyran are significantly stronger.

2.2.4 Influence of Substituents on the Photochromic System: The Geminal Methyl Groups

In 1997, Eggers and Buss[49] synthesised spiropyran **16** which had asymmetric substituents at the C3-atom of the indole which results in two different diastereomers for the spiropyran (Scheme 11). They studied how the ratio is affected upon ring opening and recyclization since they were interested if this system could be used for chiral information storage. However, when it comes to spiropyrans in modern applications, the substituents at the C3-postions are almost exclusively symmetrical. This is since spiropyrans are mainly used due to the change in physical properties upon switching to the merocyanine.

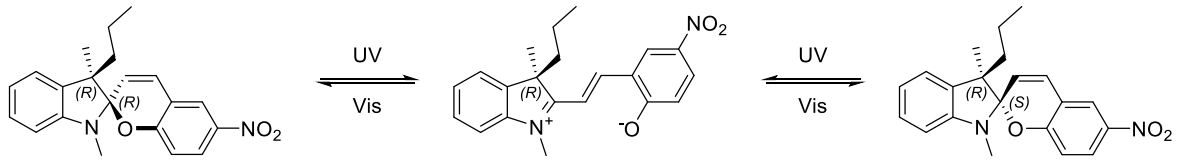

***Scheme 11*:** Chiral SP/MC system investigated by Eggers and Buss.[49]

A. Abdulla et al.[50] investigated how steric effects of the substituents can affect the photochromic behaver. Therefore, they synthesised two spiropyrans **17** and **18** with a cyclohexyl ring at the C3-atom and compared them with the methyl analogue **7** and **19** (Scheme 12**)**. The experiments were conducted at different temperatures in ethanolic solution. The experiments clearly showed that after irradiation, the thermal back reaction for the spiropyrans with the cyclohexyl moieties (**17** and **18**) were noticeably slower than those of their analogue with two geminal methyl groups (**7** and **19**). This indicates that the transformation between the *cisoid*- and *transoid*-form of the merocyanine or vice versa (Scheme 6, Chapter 2.2) is slowed down by steric hindrance caused by the cyclohexyl ring.

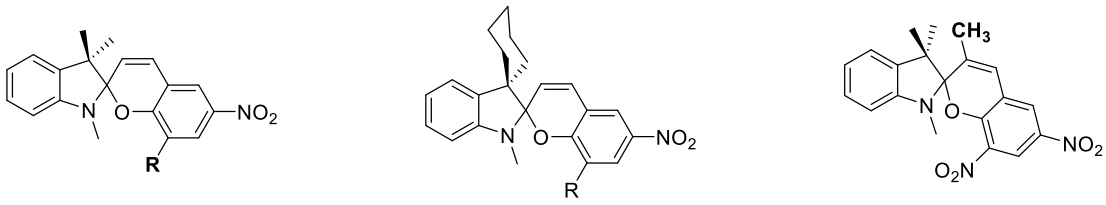

7, **R** = H
19, **R** = NO_2

17, **R** = H
18, **R** = NO_2

20

Scheme 12: Spiropyrans synthesised by Abdullah et al. concerning order to investigate sterically effect upon the SP/MC-transitions. The properties of systems with a sterically demanding cyclohexyl ring (middle) or an additional methyl group at the pyran (right) were compared to those with geminal methyl groups (left).[50]

In case of spiropyran **20** even stronger steric effects could be observed. By adding a methyl group to the C3' of the benzopyran, the formation of the merocyanine was completely prevented. Even at 410 K no merocyanine was observed. Therefore, it was proven that steric effects can have significant impact onto the photochromic properties of the SP/MC-system.

2.2.5 Influence of Solvents on the Photochromic System

The transition between spiropyrans and the corresponding merocyanines can be influenced by various stimuli. Besides the stimuli already mentioned at the beginning of Chapter 2.2, the solvent polarity has a major impact on the SP/MC-system. Spiropyrans are known for their solvatochromism for a long time. In 2014, Tian and Tian[51] investigated the effect of solvent polarity onto the position and shape of the absorption maximum of a merocyanine in the visible region in over twenty different solvents. They could show that polar solvents induce a hypsochromic shift of the absorption maximum while non-polar solvents lead to a bathochromic shift. Even more interesting was the change in shape of the absorption band. While a clear maximum was observed in polar solvents, the formation of a shoulder up to a second band was observed when switching to less polar solvents. This second absorption can be assigned to the formation of merocyanine aggregates. This aggregation can ultimately lead to the precipitation of the merocyanine.

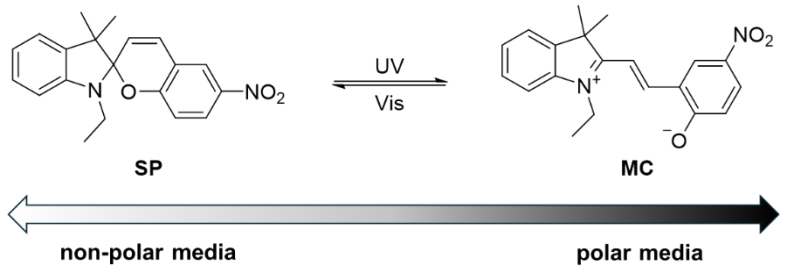

***Scheme 13*:** Photochromic system investigated by Tian and Tian in more than twenty different solvents.[51] Non-polar solvents favour the formation of the spiropyran while polar solvents favour the formation of the merocyanine.

In addition, Tian and Tian[51] reported a solvent-dependent change of the photochromic character (Scheme 13). In non-polar solvents positive photochromism and in polar solvents negative photochromism can be observed. This means that in polar solvents a coloration (MC) of the solution proceeded in the dark. The same

trends of the photochromic character were reported by Hirai and coworkers.[52] H. Görner[53] also reported a decrease in the cyclisation rate from merocyanine to spiropyran with increasing polarity of the solvent.

2.3 Influence of Spiropyrans on the Structure Biomolecules.

The potential of spiropyrans to modify the structure of biomolecules has already been reported in the 1975 by Suzuki and coworkers.[54] Therefore, the group modified the enzyme *α*-amylase with spiropyran and compared the enzymatic activity of native *α*-amylase and modified amylase after irradiation with visible and ultraviolet light. After modification with spiropyrans (Figure 2A), the activity of *α*-amylase dropped by 64 %. After irradiation with UV- or Vis-light, the activity of the modified α-amylase dropped further by 22 % and 18 % respectively. Upon incubation in the dark, the activity of the modified *α*-amylase could be regained. In subsequent studies S. Suzuki also investigated the effects of spiropyrans on other enzymes like *α*-chymotrypsin, *β*-glucosidase, urease and *β*-amylase.[55, 56] For all enzymes, a change in enzymatic activity upon the photochromic transformation of the attached spiropyrans could be reported (Figure 2B). For enzymes with hydrophilic substrates as amylose or urea, higher activity was observed when the spiropyran was in the MC form. This can be rationalised by the MC form being more hydrophilic. On the other hand, higher activity was observed for enzymes with hydrophobic substrates when the hydrophobic spiropyran form was present.

A

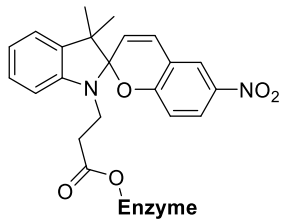

B

Modified Enzyme	Substrate	Relative activity (%)	
		MC	SP
α-Amylase	Amylose	100	64
β-Amylase	Amylose	100	13
Urease	Urea	100	62
α-Chymotrypsin	*N*-benzoyl-L-tyrosine ethylester	100	150
β-Glucosidase	*p*-Nitrophenyl-*β*-D-glucoside	100	115

***Figure 2*: A** Spiropyran used for the modification of enzymes. **B** Photochromic influence on the activity of different enzymes.[56]

The enzyme activity can also be altered by using spiropyran modified inhibitor. This was also shown by Suzuki and coworkers by modifying 20 % of the amino acids of the trypsin inhibitor ovomucoid. Upon irradiation with visible light, the inhibitor activity was reduced by 28 % and later restored by incubation in the dark.[57] There are several other examples in which the structure of peptides could be influenced directly (SP attached to the peptide)[58, 59] or indirectly (SP attached to hydrogels or

fibrils)[60, 61] based on the photochromism of spiropyrans. A great overview was published by R. Klajn.[22]

One of the few examples of biomolecules reacting with spiropyrans, without covalent bonding of the spiropyran to the biomolecule or a medium, is the interaction of cationic spiropyrans with DNA. In 2008, J. Andersson et al. reported about the ionic binding of spiropyran **1d** to calf thymus DNA (Scheme 14, left). Upon binding, the absorption spectra of the merocyanine changed significantly. Using linear dichroism analysis, it was possible to show a (partly) reversible binding of the SP/MC system to the DNA upon photochromic switching.

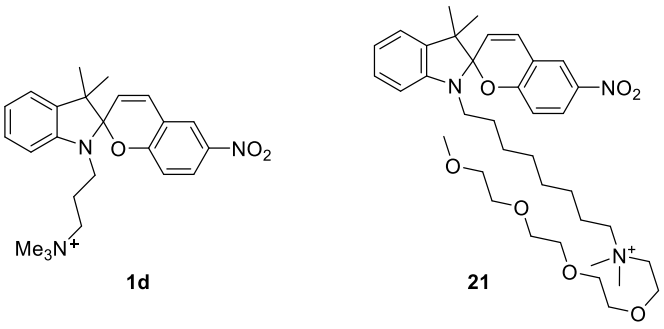

***Scheme 14*:** Structure of the spiropyran **1d** used by J. Andersson at el.[62] and spiropyran **21** used by Z. Wu et al.] for DNA binding.[63

In 2024, Z. Wu et al.[63] were able to bind the modified spiropyran **21** to a DNA with twenty-two base-pairs via noncovalent interactions. They obtained an ionic complex with two spiropyrans per negative charge in the DNA. This solid SP-DNA complex provided triple external stimuli-responsive property. The colouration based on the formation of merocyanine form could be favoured by irradiation with UV light, thermal energy or also by the relative humidity of the environment. In the future such dynamic materials could be used for several applications as optical memory devices.

2.4 Influencing the *cis*/*trans*-Equilibrium of Proline

Among the proteinogenic amino acids, proline has a role due to its unique structural properties. Since the peptide bond has a partial double bond character, it is relatively rigid. Therefore, depending on the orientation of the amino acids, a distinction can be made between *cis* and *trans* isomers. For most amino acids the *trans*-isomer is highly favoured since high sterically interaction of the side chains occurs for the *cis*-isomer (Scheme 15, left).[64, 65] In case of peptide bonds including a proline (X-P), this is different. Due to the cyclic nature of proline, steric interactions are observed in both cases leading to almost isoenergetic *cis*- and *trans*-isomers.[65] However, the *trans*-isomer is usually still slightly favoured due to a n-π*-interaction between the two carbonyls (Scheme 15, right).

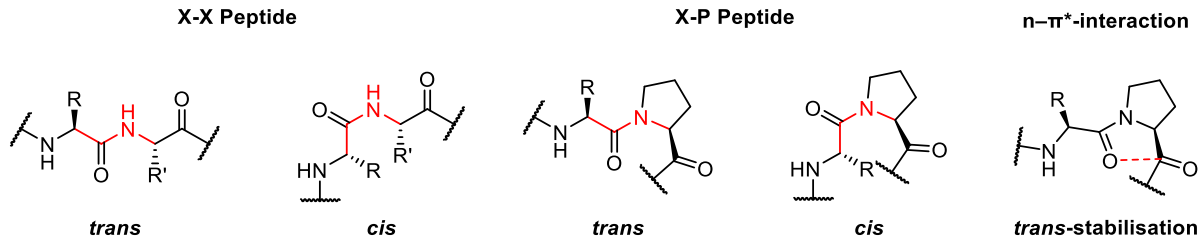

Scheme 15: General structure of the *cis*- and *trans*-isomers of non-proline containing peptide bonds (left) and proline containing peptide bonds (middle). Stabilisation of the *trans*-isomers for proline containing peptide bonds via n-π*-interaction (right).

This structural feature makes proline essential for the structure of proteins. Several examples can be found in which the *cis/trans*-isomerisation has a crucial impact on the protein folding.[65] Due to the high importance of this isomerisation, over the last two decades numerous approaches were made to alter the equilibrium between both isomers.

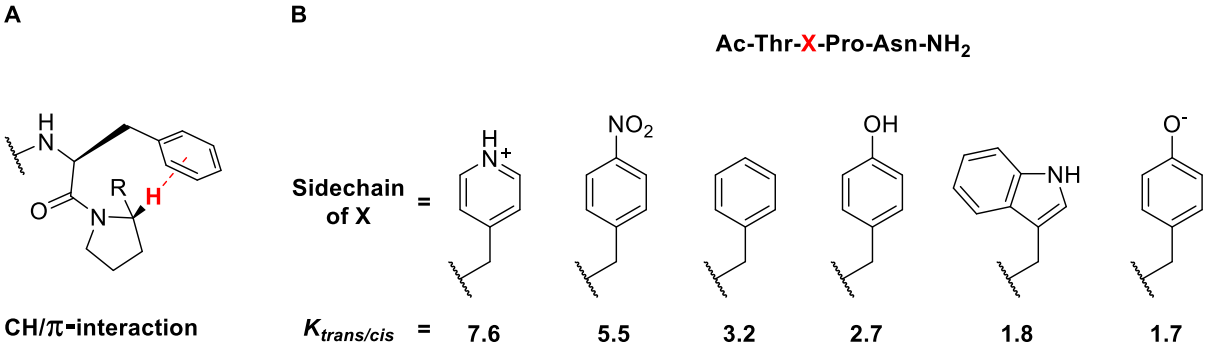

Scheme 16: **A** Illustration of the CH/π interactions between proline and aromatic amino acids. **B** Equilibrium constants of the *trans/cis*-isomerisation of selected aromatic amino acids reported by N. J. Zondlo.[68]

It was found that amino acids with aromatic side chains *N*-terminally bound to the proline stabilises the *cis*-isomer.[66–68] This stabilisation is based on a interaction of the proton at the chiral centre of the proline and the π-system of the aromatic sidechain (Scheme 16A). The efficiency of this interaction depends on the electronic character of the aromatic ring.[66–68] While the stabilisation for the *cis*-isomer is stronger for electron rich aromatics like phenolate, it is weaker for electron deficient systems like pyridinium (Scheme 16B).

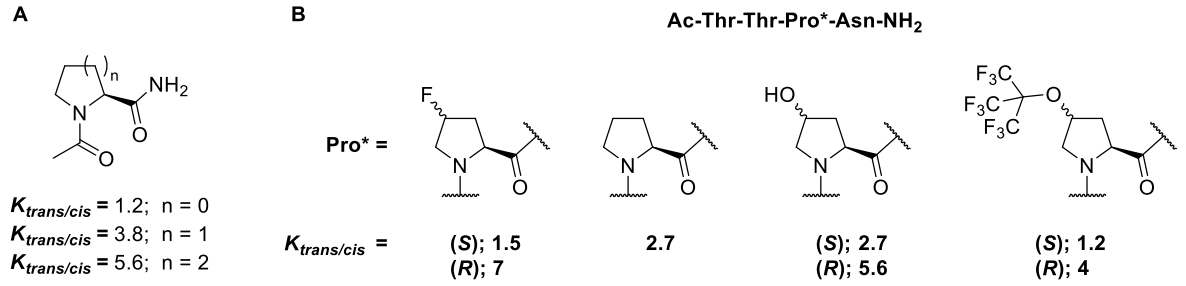

***Scheme 17*: A** Equilibrium constants of proline analogy with different ring sizes investigated by H. Wennemers and coworkers.[69] **B** Different substituted prolines and the corresponding equilibrium constants investigated by Coxon and co-workers.[70]

The influence of the proline derivatives on the *trans*/*cis*-isomerisation was subject to numerous studies. H. Wennemers and coworkers investigated the influence of proline derivates with different ring sizes (Scheme 17A) on collagen triple helices. The group could show that increasing the pyrrole ring to a piperidine ring, shifted the *trans/cis*-equilibrium towards the *trans*-isomer, while decreasing the ring to an azetidine shifted the equilibrium towards the *cis*-isomer. Coxonand co-workers investigated the influence of different proline substituents on the *trans/cis*-equilibrium. A few examples are shown in Scheme 17B. Substituents at the C4-atom with (*R*) configurated chiral centre shifted the equilibrium towards the *trans*-isomer while the derivates with a (*S*)-configuration shifted the equilibrium towards the *cis*-isomer. Those studies are only a few examples. Excellent overviews are provided by Zondlo et al.[71] and Basu et al.[72]

In 2005, S. C. R. Lummis et al.[73] published one of the most impressive examples for the utilisation of substituent influence on the isomerisation of proline. The group studied the importance of proline for the 5-HT3 receptor, a transmembrane receptor that acts as ion channel. They could show that proline isomerisation is crucial for the neurotransmitter induced opening of the ion channel. While the *cis*-isomer of proline is present in the open form of the protein, upon isomerisation to the *trans*-form the

protein is closed. By exchanging the proline with derivates with a higher affinity towards the *cis*-isomer, the concentration of neurotransmitter needed for the opening of the channel could be significantly reduced. On the other hand, changing the proline with derivates with a higher affinity towards the *trans*-isomer, the function of the protein could be stopped entirely.

Although much is already known about the influence of substituents or proline analogues on the *cis/trans*-equilibrium, there are comparatively few studies on external influence. In 2015, Wennemers et al. were interested in the effects of solvents and the dipole moments of the protected prolines (Scheme. 18A and 18B).[74]

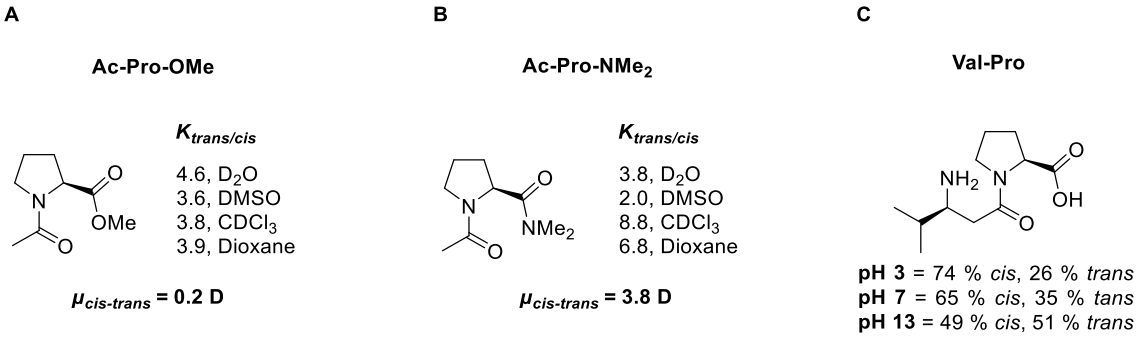

***Scheme 18*:** Influence of the solvent onto the *trans/cis*-equilibrium of **A** Ac-Pro-OMe and **B** Ac-Pro-NMe_2. The difference in dipole moment between the isomers are stated below. **C** Influence of the pH onto the *cis/trans*-ratio of the Val-Pro-dipeptide.

For Ac-Pro-OMe only minor changes of the equilibrium could be observed in different solvents (Scheme 18A). The dipole difference between the *cis*- and *trans*-isomers was calculated to be very small (0.2 D) Therefore the effects of the solvents are negligible compared to the stabilisation of the *trans*-form via the n-π*-interaction (Scheme 15, right). For the Ac-Pro-NMe_2 system, this stabilisation is smaller since the dimethylamine group lowers the electrophilicity of the carbonyl. Additionally, the dipole moment of the *cis*-isomer is 3.8 D higher than for the *trans*-isomer (Scheme 18B). In this case a significant impact of the solvent could be observed. Since the less polar *trans*-isomer is better stabilised by non-polar solvents like $CDCl_3$ and dioxane, the equilibrium in these solvents is heavily shifted towards the *trans*-conformer ($K_{trans/cis}$ = 8.5 and 6.8).

The equilibrium between proline isomers can also be affected by acid or base. V. Enchev and coworkers[75] demonstrated this on the Val-Pro-dipeptide

(Scheme 18C). The Ratio could be changed from 74 % *cis*-conformer (pH 3), through 65 % *cis*-conformer (pH 7) up to 51 % trans-conformer (pH 13).

In 2017, A. Bröhl et al.[76] investigated the influence of salts onto the *cis/trans*-isomerisation of prolines. Therefore, the equilibrium of three different prolines in the presents of different concentrations of NaOAc, NaSCN and Na_2SO_4 were determined (Scheme 19).

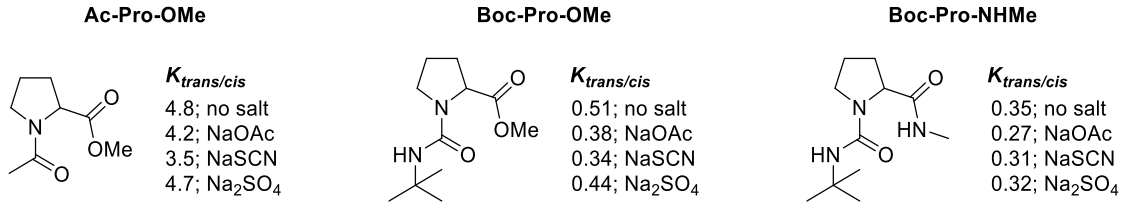

***Scheme 19*:** Changes of the *trans/cis*-equilibrium of different proline derivatives induced by different salts. For NaOAc and NaSCN concentrations up to 4 M and for Na_2SO_4 up to 1 M were used in D_2O.[76]

Concerning the *trans/cis*-equilibrium without any salts, the *trans*-conformer was highly favoured for the Ac-Pro-OMe due to the strong n-π*-interaction of the carbonyls. In case of Boc-Pro-OMe and Boc-Pro-NHMe the *cis*-conformer was favoured since the n-π*-interaction are significantly weaker due to the less nucleophilic carbamates. Upon adding salt to the solutions, the equilibrium is shifted in favour of the *cis*-conformer. However, only minor changes of the equilibrium could be noticed at high concentrations of salt (up to ~4 M). Also, no clear trends between the salt and the calculated electronic surface potential of the different prolines could be observed.

2.5 A Brief Introduction to DFT

Density functional theory (DFT) is a computational tool for the modelling of multi electron systems. For these calculations, a combination of a basis set (set of functions for the representation of electronic wavefunctions) and a functional (method for the calculation of exchange-correlation energy) is used.[77] Over the last decades numerous basis sets and functionals were established for various applications. The number of basis functions that are applied for the calculation of every valence orbital is typically described by the letter zeta (ζ). Double-ζ basis sets use two basis functions, triple-ζ basis sets use three basis functions etc. Basis sets can be divided into different categories, namely (non)polarisation functions and (non)diffuse functions. As the title suggests, polarisation functions allow the calculated orbitals to be polarised, while diffuse functions take into account the diffuse character of the orbitals.[78–86] None, light only (H and He) or heavier atoms can be included in the polarisation and diffuse functions. The number of atoms included varies between different basis sets and families of basis sets. For accurate calculations, both diffuse and polarisation functions should be utilized.[77]

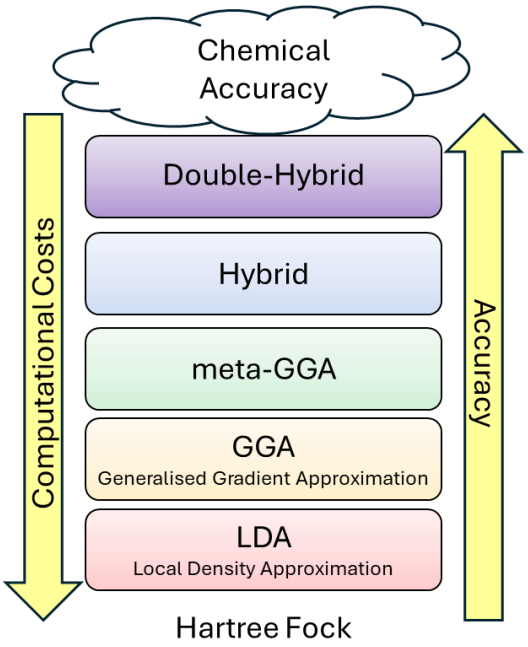

***Scheme 20**:* Jacob's ladder of density functional theory.[77]

Today hundreds of functions are known for various applications. The functionals are often categorised in classes based on the terms included. The different classes are often shown in the Jacob's ladder leading from the ground level of Hartree-Fock to the DFT heaven of chemical accuracy (Scheme 20).[77] The least accurate functional

are the so-called local density approximation functionals (LDA) where a homogeneous electron density throughout the system is presumed. On the level of generalised gradient approximation functionals (GGA) a gradient of the electron density is considered by adding the first derivatives of the electron density into the calculations.[89] For meta-GGA functional an additional term for the local kinetic energy density is taken into account. In case of hybrid functionals a part of the exchange functional is replaced by the exact exchange energy taken from the Hartree Fock theory.[89] Hybrid functionals can again be defined in different classes such as Hybrid-GGA, Hybrid-Meta-GGA and more which are not discussed as this would be beyond the scope of this thesis.

3 Motivation and Concept

Spiropyrans are showing potential for several different applications in which the structural change as well as the high change of the dipole moment upon photochromic ring opening is utilised. The first task was the calculation of the dipole moments for substituted spiropyrans and their stable *transoid* merocyanine forms using DFT. Different substituents of the indole nitrogen, the benzopyran and the indole moiety were to be included in the calculations in order to identify systems with the greatest dipole moment differences (Scheme 21).

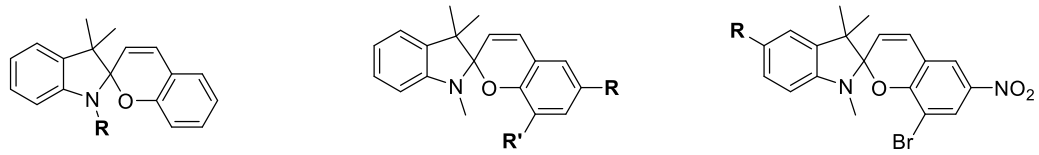

R = Me, Bzl, $(CH_2)_2COOH$ $(CH_2)_3SO_3H$, $(CH_2)_3SO_3^-$

R = NMe_2, OMe, H, Br, COOH, CN, NO_2
R' = NMe_2, OMe, H, Br, COOH, CN, NO_2

R = NMe_2, OMe, H, Br, COOH, NO_2, NMe_3^+,

Scheme 21: Different substituted spiropyran systems which are to be considered in the DFT calculation on the dipole moment changes.

The influence of substituents on photochromic behaviour has already been discussed. Although several trends of substituent effects on the rate constants of cyclisation or ring opening are already known, the mentioned data often cannot be directly compared with each other, as conditions such as solvent and temperature vary often. In order to determine the rate constant of the newly designed systems, kinetic studies are therefore conducted.

Another crucial piece of information is often not mentioned in the current literature, namely the quantity of the switching processes. However, determining the ratio of SP and MC is not trivial, since in UV/Vis analysis, only the quantitative formation of spiropyran can be observed. This is due to spiropyran exhibiting no absorption in the visible range and therefore it is possible to consider quantitative amounts of SP, if no visible absorbance is displayed. Since MC has absorption bands in both the visible and UV range, small amounts of SP can never be excluded due to overlapping signals. For the quantitative formation of merocyanine, determination via ^{1}H-NMR spectroscopy will be necessary. By combining DFT with UV/Vis and ^{1}H-NMR analysis, spiropyran/merocyanine systems with the most quantitative switching properties and high dipole moment changes will be identified.

As previously mentioned, only a few applications of spiropyrans without need to be covalent bonded to the applicant are known to date. Both our group and H. Wennemers' group have shown in the past that the *cis/trans*-equilibrium of proline derivatives can be influenced by polar interactions. Therefore, suitable spiropyrans with regard to the *cis/trans*-equilibrium of proline in photochromic SP/MC isomerisation will be tested. Various proline derivatives need to be synthesised for this purpose. In addition to simple protected prolines, such as those used by A. Bröhl[76] and H. Wennemers,[74] small peptides consisting of up to four amino acids will also be implemented. Because of the possible formation of disulfide bridges, the amino acid cysteine is included in these test models for later applications. Taking these criteria into account, the proline derivatives shown in Scheme 22 were to be synthesised. Two proline-cysteine dipeptides with different *N*-terminal protecting groups had to be included to see whether these protecting groups have an influence. The influence of cysteine protecting groups were to be investigated using the tripeptides Boc-Cys(Bzl)-Pro-Cys(Bzl)-OMe and Boc-Cys(trt)-Pro-Cys(trt)-OMe. In addition, the Boc-Cys(trt)-Pro-Phe-Cys(Acm)-OMe tetrapeptide was to be synthesised, as detailed information on its properties, including cyclisation via disulphide bridges, had already been published by the group of W. Sander.[77–79]

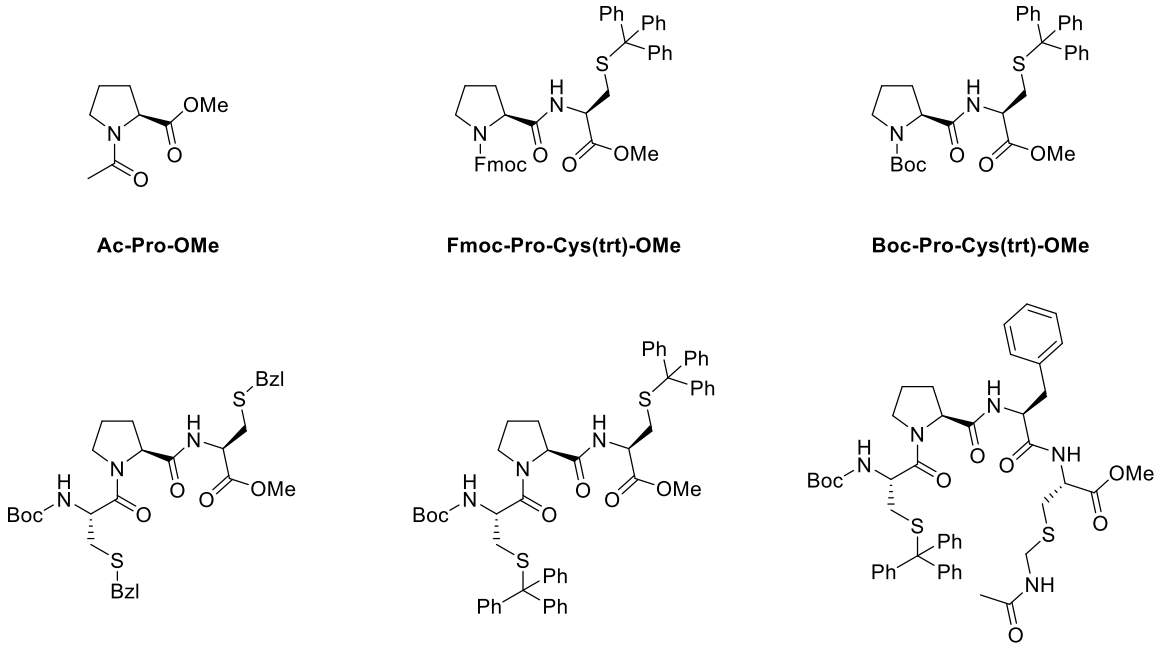

***Scheme 22*:** Proline based target molecules including the protected Ac-Pro-OMe used by A. Bröhl[76] and H. Wennemers[74] (top, left), two dipeptides (top, middle and right) and two tripeptides (bottom, left and middle) and one tetrapeptide (bottom, right) reported by W Sander.

The synthesised model peptides were then to be investigated in spiropyran-containing solutions to determine whether the *cis/trans*-equilibrium of the central proline is affected by the changes in dipole moment when switching between spiropyran and merocyanine.

4 Results and Discussion

4.1 DFT Calculations

4.1.1 Method Screening

Since we are interested if the photoisomerization from spiropyran to merocyanine can affect other molecules by polar interactions due to the change in the dipole moment, it is crucial to know the dipole moment of both isomers. Therefore, DFT based calculations were performed using the ORCA 5.0 software package.[93]

The first task was to find a suitable functional and basis set for the calculation of dipole moments of the SP/MC systems. Therefore, a small initial screening was performed. As previously mentioned, hundreds of functionals and basis sets are known today. Since the depiction of the ideal combination for specific tasks can be challenging the aug-cc-pVnZ (n = D double-ζ or T triple-ζ)[78–86] and the Karlsruhe basis sets def2-SVPD (double-ζ) and def2-TZVPPD (triple-ζ)[86–88] were selected, based on a publication by Zapata and McKemmish[94] from 2020. All basis sets include polarisation and diffuse functions. Also based on this paper the ωB97X-V[95–98] and the B3LYP D3BJ[99–102] functionals were tested in the screening. Both are hybrid functionals with additional dispersion correction (VV10 and D3BJ). Additionally the B97-V[95, 97, 98, 103] meta-GGA was included. Concerning the family of the Minnesota functionals the M06-L meta-GGA functional[104, 105] and the M06-2X hybrid meta-GGA functional[105, 106] were included. Since a screening with the SP/MC system would be demanding, the initial screening was conducted using two smaller test systems. The two systems of choice were bromobenzene and *para*-nitrophenol. These systems were chosen since they contained crucial parts of the SP/MC systems like aromatic halides, nitro-groups and acidic phenols.

The calculated dipole moments, deviation from literature values, and the computation times for bromobenzene and *p*-nitrophenol using all combinations of the five functionals and four basis sets are shown in Table 2. The last column indicates if the calculated dipole moments for both model compounds (green), one (orange) or none (red) match the literature within an ±0.1 D error range. For the bromobenzene in the gas phase, dipole moments from 1.70–1.73 D were reported in literature.[107–110] For *p*-nitrophenol in the gas phase no sufficient data are available, therefore the literature

values in dioxane of 5.38–5.43 D are used as reference.[111, 112] These might deviate from the dipole moment in the gas phase.

When comparing the results obtained by the five different functionals, the ωB97X-V and M06-2X functionals performed significantly worse than the others. The ωB97X-V functional could not yield any results that fits within the set error range of ±0.1 D. One literature match was achieved with M06-2X. Additionally, the computational demand for the calculations using the ωB97X-V was in most cases noticeably higher than for other functionals. For the remaining functionals, B3LYP-D3BJ, M06-L and B97M-L, were the results quite similar in that only one or two literature values could not be produced. It is worth mentioning that the two calculations outside the error range for the B3LYP-D3BJ functional were those using the double-ζ basis sets def2-SVPD and aug-cc-PVDZ. In case of the M06-L and B97M-L functionals, only one calculation each was not within the error range. In both cases these calculations were using the def2-SVPD base set. When assessing the data, it is noticeable that most mismatches occur with def2-SVPD basis set, which is reason why it was decided to carry out the calculations with triple-ζ base, although higher calculation costs must be expected.

Table 2: Computations for the dipole moment of bromobenzene and *p*-nitrophenol. The minimal differences between calculation and the literature range as well as the corresponding time demand are listed. The last column indicates if both (green), one (orange) or none (red) of the calculated dipole moments match the literature within an additional ±0.1 D error range.

		Bromobenzene lit.: 1.70–1.73 D[107–110]		***p*-nitrophenol lit.: 5.38–5.43 D[111, 112]**		
Functional	**Base Set**	**Time**	**min $\Delta\mu$ [D]**	**Time**	**min $\Delta\mu$ [D]**	**Match ±0.1 D**
B3LYP D3BJ	**aug-cc-pVDZ**	6.1 min	0.128	21.6 min	0	**1/2**
	aug-cc-pVTZ	13.7 min	0.090	32.1 min	–0.01218	**2/2**
	def2-SVPD	8.8 min	0.093	20.2 min	0.10534	**1/2**
	def2-TZVPPD	12.1 min	0.095	26.1 min	–0.00593	**2/2**
B97M-V	**aug-cc-pVDZ**	7.4 min	0.057	31.0 min	0.00099	**2/2**
	aug-cc-pVTZ	12.6 min	0.033	24.9 min	0	**2/2**
	def2-SVPD	13.3 min	0.020	24.8 min	0.13706	**1/2**
	def2-TZVPPD	11.2 min	–0.006	18.0 min	0	**2/2**
M06-L	**aug-cc-pVDZ**	7.8 min	0	15.6 min	0	**2/2**
	aug-cc-pVTZ	8.2 min	–0.054	21.5 min	–0.02208	**2/2**
	def2-SVPD	9.4 min	–0.024	5.5 min	0.13504	**1/2**
	def2-TZVPPD	10.9 min	–0.061	12.4 min	–0.07006	**2/2**
M06-2X	**aug-cc-pVDZ**	7.1 min	0.102	15.2 min	–0.1914	**0/2**
	aug-cc-pVTZ	12.7 min	0.132	23.2 min	–0.19386	**0/2**
	def2-SVPD	10.5 min	0.107	16.6 min	–0.07156	**1/2**
	def2-TZVPPD	11.2 min	0.137	17.5 min	–0.21847	**0/2**
ωB97X-V	**aug-cc-pVDZ**	10.4 min	0.107	20.9 min	–0.30038	**0/2**
	aug-cc-pVTZ	30.2 min	0.115	32.1 min	–0.33194	**0/2**
	def2-SVPD	9.8 min	0.110	13.0 min	–0.19003	**0/2**
	def2-TZVPPD	23.6 min	0.110	24.5 min	–0.32401	**0/2**

Comparing the results using Dunning basis sets (aug-cc-PVDZ and aug-cc-PVTZ) with those using the Karlsruhe basis sets (def2-SVPD and def2-TZVPPD), in case of the double-ζ basis sets the Duning basis set aug-cc-PVDZ yielded better results than the def2-SVPD basis set. Comparing both triple-ζ basis sets, the computational results were similar. However, in many cases the calculations using the def2-TZVPPD basis set was remarkably faster than those using the aug-cc-PVTZ basis set.

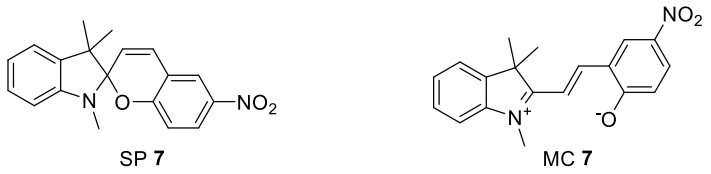

Scheme 23: Structure of spiropyran and merocyanine **7** used for the DFT screening.

Based on these results, for the calculations of the nitro substituted SP/MC system **7** (Scheme 23), the screening was narrowed to the B3LYP-D3BJ, M06-L and B97M-L functionals and the aug-cc-PVTZ and def2-TZVPPD basis sets. These results are shown in Table 3 As references for the dipole moments of SP **7** and MC **7** the publications by Levitus et al.[113] (SP = 6.4 D, MC = 14.2 D) and Lapienis-Grochowska et al.[114] (SP = 3.5 D, MC = 12.7 D) were used. Based on these publications, the dipole moment of SP **7** ranges between 3.5–6.4 D while for the MC **7** it ranges from 12.7–14.2 D.

Considering the rather wide range of dipole moment stated in the literature, it is no surprise that all calculated dipole moments for the spiropyran isomers are within this range (Table 3). However, all calculated dipole moments for the merocyanine isomers are lower than the experimental results. The data obtained using the M06-L functional deviated to most. Therefore, this functional was ruled out for the later calculations. The B3LYP-D3BJ and the B97M-V functionals gave similar results while the later had also lower computation cost. Since both functionals performed similar, the B3LYP-D3BJ functional was chosen for later computations since it also performed very well in the screening by Zapata and McKemmish.[94]

Table 3: Calculated dipole moments of SP **7** and MC **7** using B3LYP-D3BJ, B97M-V and M06-L functionals in combination with the aug-cc-PVTZ and def2-TZVPPD basis sets.

Functional	Base Set	Form	Dipole Moment [D]	Time
B3LYP D3BJ	aug-cc-pVTZ	SP	5.687	11.2 h
		MC	12.206	4.1 h
	def2-TZVPPD	SP	5.675	7.2 h
		MC	12.197	2.5 h
B97M-V	aug-cc-pVTZ	SP	13.235	7.1 h
		MC	12.231	2.3 h
	def2-TZVPPD	SP	5.582	8.0 h
		MC	12.196	1.6 h
M06-L	aug-cc-pVTZ	SP	5.703	7.7 h
		MC	12.029	2.0 h
	def2-TZVPPD	SP	5.392	4.4 h
		MC	11.849	1.1 h

Comparing the triple-ζ basis sets, the calculated results were again similar while the def2-TZVPPD was significantly more time efficient than the aug-cc-pVTZ basis set. Therefore, for all following calculations the combination of the B3LYP-D3BJ functional and the def-TZVPPD basis set were used.

4.1.2 DFT Calculation of Spiropyran and Merocyanine Derivatives

In order to ascertain the optimal methodology for computing the SP/MC system **7**, only one possible structure of the merocyanine was considered. In general, eight isomers of the merocyanine can be described, with the sole differentiating factor being the conformation of the three bonds which connect the indole- and the phenol-moieties. For the sake of clarity, the aforementioned bonds are labelled as α, β, and γ in Scheme 24.

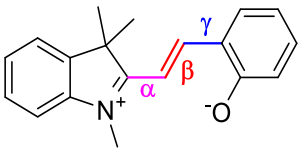

TTC

Scheme 24: Overview for the determination of the different isomers of a spiropyran.

By rotation of these bonds, four *transoid*-merocyanines and four *cisoid*-merocyanines can be described. All eight isomers are illustrated in Scheme 25. Due to the considerable steric hindrance within the *cisoid*-merocyanines, these four isomers are unlikely to be present in a reasonable concentration. In particular, the CCC isomer is

highly unlikely to be stable since it rapidly cyclises to the spiropyran. Consequently, only the four *transoid*-merocyanine structures of the desired target systems were calculated in the following.

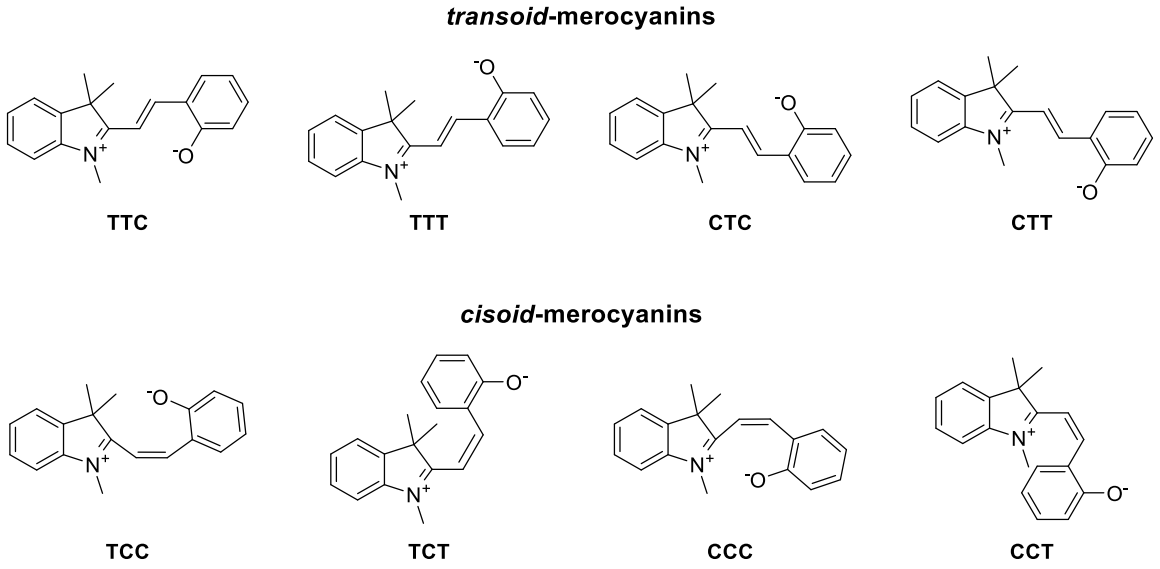

Scheme 25: The eight different isomers of **MC1**. Four *transoid*-forms (top) and four *cisoid*-forms (bottom).

In Scheme 26 the calculated dipole moments for SP **7** (left) and the four corresponding *transoid*-merocyanines (right) are depicted. A dipole moment of approximately 5.2 D was calculated for the spiropyran, while the dipole moments for the merocyanine isomers ranged from 11.2 D to 12.2 D. Therefore, the calculated change in dipole moment upon switching from the spiropyran to the merocyanine is between 6.1 D and 7.0 D

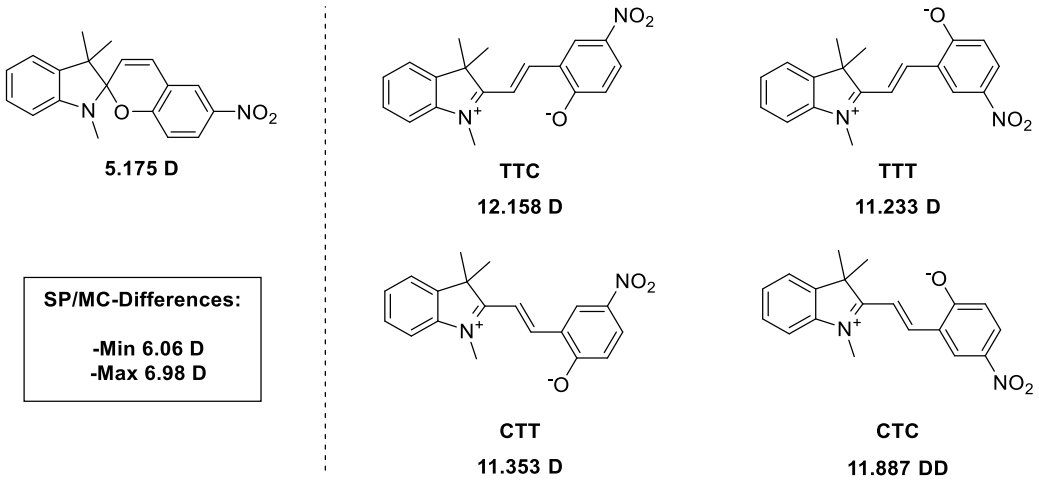

Scheme 26: Calculated dipole moments for the spiropyran and the four *transoid*-merocyanine isomers.

The differences in the dipole moments of the merocyanine isomers and the corresponding spiropyran are analysed in the following section. The objective was to investigate the impact of various substituents on the dipole moment of the SP/MC system. For this purpose, three sections of the spiropyran were substituted independently to each other. The three sections considered were the nitrogen side chain, the chromene and indole units. To facilitate comparison of the change in dipole moment, the calculated differences were colour coded. If the difference in the dipole moment of the merocyanine compared to that of the spiropyran is less than 3 D, the value is highlighted in red. In case the value is between 5 D and 7 D, it is highlighted in yellow, between 7 D and 10 D in green. Differences greater than 10 D are marked in blue.

Beginning with the nitrogen sidechain derivatisation, substituents which were considered are benzyl, propionic acid and propyl sulfonic acid (Scheme 27). In the case of the sulfonic acid substituents, both the isomers in which the sulfonic acid is protonated and those in which the phenol is protonated were considered. These substituents are then compared with the previously mentioned methyl substituent.

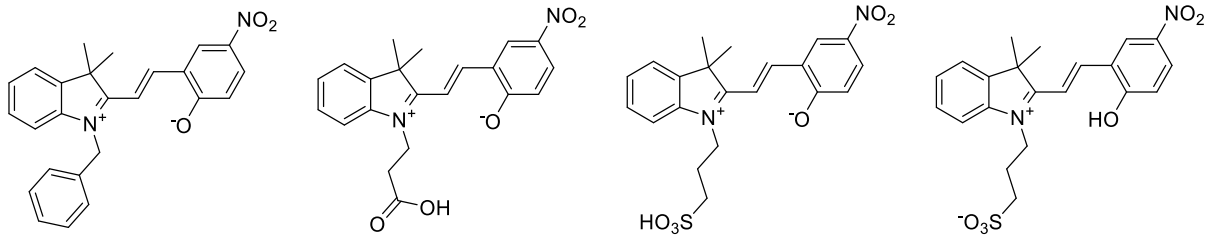

Scheme 27: Structure of the nitrogen substituted merocyanines in the TTC structure.

The dipole moments for the merocyanine isomers of the benzyl and propionic acid substituted systems are only marginally higher than those of the corresponding spiropyrans (Table 4). For the sulfonic acid substituted merocyanines the TTC isomer is the only isomer with a dipole moment change higher than 5 D. In all three cases, fluctuations in the dipole moment of up to 2.5 D were observed between the individual isomers. The dipole moment of the TTC isomer was consistently the highest. In the system in which the sulfonic acid is deprotonated and the phenol is protonated, it is notable that the dipole moment of the TTC isomer differs only slightly from that of the spiro form, with a difference of 3.6 D. The CTT and CTC isomers show an increase in the dipole moment of 5.7 D and 6.9 D respectively. A change of 9.8 D was even calculated for the TTT isomer. However, given the significant discrepancy in the dipole moments of the individual isomers, with a difference of

4.1 D, and the uncertainty regarding the precise location of the proton, the methyl group emerges as the most reliable substituent.

Table 4: Differences in dipole moments between the merocyanine isomers and the corresponding spiropyran for *N*-substituted systems. The differences of the dipole moments are colour-coded as follows: $\Delta D_{SP\text{-}MC}$ < 3 D (red), 3–7 D (yellow), 7–10 D (green), > 10 D (blue).

Sidechain	TTC	TTT	CTT	CTC
Me	7.01	6.06	6.18	6.71
Bzl	4.22	2.72	3.02	3.64
$(CH_2)_2COOH$	3.35	1.87	2.72	2.93
$(CH_2)_3SO_3H$	5.55	3.36	4.88	3.86
$(CH_2)_3SO_3^-$	3.61	9.81	5.65	6.86

As for the substitution on the chromene moiety of the system, a number of electron-withdrawing and electron-donating groups in *ortho*- and *para*-positions were considered (Scheme 28). As electron-donating groups dimethylamine- and methoxy-substituents were considered, while for electron-withdrawing substituents, bromide, nitrile, carboxylic acid and nitro-groups were tested. For those substituents all combinations of mono- and di-substitution patterns, on the specified positions in Scheme 28 were considered. The differences of the dipole moments of the MC isomers with respect to the corresponding spiropyran were colour-coded as previously established.

R = NMe_2, OMe, H, Br, COOH, CN, NO_2

R' = NMe_2, OMe, H, Br, COOH, CN, NO_2

Scheme 28: Overview of the different chromene substituted spiropyran and merocyanine derivatives included in the DFT calculations

For the systems with electron-donating groups (NMe_2 and OMe) in the *para*-position, the dipole moments of the MC-isomers were only slightly higher than those of the corresponding spiropyran (Table 5). The electron-donating substituents are presumed to increase the electron density at the phenolate moiety of the merocyanine. The conjugation shifts the electron density towards the electron-deficient indole, thereby reducing the zwitterionic character of the merocyanine. The

effect can be strengthened by further electron-donating substituents in the *ortho*-position or weakened by electron-withdrawing substituents. Therefore, the systems with additional strong electron-withdrawing substituents such as nitro-, nitrile- and carboxylic acid groups in *ortho*-position show a higher difference in the dipole moment than those with electron-donating substituents. The systems with carboxylic acid substituents stand out in particular. This phenomenon may be attributed to the interaction between the phenolate and the carboxylic acid via hydrogen bonding. Furthermore, the dipole moments for the TTT isomers are markedly higher than those of the other isomers, as in this case the electron-rich phenolate group is oriented away from the electron-deficient indole. Both trends can be applied to many of the other systems.

Table 5: Differences in dipole moments between the merocyanine isomers and the corresponding spiropyran for systems with NMe_2- and OMe-substituents in *para*-position and various substituents in *ortho*-position. The differences of the dipole moments are colour-coded as follows: $\Delta D_{SP\text{-}MC}$ < 3 D (red), 3–7 D (yellow), 7–10 D (green), > 10 D (blue).

Para	***Ortho***	**TTC**	**TTT**	**CTT**	**CTC**
NMe_2	NMe_2	**–0.05**	**1.73**	**0.60**	**0.86**
NMe_2	OMe	**0.73**	**2.23**	**1.52**	**1.55**
NMe_2	H	**1.02**	**3.21**	**2.11**	**1.93**
NMe_2	Br	**2.55**	**4.46**	**3.47**	**3.37**
NMe_2	COOH	**5.37**	**6.90**	**6.14**	**5.60**
NMe_2	CN	**3.68**	**5.81**	**4.88**	**4.55**
NMe_2	NO_2	**3.92**	**6.14**	**5.07**	**4.82**
OMe	NMe_2	**0.83**	**3.52**	**0.82**	**2.98**
OMe	OMe	**1.99**	**4.72**	**2.22**	**2.24**
OMe	H	**3.22**	**3.21**	**2.21**	**2.08**
OMe	Br	**4.10**	**4.10**	**3.22**	**3.14**
OMe	COOH	**7.55**	**8.82**	**8.21**	**8.12**
OMe	CN	**3.36**	**6.69**	**4.43**	**5.64**
OMe	NO_2	**4.76**	**5.95**	**5.36**	**3.27**

For the systems without substituents in *para*-position, dipole moment changes of 3.6 D to 6.0 D were calculated (Table 6). The obtained changes are still rather small. However, for the *para*-unsubstituted systems with strong electron-withdrawing substituent in *ortho*-position, the calculations show a high disparity of the dipole moment of 7.1–9.9 D for most of the isomers.

Table 6: Differences in dipole moments between the merocyanine isomers and the corresponding spiropyran for systems with no substituent in *para*-position and various substituents in *ortho*-position. The differences of the dipole moments are colour-coded as follows: $\Delta D_{SP\text{-}MC}$ < 3 D (red), 3–7 D (yellow), 7–10 D (green), > 10 D (blue).

Para	*Ortho*	TTC	TTT	CTT	CTC
H	NMe_2	**3.55**	**4.27**	**3.62**	**3.88**
H	OMe	**4.76**	**5.95**	**5.36**	**3.27**
H	H	**4.53**	**5.98**	**5.23**	**5.09**
H	Br	**5.76**	**7.17**	**6.46**	**6.34**
H	COOH	**9.13**	**8.67**	**9.86**	**9.65**
H	CN	**6.43**	**8.21**	**7.48**	**7.08**
H	NO_2	**7.45**	**8.60**	**8.39**	**7.41**

A similar pattern emerges when considering the *para*-bromo substituted systems, although the differences are slightly more pronounced (Table 7). Of particular interest are the systems that incorporate a nitro group (8.3–9.6 D) or a carboxylic acid (11.0–11.8 D) in the *ortho*-position.

Table 7: Differences in dipole moments between the merocyanine isomers and the corresponding spiropyran for systems with bromo-substituent in *para*-position and various substituents in *ortho*-position. The differences of the dipole moments are colour-coded as follows: $\Delta D_{SP\text{-}MC}$ < 3 D (red), 3–7 D (yellow), 7–10 D (green), > 10 D (blue).

Para	*Ortho*	TTC	TTT	CTT	CTC
Br	NMe_2	**4.76**	**4.10**	**4.04**	**4.53**
Br	OMe	**5.69**	**5.13**	**5.07**	**3.21**
Br	H	**6.00**	**6.33**	**5.96**	**6.10**
Br	Br	**7.01**	**7.57**	**7.12**	**7.25**
Br	COOH	**11.01**	**11.75**	**11.38**	**11.38**
Br	CN	**7.57**	**8.77**	**8.24**	**8.03**
Br	NO_2	**8.55**	**9.59**	**9.12**	**8.31**

For the systems with strongly electron-withdrawing substituents (NO_2, CN and COOH) in *para*-position, the difference of the dipole moments for the systems with electron-withdrawing or no substituents in *ortho*-position are below 7.0 D for the majority of the calculations (Table 8 and Table 9). The systems with only nitril- or nitro-substituents, or a combination of both, show high changes in dipole moments between 9.1 D and 10.1 D (Table 8). This is due to the electron-withdrawing substituents on the phenol unit redistributing the electron density from the already electron-deficient indole unit to the phenolate. Consequently, the zwitterionic character of the merocyanine is increased. For the systems with a nitrile- or a nitro-group in *para*-position and a carboxylic acid in *ortho*-position even higher changes of 13.0–13.7 D obtained.

Table 8: Differences in dipole moments between the merocyanine isomers and the corresponding spiropyran for systems with nitril- and nitro-substituents in *para*-position and various substituents in *ortho*-position. The differences of the dipole moments are colour-coded as follows: $\Delta D_{SP\text{-}MC}$ < 3 D (red), 3–7 D (yellow), 7–10 D (green), > 10 D (blue).

Para	***Ortho***	**TTC**	**TTT**	**CTT**	**CTC**
CN	NMe_2	**5.18**	**3.49**	**3.82**	**4.65**
CN	OMe	**5.92**	**4.46**	**4.76**	**3.02**
CN	H	**6.27**	**5.36**	**5.46**	**6.01**
CN	Br	**7.67**	**7.13**	**7.12**	**7.56**
CN	COOH	**13.12**	**13.12**	**12.99**	**13.21**
CN	CN	**9.13**	**9.41**	**9.19**	**9.27**
CN	NO_2	**9.22**	**9.50**	**9.22**	**9.39**
NO_2	NMe_2	**5.91**	**4.18**	**4.54**	**5.37**
NO_2	OMe	**6.99**	**3.43**	**3.61**	**4.31**
NO_2	H	**7.01**	**6.06**	**6.18**	**6.71**
NO_2	Br	**8.35**	**7.77**	**7.79**	**8.19**
NO_2	COOH	**13.58**	**13.60**	**13.48**	**13.68**
NO_2	CN	**9.71**	**9.99**	**9.80**	**9.77**
NO_2	NO_2	**9.75**	**10.08**	**9.83**	**9.97**

However, considering the systems with electron-withdrawing substituents in both, *ortho*- and *para*-position, the calculations for those with a carboxylic acid on *para*-position show rather unexpected results (Table 9). In these cases, the calculated changes in the dipole moment between the SP and MC form vary strongly depending on the MC isomer considered. The overall changes observed for the system with two carboxylic acid substituents remain high, however the differences are significantly reduced when considering the TTC- and TTT-isomers (9.8 D and 9.7 D), in comparison to the CTC and CTT-isomers (13.4 D and 13.2 D). The systems including a nitro- or nitrile-group in *ortho*-position show very low changes for the TTC-isomer (4.8 D and 4.6 D) and relatively high changes regarding the TTT-isomer (8.4 D and 8.2 D).

Table 9: Differences in dipole moments between the merocyanine isomers and the corresponding spiropyran for systems with carboxylic acid-substituent in *para*-position and various substituents in *ortho*-position. The differences of the dipole moments are colour-coded as follows: $\Delta D_{SP\text{-}MC}$ < 3 D (red), 3–7 D (yellow), 7–10 D (green), > 10 D (blue).

Para	***Ortho***	**TTC**	**TTT**	**CTT**	**CTC**
COOH	NMe_2	**1.86**	**3.34**	**2.38**	**3.63**
COOH	OMe	**2.75**	**2.75**	**3.27**	**2.56**
COOH	H	**5.07**	**7.33**	**3.89**	**3.33**
COOH	Br	**3.56**	**6.46**	**4.00**	**6.08**
COOH	COOH	**9.79**	**9.73**	**13.41**	**13.20**
COOH	CN	**4.57**	**8.23**	**5.25**	**7.41**
COOH	NO_2	**4.82**	**8.43**	**5.86**	**5.86**

Since predictions about the isomer ratio of MC (TTC/TTT/CTT/CTC) in solutions are difficult to make, only systems in which all four forms have a comparable dipole moment were considered for the application. Even though the dipole moment changes for acid substituted derivatives were overall very high, these derivatives were ultimately ruled out due to the difficulty in estimating the effects of acid/base interactions. Due to this and considering the accessibility, the system **19** with two nitro-substituents and the systems **9** and **10** with one nitro- and one bromo-substituent were chosen as the most promising candidates for our purpose (Scheme 29).

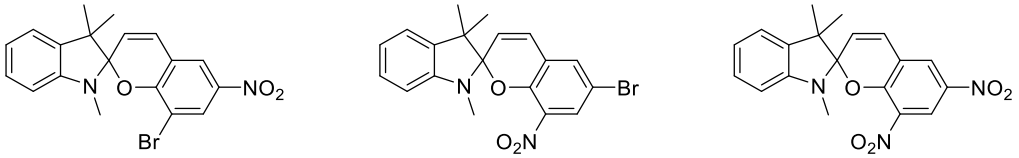

10
ΔSP–MC = 7.8–8.4 D

9
ΔSP–MC = 8.3–9.6 D

19
ΔSP–MC = 9.8–10.1 D

Scheme 29: The structures of the three substitute patterns which are promising for our purpose. Minimal and maximal changes of the dipole moment are stated below the structures.

Finally, the influence of substituents on the indole unit was investigated. Therefore, seven different substituents were considered (Scheme 30). Regarding the chromene moiety, only the substitution pattern of system **10** (Scheme 28) was tested.

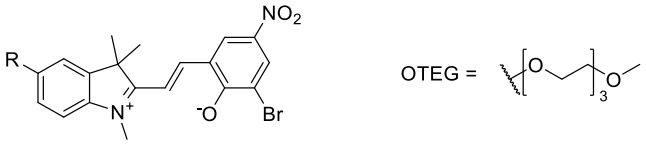

R = NMe_3^+, NO_2, COOH, H, Br, OMe, OTEG, NMe_2

Scheme 30: Overview indole substituted spiropyran and merocyanine derivatives included in the DFT calculations.

As depicted in Table 10, additional electron-donating substituents like ethers (OMe and OTEG) or amines highly increase the difference in dipole moment for all MC-isomers since in these cases, a push-pull system is created which shifts more electron density towards the phenolate unit. This further increases the zwitterionic character. The resulting change in dipole moment is between 10.9 D and 11.6 D in the dimethylamine-substituted system. Conversely, electron-withdrawing substituents, such as carboxylic acid or nitro groups, pull electron density towards the electron-deficient indole moiety, thereby reducing the zwitterionic character.

Therefore, very low changes in dipole moment (1.6–3.4 D) were calculated for the system containing a carboxylic acid at the indole unit. For the nitro-substituted system the dipole moments of the CTT- and CTC-isomers were even smaller than the one calculated for the corresponding spiropyran.

Table 10: Differences in dipole moments between the merocyanine isomers and the corresponding spiropyran for indole substituted systems. The differences of the dipole moments are colour-coded as follows: $\Delta D_{SP\text{-}MC}$ < 3 D (red), 3–7 D (yellow), 7–10 D (green), >10 D (blue).

Indole Sub.	TTC	TTT	CTT	CTC
NMe_3^+	**10.15**	**13.47**	**14.49**	**14.45**
NO_2	**0.85**	**0.61**	**–0.67**	**–0.05**
COOH	**3.40**	**3.17**	**1.62**	**2.26**
H	**8.35**	**7.77**	**7.79**	**8.19**
Br	**8.68**	**8.15**	**7.92**	**8.38**
OMe	**9.53**	**8.89**	**8.54**	**8.98**
OTEG	**9.69**	**8.56**	**8.56**	**9.14**
NMe_2	**11.60**	**10.94**	**11.01**	**11.41**

For the system containing a trimethylammonium-group at the indole, also high changes of the dipole moment were calculated ranging from 10.1–14.5 D. The absence of a mesomeric effect and the presence of a negative inductive effect result in a slight electron-withdrawing effect. However, this effect is completely ruled out by the additional positive charge, which leads to a high charge separation in the merocyanine form. Moreover, dipole moments for this system are typically high in comparison to other systems, due to the aforementioned charge. The dipole moments for the merocyanine-isomers range from 34.4–38.7 D, while one of 24.3 D was calculated for the spiropyran. The calculated dipole moments for all isomers can be found in the appendix.

Based on these calculations, systems with electron-donating groups like ethers or amines are most promising for the desired application of influencing other molecules via polarity changes.

4.2 Synthesis of Spiropyrans and Merocyanines

4.2.1 Synthesis of *N*-Substituted Spiropyrans and Merocyanines

The synthesis of the *N*-substituted indolium salts **22**, **23** and **24** was achieved by refluxing indole **25** with the corresponding reagents **26–28**, based on the procedures provided by Y. Zhang et al.[115], A. R. Tyler et al. [116] and D. E. Lynch et al.[117] In all cases even with a high excess of the corresponding alkylation agent and increased reaction times of several days, full conversion of indole **25** was never achieved. Since full conversion was not achieved, unfortunately only moderate yields of 46–61 % were achieved (Scheme 31).

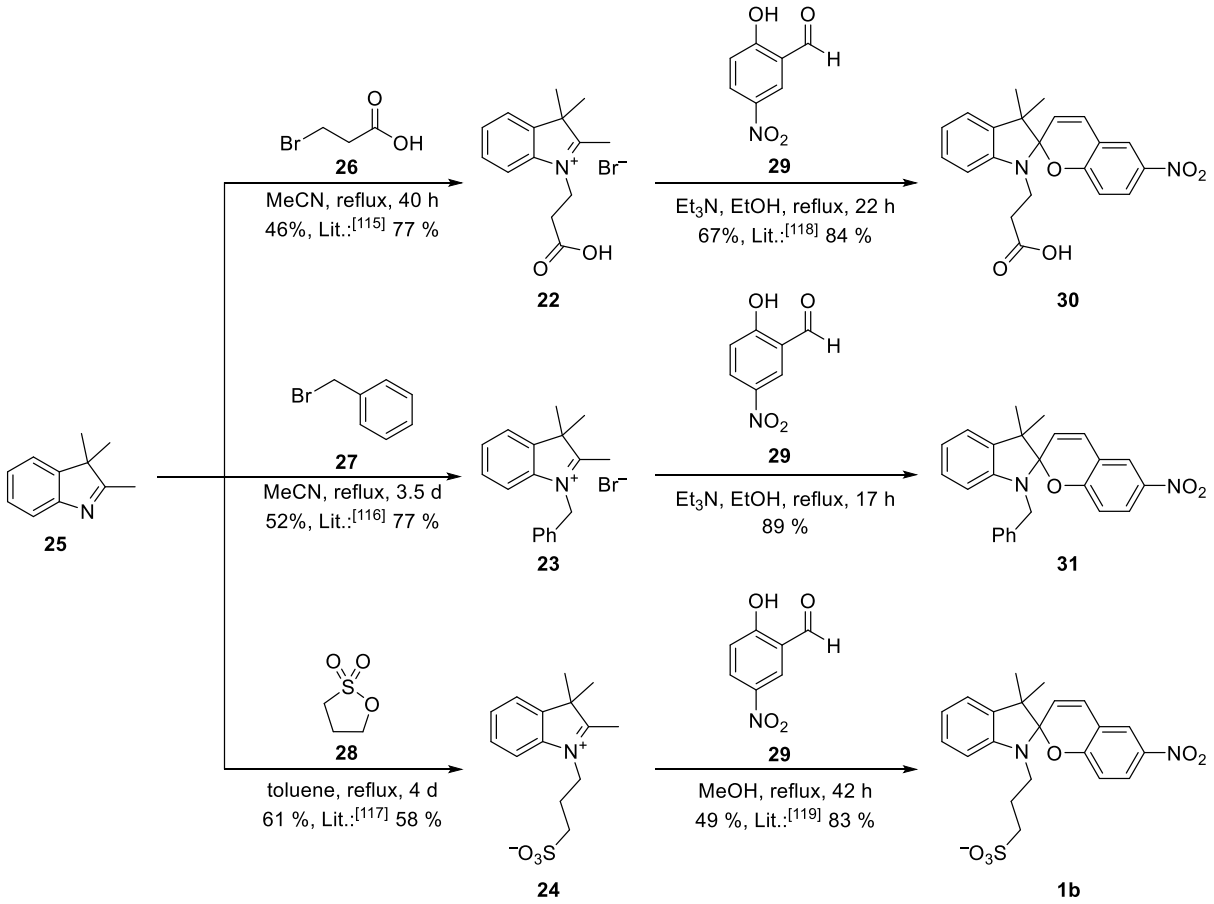

***Scheme 31*:** Synthetic scheme for the synthesis of *N*-substituted spiropyrans **30**, **31** and **1b** starting from indole **25**.

The obtained indolium salts were used in a condensation reaction with 2-hydroxy-5-nitro benzaldehyde (**29**) to obtain the corresponding spiropyrans in moderate to good yields, following the protocols by W. Zhang et al.[118] and J. Liu et al.[119] In case of the spiropyrans **30** and **31** base was added to trap the bromide. The low yields are due to high product loss during the recrystallisation.

4.2.2 Synthesis of Chromene Substituted Spiropyrans and Merocyanines

For the synthesis of spiropyrans with different substituted chromene moieties, two different methods were used. For the synthesis of **8**, **9** and **32**, indolium **33** was refluxed with the appropriate salicylic aldehyde (**34**, **35** and **36)** to obtain the corresponding merocyanine hydro iodide-salts **37**, **38** and **39** (Scheme 32). The salts were transformed to the free spiropyrans by adding Et_3N. For both steps good to excellent yields were obtained. In case of spiropyran **32** the corresponding salt **36** was not isolated.

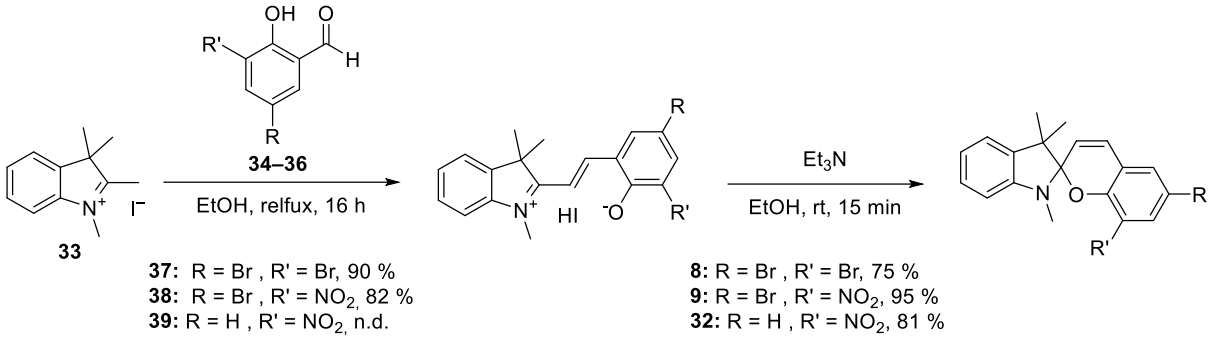

***Scheme 32*:** Results of the two-step synthesis of Spiropyrans **8**, **9** and **32** starting from indolium **33**.

Based on a modified procedure by Roxburgh et al.[120] spiropyrans **7**, **9**, **19**, **40** and **41** were synthesised in one step from Fisher-Base **43** instead of indolium **33** (Scheme 33). Therefore, no base was needed to remove HI. The spiropyrans were obtained in yields between 66 % and 93 % by refluxing Fisher-Base **43** with the corresponding salicylic aldehydes **44–47** and **29**.

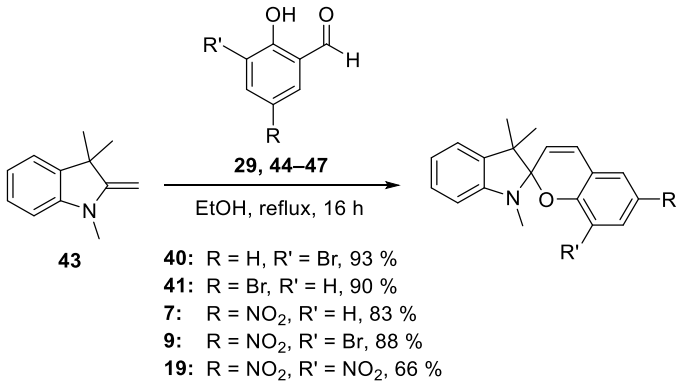

***Scheme 33*:** Results obtained by the one-step synthesis of spiropyrans **7**, **9**, **19**, **40** and **41**.

While the two-step approach resulted slightly lower yields the purification of the products was often easier than for those obtained by the one-step synthesis. Therefore, none of the methods is clearly preferable.

4.2.3 Synthesis of Indole Substituted Spiropyrans and Merocyanines

The synthesis of spiropyrans **48–51** was achieved over three steps. Starting from the corresponding phenyl hydrazine salts, a Fisher-Indole synthesis with isopropyl methyl ketone was performed following the procedures by H. Goa et al.[121] The substituted indoles **52–55** were obtained in yields between 66–98 % (Scheme 34). Methylation to the corresponding indolium salts **56–59** with iodomethane was performed in good to excellent yields. The condensation between the indolium salts and salicylic aldehyde **46** was achieved by heating in ethanol in the presence triethylamine. Since triethylamine was used to scavenge the released HI, the spiropyrans **48–51** were directly obtained instead of the corresponding HI-adducts as mentioned in the previous chapter.

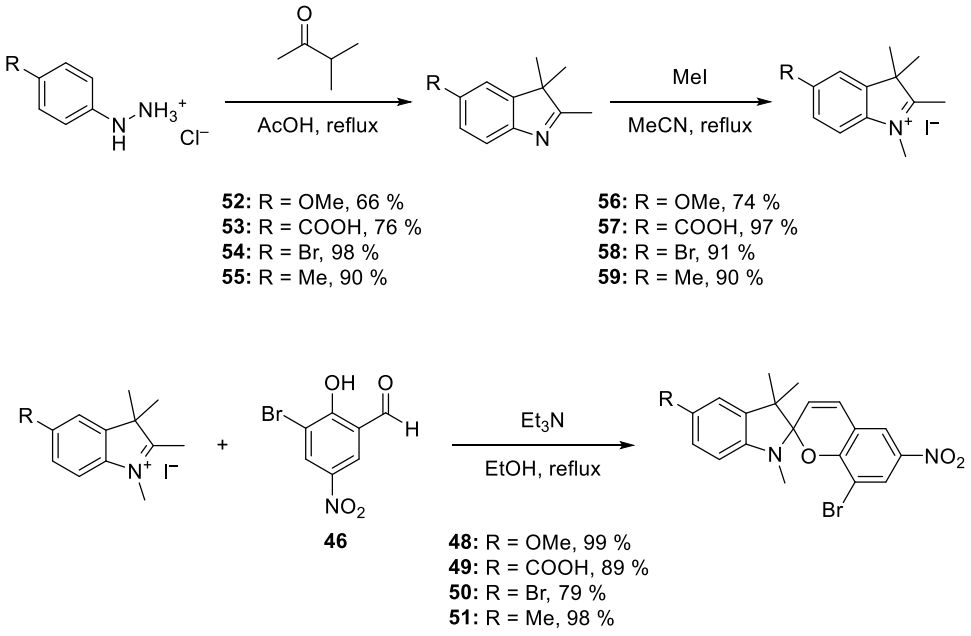

***Scheme 34*:** Synthesis of different indole substituted spiropyrans starting from substituted hydrazine salts.

Following the procedure by Kele and coworkers,[122] indole **60** was synthesised via nitration of indole **25** (Scheme 35). The yield of 87 % was slightly lower than reported in the literature.

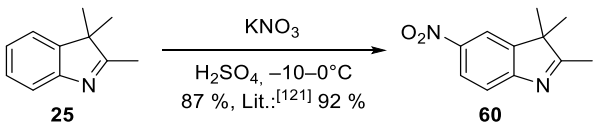

***Scheme 35*:** Nitration of indole **25**.

Nitro indole **60** was used as substrate for synthesis of spiropyran **61** and **62** (Scheme 36). For the synthesis of **61**, nitro indole was first methylated to indolium **63**

in 91 % yield following a procedure by Berizin et al.[123] The final condensation to the spiropyran **61** was achieved in 85 % yield.

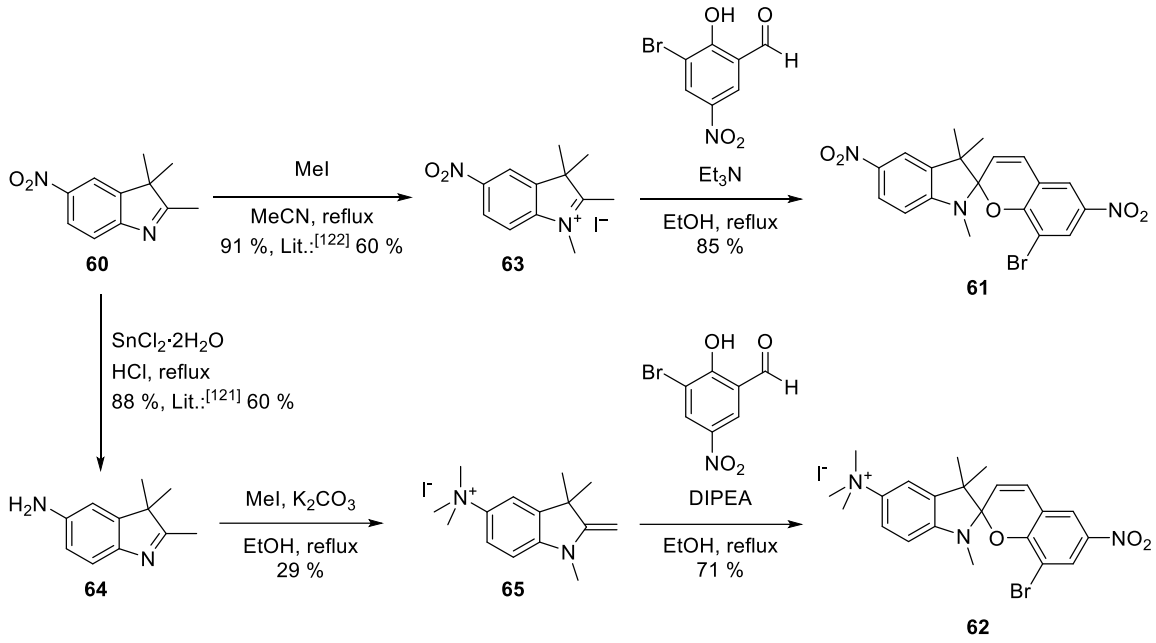

Scheme 36: Synthesis of Spiropyran **61** (top) and **62** (bottom) starting from nitro indole **60**.

In order to synthesize the compound spiropyran **62** (Scheme 36, bottom), nitro indole **60** was first reduced with tin chloride, following the procedure described by Kele and colleagues.[122] The resulting amino indole **64** was then methylated with iodomethane, after which it underwent condensation with the previously synthesized spiropyran **62** to yield the final product. While most products were obtained in good yields, the methylation of amino indole **64** was rather challenging. After refluxing the reaction for 18 h with over stoichiometric amounts iodomethane, several spots were observed by TLC. Via GC-MS analysis manly the methylated indoles **66** and **67** and traces of **65** were observed (Scheme 37). Therefore, additional iodomethane was added and the reaction was heated for further 20 h. Since **66** and **67** were still the mayor species, the reaction was heated again with additional iodomethane. After refluxing for in total 44 h, the reaction was stopped since an additional species was forming which was identified as indole **68** by a crude ^{1}H-NMR. After column chromatography, only spiropyran **65** could be isolated in a moderate yield of 29 %.

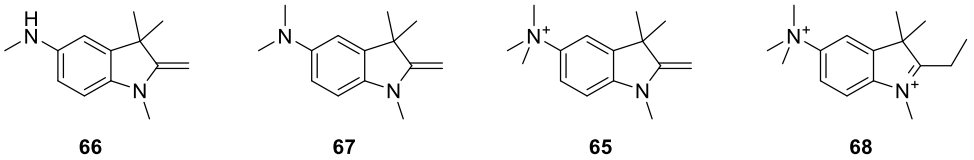

***Scheme 37*:** Different indoles which were observed during the methylation of indole **64**.

The synthesis of spiropyran **69** with a triethylene glycol (TEG) moiety at the indole was achieved over four steps starting from methoxy substituted indole **52** (Scheme 38). The methoxy group was deprotected to the free alcohol **70** in 88 % using BBr_3. The alcohol was then converted to the ethylene glycol ether **71** using tosylate **72**. This was done under basic conditions to increase the reactivity of the alcohol to avoid the substitution of the indole nitrogen. After methylation with iodomethane, indolium iodide **73** was obtained in quantitative yield. The condensation to the spiropyran **69** was also achieved in a good yield of 85 %.

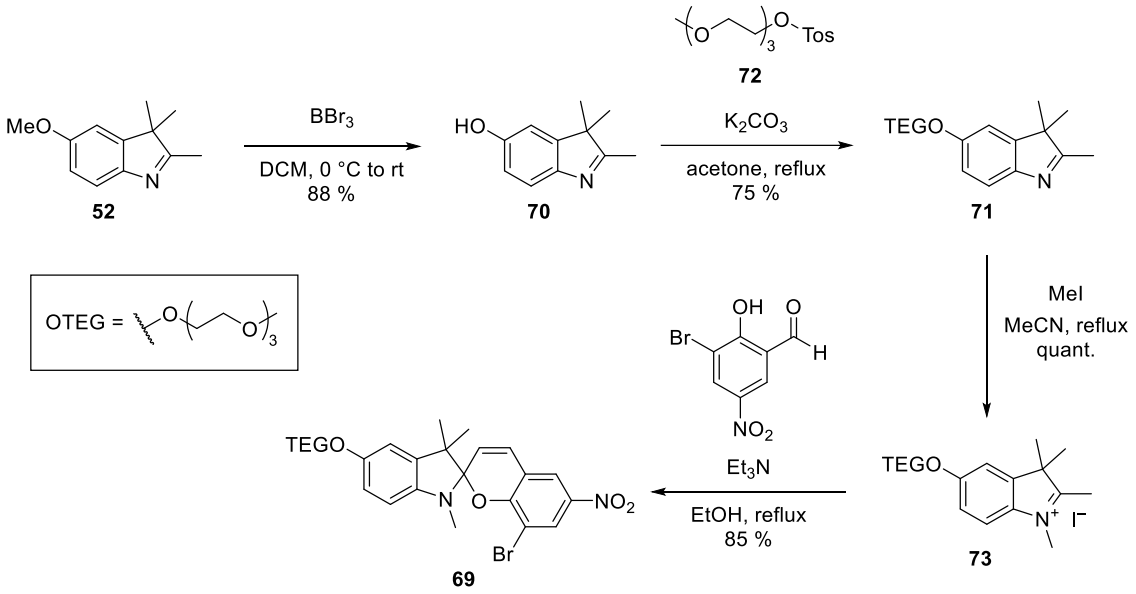

Scheme 38: Four step synthesis towards triethylen glycol substituted spiropyran **69** starting from indole **52**.

4.2.4 Synthesis of Spiropyrans with Substituents at the Geminal Methyl Groups

For the synthesis of spiropyran **74**, ketone **75** should be used in the Fischer-indole synthesis. This ketone was synthesised over six steps starting from benzophenone (**76**) (Scheme 39).

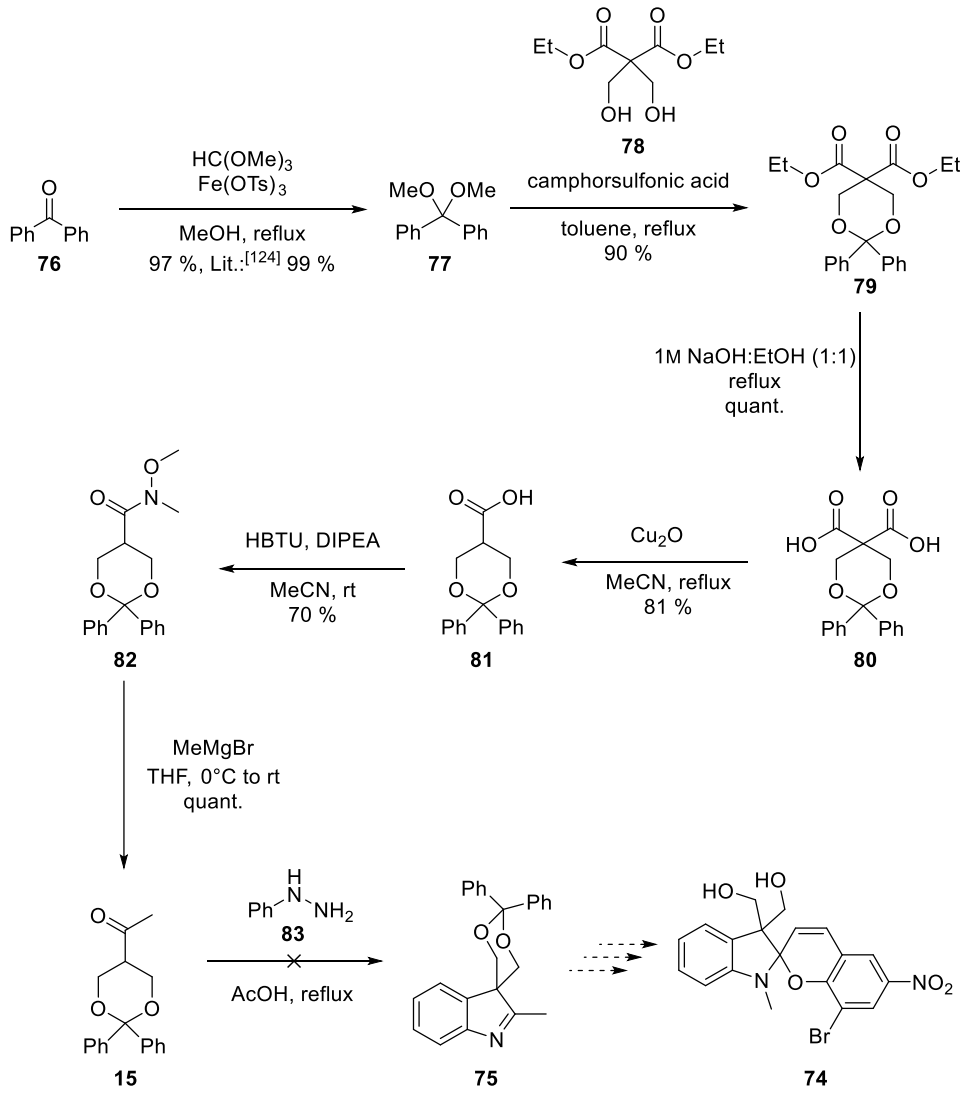

Scheme 39: Synthesis of ketone **75** as key intermediate for the synthesis of **74**.

According to a procedure reported by H. Mansilla and M. Alfonso[124], dimethylketal **77** was synthesised using iron(III)tosylate as catalyst. The dimethylketal was then used to protect diol **78** to obtain dioxane **79**. After saponification, the dicarboxylic acid **80** was decarboxylated according to a procedure by J. Ehrler and D. Seebach[125] using Cu_2O. The monocarboxylic acid **81** was then transferred to the Weinreb-amide **82** using HBTU and DIPEA. By treating the Weinreb-amide **82** with MeMgBr,

ketone **75** was obtained. All synthesis steps were performed in good to quantitative yields.

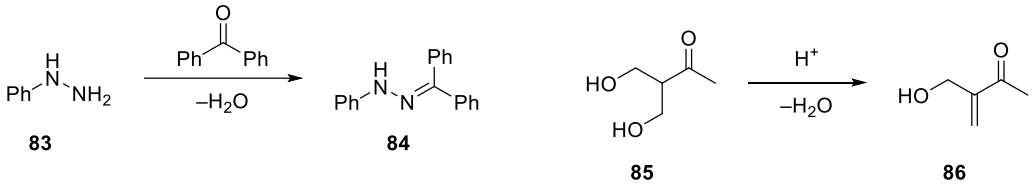

83 **84** **85** **86**

***Scheme 40**:* Possible by-products and side reactions of the indole synthesis after cleavage of the acetal.

The Fisher Indole synthesis towards indole **75** did not yield the desired product. A complex mixture was obtained with no clear major product. Since the indole synthesis is typically performed under acidic conditions and high temperature, the acetal might be cleaved to the corresponding diol and benzophenone, which enables several side reactions (Scheme 40). The benzophenone could react with the hydrazine **83** forming hydrazone **84**. Under these harsh conditions the unprotected diol **85** is also likely to eliminate water hence forming a α,β-unsaturated ketone **86** which can further react.

Due to the synthetic problems and since the results of the DFT calculations of the dipole moments looked only moderately promising for our applications, the synthesis of spiropyran **74** was not further pursuit. If this molecule should be synthesised for other applications, the use of more stable protection groups like bulky silyls (e.g. DIPS) or ethers should be considered.

For the synthesis of spiropyran **87**, a synthesis starting from nipecotic acid (**88**) was pursued (Scheme 41). After protecting the amine, the corresponding carboxylic acid **89** was transferred to the Weinreb amide **90** using HBTU as amide coupling agent. According to H. Ito and co-workers,[126] the Weinreb amide **90** was transferred to ketone **91** using MeMgBr. The Fischer-indole synthesis of indole **92** using ketone **91** and phenyl hydrazine (**83**) was not successful due to the acid lability of the Boc-protecting group, which enables a considerable amount of side reactions. This could be avoided by using acid stable protecting groups like Fmoc or Cbz.

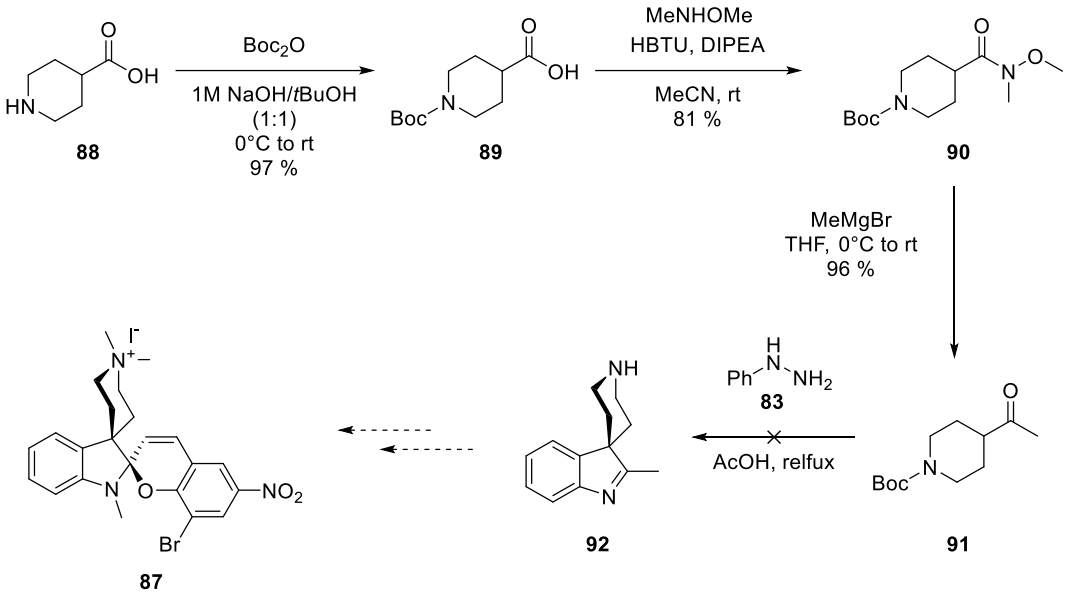

Scheme 41: Overview of the synthesis of ketone **91** as key intermediate in the synthesis of spiropyran **87**.

Another alternative to avoid this side reaction, is the controlled deprotection with subsequent methylation of the amine to the piperidinium salt **93** (Scheme 42).

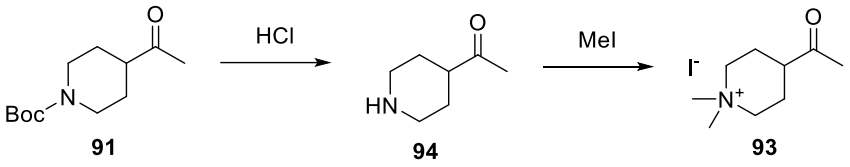

Scheme 42: Synthesis plan for piperidinium salt **14** as acid stable alternative for the Fischer-indole synthesis.

The Fisher-indole synthesis with ammonium salt **93** was tested by C. Weißelberg during his E-Module. However, the desired indole could not be isolated. Since the DFT calculation for the dipole moments final spiropyran and merocyanine were not promising for our desired applications, the synthesis of spiropyran **87** was not further pursuit.

4.3 UV/Vis Analysis of Substituted Spiropyrans and Merocyanines

4.3.1 Influence of Chromene Substituents on the UV/Vis-Spectra of Spiropyrans and Merocyanines

In the following, the UV/Vis spectra of spiropyrans and merocyanines with different bromine and nitro substitution patterns at the chromene part of the system are compared. All spectra were obtained from 0.025 mM methanolic solutions at 20 °C. Three spectra were recorded for the system. Once at a thermal equilibrium in the dark (blue) and the other after irradiation with UV (red) or visible light (green).

The UV/Vis-spectra of the SP/MC system **7** are shown in Scheme 43. The spectra obtained after irradiation with visible light and after incubation in the dark are almost identical. In both cases primarily the spiropyran from is present and only traces of the merocyanine can be observed indicated by the small absorption at λ = 529 nm. The spiropyran exhibits four absorption bands with λ = 339 nm, 298 nm, 266 nm and 242 nm. After irradiation with UV light the absorption maxima at 266 nm and 242 nm are reduced in intensity (hypochromic shift) while the characteristic merocyanine band at λ = 529 nm is significantly increased (hyperchromic shift). The maxima at 339 nm and 298 nm are shifted in the higher wavelength region (bathochromic) to 352 nm and 307 nm respectively.

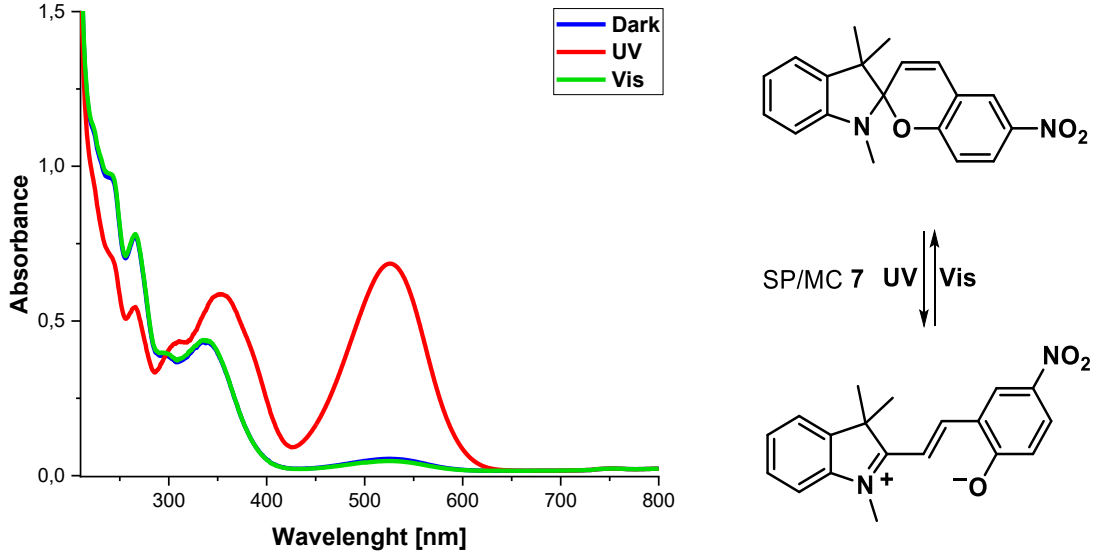

Scheme 43: UV/Vis-spectra of SP/MC **7** at the thermal equilibrium in the dark (blue) and after irradiation with UV (red) or visible (green) light. All spectra were recorded in 0.025 mM methanolic solutions at 20 °C.

Since the spectrum obtained at the thermal equilibrium is almost identical with the one obtained after irradiation with visible light, the spiropyran form is highly favoured

for this system. However, even after irradiation with visible light, traces of the merocyanine absorption at 529 nm was detected.

The UV/Vis spectrum of the SP/MC system **9** with an additional bromine substitution in *ortho*-position also shows an incomplete cyclisation after irradiation with visible light (Scheme 44). For the spiropyran three absorption maxima with λ = 330 nm, 272 nm and 243 nm can be determined. After irradiation with UV light two defined maxima at 523 nm and 365 nm can be detected for the merocyanine. Also, several smaller absorptions can be detected between 200–300 nm. These absorptions are strongly hypochromic shifted compared to those of the spiropyran.

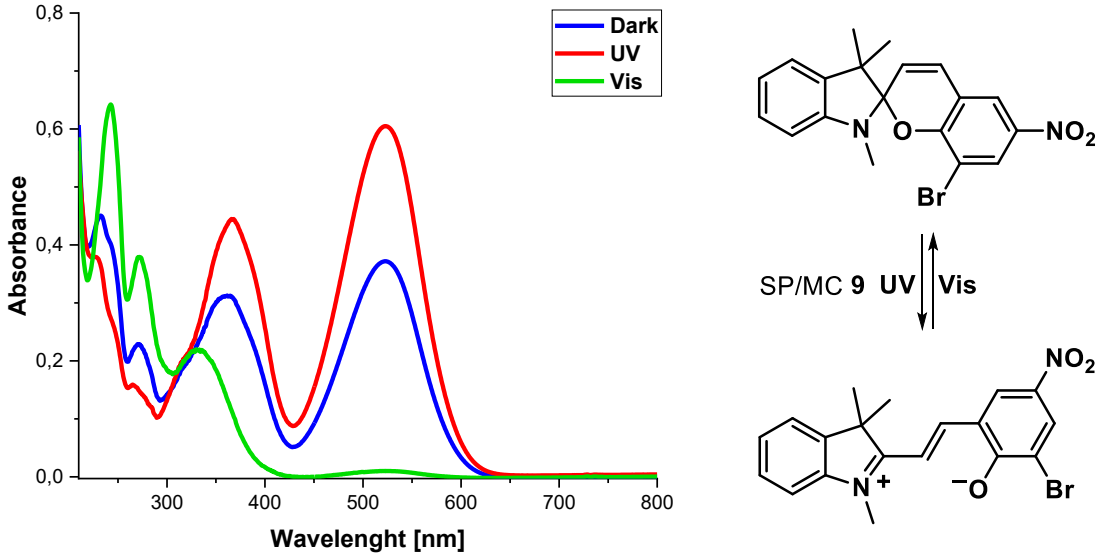

Scheme 44: UV/Vis-spectra of SP/MC **9** at the thermal equilibrium in the dark (blue) and after irradiation with UV (red) or visible (green) light. All spectra were recorded in 0.025 mM methanolic solutions at 20 °C.

The UV/Vis spectrum which was recorded after incubation in the dark resembles the spectrum obtained after irradiation with UV light. This indicates a shift of the equilibrium towards the merocyanine induced by the additional bromine substituent.

For system **32** with the nitro group in *ortho*-position three absorption maxima with λ = 353 nm, 281 nm and 245 nm are detected for the spiropyran (Scheme 45, green). Upon irradiation with UV light an absorption maximum at 543 nm is observed for the merocyanine. Again, the maxima below 300 nm are decreased in intensity, while the intensity of the absorption at 353 nm is increased and bathochromic shift to 364 nm upon formation of the merocyanine. At the equilibrium in the dark, the UV/Vis spectrum is almost identical with spectrum of the spiropyran between 200–300 nm but clearly shows the absorption of the merocyanine at higher wavelength.

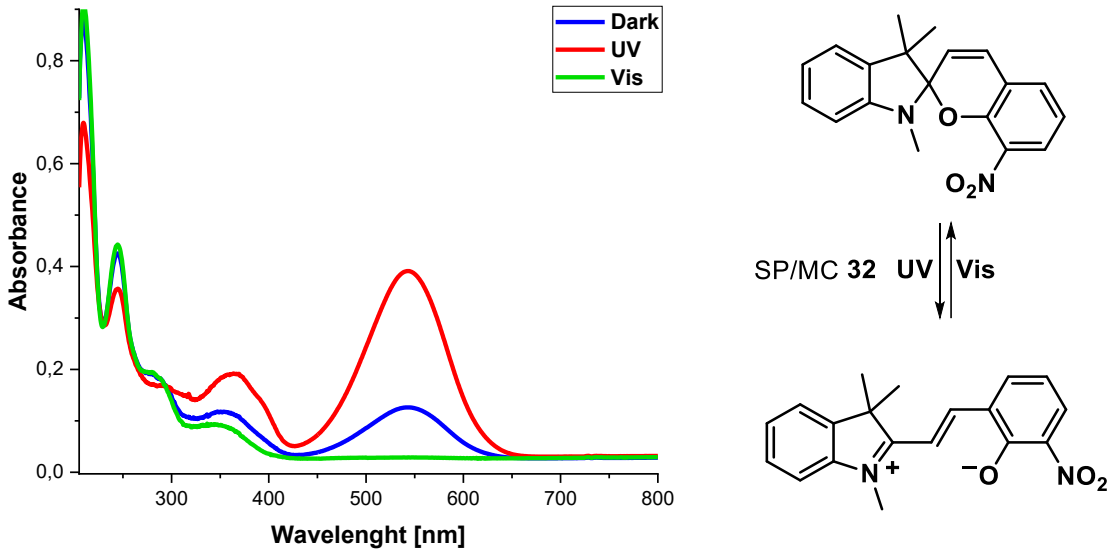

Scheme 45: UV/Vis-spectra of SP/MC **32** at the thermal equilibrium in the dark (blue) and after irradiation with UV (red) or visible (green) light. All spectra were recorded in 0.025 mM methanolic solutions at 20 °C.

The addition of a bromine substituent in *para*-position of system **10** shifts the equilibrium further towards the merocyanine (Scheme 46, blue). Therefore, the UV/Vis-spectra of **10** recorded in the dark and after irradiation with UV light are similar. For the merocyanine, two absorptions, with λ = 554 nm and 365 nm are observed while for the corresponding spiropyran an absorption maximum at 361 nm is detected. For both forms the absorptions between 200–300 nm are not well defined. As with system **32**, complete cyclisation to spiropyran can be observed for system **10** after irradiation with visible light.

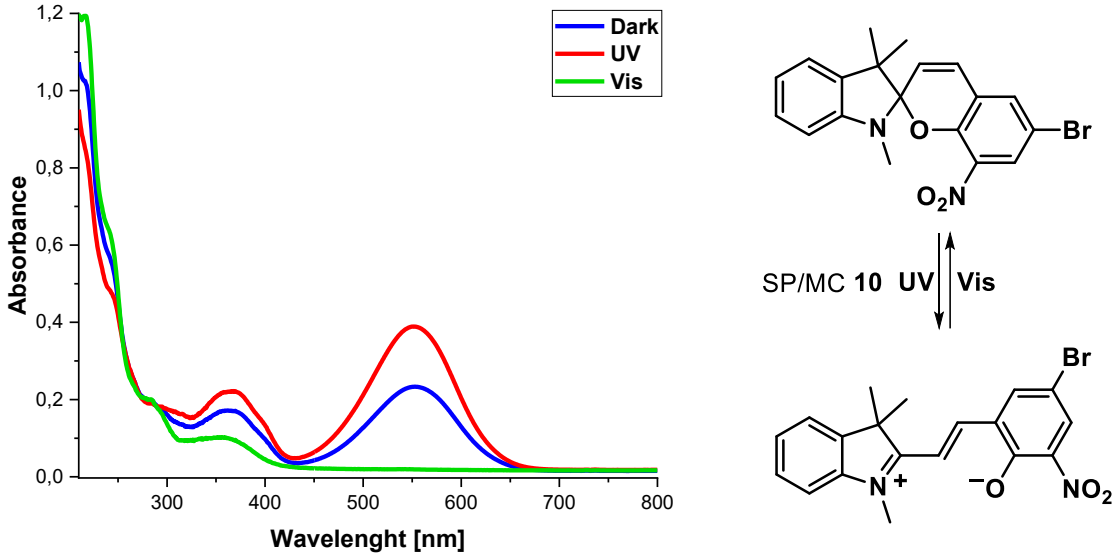

Scheme 46: UV/Vis-spectra of SP/MC **10** at the thermal equilibrium in the dark (blue) and after irradiation with UV (red) or visible (green) light. All spectra were recorded in 0.025 mM methanolic solutions at 20 °C.

Quantitative cyclisation was also observed for spiropyran **19** with two nitro substituents after irradiation with visible light (Scheme 47, green). The spiropyran has two absorptions in the UV region with λ = 339 nm and 255 nm. The corresponding merocyanine exhibits strong absorption maxima at 507 nm, 378 nm and 360 nm, as well as two weaker absorptions at 302 nm and 363 nm.

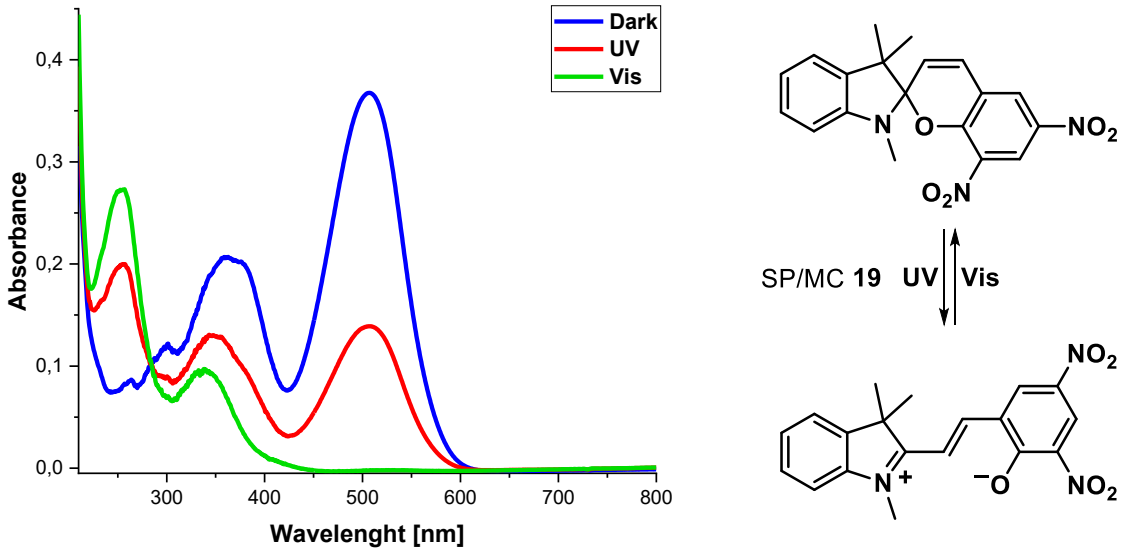

Scheme 47: UV/Vis-spectra of SP/MC **19** at the thermal equilibrium in the dark (blue) and after irradiation with UV (red) or visible (green) light. All spectra were recorded in 0.025 mM methanolic solutions at 20 °C.

It should be emphasised that for this system the absorption of merocyanine obtained after incubation in the dark exceeds the absorption after excitation with UV light. On one hand this shows a high stabilisation of the merocyanine based on the electron withdrawing character of the nitro groups. On the other hand, this leads to the assumption that exposure to UV light can also induce the cyclisation to a small extent. This is probably due to the superposition of the absorption bands of both species in the UV range.

For the SP/MC system **8** with two bromine substituents the spectrum after irradiation with UV light and the spectrum after incubation in the dark are identical (Scheme 48). In both cases only the spiropyran is present. In total four absorption bands can be observed for the spiropyran with λ = 326 nm, 296 nm, 240 nm and 232 nm. After irradiation with UV light two additional absorption maxima of the merocyanine at 566 nm and 384 nm are detected. However, for this system the equilibrium is highly shifted towards the spiropyran and only small amounts of merocyanine are formed upon irradiation with UV light. Additionally, decomposition of the system is observed after irradiation with UV light for few minutes (Scheme 48, orange). This

decomposition can be identified by the appearance of a new absorption maximum at 451 nm and the significant hypochromic shift of the absorptions between 200–300 nm.

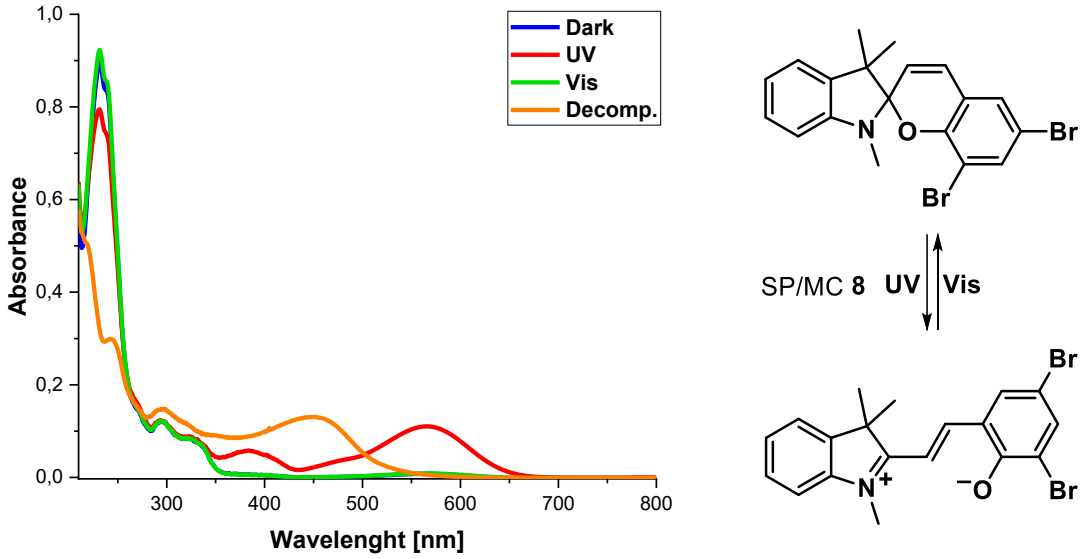

Scheme 48: UV/Vis-spectra of SP/MC **8** at the thermal equilibrium in the dark (blue) and after irradiation with UV (red) or visible (green) light. Decomposition (orange) was observed after longer exposure to UV light. All spectra were recorded in 0.025 mM methanolic solutions at 20 °C.

In summary, for all systems a hypochromic shift of the absorption maxima between 200–300 nm can be observed upon formation of the merocyanine while for all nitro substituted system the maximum at around 350 nm is increased in intensity (hyperchromic shit) and bathochromic shifted. Comparing the absorption maxima of the different substituted merocyanines a trend can be observed (Scheme 49).

With increasing electron withdrawing substituents at the phenolate moiety the absorption maximum in the visible region of the spectra is hypsochromic shifted. For merocyanine **7** with only a nitro group in *para*-position the absorption maximum was found at 543 nm. By adding a bromine or a nitro group in *ortho*-position the maximum is shifted to 523 nm and 507 nm respectively. By replacing the nitro group with two bromine substituents the absorption maximum is bathochromic shifted to 566 nm. Comparing the maxima of merocyanine **7** (λ = 529 nm) and **32** (λ = 543 nm) the nitro substituent in *ortho*-position has a lesser impact on the electron density of the system which can be addressed to steric effects between the ortho-substituents.

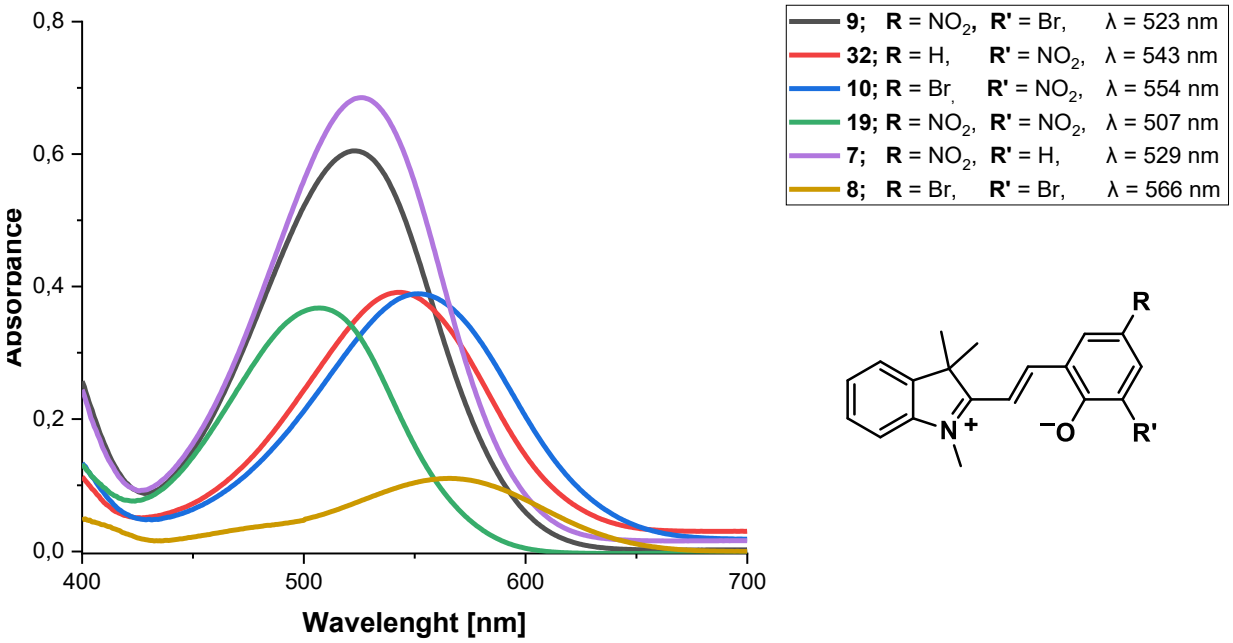

Scheme 49: Comparison of the characteristic absorption maxima of chromene substituted merocyanines. All spectra were recorded in 0.025 mM methanolic solutions at 20 °C. For each system the spectrum with the strongest merocyanine absorption is shown.

4.3.2 Influence of Chromene Substituents on the UV/Vis-Spectra of Spiropyrans and Merocyanines

In the following, the UV/Vis spectra of spiropyrans and merocyanines with different substituents at the indole part of the system are compared. For all systems the chromene substituents were kept the same. All spectra were obtained from 0.025 mM methanolic solutions at 20 °C. Three spectra were recorded for every system. One at thermal equilibrium in the dark (blue) and one each after irradiation with UV (red) and visible light (green). As reference the spiropyran/merocyanine system **9** with a nitro group at the *para*-position and a bromine substituent in *ortho*-position was selected since it showed a good switchability between both forms. Additionally, for this system the thermal equilibrium in the dark was shifted towards the merocyanine. This is desirable for our applications since irradiation with Vis-light (MC→SP) is less destructive than irradiation with UC light (SP→MC).

In Scheme 50 the spectra obtained for SP/MC **51** with a methyl substituent at the indole are shown. The general forms of the spectra are very similar compared to those of system **9**. For the spiropyran four absorptions at λ = 334 nm, 307 nm,

273 nm, and 243 nm and four absorptions for the merocyanine at λ = 521 nm, 371 nm, 318 nm and 270 nm are detected.

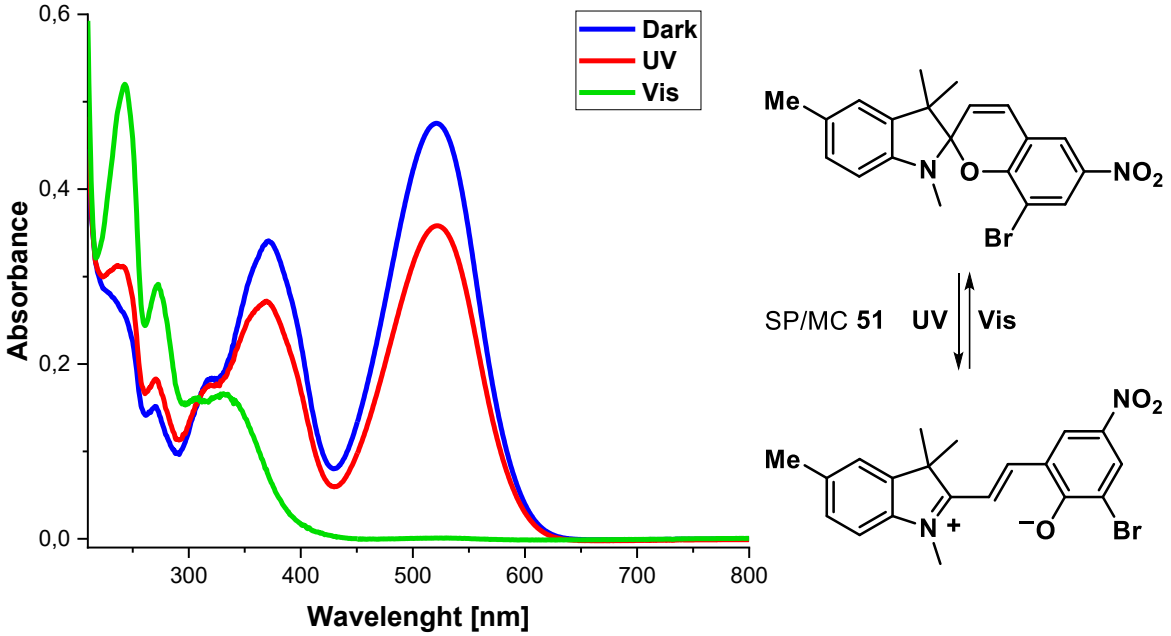

Scheme 50: UV/Vis-spectra of SP/MC **51** at the thermal equilibrium in the dark (blue) and after irradiation with UV (red) or visible (green) light. All spectra were recorded in 0.025 mM methanolic solutions at 20 °C.

The electron donating effect of the methyl group shifts the SP/MC equilibrium further towards the merocyanine. This results in a negative photochromism of this system. Therefore, the strongest absorbance of characteristic absorption band of the merocyanine at 521 nm was detected after incubation in the dark.

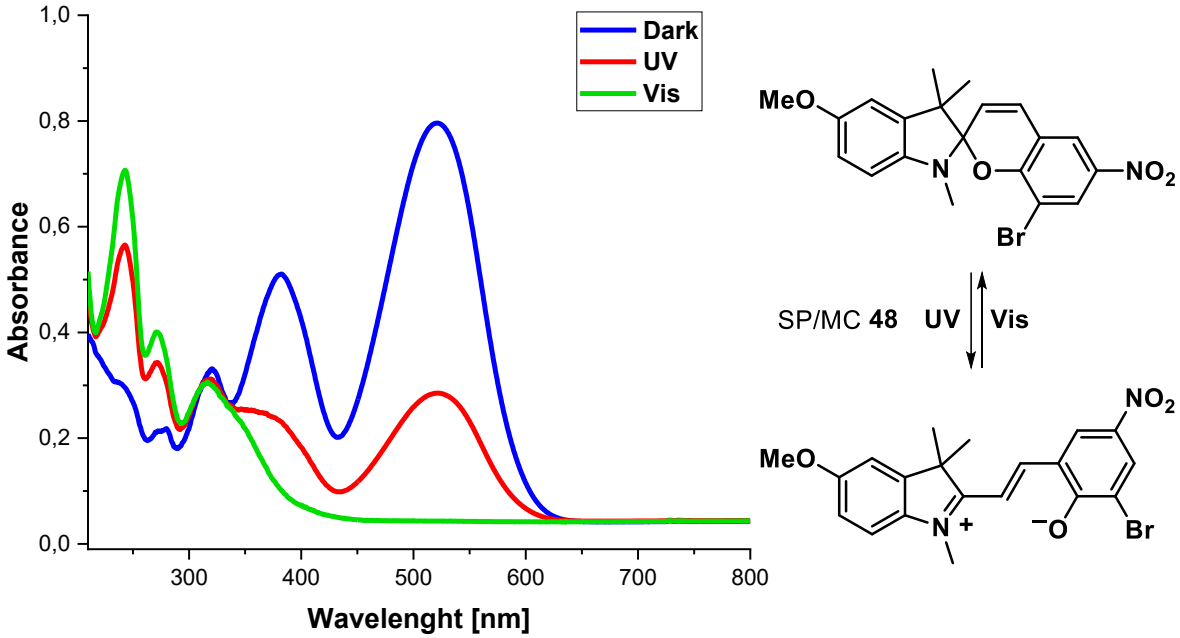

Scheme 51: UV/Vis-spectra of SP/MC **48** at the thermal equilibrium in the dark (blue) and after irradiation with UV (red) or visible (green) light. All spectra were recorded in 0.025 mM methanolic solutions at 20 °C.

The same trend can be seen for the methoxy substituted system **51**. In this instance, the differences are even more pronounced (Scheme 52). Once more, four absorptions were identified for the spiropyran (346 nm, 317 nm, 280 nm and 272 nm) and the merocyanine (521 nm, 382 nm, 280 nm and 272 nm).

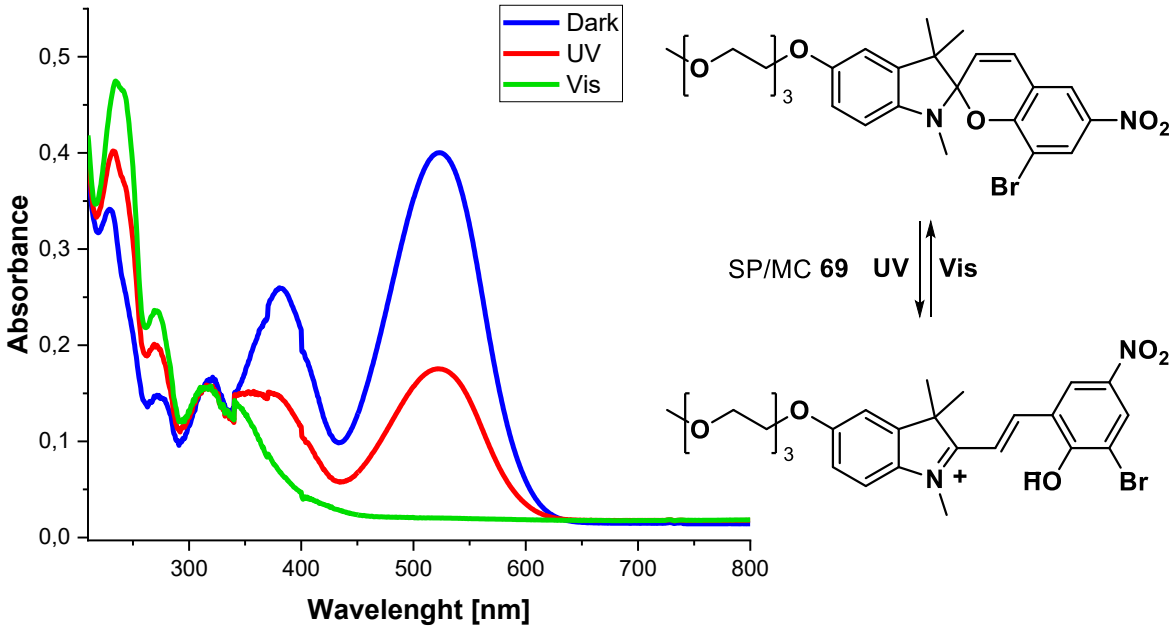

***Scheme 52*:** UV/Vis-spectra of SP/MC **48** at the thermal equilibrium in the dark (blue) and after irradiation with UV (red) or visible (green) light. All spectra were recorded in 0.025 mM methanolic solutions at 20 °C.

The spectra recorded for system **69** with a triethylen glycol ether substituent are almost identical to those of the methoxy substituted system **48**. The merocyanine shows five absorption bands at 521 nm, 382 nm, 321 nm, 377 nm and 230 nm (Scheme 52). The highest absorption of merocyanine was detected at the equilibrium in the dark. After irradiation with visible light, four absorptions with λ = 343 nm, 316 nm, 272 nm and 235 nm could be observed.

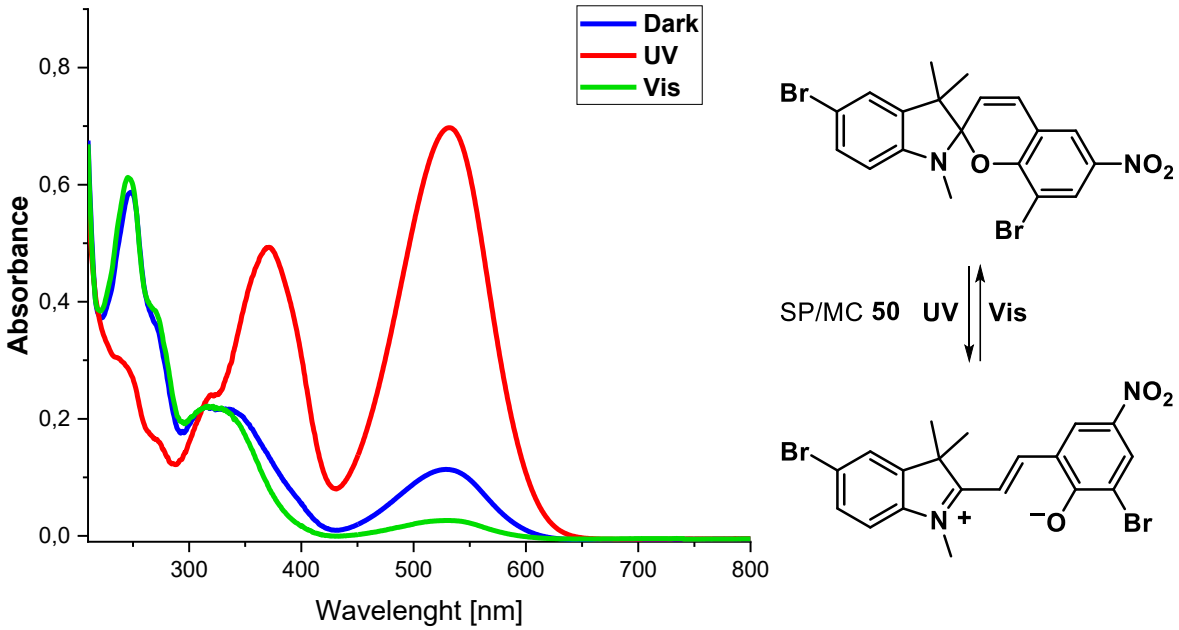

Scheme 53: UV/Vis-spectra of SP/MC **50** at the thermal equilibrium in the dark (blue) and after irradiation with UV (red) or visible (green) light. All spectra were recorded in 0.025 mM methanolic solutions at 20 °C.

While the stabilisation of the merocyanine was observed for the systems with electron donating substituents at the indole moiety the opposite can be observed for systems with electron withdrawing substituents. After irradiation with UV light, for merocyanine **50** two intense absorption with λ = 541 nm and 371 nm can be detected as well as three less defined absorption at 320 nm, 273 nm and 239 nm (Scheme 53). When exposed to visible light, the strong absorption at 541 nm disappears almost completely and the maximum at 371 nm is blue shifted to 335 nm and decreased in intensity (hypochromic shift). On the other hand, the absorptions between 200–300 nm undergo a hyperchromic shift. Due to the detection of a small absorbance at 541 nm after irradiation with visible light, indicates uncomplete cyclisation towards the spiropyran or a fast ring opening reaction. After incubation in the dark, the absorption at 541 nm is slightly increased in intensity. However, the spectrum recorded at the thermal equilibrium still highly resembles the spiropyran.

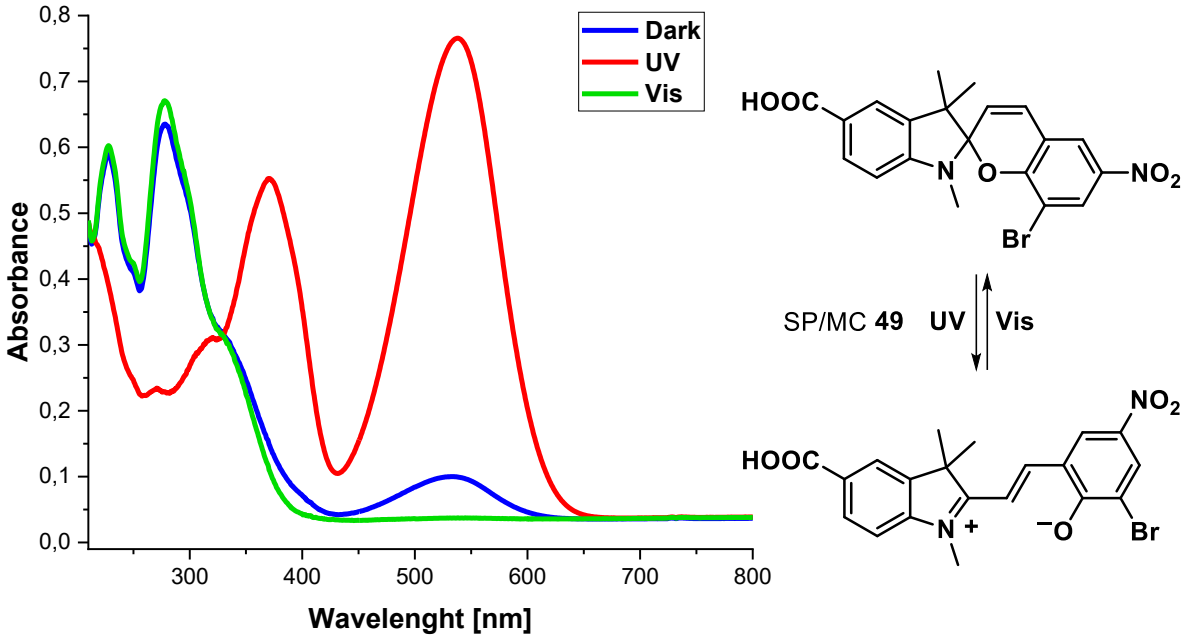

Scheme 54: UV/Vis-spectra of SP/MC **49** at the thermal equilibrium in the dark (blue) and after irradiation with UV (red) or visible (green) light. All spectra were recorded in 0.025 mM methanolic solutions at 20 °C.

Similar behaviour was observed for system **49** containing a carboxylic acid at the indole moiety (Scheme 54). After irradiation with UV light, two intense absorption maxima at 541 nm and 371 nm and two less defined maxima at 320 nm and 271 nm are detected. Upon cyclisation to the spiropyran (green) the absorptions at 541 nm and 371 nm disappear while two strong absorption bands at 230 nm and 271 nm are formed. After incubation in the dark, partial formation of the merocyanine was observed, indicated by a weak absorption at 541 nm.

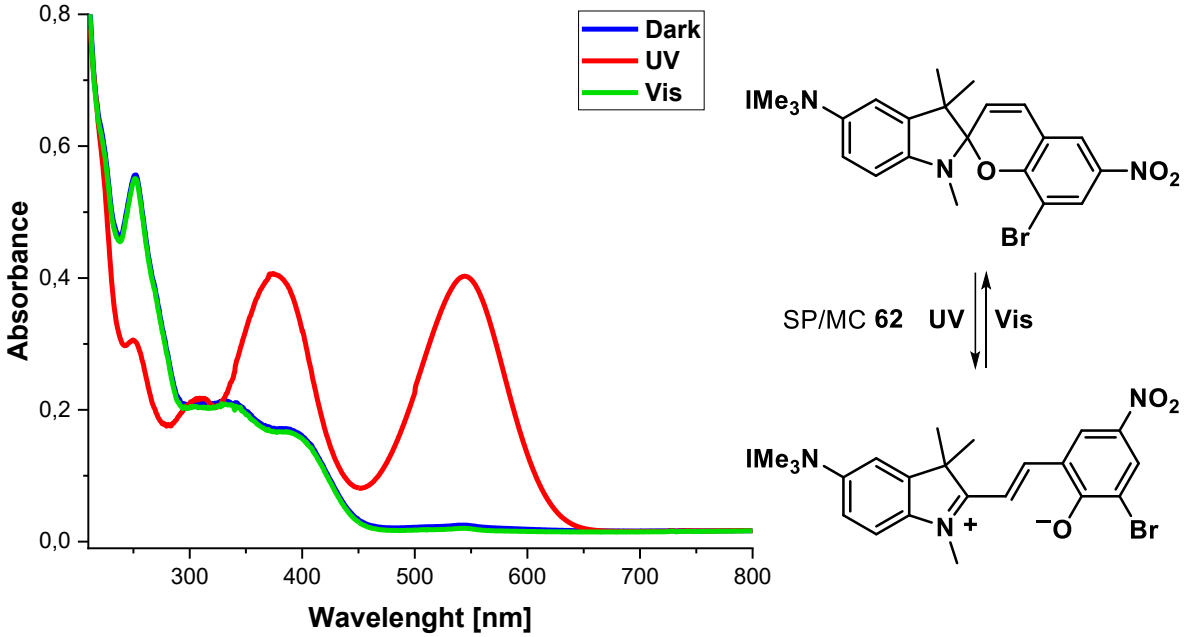

Scheme 55: UV/Vis-spectra of SP/MC **62** at the thermal equilibrium in the dark (blue) and after irradiation with UV (red) or visible (green) light. All spectra were recorded in 0.025 mM methanolic solutions at 20 °C.

When switching to even stronger electron donating withdrawing substituents (Scheme 55) the thermodynamic equilibrium is further shifted towards the cyclic spiropyran. This can be seen on the example of spiropyran **62** containing a trimethylammonium substituent. In this case the spectra recorded in the dark is almost identical with the one after irradiation was visible light. In both cases almost exclusively the spiropyran form is present. One defined absorption at 252 nm and two smaller absorptions at 336 nm and 388 nm can be assigned. Formation of the merocyanine leads to the formation of two strong maxima at 544 nm and 376 nm. The absorptions between 200–300 nm are decreased in intensity. Two absorptions with λ = 309 nm and 250 nm can be detected.

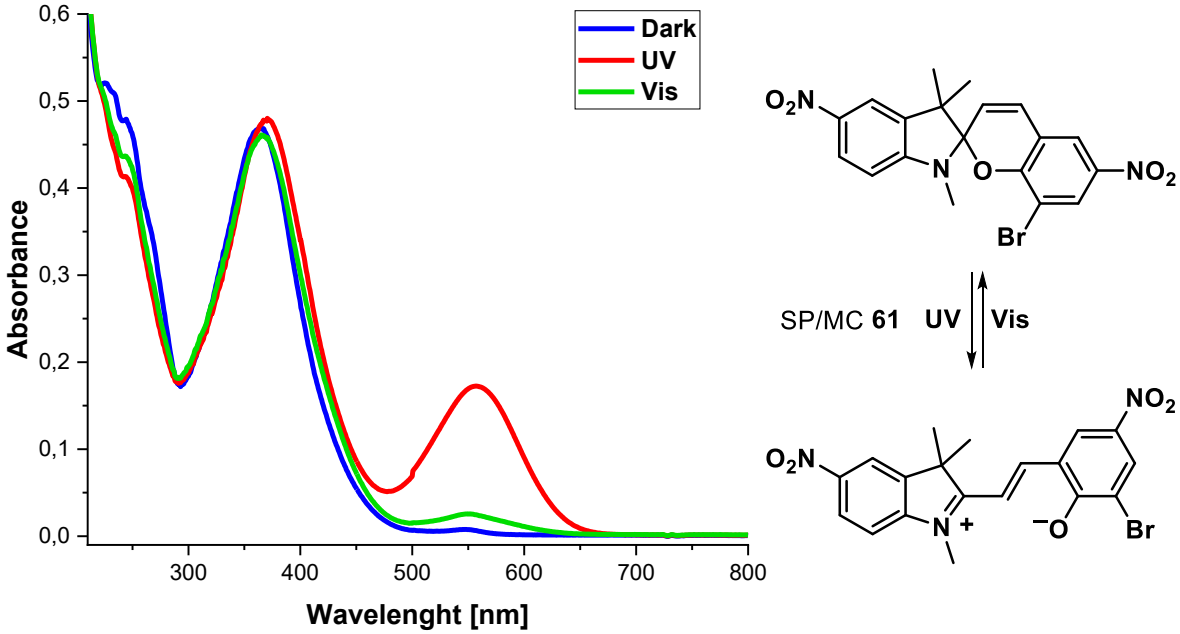

Scheme 56: UV/Vis-spectra of SP/MC **61** at the thermal equilibrium in the dark (blue) and after irradiation with UV (red) or visible (green) light. All spectra were recorded in 0.025 mM methanolic solutions at 20 °C.

In case of nitro substituted system **61**, the absorption bands in the UV region of the spectrum are very similar with two merging absorption maxima with λ = 246 nm and 226 nm and an intense absorption at 365 nm for the spiropyran and at 370 nm for the merocyanine (Scheme 56). Even after irradiation with UV light, only a weak absorption at 559 nm can be detected which indicates a highly disfavoured merocyanine due to the additional nitro group. In the dark and after exposure to visible light, only traces of merocyanine can be detected.

In summary, the following substituent-dependent trends can be recognised in the UV/Vis spectra. The most noticeable trend is concerning the equilibrium in the dark.

For the systems with electron donating substituents, the equilibrium is shifted towards the merocyanine form while electron withdrawing substituents shift the equilibrium towards the spiropyran. The substituents also affect the position of the absorption maxima (Scheme 57). For electron donating substituents the characteristic maximum of the spiropyran, is hypsochromic shifted from 523 nm (R = H) to 521 nm (R = OMe). On the other hand, electron withdrawing substituents induce a bathochromic shift up to 559 nm (R = NO_2). The absorption maximum around 370 nm is also bathochromic shifted. The absorption maximum at 370nm is bathochromic shifted by additional substituents regardless of the electronic properties. The same can be seen for the spiropyran absorption between 330–380 nm.

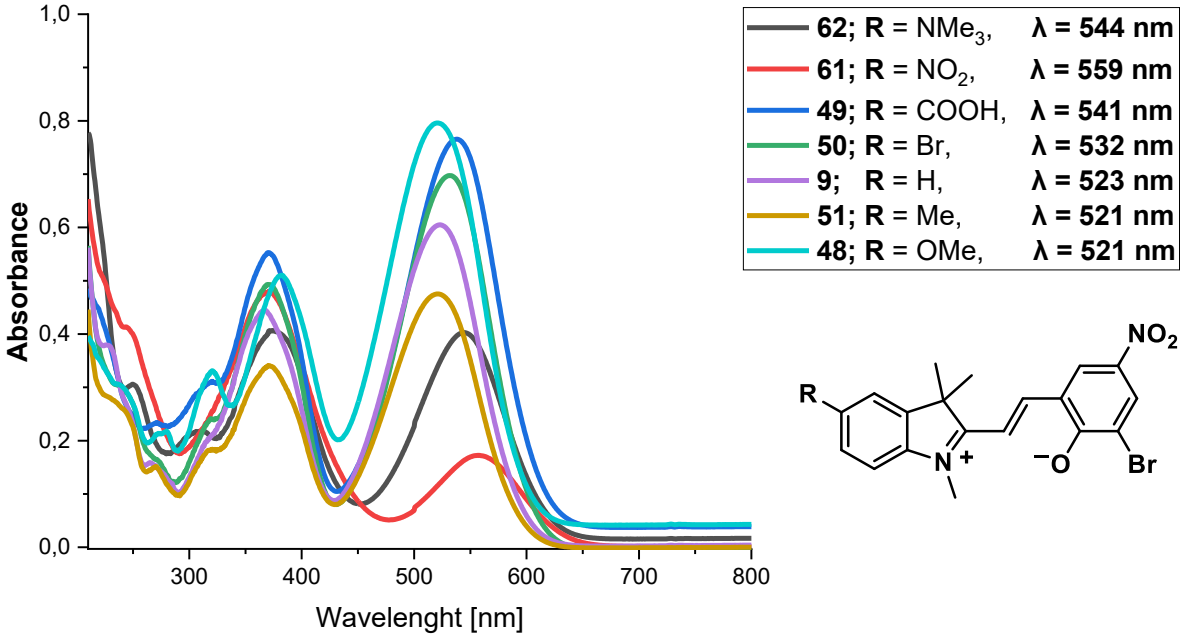

***Scheme 57*:** Comparison of the characteristic absorption maxima of chromene substituted merocyanines. All spectra were recorded in 0.025 mM methanolic solutions at 20 °C. For each system the spectrum with the strongest merocyanine absorption is shown.

4.3.3 General Information on the Kinetic Measurements

In the following chapter, the rate constants (k_{obs}) of the of the cyclisation (MC→SP, decolourisation) or the ring-opening reaction (SP→MC, colourisation) for substituted spiropyrans and merocyanines are compared. In order to observe the ring opening reaction, the sample was irradiated with UV light (254 nm) to maximise the concentration of merocyanine. The sample was then kept in the dark and the absorption spectrum was measured in regular intervals. Through this, the decrease in absorption in the visible range could be monitored over time. To investigate the ring-opening reaction, the sample was irradiated with visible light instead. The sample was again placed in the dark and the absorption spectrum was measured over time. Afterwards the increase in intensity of the π–π* absorption band between 520–560 nm was observed. All measurements were conducted using 0.025 mM methanolic solutions at 20 °C. These kinetic measurements were used to determine the rate constants for the different SP/MC systems using the following equations:

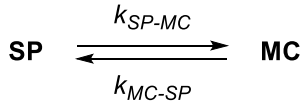

The observed rate constant can be described by the sum of the rate constants of the ring-opening reaction ($k_{SP–MC}$) and the cyclisation ($k_{MC–SP}$) (Equation (1)).[127]

$$k_{obs} = k_{SP-MC} + k_{MC-SP} \tag{1}$$

The cyclisation of the merocyanine and the ring opening reaction of the spiropyran are first order reactions.[43] Therefore, both reactions can be described by Equation (2), with [X] being the concentration of species X (SP or MC) at a given time and $[X]_0$ being the concentration of the same species at the beginning of the reaction.

$$[X] = [X]_0 e^{-kt} \tag{2}$$

Equation (2) can be rearranged to Equation (3).

$$k = -\frac{1}{t}\ln\left(\frac{[X]}{[X_0]}\right) \tag{3}$$

Utilising the relaxation method this can be written as follows:[127, 128]

$$k_{obs} = -\frac{1}{t}\ln\left(\frac{[X]_t - [X]_e}{[X]_i - [X]_e}\right) \tag{4}$$

Based on the Beer–Lambert law, concentration is proportional to absorption.

$$[X] \propto A \tag{5}$$

Equation (6) is obtained by combining Equation (4) and (5).

$$k_{obs} = -\frac{1}{t}\ln\left(\frac{A_t - A_e}{A_i - A_e}\right) \tag{6}$$

In Equation (6), A_e is defined as the absorption at the equilibrium and A_i is the initial absorption directly after the equilibrium is shifted by an external trigger. In case of the cyclisation, A_i is measured directly after the irradiation with UV light, while for the ring-opening reaction A_i is measured after irradiation with visible light. A_t is the absorption at a given time *t* after the initial irradiation. Rearrangement leads to Equation (7).

$$\ln\left(\frac{A_t - A_e}{A_i - A_e}\right) = -k_{obs}t \tag{7}$$

Utilising Equation (7), the rate constant $-k_{obs}$ be determined as the slope of the linear regression of the time plotted against the logarithmic absorption ratios. Unless otherwise stated, only the first data points up to a conversion of 30 % were used to determine the rate constant. For simplification in the following chapter k_{obs} is only written as *k.*

4.3.4 Influence of the Chromene Substituents onto the Reaction Kinetics

In Scheme 58, the kinetic UV/Vis measurements for the cyclisation of merocyanine **7** to the corresponding spiropyran are shown. After irradiation with UV light (254 nm), the sample was kept in the dark while the absorbance of the merocyanine at 523 nm was measured until the equilibrium between merocyanine and spiropyran was reached (Scheme 58, left). Utilizing equation (10), the exponential curve can be converted to a linear plot with the negative rate constant (–*k*) as slope (Scheme 58, right). Using this method, a rate constant of $k = 1.085 \times 10^{-4}$ s^{-1} was determined for the cyclisation of merocyanine **7**.

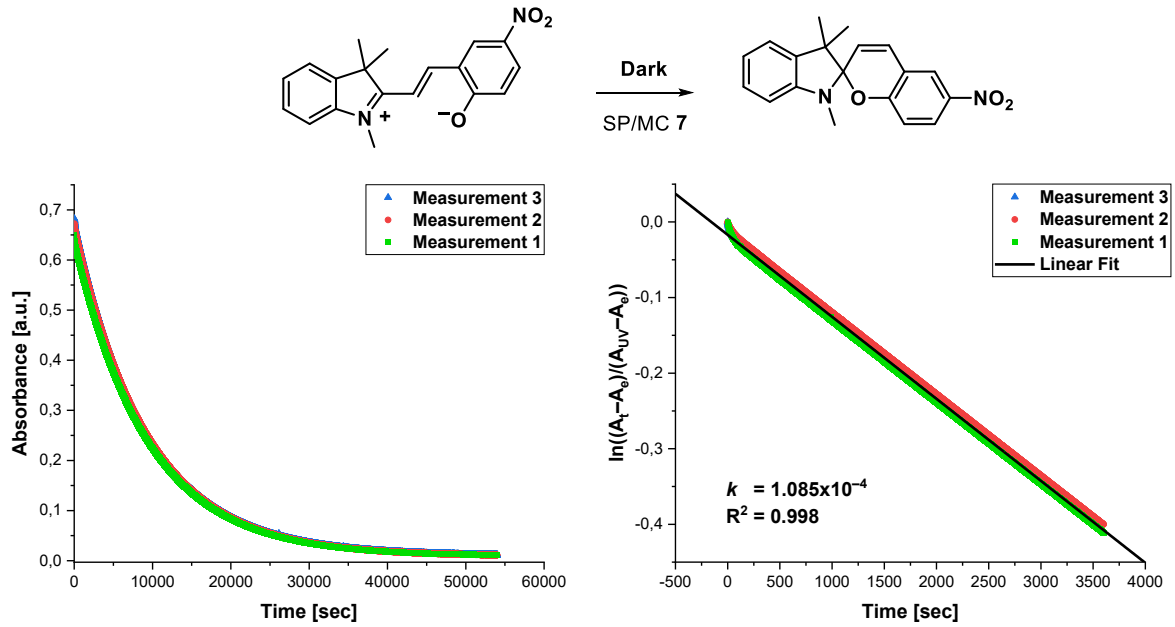

Scheme 58: Kinetics for the cyclisation of the merocyanine **7** to the corresponding spiropyran. Plot of the absorbance at the absorption maximum (529 nm) of the merocyanine against time (left) and logarithmic plot of the first 30 % conversion to determine the rate constant (right). All measurements were repeated three times and conducted with 0.025 mM methanolic solutions at 20 °C.

For merocyanine **32** the cyclisation to the spiropyran was monitored as well. The equilibrium was reached at an absorbance of 0.15 a.u. (Scheme 59, left). A rate constant of k = 5.202 x 10^{-4} s^{-1} was determined.

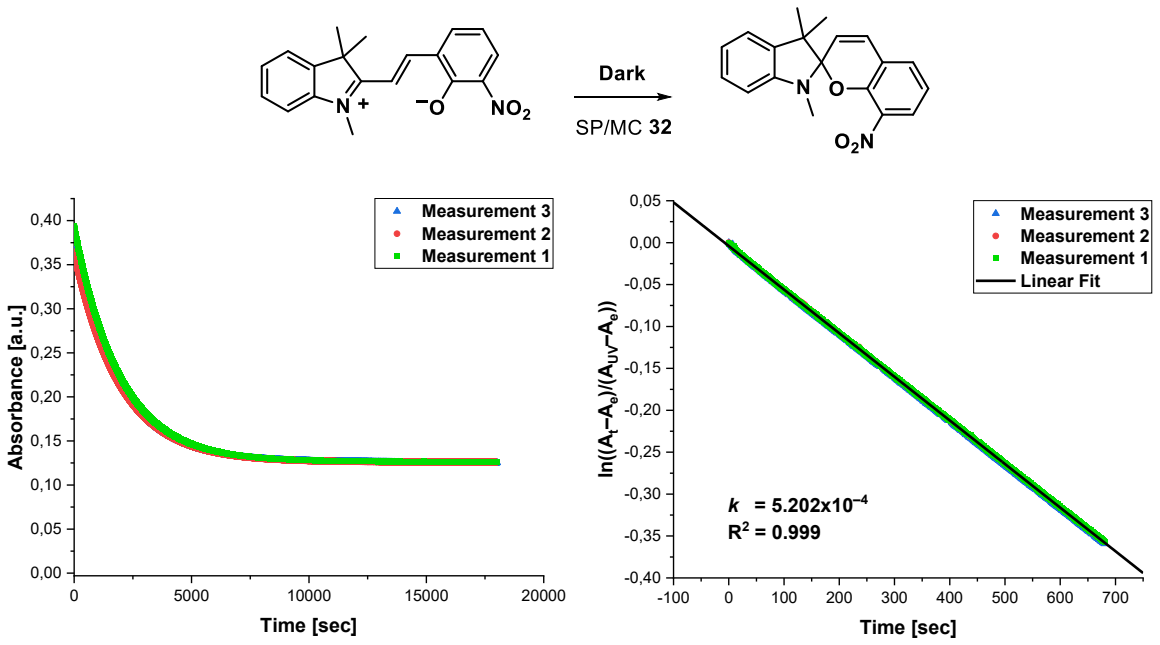

Scheme 59: Kinetics for the cyclisation of the merocyanine **32** to the corresponding spiropyran. Plot of the absorbance at the absorption maximum (543 nm) of the merocyanine against time (left) and logarithmic plot of the first 30 % conversion to determine the rate constant (right). All measurements were repeated three times and conducted with 0.025 mM methanolic solutions at 20 °C.

In the case of system **9**, in which the nitro group in the *para*-position is supplemented with a bromine substituent in the *ortho*-position, the equilibrium is shifted towards the merocyanine. Therefore, the kinetics of the ring opening reaction of the spiropyran to the merocyanine were monitored (Scheme 60). The obtained rate constant of k = 2.670 x 10^{-5} s^{-1} is approximately a fourth of than for system **7**.

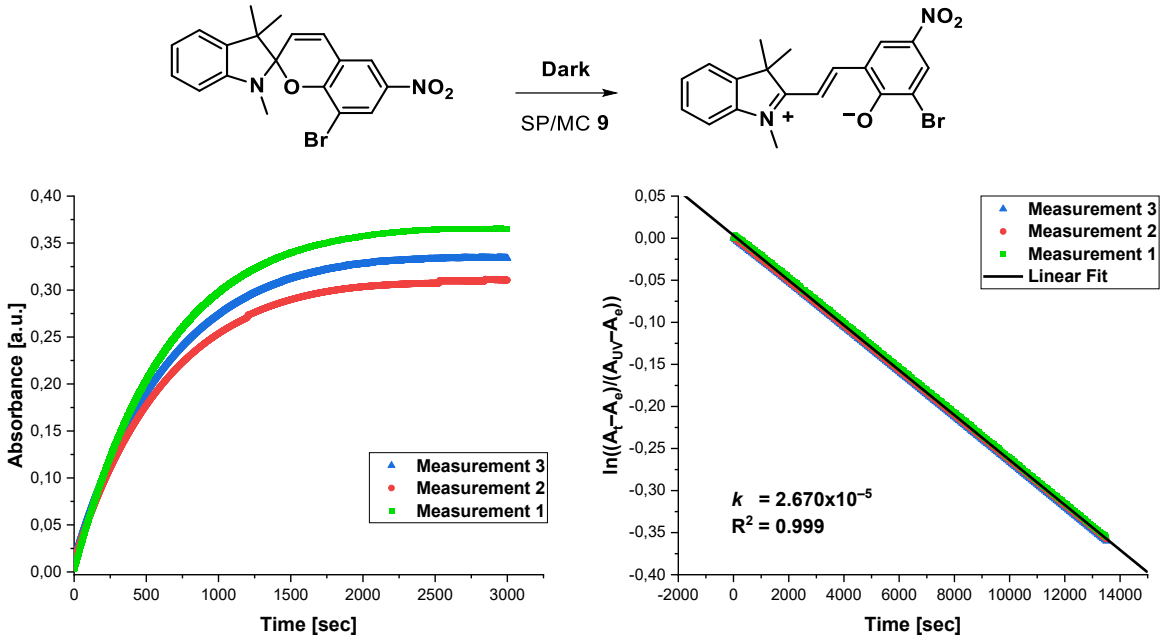

***Scheme 60*:** Kinetics for the ring opening reaction of spiropyran **9** to the corresponding merocyanine. Plot of the absorbance at the absorption maximum (523 nm) of the merocyanine against time (left) and logarithmic plot of the first 30 % conversion to determine the rate constant (right). All measurements were repeated three times and conducted with 0.025 mM methanolic solutions at 20 °C.

For system **10**, where the position of the bromine substituent and the nitro group are switched, a rate constant of k = 8.288 x 10^{-5} s^{-1} can be observed (Scheme 61). This is noticeably lower than the rate constant determined for the inverted system **9** (k = 2.670 x 10^{-5} s^{-1}).

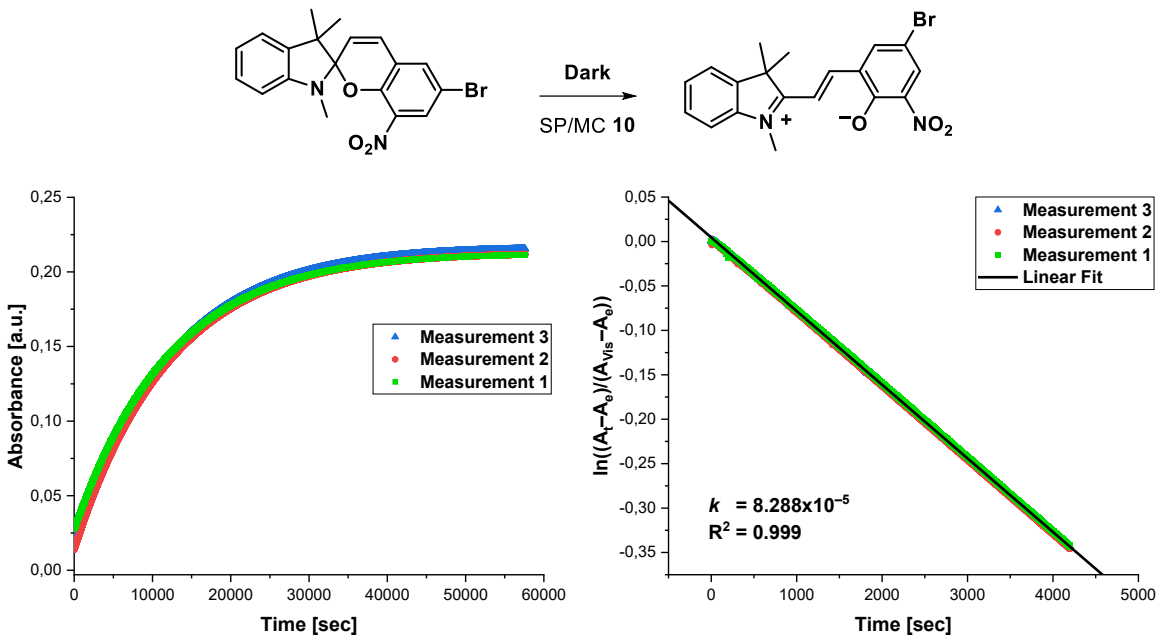

***Scheme 61*:** Kinetics for the ring opening reaction of spiropyran **10** to the corresponding merocyanine. Plot of the absorbance at the absorption maximum (554 nm) of the merocyanine against time (left) and logarithmic plot of the first 30 % conversion to determine the rate constant (right). All measurements were repeated three times and conducted with 0.025 mM methanolic solutions at 20 °C.

For compound **19**, solubility problems were encountered during the kinetic measurements. In addition, a none-linear phase at the start of the ring opening reaction was observed in the logarithmic plot (Scheme 62). This could be related to the solubility problems, but further investigations would be necessary to determine this. However, in order to minimise the influence of this non-linear initial phase, in this case the data points up to a turnover of 60 % were used to determine the rate constant (Scheme 60). The graph of the commonly used 30 % turnover can be found in the appendix. With this additional data, a rate constant of k = 1.503 x 10^{-5} s^{-1} was determined.

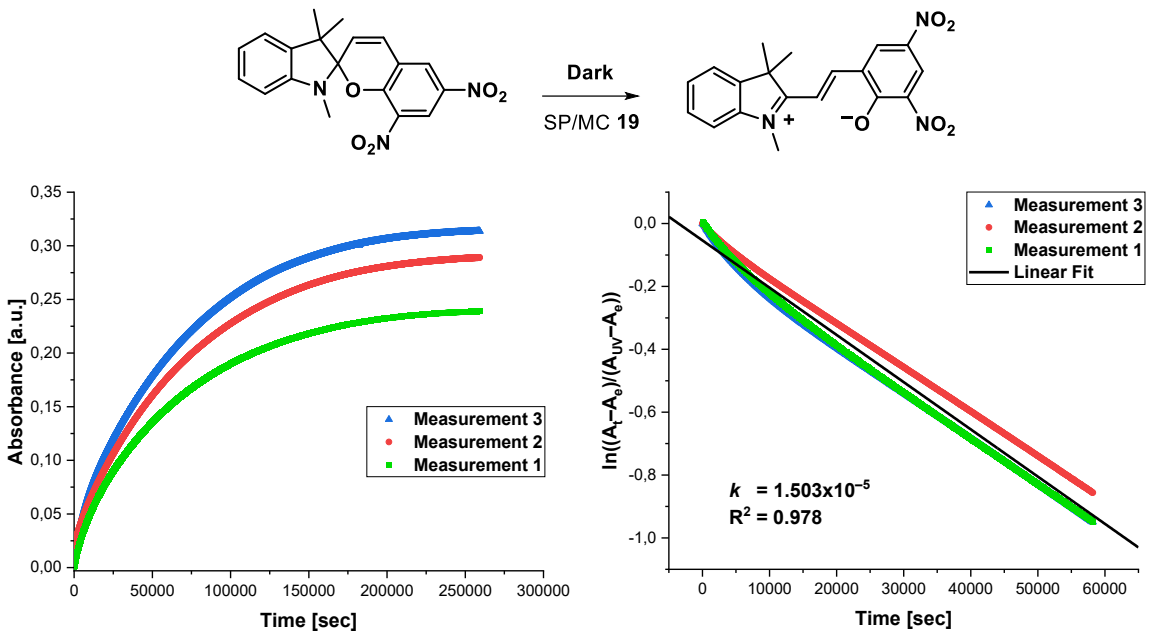

Scheme 62: Kinetics for the ring opening reaction of spiropyran **19** to the corresponding merocyanine. Plot of the absorbance at the absorption maximum (507 nm) of the merocyanine against time (left) and logarithmic plot of the first 60 % conversion to determine the rate constant (right). All measurements were repeated three times and conducted with 0.025 mM methanolic solutions at 20 °C.

For the SP/MC system **8** with two bromine substituents at the chromene moiety, the cyclisation of the merocyanine to the spiropyran was monitored (Scheme 63, left). A complete cyclisation of merocyanine **8** could be observed within a few minutes. A rate constant of k = 0.0129 was determined.

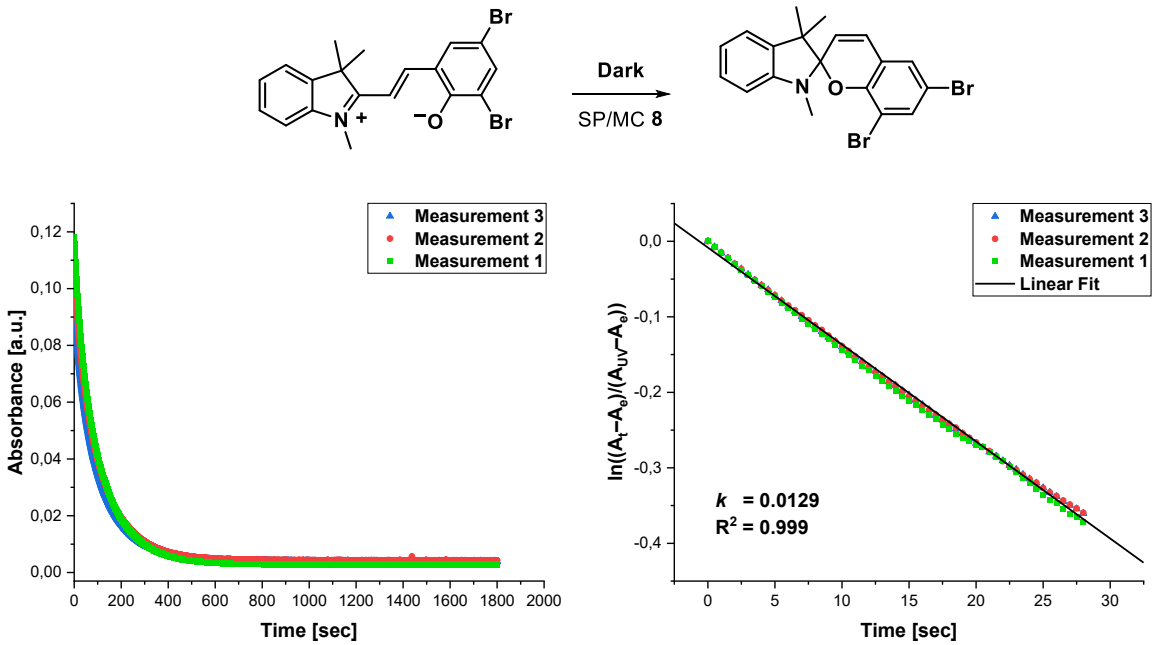

Scheme 63: Kinetics for the cyclisation of the merocyanine **8**o the corresponding spiropyran. Plot of the absorbance at the absorption maximum (566 nm) of the merocyanine against time (left) and logarithmic plot of the first 30 % conversion to determine the rate constant (right). All measurements were repeated three times and conducted with 0.025 mM methanolic solutions at 20 °C.

For the system **8** with two bromine substituents at the chromene moiety, the fastest cyclisation was observed. The rate constant of the system was by far the largest with $k = 0.0129\ s^{-1}$. The rate constants for the nitrated systems **7** and **32** were significantly smaller with $k = 1.085 \times 10^{4}\ s^{-1}$ and $k = 5.202 \times 10^{-4}\ s^{-1}$. For both systems **9** and **10** with an additional bromine substituent, the rate constants of $k = 2.670 \times 10^{-5}\ s^{-1}$ and $k = 8.288 \times 10^{-5}\ s^{-1}$ were even smaller by one order of magnitude. The smallest rate constant of $k = 1.503 \times 10^{-5}\ s^{-1}$ was determined for the system **19** with two nitro groups. This shows that the rate constant is decreased by the increasing number and strength of the electron-withdrawing substituents at the chromene part. As the name implies, electron withdrawing substituents lower the electron density at the phenolate moiety of the merocyanine. This lowers the nucleophilicity of the phenolate which is crucial for the cyclisation towards the spiropyran (Scheme 64, left). In the spiropyran, the lowered electron density at the chromene part also leads to a stronger polarisation, and therefore weakening, of the C-O bond which is cleaved upon isomerisation to the merocyanine (Scheme 64, right). Due to this, a change from positive to negative photochromism can be detected with increasing electron-withdrawing substituents. In contrast, electron-donating substituents at the indole moiety increase the nucleophilicity of the phenolate and stabilise the C-O bond of the spiropyran. This could be demonstrated by M. S. Vogt during her bachelor thesis were methoxy substitute at the chromene moiety completely inhibited the ring opening at ambient temperature.[129] As already mentioned, the obtained rate constant is the sum of the rate constants of the cyclisation (k_{SP-MC}) and the ring opening reaction (k_{MC-SP}). It was shown that electron withdrawing groups disfavoured the cyclisation of the merocyanine to the spiropyran and therefore decrease the rate constant k_{SP-MC}. Since the equilibrium constant K is the ration between k_{SP-MC} and k_{MC-SP}, the decrease of k_{SP-MC} by the electron withdrawing groups also result in a decrease of the equilibrium constant.

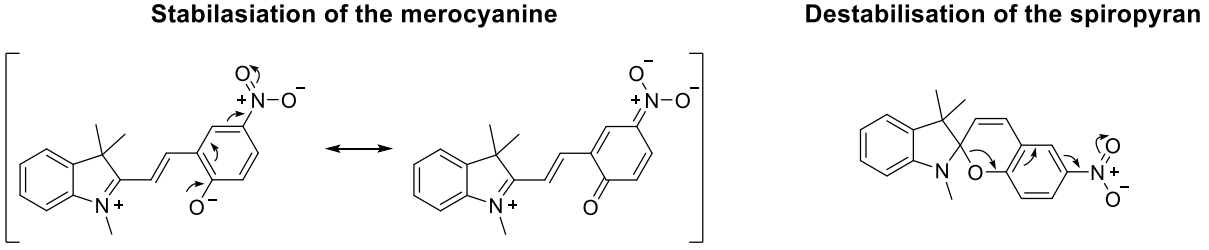

***Scheme 64*:** Visualisation of the stabilisation of the merocyanine form (left) and the destabilisation of the spiropyran (right) by electron-withdrawing substituents.

Comparing **7** and **32**, the rate constant of the latter one is almost five times larger, leading to a faster cyclisation of the merocyanine. This indicates that a nitro substituent in *ortho*-position stabilises the merocyanine to a lesser degree than a nitro group in *para*-position. The same can be seen when comparing the rate constants of **9** and **10**. This can be contributed to interactions that are of neither inductive nor mesomeric nature, such as repulsive interactions between the phenolate and the nitro group (Scheme 65, left). This could lead to an out of plane twist of the nitro group, thus lowering its mesomeric effect (–M). Additionally, hydrogen bonding involving the solvent could hinder the nucleophilic attack of the phenolate (Scheme 65, right). These additional interactions are only possible for *ortho*-substituents.

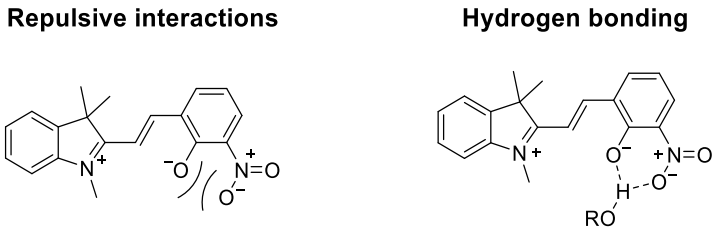

***Scheme 65*:** Visualisation of repulsive interactions between ortho-substituents (left) and hydrogen bonding with a solvent molecule (right).

4.3.5 Influence of the Indole Substituents on the Reaction Kinetics

In this chapter the influence of different indole substituents on the kinetics of the SP/MC equilibrium are analysed and compared. The substituents were always at the *para*-position relative to the indole nitrogen. As previously mentioned, the ideal system for our desired application should provide quantitative transformation between merocyanine and spiropyran. Additionally, the system should have a favoured merocyanine form at the given conditions. This is desirable for envisioned applications since the isomerisation of the merocyanine to the spiropyran is a milder process then the reverse, as it employs visible light instead of higher energy UV light. Though the system **19** with two nitro substituents is the most promising system of those introduced in the previous section under these criteria, it was ultimately excluded due to its poor solubility. Therefore, the rate constant of system **9** with k = 2.670 x 10^{-5} s^{-1} is used as reference.

In case of the system **51** a methyl group was added to the indole moiety. For the kinetic measurements of the system, the ring opening reaction of the spiropyran (colourisation) was monitored (Scheme 66, left). The equilibrium is reached at an absorption of 0.41. A rate constant of k = 1.943 x 10^{-5} s^{-1} was determined, which is slightly smaller than the rate constant of the references system **9**.

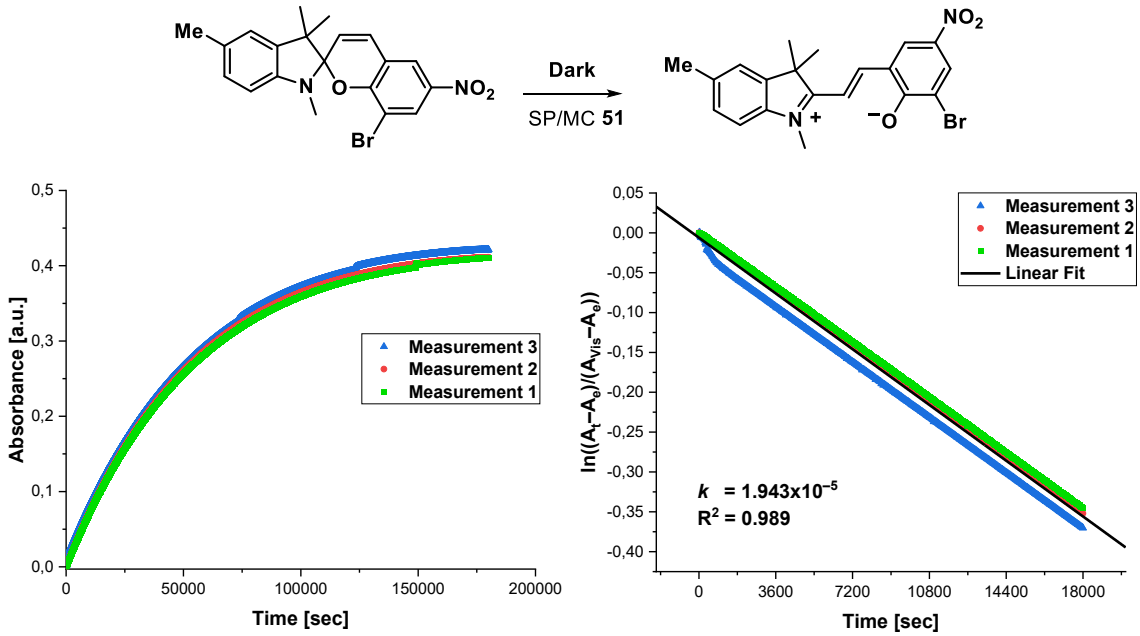

Scheme 66: Kinetics for the ring opening reaction of spiropyran **51** to the corresponding merocyanine. Plot of the absorbance at the absorption maximum (521 nm) of the merocyanine against time (left) and logarithmic plot of the first 30 % conversion to determine the rate constant (right). All measurements were repeated three times and conducted with 0.025 mM methanolic solutions at 20 °C.

When the formation of the merocyanine **48** was monitored through the absorption maximum at 521 nm, the equilibrium was reached at an absorption of approximately 0.52 a.u. (Scheme 67, left). A rate constant of k = 1.658 x 10^{-5} s^{-1} was calculated for the colourisation, which is even smaller that the constants determined for SP/MC **48**.

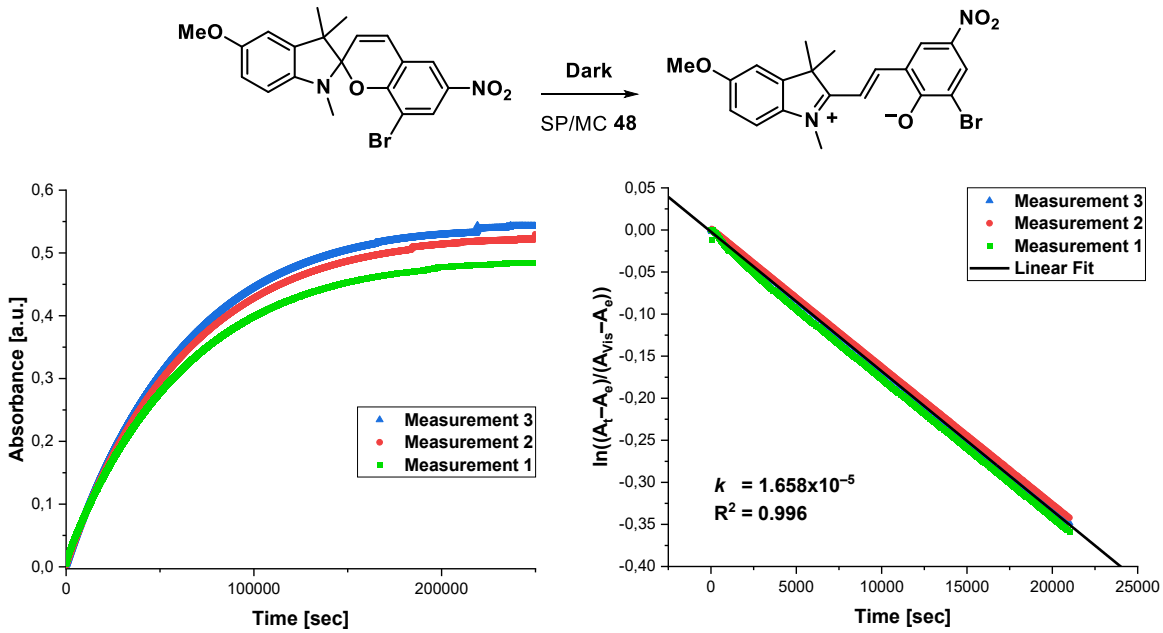

Scheme 67: Kinetics for the ring opening reaction of spiropyran **48** to the corresponding merocyanine. Plot of the absorbance at the absorption maximum (521 nm) of the merocyanine against time (left) and logarithmic plot of the first 30 % conversion to determine the rate constant (right). All measurements were repeated three times and conducted with 0.025 mM methanolic solutions at 20 °C.

In case of system **69** with a triethyl glycol ether as substituent the obtained rate constant k = 2.232 x 10^{-5} was slightly bigger than for systems **51** and **48** (Scheme 68, right). The R^2-value of 0.917 is also not ideal. The reason for this can be clearly seen in the absorbance measurements (Scheme 68, left). Over the three measurements, the total absorbance at the equilibration point decreased for each subsequent measurement. This indicates a decrease in concentration of the merocyanine which might be due to agglomeration of the molecules. This phenomenon is already known. However, typically this occurs after several isomerisation cycles or in non-polar solvents like cyclohexane and toluene.[51] It might be possible that the long ethylene glycol chain enables faster agglomeration but further experiments and other reference systems would be necessary to verify this hypothesis.

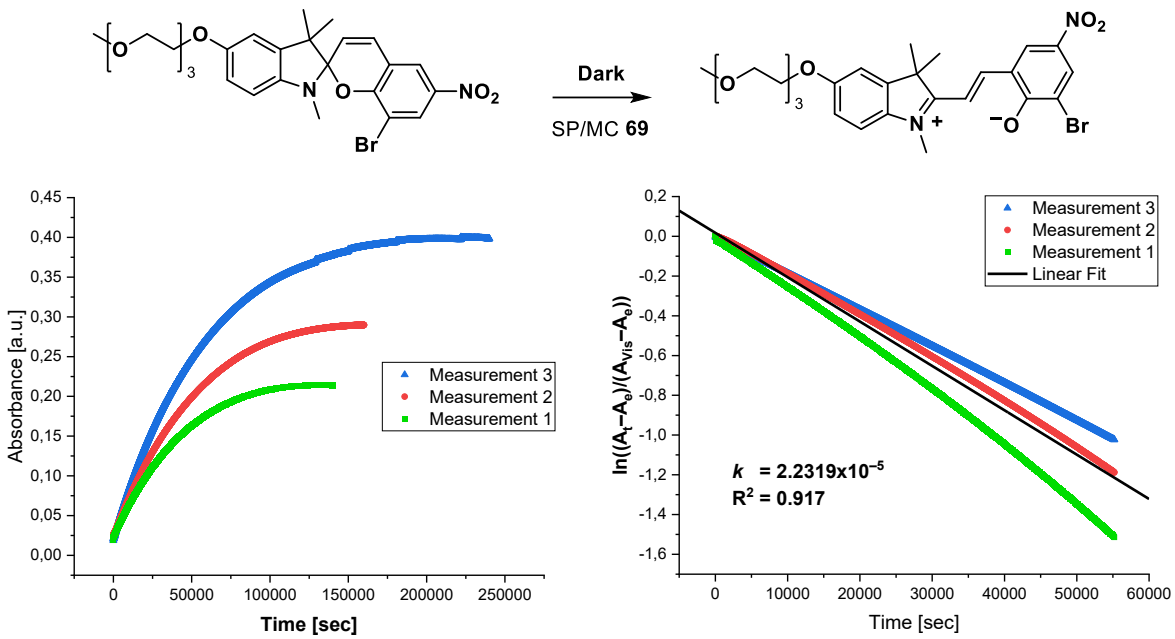

Scheme 68: Kinetics for the ring opening reaction of spiropyran **69** to the corresponding merocyanine. Plot of the absorbance at the absorption maximum (521 nm) of the merocyanine against time (left) and logarithmic plot of the first 30 % conversion to determine the rate constant (right). All measurements were repeated three times and conducted with 0.025 mM methanolic solutions at 20 °C.

By comparing the kinetics of **51**, **69** and **48** with **9** it can be seen that electron-donating substituents at the indole moiety lower the rate constant of the isomerisation between spiropyran and merocyanine.

For the system **50** with a bromine substituent at the indole moiety the equilibrium in the dark was reached at an absorption of approximately 0.11 a.u. (Scheme 69, left). Therefore, in case of this system the decolourisation after irradiation with UV light was investigated in the kinetic studies. The determined rate constant of k = 8.041 x 10^{-5} is three times higher than of system **9**.

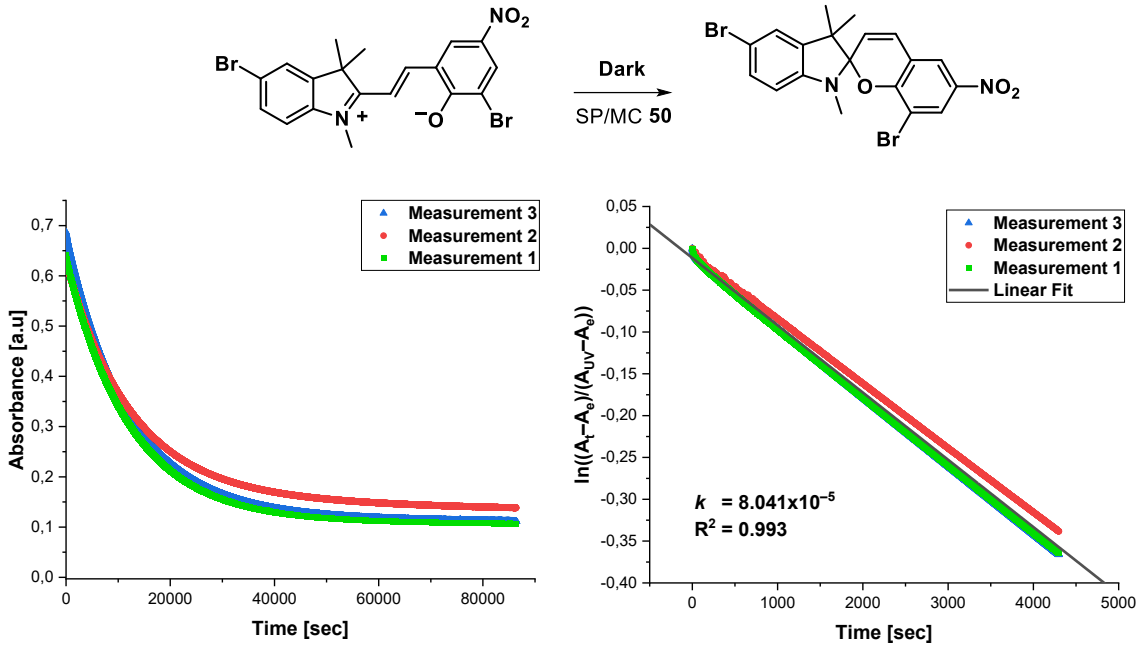

Scheme 69: Kinetics for the cyclisation of the merocyanine **50** to the corresponding spiropyran. Plot of the absorbance at the absorption maximum (532 nm) of the merocyanine against time (left) and logarithmic plot of the first 30 % conversion to determine the rate constant (right). All measurements were repeated three times and conducted with 0.025 mM methanolic solutions at 20 °C.

In the cyclisation of merocyanine **49,** the absorption maximum at 541 nm completely disappeared upon reaching the equilibrium in the dark (Scheme 70, left). A rate constant of $k = 5.091 \times 10^{-4}\ s^{-1}$ was determined. The logarithmic plot used for the determination of the rate constant shows a short non-linear phase within the first 8–9 % of conversion. This might be due to the acidic proton of the carboxylic acid. The carboxylic acid can protonate the phenolate. The resulting carboxylate has no electron-withdrawing character anymore ($\sigma = 0.00$),[42] thus resulting in a faster cyclisation. Upon cyclisation to the spiropyran, the proton is released to the solution. However, the correlation coefficient ($R^2 = 0.982$) is still sufficient. With a rate constant of $5.091 \times 10^{-4}\ s^{-1}$, the reaction is almost twenty times faster than for the system **9** without an additional indole substituent.

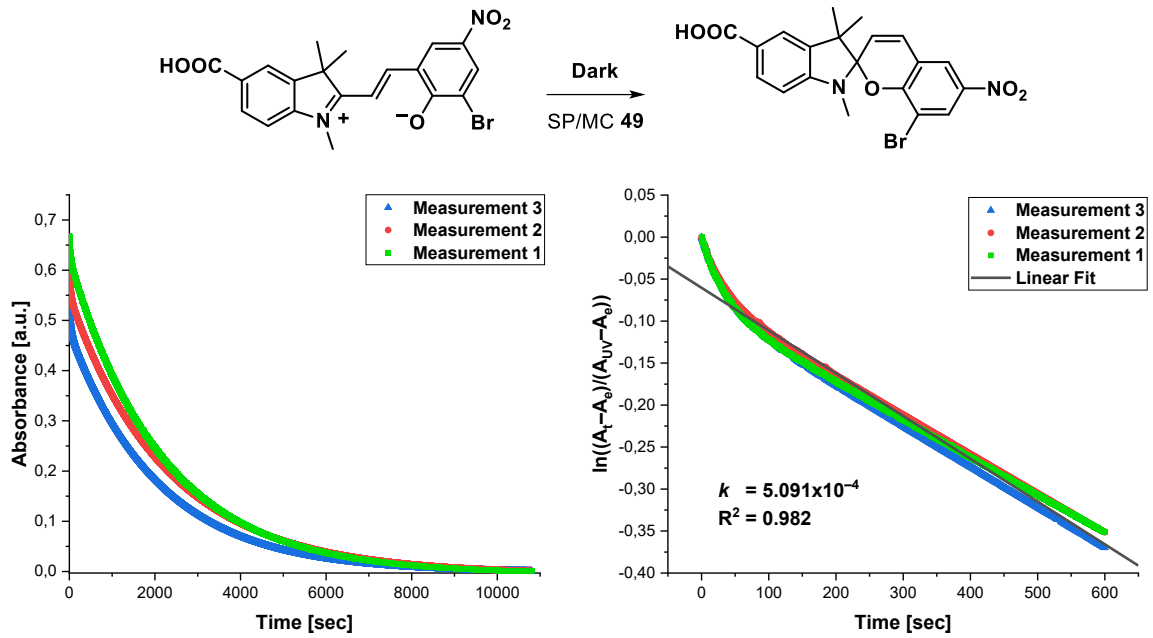

Scheme 70: Kinetics for the cyclisation of the merocyanine **49** to the corresponding spiropyran. Plot of the absorbance at the absorption maximum (541 nm) of the merocyanine against time (left) and logarithmic plot of the first 30 % conversion to determine the rate constant (right). All measurements were repeated three times and conducted with 0.025 mM methanolic solutions at 20 °C.

For the system **62** a fast cyclisation to the spiropyran was observed (Scheme 71). The determined rate constant of $k = 0.010\ s^{-1}$ is more than 350 times bigger than for the unsubstituted system.

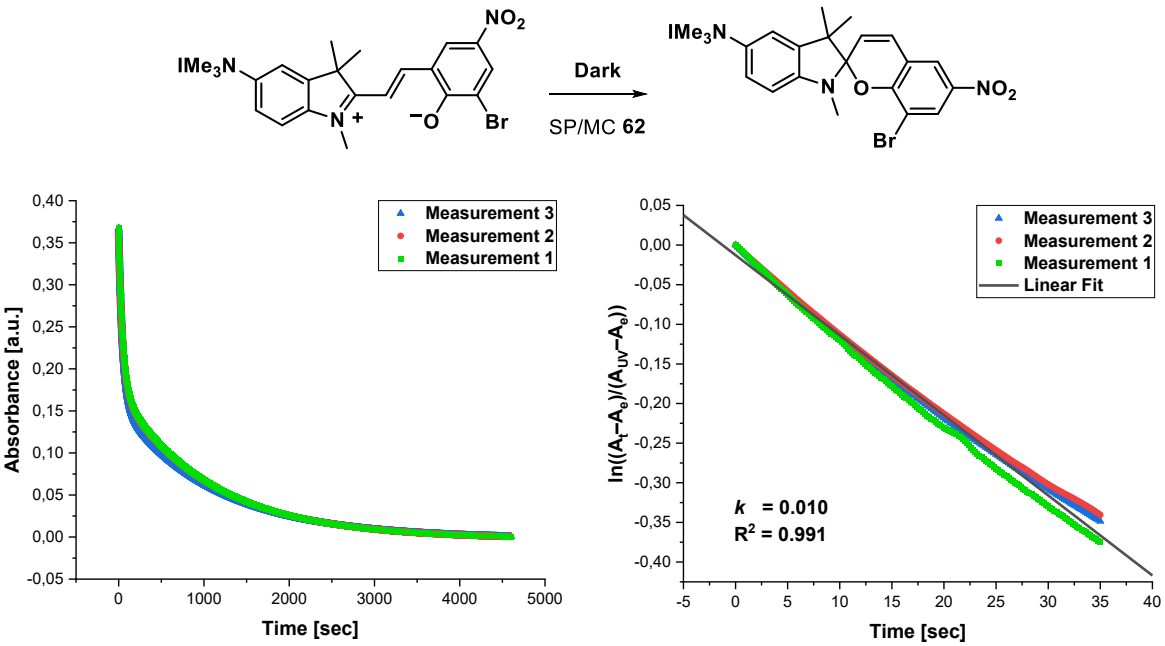

Scheme 71: Kinetics for the cyclisation of the merocyanine **62** to the corresponding spiropyran. Plot of the absorbance at the absorption maximum (544 nm) of the merocyanine against time (left) and logarithmic plot of the first 30 % conversion to determine the rate constant (right). All measurements were repeated three times and conducted with 0.025 mM methanolic solutions at 20 °C.

For the nitro substituted system **61** an even higher rate constant of 0.030 s^{-1} was calculated (Scheme 72).

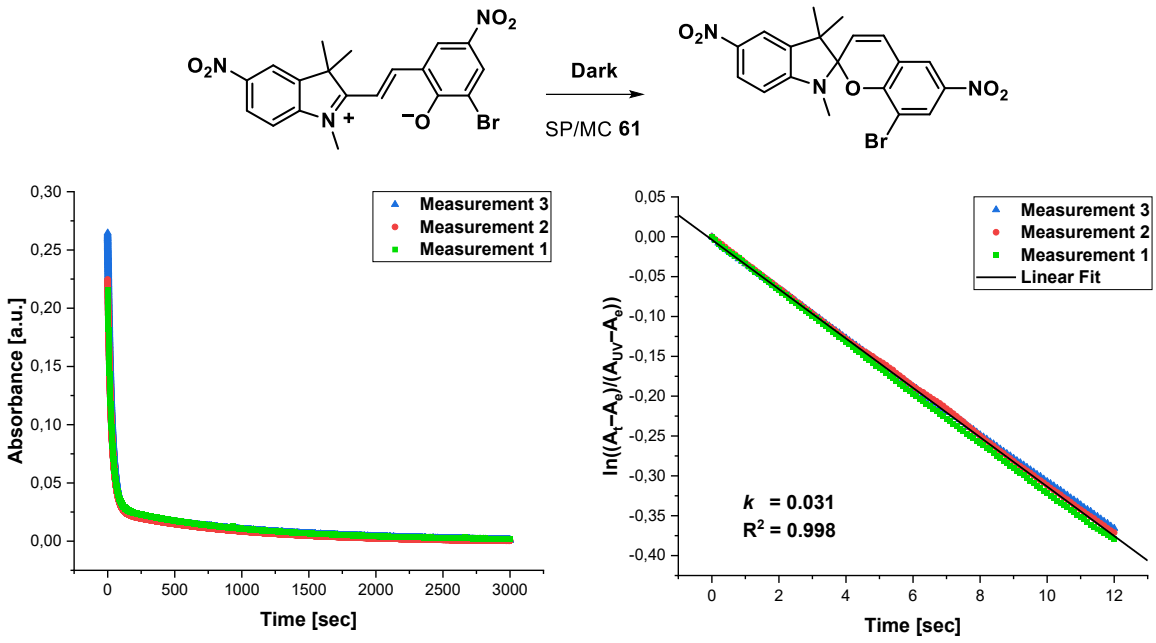

***Scheme 72*:** Kinetics for the cyclisation of the merocyanine **61** to the corresponding spiropyran. Plot of the absorbance at the absorption maximum (559 nm) of the merocyanine against time (left) and logarithmic plot of the first 30 % conversion to determine the rate constant (right). All measurements were repeated three times and conducted with 0.025 mM methanolic solutions at 20 °C.

As already mentioned, the cyclisation reactions for the systems **62** and **61** are very fast. For the trimethylammonium substituted system **62** the 30 % conversion were reached after 35 seconds. In case of the nitro substituted system **61** 30 % conversion were already reached after 12 seconds. Since the samples are transferred manually into the UV/Vis-spectrometer, the first few seconds after irradiation with UV light are not recorded. Therefore, the calculated rates constants might be a little lower than the real ones. It is also worth mentioning that for both systems a change of the rate constant can be observed. For the cyclisation of **62** the change can be observed after approximately 200 seconds and 60–65 % conversion. In case of the nitro substituted system **61** the change of the reaction rate was observed after approximately 100 seconds and 85–90 % conversion. Since the first seconds of the reactions were not monitored the real conversion at which this change occurs might be bigger. The reason for the change of the reaction rate is unknown. However, since these changes are only observed at high conversions, the rate constants obtained by using the initial rates can still be used to discuss the influence of the different indole substituents.

A correlation can be observed between the characteristics of the indole substituents and the rate constants as can be seen in the Hammett plot shown in Scheme 73. While electron-donating groups lead to a smaller initial rate, higher rates are obtained with increasing electron-withdrawing character of the substituents.

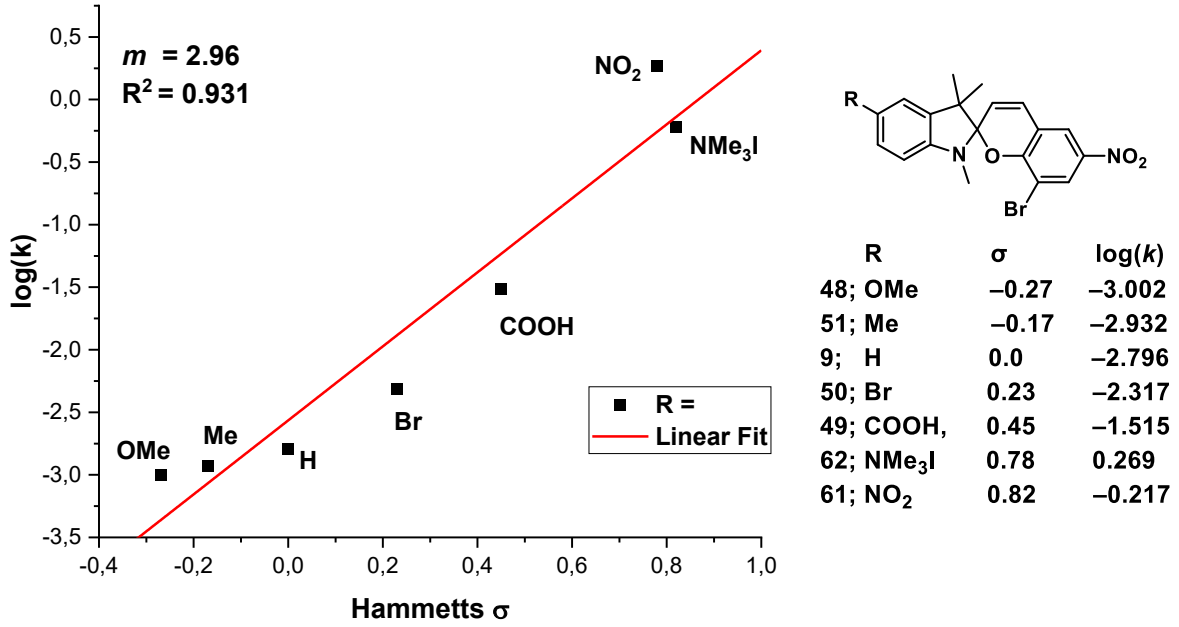

R	σ	log(*k*)
48; OMe	–0.27	–3.002
51; Me	–0.17	–2.932
9; H	0.0	–2.796
50; Br	0.23	–2.317
49; COOH,	0.45	–1.515
62; NMe_3I	0.78	0.269
61; NO_2	0.82	–0.217

Scheme 73: Hammett plot for isomerization of indole substituted spiropyrans and merocyanines.

The observed rates correlate with the stabilisation of the merocyanine. For systems with a stabilised merocyanine form, small rate constants can be observed while those with a none-stabilised merocyanine exhibit higher rate constants. As mentioned before, the merocyanine can be stabilised by introduction of electron-withdrawing substituents at the chromene moiety (Chapter 4.3.4). This lowers the electron density and therefore the nucleophilicity of the phenolate. On the other hand, electron-donating substituents at the indole can stabilise the merocyanine form by increasing the electron density at the iminium of the merocyanine and thus decreasing its electrophilicity (Scheme 74, left). Therefore, the nucleophilic attack of the phenolate, which is crucial for the cyclisation to the spiropyran, is hindered. In the spiropyran form, electron-donating groups also favours the cleavage of the C-O bond. Additionally, a higher electron density at the indole, favours the ring-opening of the spiropyran (Scheme 74, right).

Stabilisation of the merocyanine **Destabilisation of the spiropyran**

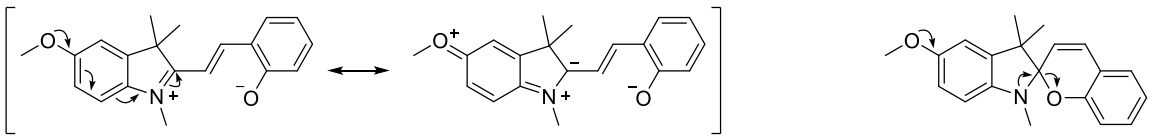

***Scheme 74*:** Visualisation of the stabilisation of the merocyanine (left) and the destabilisation of the spiropyran (right) by electron-donating substituents at the indole moiety.

Electron-withdrawing substituents at the indole moiety show the opposite effect. Due to the lower electron density, the electrophilicity of the iminium of the spiropyran is increased and therefore the nucleophilic attack of the phenolate favoured (Scheme 75, left). Additionally, low electron density at the indole stabilises the C-O bond of the spiropyran (Scheme 75, right).

Destabilisation of the merocyanine **Stabilisation of the spiropyran**

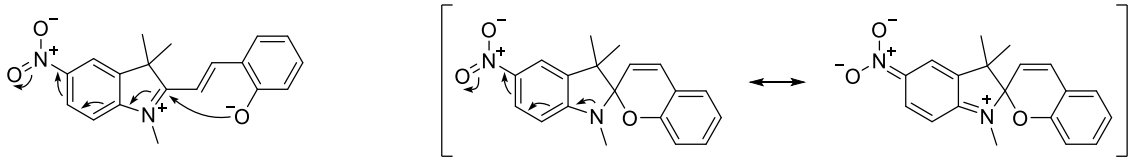

Scheme 75: Visualisation of the destabilisation of the merocyanine (left) and the stabilisation of the spiropyran (right) by electron-withdrawing substituents at the indole moiety.

A graph with all rate constants of the different indole substituted merocyanine and spiropyran systems as well as those with different chromene substituents is shown in Scheme 76.

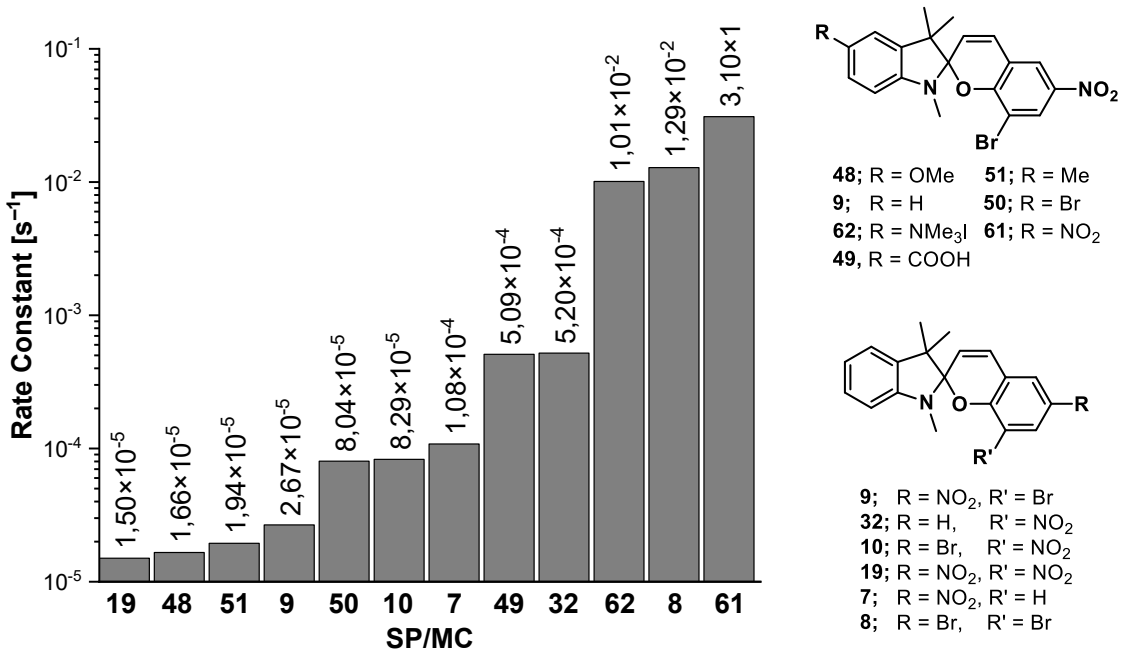

***Scheme 76*:** Rate constants for the isomerisation of all spiropyrans and merocyanines discussed in chapter 4.3.4 and 4.3.5.

The fastest SP/MC isomerisation can be observed for the systems with strong electron donating substituents at the indole moiety like a nitro **61** or an ammonium group **62** or when only weak electron withdrawing substituents are at the chrome moiety e.g. **8**. The fastest isomerisation rates were obtained for systems with strong electron withdrawing substituents at the chromene part of the system **19** and and/or electron donating substituents at the indole like methyl **51** or methoxy groups **48**. Since for the systems **19** and **48** similar rates were obtained, but the latter one is notably better soluble in polar solvents, **48** seems to be most suitable for the envisioned application.

4.4 ^{1}H-NMR Ratio of Spiropyran and Merocyanine

In the previous chapter it was shown that via UV/Vis-spectroscopy, a quantitative cyclisation to the spiropyran can be detected. For the quantification of the ring-opening reaction towards the merocyanine UV/Vis-spectroscopy is not suitable due to an overlay of the characteristic absorptions of the spiropyran with the absorptions of the merocyanine. Therefore, the SP/MC ratio was determined using ^{1}H-NMR spectroscopy.

In Scheme 77, a selected part (5.5–9.0 ppm) of the ^{1}H-NMR spectra of the SP/MC system **46** obtained from DMSO-d_6 is shown. The spectrum shown in black was obtained after the samples was kept in the dark for 72 h. The red spectrum was measured directly after the samples was irradiated with visible light for one minute. Upon cyclisation the aromatic signals are all high-field shifted (smaller chemical shift) since the conjugated system is disrupted by the spiro centre. Also very characteristic are the coupling constants of the CH=CH group which connect the two parts of the system, which change from approximately 15.6 Hz for the merocyanine to 10.4 Hz for the spiropyran. This is due to the *trans/cis*-isomerisation upon the cyclisation.

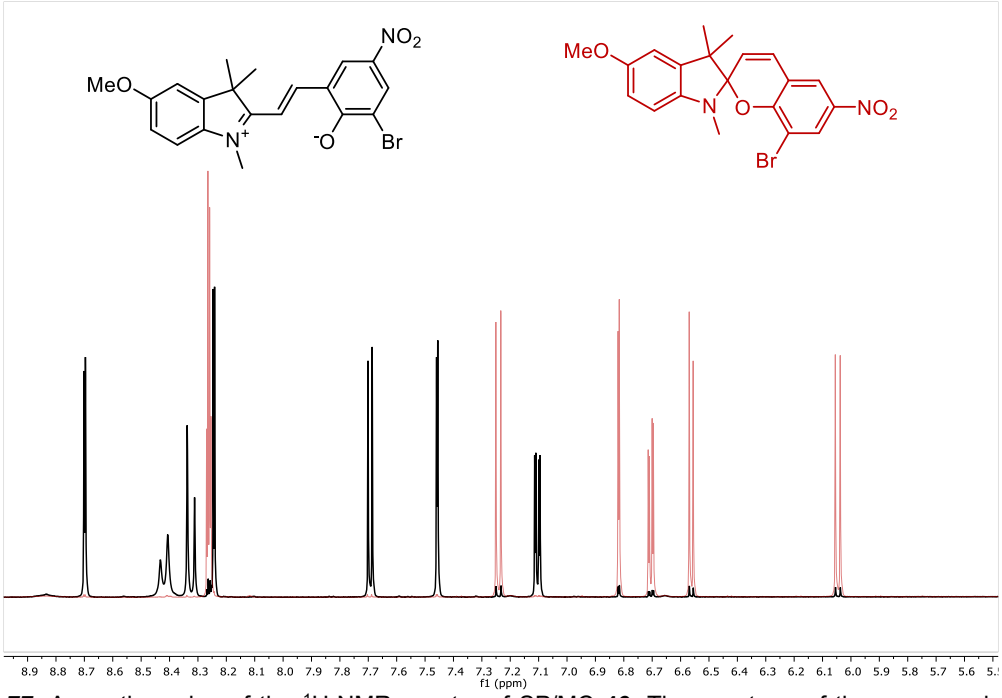

***Scheme 77*:** Aromatic region of the ^{1}H-NMR spectra of SP/MC **46**. The spectrum of the merocyanine (black) was recorded after incubation in the dark. The spectrum of the spiropyran (red) was recorded directly after irradiation of the sample with visible light for one minute. For both spectra DMSO-d_6 was used as solvent.

The signals of the geminal methyl groups and the methyl group at the indole nitrogen also show characteristic differences which can be seen in the appendix. For the

determination of the ratio of spiropyran and merocyanine, the average integrals of at least two signals of each isomer were used. All spectra with the corresponding integrals can be found in the appendix. The average integrals and the determined ratios for the different derivatives are summarised in Table 11.

Table 11: ^{1}H-NMR ratios of spiropyran and merocyanine for different indole substituted derivatives. The ratios were determined after the samples were kept in the dark for three days (left) or irradiated with visible light for one minute (right). All samples were dissolved in DMSO-d_6.

	Dark			Vis		
System	**SP**	**MC**	**% MC**	**SP**	**MC**	**% MC**
69	0.11	1.00	90	1.00	<0.05	<5
48	0.06	1.00	94	1.00	<0.05	<5
51	0.29	0.99	77	1.00	<0.05	<5
9	0.56	1.01	64	1.00	<0.05	<5
50	1.06	0.49	32	1.00	<0.05	<5
49	1.00	0.09	8	1.00	<0.05	<5
61	0.99	nd	<5	1.00	nd	<5
62	1.00	0.09	9	1.00	<0.05	<5

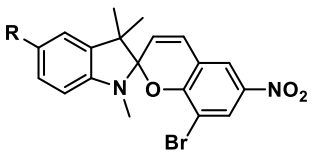

69; R = $O(CH_2CH_2O)_3Me$
48; R = OMe
51; R = Me
9; R = H
50; R = Br
62; R = NMe_3I
61; R = NO_2
49, R = COOH

For system **9** without any indole substituent, the SP/MC equilibrium in the dark is with 64 % slightly in favour of the merocyanine. Electron-donating groups can further shift the equilibrium towards the merocyanine form. For the ethers **48** and **69**, a merocyanine ratio of 94 % and 90 % was determined. Electron withdrawing substituents on the other hand stabilises the spiropyran form. Therefore, less than 10 % of merocyanine were obtain for the systems **49, 61** and **62**. In all cases, an almost quantitative cyclisation of the merocyanine could be obtained by irradiation with visible light. These results are in line with those discussed for the UV/Vis analysis.

***Table 12*:** ^{1}H-NMR ratios of spiropyran and merocyanine for different indole substituted derivatives. The ratios were determined after the samples were kept in the dark for three days (left) or irradiated with visible light for one minute (right). All samples were dissolved in methanol-d_4.

	Dark			Vis		
System	**SP**	**MC**	**% MC**	**SP**	**MC**	**% MC**
69	0.11	1.00	90	1.00	<0.05	<5
48	0.06	1.00	94	1.00	<0.05	<5
51	0.29	0.99	77	1.00	<0.05	<5
9	0.56	1.01	64	1.00	<0.05	<5

For a better comparison with the UV/Vis analysis, the same experiments were repeated with methanol-d_4 as solvent. Unfortunately, the solubility of the spiropyrans was not as good as in DMSO. Therefore, only reliable results could be obtained for the systems **69**, **48**, **51** and **9.** The results are shown in Table 12. Again, a stabilisation of the merocyanine form by the electron-donating substituents was observed. However, for all systems the overall amount of merocyanine was lower in methanol compared to DMSO.

4.5 Synthesis of Proline Based Model Peptides

The synthesis of the Boc-Cys(*t*Bu)-Pro-OMe dipeptide **94** was achieved over three steps in an overall yield of 48 % (Scheme 78). Following a procedure by Pastuszak and Chimiak[130], cysteine **95** was protected using *t*BuOH and hydrochloric acid. The obtained cysteine **96** was then Boc-protected in 68 % yield. The twice protected cysteine **97** was than coupled with proline methylester **98** in 73 % yield, using a self-established procedure with HBTU as coupling reagent.

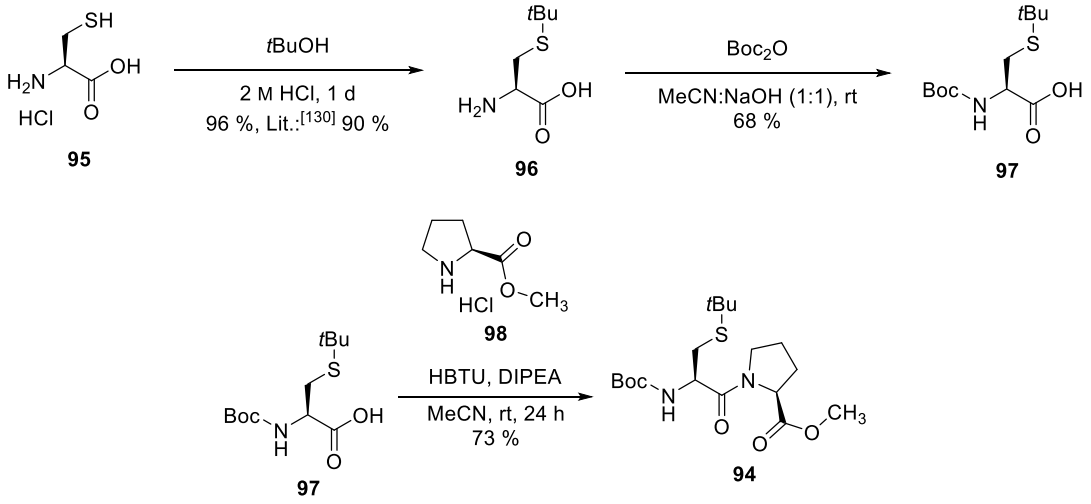

***Scheme 78*:** Results for the synthesis of Boc-Cys(tBu)-Pro-OMe dipeptide **94**.

For the synthesis of the Fmoc-Cys(trt)-Pro-Cys(trt) tripeptide **99**, the protected proline **100** and protected cysteine **101** were coupled to the dipeptide **102** using HBTU as amide coupling reagent (Scheme 79). The dipeptide deprotected and subsequently coupled with the cysteine **103**. The synthesis of tripeptide **99** was achieved in an overall yield of 55 %. The same synthesis was also tested in a one-pot approach with an overall yield of 61 %.

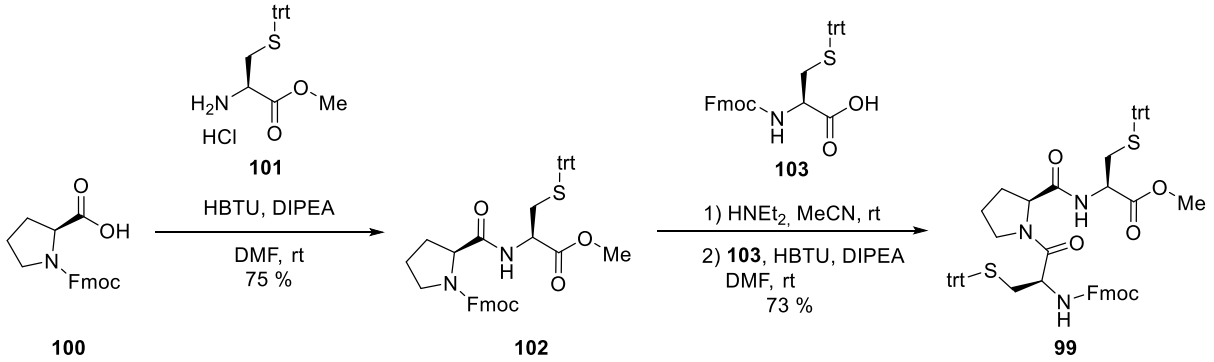

***Scheme 79*:** Two step synthesis towards the Fmoc-Cys(trt)-Pro-Cys(trt) tripeptide **99**.

The synthesis of the Boc-Cys(trt)-Pro-Cys(trt)-OMe tripeptide **104** was realised in a similar fashion (Scheme 80). Starting from Boc-protected proline **105**, a amid coupling with cysteine **101** was performed in 90 % yield. The Boc-protecting group of the dipeptide **106** was than quantitatively removed under acidic conditions. The amid coupling between cysteine **107** and dipeptide **108** was performed with a yield of 73 %.

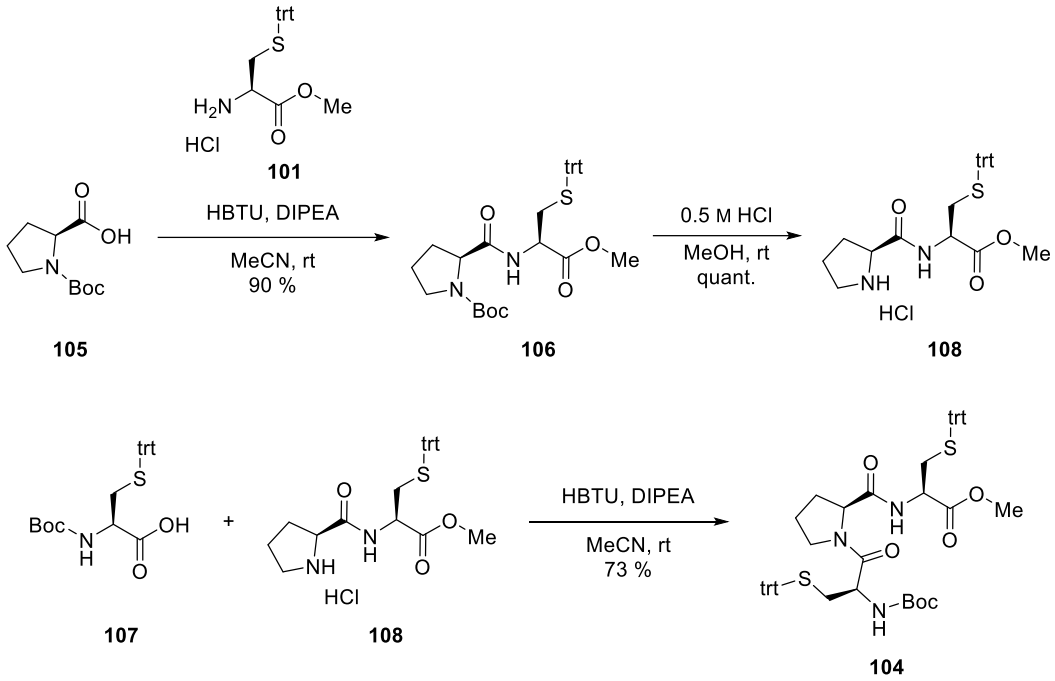

Scheme 80: Three step synthesis towards the Boc-Cys(trt)-Pro-Cys(trt) tripeptide **104**.

For the synthesis of the Boc-Cys(Bz)-Pro-Cys(Bz)-OMe tripeptide **109** the two protected cysteines **110** and **111** were synthesised (Scheme 81). Following a procedure by Jia et al.[131] cysteine **112** was protected with benzyl bromide and directly converted to cysteine **113**. For the synthesis of cysteine **111** the benzyl-protected cysteine **114** was Boc-protected using Boc_2O.

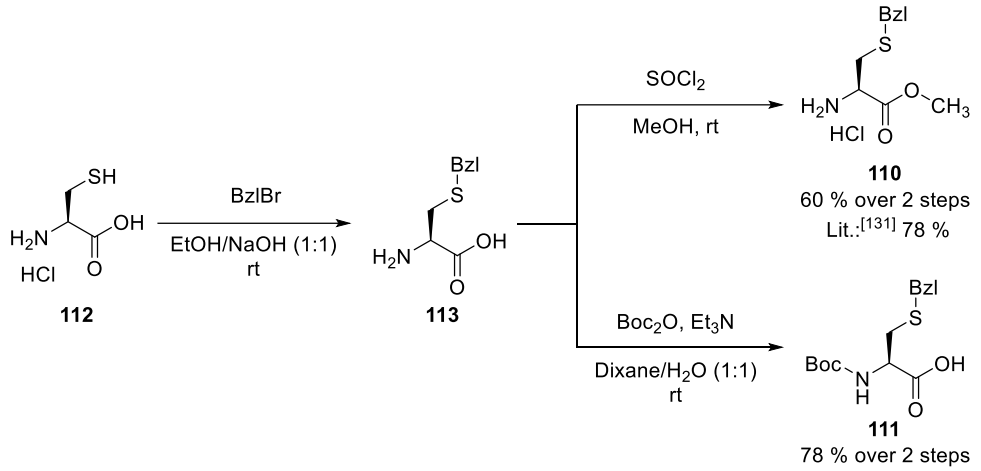

Scheme 81: Synthesis of double protected cysteines **110** and **111**.

Via an amide coupling with HBTU, dipeptide **114** was obtained from proline **100** and cysteine **110** (Scheme 82). The Fmoc-protecting group of the dipeptide was cleaved with diethylamine and the deprotected dipeptide was directly coupled with cysteine **111**. The desired product **109**, was detected by ^{1}H-NMR. Unfortunately, the product was not isolatable via column chromatography. Recrystallisation attempts from acetonitrile, methanol and acetone were also not successful. Additionally, the purification after the cleavage of the Boc-protecting group was tested without any success.

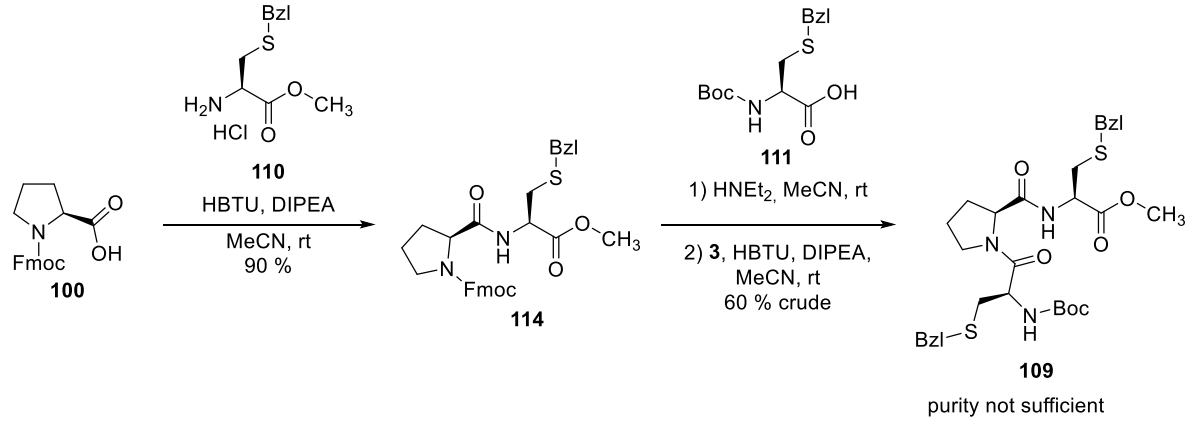

Scheme 82: Two step synthesis towards the Boc-Cys(Bz)-Pro-Cys(Bz) tripeptide **109**.

The synthesis of the Boc-Cys(trt)-Pro-Phe-Cys(Acm)-OMe tetrapeptide **115** via a linear synthesis was already reported by W. Sander and coworkers,[90] but in this work a convergent approach has been chosen (Scheme 83). Therefore, the dipeptides **116** and **117** were synthesised first. The synthesis of dipeptide **116** was started from proline **118** which was first transferred to ester **119** and then couplet with Boc-protected cysteine **107**. The fully protected dipeptide **120** was saponified to remove the *C*-terminal protecting group. For the synthesis of the second

dipeptide **117**, cysteine **121** was deprotected at the *N*-terminus and esterified at the *C*-terminus. The obtained cysteine **122** was then used for the amide coupling with phenylalanine **123**. The obtained dipeptide **124** was deprotected to compound **117**. The two dipeptides **116** and **117** were finally coupled to the tetrapeptide **109** using HBTU as amide coupling reagent. For all synthetic steps, good to excellent yields were obtained. Only for the last step the achieved yield of 49 % was moderate due to purification issues.

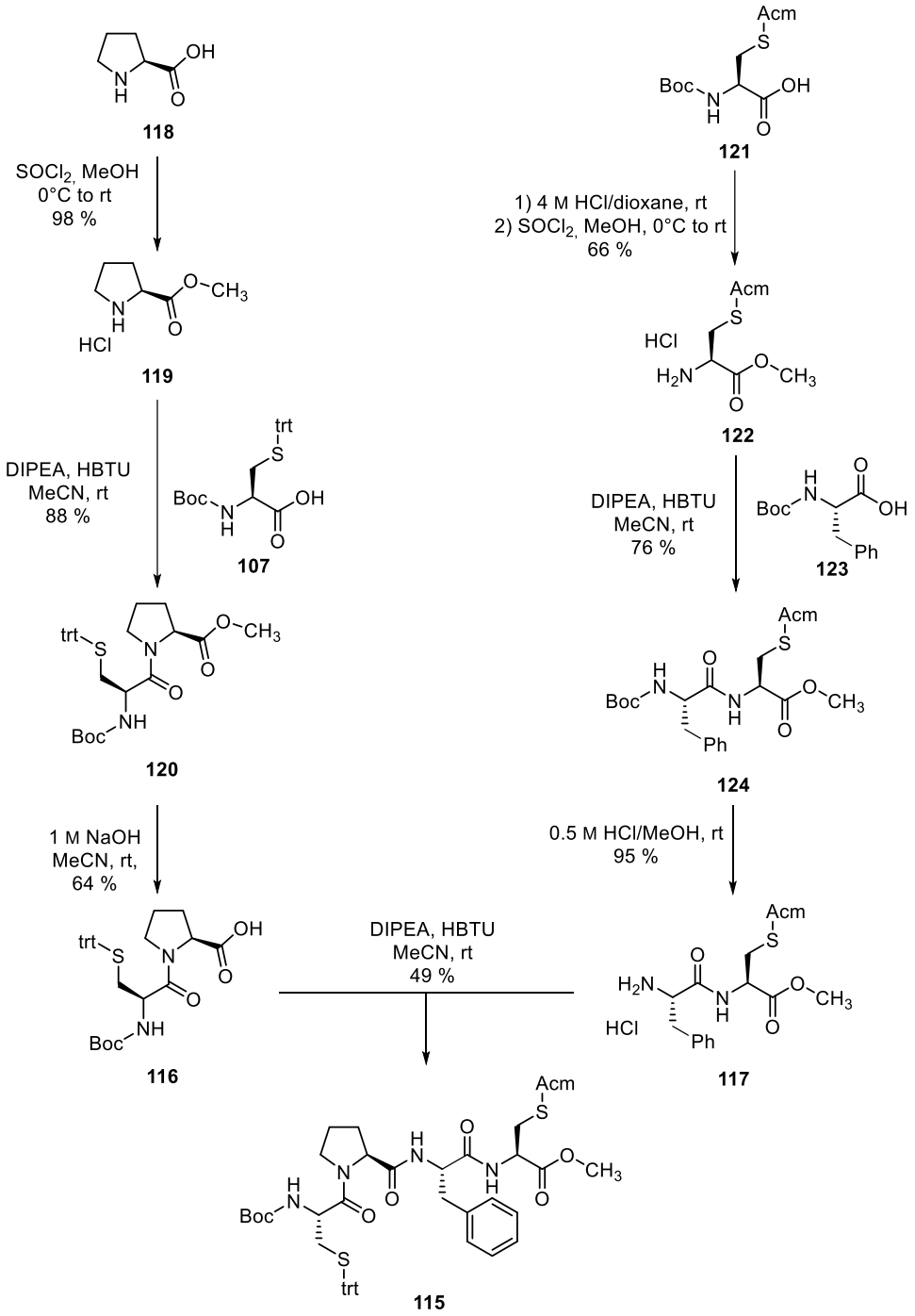

Scheme 83: Convergent synthesis towards the Boc-Cys(trt)-Pro-Phe-Cys(Acm)-OMe tetrapeptide **115** via the dipeptides **116** and **117**.

In summary, all targeted peptides could be successfully synthesised within this thesis (Schem 84). Unfortunately, the purity the Boc-Cys(Bzl)-Pro-Cys(Bzl)-OMe tripeptides was not sufficient enough for isomerisation test in combination with the spiropyran/merocyanine systems. However, the isomerisation experiments including the four other peptides are discussed in the next chapter.

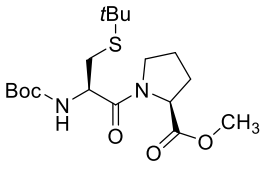

Boc-Cys(*t*Bu)-Pro-OMe

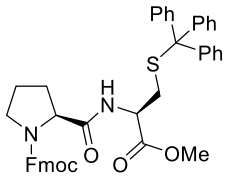

Fmoc-Pro-Cys(trt)-OMe

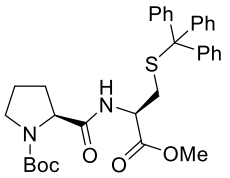

Boc-Pro-Cys(trt)-OMe

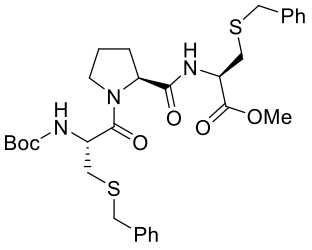

Boc-Cys(Bzl)-Pro-Cys(Bzl)-OMe

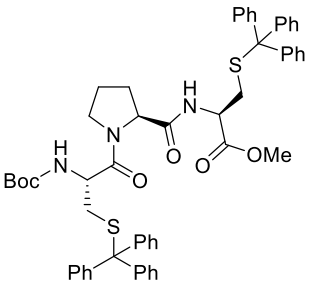

Boc-Cys(trt)-Pro-Cys(trt)-OMe

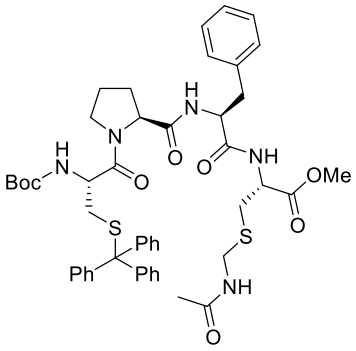

Boc-Cys(trt)-Pro-Phe-Cys(acm)-OMe

Scheme 84: Synthesised proline-based peptides.

4.6 Isomerisation Experiments for Proline-Based Peptides in the Presence of Photochromic Spiropyrans and Merocyanines

In Chapter 4.4 indicated that SP/MC system **48** has the best photochromic properties in terms of quantity. Upon irradiation with visible light, a change from 94 % of merocyanine towards almost exclusively spiropyran was observed. However, the system was ultimately ruled out due to poor solubility after initial tests. Therefore, the SP/MC system **69**, which has similar photochromic properties but a much better solubility, was chosen for all isomerisation experiments.

In Scheme 85, the results of the isomerisation experiment of Ac-Pro-OMe with SP/MC **69** are depicted. For the experiment, a 10 mM stock solution of **69** in DMSO-d_6 was prepared and stored in the dark for at least 72 h to ensure a proper equilibration. In the dark, 500 µL of the stock solution was mixed with 25 µL of a 200 mM stock solution of Ac-Pro-OMe. The first ^{1}H-NMR spectrum (black) was recorded in the dark while the second spectrum (red) was obtained after the sample was irradiated with visible light until the decolourisation was observed.

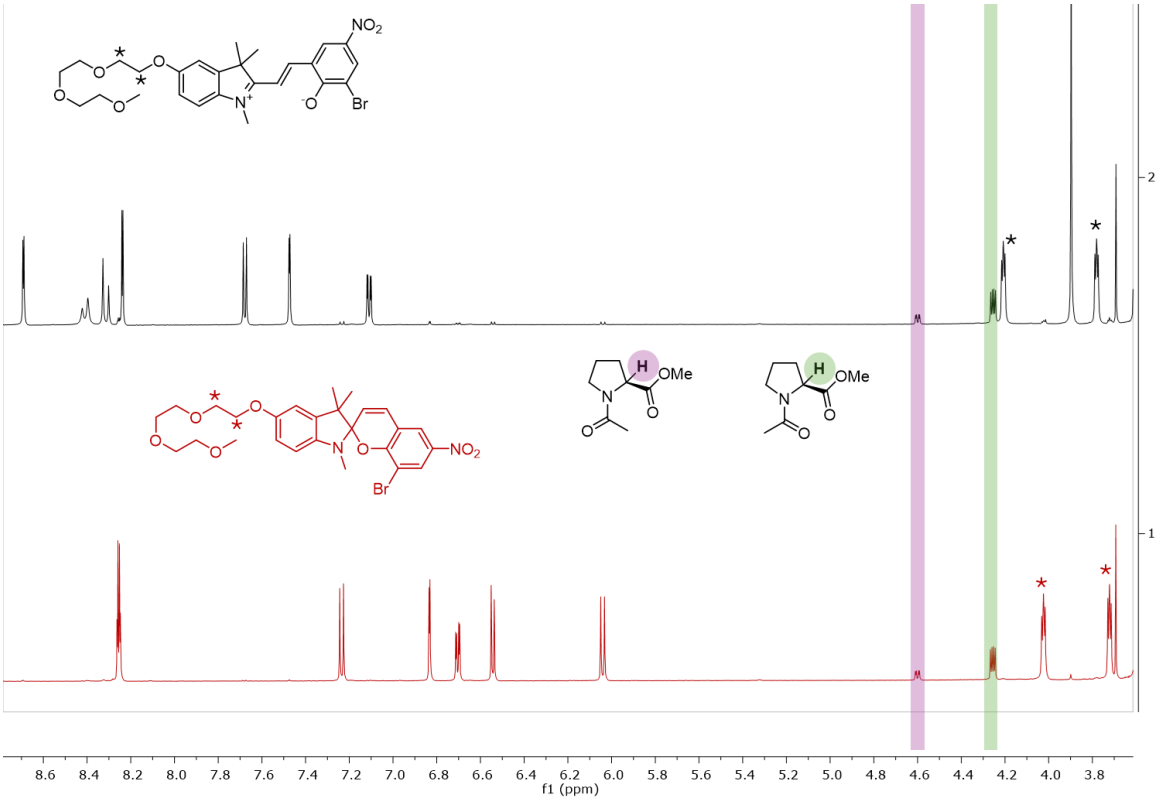

Scheme 85: ^{1}H-NMR isomerisation experiment with 5 µmol Ac-Pro-OMe and 5 µmol SP/MC **69** (1:1) in DMSO-d_6. The upper spectrum (black) was recorded after storing the sample in the dark, while the spectrum at the bottom (red) was obtained after irradiation with visible light. The signals that can be used to determine the *cis/trans*-ratio are highlighted in purple and green.

As already mentioned in Chapter 4.4, upon irradiation with visible light, an almost quantitative isomerisation from merocyanine to spiropyran is detected. The CH-group of the proline is highlighted in green for the *trans*-isomer and purple for the *cis*-isomer. Upon switching from the polar merocyanine to the less polar spiropyran, no change of the *cis/trans*-ratio of Ac-Pro-OMe could be observed.

For the experiments with the more complex peptides, the sample preparation was adjusted. Again, a stock solution of SP/MC **69** in DMSO-d_6 was used at a concentration of 10 mM. This solution was kept in the dark for at least 72 h to ensure a proper equilibration. In the dark, 500 µL of the stock solution were used to directly dissolve 5 µmol of the respective peptide. After the ^{1}H-NMR of the sample was recorded (black), the same sample was irradiated with visible light until the decolourisation of the purple solution was observed (approximately 1 min). The second spectrum was recorded immediately after (red). In Scheme 86 parts of the spectra using Boc-Cys(*t*Bu)-Pro-OMe are shown.

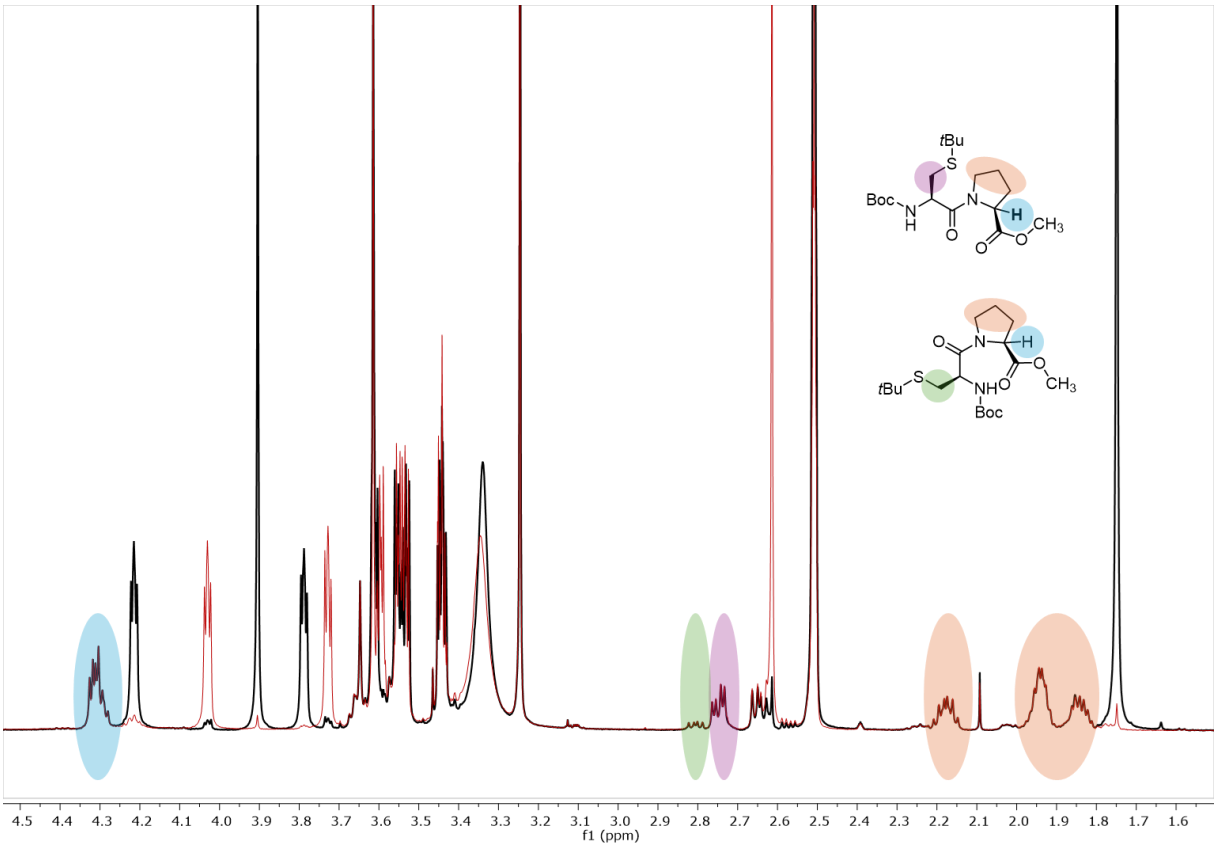

Scheme 86: ^{1}H-NMR isomerisation experiment with 5 µmol Boc-Cys(*t*Bu)-Pro-OMe and 5 µmol SP/MC **69** in DMSO-d_6. The spectrum shown in black was recorded in the dark while the spectrum shown in red was recorded after irradiation with visible light. The signals that can be used to determine the *cis/trans*-ratio are highlighted in purple and green.

Since the ^{1}H-NMR spectra for peptide models are much more complex than those of the protected proline, the spectra before and after irradiation with visible light are superimposed for better comparison. The signals of the CH group of proline are merged for both isomers in the case of Boc-Cys(*t*Bu)-Pro-OMe. However, from the CH_2 signals of the cysteine, the ratio of the *cis/trans*-isomers can be distinguished. Note that when switching from the merocyanine (black) to the spiropyran (red), the signals of the proline isomers do not change. The same is true for the Boc-Pro-Cys(trt)-OMe, Fmoc-Pro-Cys(trt)-OMe, Boc- Cys(trt)-Pro-Cys(trt)-OMe and Boc-Cys(trt)-Pro-Phe-Cys(Acm)-OMe peptides as well. A complete list of the superimposed spectra for all peptides of all experiments are depicted in the appendix.

In summary, no effect of the SP/MC isomerisation of **69** on the *cis/trans*-ratio of proline could be detected. Given that the difference in dipole moments for the merocyanine isomers and spiropyran is already very high at 8.6–9.7 D, testing other SP/MC systems is unlikely to alter the outcome of the experiments. It may be advantageous to alter the ratio between photoswitch and peptide in favour of the photoswitch, given that the overall polarity of the solution would be more pronounced. This approach has already been tested in preliminary experiments. However, due to the solubility issues associated with the SP/MC, the amount of peptide had to be reduced, which unfortunately resulted in the inability to clearly analyse the peptide signals. Consequently, in order to test this hypothesis, further efforts would have to be made to synthesise even more soluble photoswitches.

Another possibility to achieve a change in the *cis/trans*-equilibrium of the proline via the dipole moment changes of the photoswitch, might be the utilisation of less polar solvents then DMSO. In a polar environment, the impact of the change in dipole moments of the photoswitch may be preponderate by the polarity of the solvent. Consequently, in non-polar solvents (like DCM or chloroform), the impact of the photoisomerisation of the SP/MC system may be higher. This approach may prove to be the most promising for further experiments. However, the solubility and the photochromic properties of the photoswitch, as well as the solubility of the peptide models, must first be assessed.

5 Summary and Outlook

As part of this work, a small DFT screening was carried out to find suitable functionals and basis sets for the calculation of dipole moments. For the initial screening bromobenzene and *p*-nitrophenol were used as model-systems and the DFT results were compared with experimental results from the literature. After the combination of functionals and basis sets were narrowed to a smaller selection the dipole moments of SP/MC system **7** were calculated. The combination of the B3LYP-D3BJ functional and the def2-TZVPP basis set was selected after comparison of the results with the literature. This method was employed to calculate the dipole moments of 310 isomers for 62 different substituted spiropyran and merocyanine systems. The focus of the derivatisation was on the substituent pattern at the chromene and indole moieties of the system (Scheme 87).

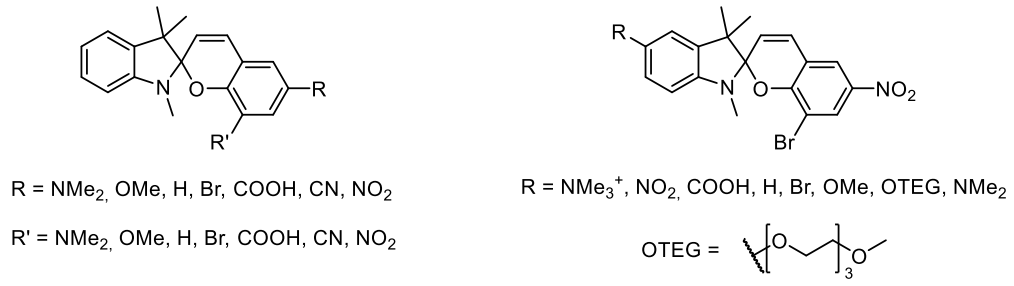

***Scheme 87*:** Selection of SP/MC systems included in the DFT studies on the dipole moments.

Detailed UV/Vis analysis was carried out on twelve of the synthesised SP/MC systems. This included analysis of the UV/Vis spectra after irradiation with UV and visible light and at equilibrium in the dark. A clear trend between the electronic character of the substituents and the equilibrium of the system could be shown. While electron-withdrawing substituents on the chromene moiety shift the equilibrium towards the merocyanine, on the indole moiety these substituents shift the equilibrium towards the spiropyran. For electron donating substituents these effects are reversed. With increasing strength of the electron-withdrawing substituents at the chromene, or electron-donating substituents at the indole, a change from positive to negative photochromism was observed. Additionally kinetic studies on the isomerisation on the of the systems were conducted and the rate constants were determined. Lower rate constants were obtained for those systems with electron-deficient chromene and electron-rich indole moieties (Scheme 88).

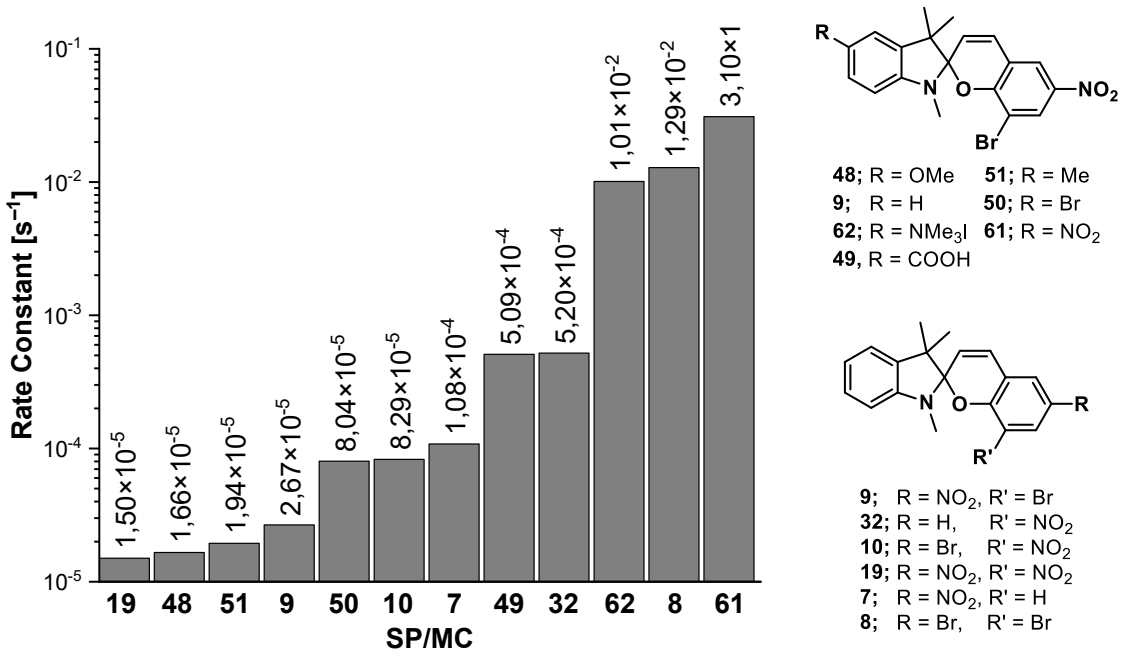

Scheme 88: Overview of the determined rate constants of substituted SP/MC systems.

The SP/MC ratio in the dark and after irradiation with visible light was also investigated via 1H-NMR spectroscopy for the indole substituted systems since the quantification of the Merocyanine is not possible via UV/Vis (Table 13). This was done in DMSO-d_6 and where applicable also in methanol-d_4. For all systems an almost quantitative formation of the spiropyran could be observed after irradiation with visible light.

Table 13: SP/MC ratio determined by ^{1}H-NMR spectroscopy in DMSO-d_6. The ratios were determined after the samples were kept in the dark for three days (left) or irradiated with visible light for one minute (right).

	Dark			Vis		
System	**SP**	**MC**	**% MC**	**SP**	**MC**	**% MC**
69	0.11	1.00	90	1.00	<0.05	<5
48	0.06	1.00	94	1.00	<0.05	<5
51	0.29	0.99	77	1.00	<0.05	<5
9	0.56	1.01	64	1.00	<0.05	<5
50	1.06	0.49	32	1.00	<0.05	<5
49	1.00	0.09	8	1.00	<0.05	<5
61	0.99	nd	<5	1.00	nd	<5
62	1.00	0.09	9	1.00	<0.05	<5

Regarding the SP/MC ratio in the dark, the trend described early was again verified with the lowest amount of merocyanine detected for nitro substituted system **61**

(<5 %) and the highest amount determined for methoxy substituted system **48** (94 %).

For proline isomerisation experiments six test systems were synthesized (Scheme 89). Five of these systems as well as the protected proline Ac-Pro-OMe were analysed regarding their *cis/trans*-ratio of the central proline in the presents of photoswitch **69** using ^{1}H-NMR spectrosopy. Unfortunately, for none of the tested systems, an influence of the *cis/trans*-ration of the proline could be observed upon the photochromic transition of the merocyanine to the spiropyran.

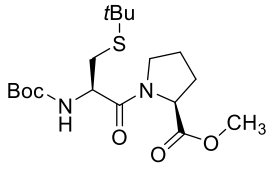

Boc-Cys(*t*Bu)-Pro-OMe
48 %

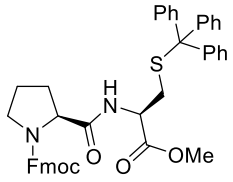

Fmoc-Pro-Cys(trt)-OMe
75 %

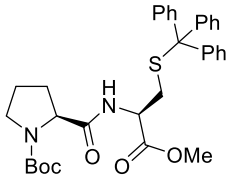

Boc-Pro-Cys(trt)-OMe
90 %

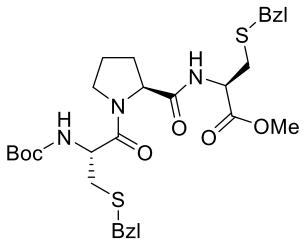

Boc-Cys(Bzl)-Pro-Cys(Bzl)-OMe
purity not sufficent for final tests

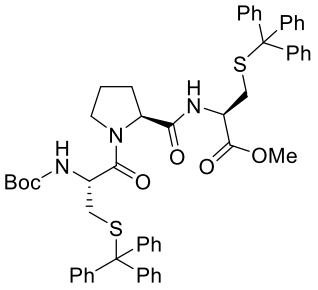

Boc-Cys(trt)-Pro-Cys(trt)-OMe
66 %

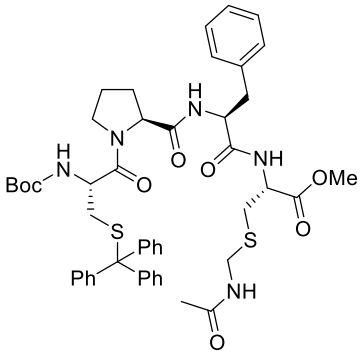

Boc-Cys(trt)-Pro-Phe-Cys(acm)-OMe
27 %

***Scheme 89*:** Proline-based peptides synthesised within this thesis.

Assuming that the *cis/trans*-ratio of the proline can be sufficiently influenced by dipolar interactions, the system **69** should be suitable since a large dipole moment change was calculated for the SP/MX isomerisation and the compound exhibits an almost quantitative switching behaviour. H. Wennemers[74] could show that the *cis/trans*-ratio of the protected proline Ac-Pro-NMe_2 could be affected by switching from polar solvents like H_2O and DMSO to less polar solvents like chloroform and dioxane. Therefore, in future experiments solvent should be changed from MeOH and DMSO less polar solvents. In less polar solvents the changes in dipole moment of the SP/MC system might have a higher impact while in very polar solvents these changes might be neglectable for the overall polarity. Before the real experiments on

the peptide models can be conducted, the studies on the reaction kinetics and the NMR ratios for the most promising photo switchable systems (**69** and **48**) are to be repeated in less polar solvents. Solubility problems could arise again during these experiments. The spiropyran shown in Scheme 90 might be very interesting for further application. The additional ethylene glycol chain should improve the overall solubility while the electron-donating amine substituent at the indole moiety might lead to a further stabilisation of the merocyanine form.

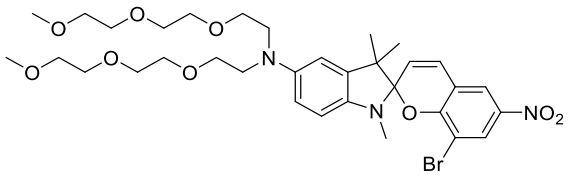

***Scheme 90*:** Structure of a new spiropyran which might further improve the solubility and the photochromic behaviour.

If after these adjustments an influence on the *cis/trans*-ratio of proline based on the photochromic SP/MC-isomerisation is detectable, the model systems should be adjusted. During this thesis it could be shown that a clear distinguishing between the proline isomers is often not possible even for smaller peptides. In 2023, Killoran et al.[132] were able to demonstrate that it is possible to distinguish between the proline isomers via ^{19}F-NMR if a *p*-fluor-phenylalanine amino acid is *C*-terminal bound to the proline. This is also possible if up to six other amino acids are between the proline and the substituted phenylalanine. Therefor the incorporation of this unnatural amino acid is very beneficial for our desired purpose.

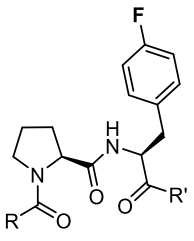

***Scheme 91*:** Structure of possible model compounds for future experiments. The fluorine substituent enables easier distinguishment between the proline isomers.

6 Experimental Part

6.1 General Information

Chemicals

All chemicals were bought from Sigma Aldrich, TCI, Fisher Scientific, Carl Roth and BLD Pharm and were, if not mentioned otherwise, directly used without further purification.

Solvents

All solvents were purchased in technically grade and freshly distilled before used. Dry solvents were purchased from Thermo Fisher/Acros Organic over molecular sieve under Acroseal. HPLC and LCMS grade solvents were purchased from Fisher Scientific.

Inert Conditions

As inert gas BIP© Argon (O_2 < 10 ppb, H_2O < 20 ppb, CO + CO_2 < 100 ppb) from AirProdukts was used. Inert reactions were performed using standard Schlenk technic.

Journal Numbers

For every procedure the reaction code of the corresponding entry in the laboratory journal is given in brackets [NIH-PXXX] at the upper left corner of the protocol. If the reaction was repeated, the revered procedure is highlighted in bold.

Thin Layer Chromatography (TLC) and Column Chromatography

For TLC, aluminium plates coated with Silicagel by *Merck* (Silica 60, F_{254}) were used. Detection was performed by UV-light (λ= 254 nm and 366 nm) or by staining with potassium permanganate or ninhydrin and subsequent heating. Silica gel for column chromatography was purchased from Acros Organics (0.035−0.070 mm, 60 Å).

Electrospray-Ionisation-Mass Spectrometry (Low resolution ESI-MS)

ESI-MS measurements were performed using an Agilent 1100 Series LC/MSD mass spectrometer with an G1313A autosampler, binary pump G1312A and mass selective G1956A detector.

HR ESI-MS

High resolution ESI-MS measurements were performed by Michael Neihs using a Thermo Scientific LTQ Orbitrap XL spectrometer with a FTMS analyser using a spray voltage of 3.2 KV.

Gas Chromatography-Mass Spectrometry (GC-MS)

GC-MS measurements were performed using a Hewlett-Packard HP 6890 Series gas chromatograph coupled with a HP 5973 mass detector column: HP-5: Crosslinked Methyl silicone gum capillary column, 25 m, 0.2 µm, 0.33 µm.: Carrier gas: H_2. Temperature program (Stand 50): 50 °C (2 min), 20 °C/min, 280 °C (10 min). Relative intensities are given in brackets and normalized to the strongest peak.

Nuclear Magnetic Resonance (NMR) Spectroscopy

^{1}H-NMR-spectra were recorded with Avance 300 (300 MHz) and 500 (500 MHz) spectrometers by Bruker. For measurements, the substances were dissolved in deuterated solvents ($CDCl_3$, DMSO-d_6, MeOD-d_4, D_2O). The chemical shifts are referenced on TMS (δ = 0 ppm) (^{1}H-spectra) or the characteristic solvent peaks (^{13}C-spectra). Assignment was done with the software MestReNova 11.0. Multiplicities for proton signals were characterized using “br” for broad signals, “s” for singlet, “d” for doublet, “dd” for doubled of doublets, “t” for triplet and “dt” for doublet of triplets. The scalar coupling constants are presented in Hertz (Hz). ^{13}C-NMR spectra were recorded with 75 MHz or 125 MHz. The assignment of the ^{1}H and ^{13}C resonances was obtained from ^{1}H-COSY, ^{1}H-, ^{13}C- HSQC and HMBC experiments. For reasons of clarity the carbon atoms of the compound were numbered in a way which not necessarily correlates with IUPAC nomenclature. The switching experiments were all performed with an AVANCE II+ 600 by Bruker.

Fourier-Transform Infrared Spectroscopy (FT-IR)

IR-spectra were recorded using a IRAffinity-1S FT-IR spectrometer by *Shimadzu* at 25 °C. Absorption bands are given in wavenumbers (v [cm^{-1}]) and marked as s (strong), m (medium) or w (weak) with a prefixed br indicating broad signals.

UV/Vis-Spectroscopy

UV/Vis analysis was performed using a Jasco V-730 spectrometer with an ETCS-761 Peltier thermostatic single position cell holder. all measurements were performed in

0.025 mM solutions at 20 °C using HPLC or LCMS grade solvents. Suprasil 110-QS cuvettes by the company Hellma were used.

Irradiation of the samples

UV-irradiation was done using a Konrad Benda UV-C lamp with 15 W and a wavelength of 254 nm. For irradiation with visible light a 100 W LED construction spotlight was used.

DFT Calculations

The ORCA 5.0 software package[93] was used for all calculations. The calculations were performed on the CHEOPS HPC cluster. After the initial screening all calculations were done as follows. The geometry optimisation of the structures was performed using the B3LYP functional with the D3BJ dispersions correction and the def2-TZVPPD triple-ζ basis set with polarisation functions for light and heavy atoms and a set of diffuse functions. Frequency analysis of the optimised structures was done to exclude negative frequencies. Afterward the single point energy of the optimised structure was calculated using the B3LYP D3BJ functional and the def2-QZVPPD quadruple- ζ basis set with polarisation functions for light and heavy atoms and a set of diffuse functions.

6.2 Derivatisation of the Sidechain

Synthesis of 1-(2-carboxyethyl)-2,3,3-trimethyl-3H-indol-1-ium bromide

[NIH_P132, **VAG_03**]

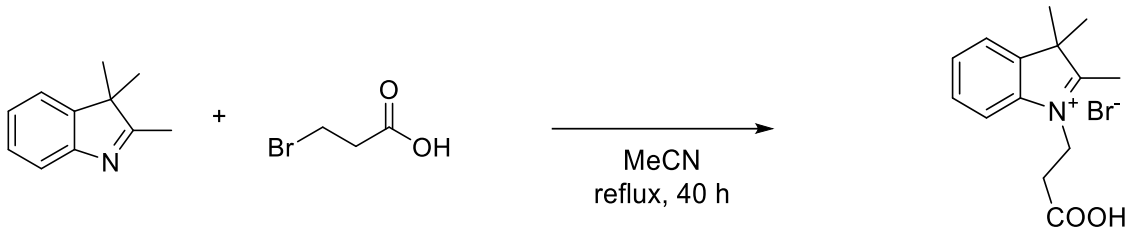

25 **26** **22**

Under argon atmosphere, 3-bromopropionic acid (**26**) (10.6 g, 69.2 mmol, 1.1 eq.) and indole **25** (10.0 g, 62.8 mmol, 1.0 eq.) were dissolved in dry MeCN (20 mL) and heated to reflux. After 22 h, TLC only indicated a partial conversion. Therefore, additional 3-bromopropionic acid (**26**) (2.87 g, 18.8 mmol, 0.3 eq.) was added and the reaction was refluxed for further 18 h. After cooling to ambient temperature, the solvent was removed under reduced pressure. Et_2O was added to the residue and the solvent was decanted. The remaining solid was recrystallised from acetone. The product was filtered off and washed with cold acetone. Indolium **22** was obtained as beige solid in 46 % (9.02 g, 28.9 mmol) yield.

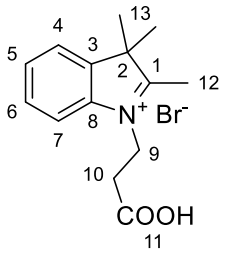

M($C_{14}H_{18}NO_2Br$)**:** 312.21 g·mol^{-1}.

Habitus: Beige solid.

Yield: 9.02 g (28.9 mmol, 46 %, Lit.:[115] 77 %).

R_f: 0.1 (3:1, DCM:MeOH).

Mp.: 175–176 °C (Lit.:[133] 174–176 °C).

^{1}H-NMR: (500 MHz, DMSO-d_6) δ [ppm] = 12.71 (s, 1H, H-11), 8.03 – 7.96 (m, 1H), 7.88 – 7.80 (m, 1H), 7.66 – 7.59 (m, 2H), 4.66 (t, $^3J_{H9\text{-}H10}$ = 7.0 Hz, 2H, H-9), 2.99 (t, $^3J_{H10\text{-}H9}$ = 7.0 Hz, 2H, H-10), 2.87 (s, 3H, H-12), 1.53 (s, 6H, H-13, H-13').

^{13}C-NMR: (126 MHz, DMSO-d_6) δ [ppm] = 197.9 (C_q, 1C, C-1), 171.5 (C_q, 1C, C-11), 141.8 (C_q, 1C, C-3), 140.8 (C_q, 1C, C-8), 129.3 (CH_{Ar}, 1C), 128.9 (CH_{Ar}, 1C), 123.5 (CH_{Ar}, 1C), 115.6 (CH_{Ar}, 1C), 54.3 (C_q, 1C, C-2), 43.5 (CH_2, 1C, C-9), 31.1 (CH_2, 1C, C-10), 21.9 (CH_3, 2C, C-13), 14.4 (CH_3, 1C, C-12).

Due to an overlap in the NMR-spectra, the signals cannot be completely assigned.

FT-IR (ATR): $\tilde{\nu}$ [cm^{-1}] = 3312 (w), 3028 (w), 2982 (br, w), 2837 (w), 1715 (s), 1622 (w), 1591 (w), 1456 (m), 1408 (m), 1366 (m), 1329 (w), 1298 (w),1269 (m), 1233 (m), 1223 (m), 1186 (s), 1128 (w), 1047 (w), 1032 (w), 991 (w), 966 (w), 932 (m), 914 (w), 880 (w), 843 (m), 800 (w), 773 (s), 758 (m), 687 (w), 665 (m), 637 (m).

The analytic data are in agreement with the literature[115, 133]

Synthesis of 3-(3',3'-dimethyl-6-nitrospiro[chromene-2,2'-indolin]-1'-yl)propanoic acid

[VAG_06]

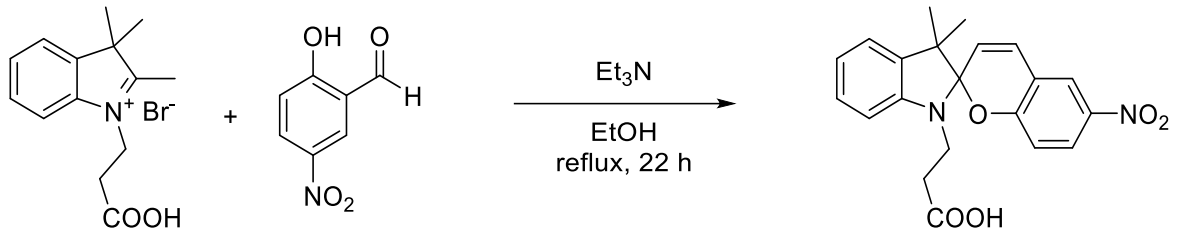

22 **29** **30**

Under argon atmosphere, indolium **22** (3.27 g, 10.5 mmol, 1.00 eq.) and salicylic aldehyde **29** (1.84 g, 11.0 mmol, 1.05 eq.) were dissolved in EtOH (70 mL, HPLC grade) and triethylamine (1.70 mL, 12.3 mmol, 1.17 mmol) was added. The solution was refluxed for 22 h and then cooled to ambient temperature. The precipitated solid was filtered off and washed with cold EtOH. After recrystallisation from MeOH, spiropyran **30** was obtained as a yellow solid in 67 % (2.68 g, 7.05 mmol) yield.

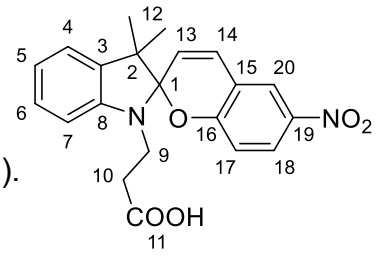

M($C_{21}H_{20}N_2O_5$)**:** 380.40 g·mol^{-1}.

Habitus: Yellow solid.

Yield: 2.68 g (7.05 mmol, 67 %, Lit.:[118] 84 %).

R_f: 0.3 (20:1, DCM:MeOH).

Mp.: 195 °C (decomp.).

^{1}H-NMR: (500 MHz, DMSO-d_6) δ [ppm] = 12.23 (s, 1H, H-11), 8.22 (d, $^4J_{H20\text{-}H18}$ = 2.8 Hz, 1H, H-20), 8.00 (dd, $^3J_{H18\text{-}H17}$ = 9.0 Hz, $^4J_{H18\text{-}H20}$ = 2.8 Hz, 1H, H-18), 7.21 (d, $^3J_{H14\text{-}H13}$ = 10.4 Hz, 1H, H-14),

7.18 – 7.08 (m, 2H, H-4, H-6), 6.87 (d, $^{3}J_{H17\text{-}H18}$ = 9.0 Hz, 1H, H-17), 6.81 (t, $^{3}J_{H5\text{-}H4,\ H5\text{-}H6}$ = 7.4 Hz, 1H, H-5), 6.67 (d, $^{3}J_{H7\text{-}H6}$ = 7.7 Hz, 1H, H-7), 6.00 (d, $^{3}J_{H13\text{-}H14}$ = 10.4 Hz, 1H, H-13), 3.50 (ddd, $^{2}J_{H9\text{-}H9}$ = 14.8 Hz, $^{3}J_{H9\text{-}H10}$ = 8.3 Hz, $^{3}J_{H9\text{-}H10}$ = 6.7 Hz, 1H, H-9), 3.38 (ddd, $^{2}J_{H9\text{-}H9}$ = 14.8, $^{3}J_{H9\text{-}H10}$ = 8.0 Hz, $^{3}J_{H9\text{-}H10}$ = 5.9 Hz, 1H, H-9), 2.65 – 2.54 (m, 1H, H-10), 2.46 (ddd, $^{2}J_{H10\text{-}H9}$ = 15.9 Hz, $^{3}J_{H10\text{-}H9}$ = 8.3 Hz, $^{3}J_{H10\text{-}H9}$ = 5.9 Hz, 1H, H-10), 1.19 (s, 3H, H-12/H-12'), 1.08 (s, 3H, H-12/H-12').

^{13}C-NMR: (75 MHz, DMSO-d_6) δ [ppm1] = 172.8 (C_q, 1C, C-11), 159.1 (C_q, 1C, C-16), 146.1 (C_q, 1C, C-8), 140.5 (C_q, 1C, C-19), 135.6 (C_q, 1C, C-3), 128.2 (CH_{Ar}, 1C, C-14), 127.6 (CH_{Ar}, 1C, C-6), 125.7 (CH_{Ar}, 1C, C-18), 122.8 (CH_{Ar}, 1C, C-20), 121.8 (CH_{Ar}, 2C, C-4, C-13), 119.2 (CH_{Ar}, 1C, C-5), 118.8 (C_q, 1C, C-15), 115.5 (CH_{Ar}, 1C, C-17), 106.6 (CH_{Ar}, 1C, C-7), 106.5 (C_q, 1C, C-1), 52.4 (C_q, 1C, C-2), 38.9 (CH_2, 1C, C-9), 33.2 (CH_2, 1C, C-10), 25.6 (CH_3, 1C, C-12), 19.5 (CH_3, 1C, C-12).

FT-IR (ATR): $\tilde{\nu}$ [cm^{-1}] = 3078 (w), 2972 (w), 2901 (w), 2870 (w), 1701 (m), 1655 (w), 1601 (w), 1574 (w), 1508 (m), 1483 (m), 1456 (w), 1441 (w), 1404 (w), 1377 (w), 1360 (w), 1325 (m), 1296 (m), 1269 (m), 1211 (w), 1196 (w), 1159 (m), 1142 (w), 1126 (w), 1086 (m), 1055 (w), 1028 (m), 997 (w), 935 (s), 914 (s), 835 (m), 802 (s), 781 (m), 750 (s), 716 (w), 679 (m), 633 (w).

The analytic data are in agreement with the literature[118]

Synthesis of 1-benzyl-2,3,3-trimethyl-3H-indol-1-ium bromide

[NIH_P133]

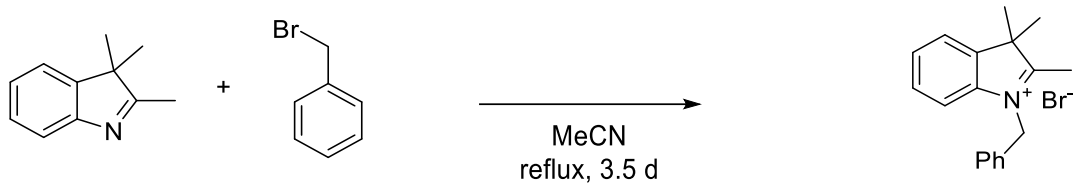

25 **27** **23**

Under argon atmosphere, indole **25** (5.0 mL, 31 mmol, 1.0 eq.) was dissolved in dry acetonitrile (50 mL). Benzyl bromide (**27**) (5.5 mL, 47 mmol, 1.5 eq.) was added and the reaction was heated to reflux for 3.5 d. Even though TLC indicated no full conversion, the reaction was stopped. After cooling to ambient temperature, the solvent was removed under reduced pressure and the remaining residue was recrystallised from acetone. Indolium bromide **23** was obtained as a pale-yellow solid in 52 % (5.2 g, 16 mmol) yield.

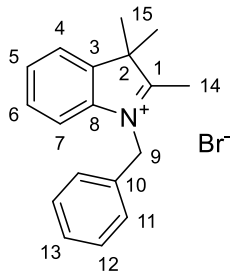

M($C_{18}H_{20}BrN$): 330.27 g·mol^{-1}.

Habitus: Pale-yellow solid.

Yield: 5.2 g (16 mmol, 52 %, Lit.:[116] 77 %).

Mp.: 183–186 °C, Lit.:[116] 226–230 °C.

^{1}H-NMR: (500 MHz, DMSO-d_6) δ [ppm] = 7.89 (d, $^3J_{H4\text{-}H5}$ = 7.4 Hz, 1H, H-4), 7.83 (d, $^3J_{H7\text{-}H6}$ = 7.9 Hz, 1H, H-7), 7.61 (φt, $^3J_{H5\text{-}H4,\ H5\text{-}H6}$ = 7.4 Hz, 1H, H-5), 7.56 (φt, $^3J_{H6\text{-}H5,\ H6\text{-}H7}$ = 7.6 Hz, 1H, H-6), 7.47 – 7.37 (m, 5H, H-11, H-12, H-13), 5.88 (s, 2H, H-9), 3.02 (s, 3H, H-14), 1.62 (s, 6H, H-15, H-15').

^{13}C-NMR: (75 MHz, DMSO-d_6) δ [ppm] = 198.1 (C_q, 1C, C-1), 141.9 (C_q, 1C, C-3), 141.0 (C_q, 1C, C-8), 132.1 (C_q, 1C, C-10), 129.5 (CH_{Ar}, 1C, C-5), 129.2 (CH_{Ar}, 2C, C-12), 128.9 (CH_{Ar}, 1C, C-6), 128.7 (CH_{Ar}, 1C, C-13), 127.4 (CH_{Ar}, 2C, C-11), 123.6 (CH_{Ar}, 1C, C-4), 115.9 (CH_{Ar}, 1C, C-7), 54.5 (C_q, 1C, C-2), 50.7 (CH_2, 1C, C-9), 22.2 (CH_3, 2C, C-15, C-15'), 14.7 (CH_3, 1C, C-14).

FT-IR: $\tilde{\nu}$ [cm^{-1}] = 2968 (w), 2901 (w), 2870 (w), 1626 (w), 1607 (w), 1477 (w), 1445 (m), 1362 (w), 1342 (w), 1302 (w), 1261 (w),

1231 (w), 1202 (w), 1080 (w), 1057 (w), 1020 (w), 997 (w), 957 (w), 928 (w), 910 (w), 822 (w), 764 (s), 743 (s), 694 (m), 665 (w).

LR-ESI-MS: m/z = pos: 250.1 $[M–Br]^+$.

The analytic data are in agreement with the literature[116]

Synthesis of 1'-benzyl-3',3'-dimethyl-6-nitrospiro[chromene-2,2'-indoline]

[VAG_18]

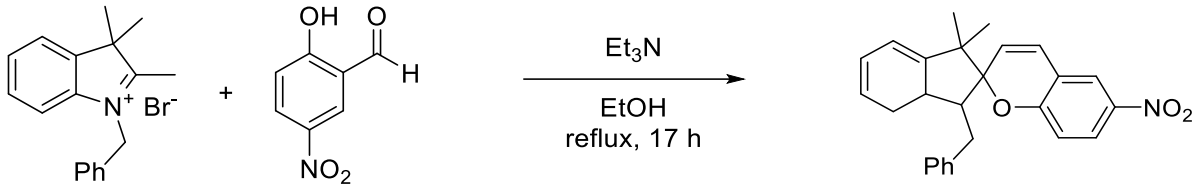

23 **29** **31**

Under argon atmosphere, indolium **23** (1.65 g, 5.00 mmol, 1.0 eq.) and salicylic aldehyde **29** (0.91 g, 5.5 mmol, 1.1 eq.) were dissolved in EtOH (45 mL, HPLC grade) and triethylamine (0.82 mL, 5.9 mmol, 1.2 eq.) was added. The reaction was refluxed for 17 h. After cooling to ambient temperature, the precipitated solid was filtered off and washed with cold EtOH. Spiropyran **31** was obtained as a yellow solid in 89 % (1.77 g, 4.44 mmol) yield.

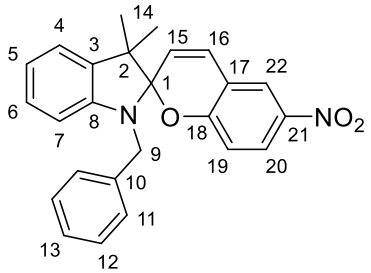

M($C_{25}H_{22}N_2O_3$)**:** 398.46 g·mol^{-1}.

Habitus: Yellow solid.

Yield: 1.77 g (4.44 mmol, 89 %).

R_f: 0.5 (2:1, *c*Hex:DCM).

Mp.: 159–161 °C (Lit.:[50] 162–163 °C).

^{1}H-NMR: (500 MHz, $CDCl_3$) δ [ppm] = 7.97 (dd, $^3J_{H20\text{-}H19}$ = 8.8 Hz, $^4J_{H20\text{-}H22}$ = 2.8 Hz, 1H, H-20), 7.95 (d, $^4J_{H22\text{-}H20}$ = 2.8 Hz, 1H, H-22), 7.30 – 7.24 (m, 4H, H-11, H-12), 7.23 – 7.18 (m, 1H, H-13), 7.11 (d, $^3J_{H4\text{-}H5}$ = 7.2 Hz, 1H, H-4), 7.04 (t, $^3J_{H6\text{-}H5,\ H6\text{-}H7}$ = 7.6 Hz, 1H, H-6), 6.89 – 6.80 (m, 2H, H-5, H-16), 6.72 (d, $^3J_{H19\text{-}H20}$ = 8.8 Hz, 1H, H-19), 6.34 (d, $^3J_{H7\text{-}H6}$ = 7.8 Hz, 1H, H-7), 5.90 (d, $^3J_{H15\text{-}H16}$ = 10.4 Hz, 1H, H-15), 4.51 (d, $^2J_{H9\text{-}H9}$ = 16.5 Hz, 1H, H-9), 4.21 (d,

$^{2}J_{H9\text{-}H9}$ = 16.5 Hz, 1H, H-9), 1.34 (s, 3H, H-14/H-14'), 1.30 (s, 3H, H-14/H-14').

^{13}C-NMR: (126 MHz, $CDCl_3$) δ [ppm] = 159.6 (C_q, 1C, C-18), 147.1 (C_q, 1C, C-8), 141.0 (C_q, 1C, C-21), 138.6 (C_q, 1C, C-10), 136.1 (C_q, 1C, C-3), 128.6 (CH_{Ar}, 2C, C-11/C-12), 128.5 (CH_{Ar}, 1C, C-16), 127.8 (CH_{Ar}, 1C, C-6), 127.1 (CH_{Ar}, 1C, C-13), 126.6 (CH_{Ar}, 2C, C-11/C-12), 125.9 (CH_{Ar}, 1C, C-20), 122.7 (CH_{Ar}, 1C, C-22), 121.7 (CH_{Ar}, 1C, C-15), 121.6 (CH_{Ar}, 1C, C-4), 120.0 (CH_{Ar}, 1C, C-5), 118.6 (C_q, 1C, C-17), 115.5 (CH_{Ar}, 1C, C-19), 107.9 (CH_{Ar}, 1C, C-7), 106.8 (C_q, 1C, C-1), 52.8 (C_q, 1C, C-2), 47.7 C_q, 1C, C-9), 26.2 (CH_3, 1C, C-14/C-H14'), 19.9 (CH_3, 1C, C-14/C-H14').

FT-IR (ATR): $\tilde{\nu}$ [cm^{-1}] = 3096 (w), 3059 (w), 2988 (w), 2965 (w), 2907 (w), 1649 (w), 1609 (w), 1574 (w), 1510 (m), 1479 (m), 1450 (w), 1331 (s), 1314 (w), 1275 (s), 1161 (m), 1124 (m), 1090 (m), 1065 (w), 1034 (m), 993 (w), 949 (s), 934 (m), 916 (s), 899 (m), 810 (m), 795 (m), 772 (m), 745 (s), 729 (s), 694 (s), 662 (m).

GC-MS: τ_R= min; $^{m}/_{z}$ (%) = 398 [M^+, (100)], 307 (29), 235 (17), 207 (10), 91 (45).

The analytic data are in agreement with the literature[134]

Synthesis of 3-(2,3,3-trimethyl-3H-indol-1-ium-1-yl)propane-1-sulfonate

[NIH_P117; NIH_P119, **VAG_13**]

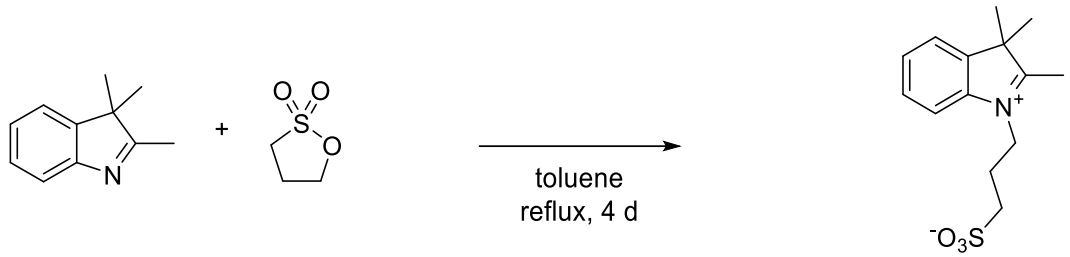

25 **28** **24**

Under argon atmosphere, 1,3-propansultone (**28**) (2.56 g, 21.0 mmol, 1.1 eq.) and indole **25** (3.01 g, 18.9 mmol, 1.0 eq.) were dissolved in dry toluene (150 mL) and heated to reflux. After 2.5 d, additional 1,3-propansultone (**28**) (1.45 g, 11.9 mmol, 0.6 eq.) was added since TLC only indicated partial conversion. After 22 h, additional 1,3-propansultone (**28**) (1.45 g, 11.9 mmol, 0.6 eq.) as well as dry toluene (20 mL) were added and the mixture was refluxed for 5 h. After refluxing for almost four days in total, TLC still indicated uncompleted conversion. The solvent was removed under reduced pressure and the residue was purified by column chromatography over silica (100 % DCM to 5:1, DCM: MeOH). The residue was dissolved in water and HCl (6 M) was added until a pH of two was obtained. The solvent was removed under reduced pressure and indolium **24** was obtained as a red solid in 61 % (3.25 g, 11.6 mmol) yield.

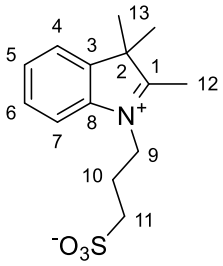

M($C_{14}H_{19}NO_3S$)**:** 281.37 g·mol^{-1}.

Habitus: Red solid.

Yield: 3.25 g (11.6 mmol, 61 %).

R_f: 0.2 (5:1, DCM:MeOH).

Mp.: 96 °C. Lit[117] 242–243 °C

^{1}H-NMR: (500 MHz, DMSO-d_6) δ [ppm] = 8.10 – 8.02 (m, 1H, H-5/H-7), 7.88 – 7.79 (m, 1H, H-4), 7.65 – 7.58 (m, 2H, H-6, H-5/H-7), 4.76 – 4.60 (m, 2H, H-9), 2.85 (s, 3H, H-12), 2.64 (t, $^3J_{H11\text{-}H10}$ = 6.5 Hz, 2H, H-11), 2.21 – 2.13 (m, 2H, H-10), 1.54 (s, 6H, H-13).

^{13}C-NMR: (126 MHz, DMSO-d_6) δ [ppm] = 197.1 (C_q, 1C, C-1), 142.4 (C_q, 1C, C-3), 141.7 (C_q, 1C, C-8), 129.8 (CH_{Ar}, 1C, C-5/C-7), 129.4 (CH_{Ar}, 1C, C-6), 123.9(CH_{Ar}, 1C, C-4), 115.9 (CH_{Ar}, 1C, C-5/C-7),

54.6 (C_q, 1C, C-2), 47.9 (CH_2, 1C, C-11), 47.1 (CH_2, 1C, C-9), 24.2 (CH_2, 1C, C-10), 22.5 (CH_3, 2C, C-13), 14.3 (CH_3, 1C, C-12).

FT-IR (ATR): $\tilde{\nu}$ [cm^{-1}] = 3362 (br, w), 3022 (w), 2976 (w), 2934 (w), 2878 (w), 1715 (w), 1626 (w), 1607 (w), 1593 (w), 1479 (m), 1460 (m), 1420 (w), 1395 (w), 1369 (w), 1333 (w), 1300 (w), 1271 (w), 1215 (s), 1152 (s), 1124 (s), 1034 (s), 934 (m), 766 (s), 723 (s), 683 (s), 660 (s), 613 (s).

The NMR data are in agreement with the literature[116]

Synthesis of 3-(3',3'-dimethyl-6-nitrospiro[chromene-2,2'-indolin]-1'-yl)propane-1-sulfonate

[VAG_10]

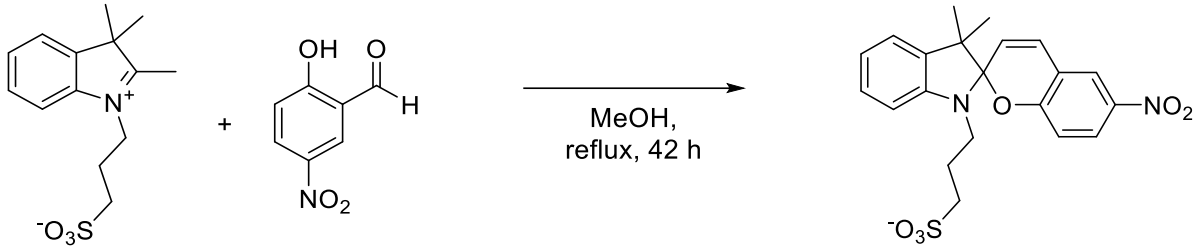

24 **29** **1b**

Under argon atmosphere, indole **24** (1.69 g, 6.00 mmol, 1.0 eq.) and salicylic aldehyde **29** (1.3 g, 7.8 mmol, 1.3 eq.) were suspended in dry methanol (35 mL) and heated to reflux. After 42 h, the reaction was cooled to ambient temperature, the solvent was removed under reduced pressure and the crude product was purified by column chromatography over silica (5:1, DCM:MeOH). Spiropyran **1b** was isolated a yellow solid in 49 % (1.27 g, 2.96 mmol) yield.

M($C_{21}H_{21}N_2O_6S^-$)**:** 430.48 g·mol^{-1}.

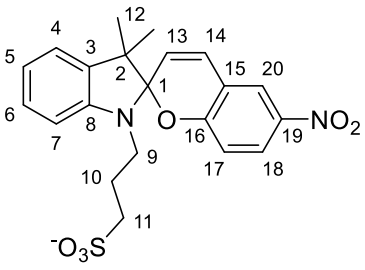

Habitus: Yellow solid.

Yield: 1.27 g (2.96 mmol, 49 %, Lit.:[119] 83 %).

R_f: 0.3 (5:1, DCM:MeOH).

Mp.: 285°C (decomp.).

^{1}H-NMR: (500 MHz, DMSO-d_6) δ [ppm] = 8.21 (d, $^{4}J_{H20\text{-}H18}$ = 2.9 Hz, 1H, H-20), 7.99 (dd, $^{3}J_{H18\text{-}H17}$ = 9.0 Hz, $^{4}J_{H18\text{-}H17}$ = 2.9 Hz, 1H, H-18), 7.21 (d, $^{3}J_{H14\text{-}H13}$ = 10.4 Hz, 1H, H-14), 7.14 – 7.07 (m, 2H, H-4, H-6), 6.86 (d, $^{3}J_{H17\text{-}H18}$ = 9.0 Hz, 1H, H-17), 6.78 (t, $^{3}J_{H5\text{-}H4,\ H5\text{-}H6}$ = 7.4 Hz, 1H, H-5), 6.70 (d, $^{3}J_{H7\text{-}H6}$ = 7.6 Hz, 1H, H-7), 5.98 (d, $^{3}J_{H13\text{-}H14}$ = 10.4 Hz, 1H, H-13), 3.22 (t, $^{3}J_{H9\text{-}H10}$ = 7.4 Hz, 2H. H-9), 2.48 – 2.37 (m, 2H, H-11), 1.92 – 1.78 (m, 2H, H-10), 1.20 (s, 3H, H-12/H-12'), 1.10 (s, 3H, H-12/H-12').

^{13}C-NMR: (126 MHz, DMSO-d_6) δ [ppm] =159.3 (C_q, 1C, C-16), 146.9 (C_q, 1C, C-8), 140.4 (C_q, 1C, C-19), 135.5 (C_q, 1C, C-3), 128.1 (CH_{Ar}, 1C, C-14), 127.6 (CH_{Ar}, 1C, C-6), 125.7 (CH_{Ar}, 1C, C-18), 122.8 (CH_{Ar}, 1C, C-20), 121.8 (CH_{Ar}, 1C, C-13), 121.6 (CH_{Ar}, 1C, C-4), 118.9 (CH_{Ar}, 1C, C-5), 118.8 (C_q, 1C, C-15), 115.5 (CH_{Ar}, 1C, C-17), 106.7 (CH_{Ar}, 1C, C-7), 106.5 (C_q, 1C, C-1), 52.4 (CH_{Ar}, 1C, C-2), 49.0 (CH_2, 1C, C-11), 42.3 (CH_2, 1C, C-9), 25.8 (CH_3, 1C, C-12/C-12'), 24.8 (CH_2, 1C, C-10), 19.5 (CH_3, 1C, C-12/C-12').

FT-IR (ATR): $\tilde{\nu}$ [cm^{-1}] = 3065 (w), 2976 (w), 2932 (w), 2704 (w), 1605 (m), 1584 (w), 1539 (m), 1514 (w), 1489 (w), 1472 (w), 1435 (w), 1369 (w), 1339 (s), 1321 (w), 1298 (m), 1256 (m), 1233 (s), 1198 (w), 1153 (s), 1128 (m), 1088 (m), 1078 (m), 1032 (s), 980 (m), 961 (w), 901 (w), 868 (m), 858 (m), 839 (m), 797 (w), 773 (m), 745 (s), 700 (w), 617 (w).

The analytic data are in agreement with the literature[119]

6.3 Derivatization of the Chromene

Synthesis of (*E*)-2-(3,5-dibromo-2-hydroxystyryl)-1,3,3-trimethyl-3H-indol-1-ium iodide

[NIH_P304]

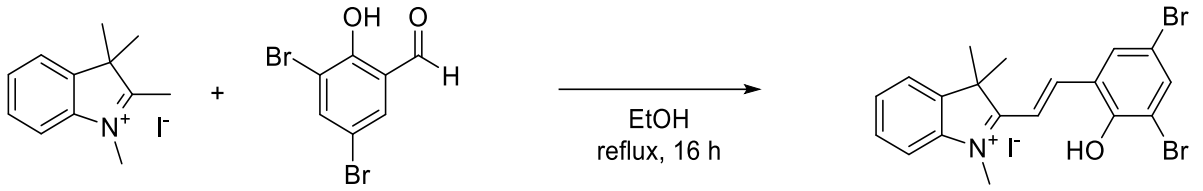

33 **34** **35**

Under argon atmosphere, indolium **33** (1.51 g, 5.00 mmol, 1.0 eq.) and salicylic aldehyde **34** (1.40 g, 5.00 mmol, 1.0 eq.) were suspended in dry EtOH (20 mL) and heated to reflux. After 16 h, full conversion was confirmed by TLC. The solution was cooled to ambient temperature and the precipitated product was filtered of and dried under reduced pressure. Indolium iodide **35** was obtained as a bright orange solid in 90 % (2.53 g, 4.49 mmol) yield.

M($C_{19}H_{18}Br_2INO$)**:** 563.07 g·mol^{-1}.

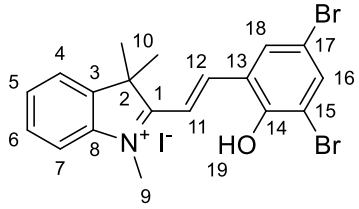

Habitus: Bright orange solid.

Yield: 2.53 g (4.49 mmol, 90 %).

Mp.: 221–223 °C.

^{1}H-NMR: (500 MHz, DMSO-d_6) δ [ppm] = 8.46 (d, $^4J_{H16\text{-}H18}$ = 2.4 Hz, 1H, H-16), 8.39 (d, $^3J_{H12\text{-}H11}$ = 16.5 Hz, 1H, H-12), 8.02 (d, $^4J_{H18\text{-}H16}$ = 2.4 Hz, 1H, H-18), 7.98 – 7.93 (m, 1H, H-7), 7.91 – 7.85 (m, 1H, H-4), 7.76 (d, $^3J_{H11\text{-}H12}$ = 16.5 Hz, 1H, H-11), 7.74 – 7.63 (m, 2H, H-5, H-6), 4.18 (s, 3H, H-9), 1.77 (s, 6H, H-10).

^{13}C-NMR: (126 MHz, DMSO-d_6) δ [ppm] = 181.7 (C_q, 1C, C-1), 153.8 (C_q, 1C, C-14), 145.1 (CH, 1C, C-12), 143.6 (C_q, 1C, C-3), 141.8 (C_q, 1C, C-8), 138.6 (CH_{Ar}, 1C, C-16), 130.3 (CH_{Ar}, 1C, C-18), 129.7 (CH_{Ar}, 1C, C-5), 129.1 (CH_{Ar}, 1C, C-6), 126.0 (C_q, 1C, C-13), 122.9 (CH_{Ar}, 1C, C-4), 115.5 (CH_{Ar}, 1C, C-7), 114.9 (CH, 1C, C-11), 114.3 (C_q, 1C, C-15), 112.5 (C_q, 1C, C-17), 52.3 (C_q, 1C, C-2), 34.9 (CH_3, 2C, C-9), 25.5 (CH_3, 2C, C-10).

Spiropyran:

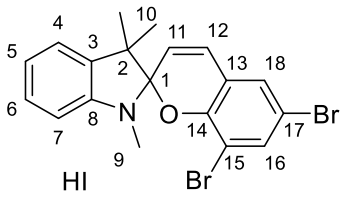

^{1}H-NMR: (500 MHz, DMSO-d_6) δ [ppm] = 7.58 (d, $^{4}J_{H16\text{-}H18}$ = 2.4 Hz, 1H, H16), 7.48 (d, $^{4}J_{H18\text{-}H16}$ = 2.4 Hz, 1H, H-18), 7.16 – 7.09 (m, 2H, H-4, H-6), 7.04 (d, $^{3}J_{H12\text{-}H11}$ = 10.3 Hz, 1H, H-12), 6.79 (φtd, $^{3}J_{H5\text{-}H4;\ H5\text{-}H6}$ = 7.4 Hz, $^{4}J_{H5\text{-}H7}$ = 1.0 Hz, 1H, H-5), 6.62 – 6.59 (m, 1H, H-7), 5.92 (d, $^{3}J_{H11\text{-}H12}$ = 10.2 Hz, 1H, H-11), 2.65 (s, 3H, H-9), 1.22 (s, 3H, H-10/H-10'), 1.10 (s, 3H, H-10/H-10').

^{13}C-NMR: (126 MHz, DMSO-d_6) δ [ppm] = 149.6 (C_q, 1C, C-14), 147.4 (C_q, 1C, C-8), 135.9 (C_q, 1C, C-3), 133.9 (CH_{Ar}, 1C, C-16), 128.6 (CH_{Ar}, 1C, C-18), 128.0 (CH_{Ar}, 1C, C-12), 127.5 (CH_{Ar}, 1C, C-6/4), 122.0 (C_q, 1C, C-13), 121.8 (CH_{Ar}, 1C, C-11), 121.4 (CH_{Ar}, 1C, C-6/4), 119.3 (CH_{Ar}, 1C, C-5), 111.4 (C_q, 1C, C-15/C-17), 109.2 (C_q, 1C, C-15/C-17), 106.9 (CH_{Ar}, 1C, C-7), 105.7 (C_q, 1C, C-1), 51.7 (C_q, 1C, C-2), 28.5 (CH_3, 1C, C-9'), 25.6 (CH_3, 1C, C-10/C-10'), 19.9 (CH_3, 1C, C-10/C-10').

FT-IR (ATR): $\tilde{\nu}$ [cm^{-1}] = 3092 (m), 3042 (m), 2968 (m), 2924 (m), 1605 (s), 1555 (s), 1476 (m), 1443 (s), 1396 (m), 1310 (s), 1292 (s), 1240 (s), 1229 (s), 1169 (s), 1117 (s), 1094 (s), 1045 (s), 1018 (s), 959 (s), 918 (m), 841 (s), 826 (s), 791 (s), 743 (s), 735 (s), 719 (s), 687 (s).

Synthesis of 6,8-dibromo-1',3',3'-trimethylspiro[chromene-2,2'-indoline]

[NIH_P308]

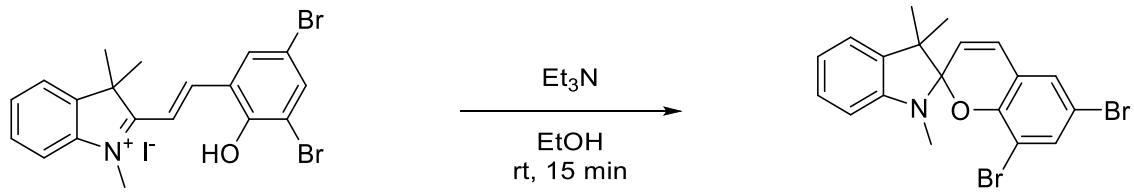

35 **8**

Indolium iodide **35** (1.12 g, 2.00 mmol, 1.0 eq.) and triethylamine (0.31 mL, 2.3 mmol, 1.1 eq.) were suspended in EtOH (7 mL, HPLC grade) and stirred for 15 min at ambient temperature. The solvent was removed under reduced pressure and the residue was refluxed for 15 min in water (25 mL). After cooling to ambient temperature, the solvent was filtered of and dried under reduced pressure. Spiropyran **8** was obtained as a beige solid in 75 % (0.66 g, 1.5 mmol) yield.

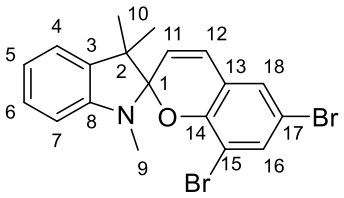

M($C_{19}H_{17}Br_2NO$)**:** 435.16 g·mol^{-1}.

Habitus: Beige solid.

Yield: 0.66 g (1.5 mmol, 75 %).

Mp.: 117–119°C, turns blue upon melting.

^{1}H-NMR: (500 MHz, DMSO-d_6) δ [ppm] = 7.58 (d, $^4J_{H16\text{-}H18}$ = 2.3 Hz, 1H, H-16), 7.48 (d, $^4J_{H18\text{-}H16}$ = 2.3 Hz, 1H, H-18), 7.15 – 7.09 (m, 2H, H-4, H-6), 7.03 (d, $^3J_{H12\text{-}H11}$ = 10.3 Hz, 1H, H-12), 6.79 (td, $^3J_{H5\text{-}H4,\ H5\text{-}H6}$ = 7.4 Hz, $^4J_{H5\text{-}H7}$ = 1.0 Hz, 1H, H-5), 6.60 (d, $^3J_{H7\text{-}H6}$ = 7.6 Hz, 1H, H-7), 5.92 (d, $^3J_{H11\text{-}H12}$ =10.3 Hz, 1H, H-11), 2.65 (s, 3H, H-9), 1.22 (s, 3H, H-10/H-10'), 1.10 (s, 3H, H-10/H-10').

^{13}C-NMR: (126 MHz, DMSO-d_6) δ [ppm] = 149.6 (C_q, 1C, C-14), 147.4 (C_q, 1C, C-8), 135.9 (C_q, 1C, C-3), 134.0 (CH_{Ar}, 1C, C-16), 128.6 (CH_{Ar}, 1C, C-18), 128.0 (CH_{Ar}, 1C, C-12), 127.5 (CH_{Ar}, 1C, C-6), 122.0 (C_q, 1C, C-13), 121.8 (CH_{Ar}, 1C, C-11), 121.4 (CH_{Ar}, 1C, C-4), 119.3 (CH_{Ar}, 1C, C-5), 111.4 (C_q, 1C, C-17), 109.2 (C_q, 1C, C-15), 106.9 (CH_{Ar}, 1C, C-7), 105.7 (C_q, 1C, C-1), 51.7 (C_q, 1C, C-2), 28.5 (CH_3, 1C, C-9), 25.6 (CH_3, 1C, C-10/H-10'), 19.9 (CH_3, 1C, C-10/H-10').

FT-IR (ATR): $\tilde{\nu}$ [cm^{-1}] = 3057 (w), 2963 (w), 2864 (w), 1649 (w), 1607 (w), 1549 (w), 1485 (m), 1445 (s), 1420 (m), 1360 (m), 1302 (m), 1261 (s), 1209 (w), 1153 (m), 1101 (m), 964 (s), 887 (s), 856 (m), 824 (w), 743 (s), 708 (s).

HRMS (ESI): $^{m}/_{z}$ calcd. for $C_{19}H_{17}Br_2NO$: 433.9749659 $[M+H]^+$;
found: 433.97533.
$^{m}/_{z}$ calcd. for $C_{19}H_{17}Br_2NO$: 455.9569106 $[M+Na]^+$;
found: 455.95697.

UV/Vis: $\tilde{\nu}$ [nm]: λ_{max} (MeOH, 0.025 mM): MC = 566, 384, 326, 296, 240; SP = 326, 296, 240, 232.

Synthesis of (*E*)-2-(5-bromo-2-hydroxy-3-nitrostyryl)-1,3,3-trimethyl-3H-indol-1-ium iodide

[NIH_P306]

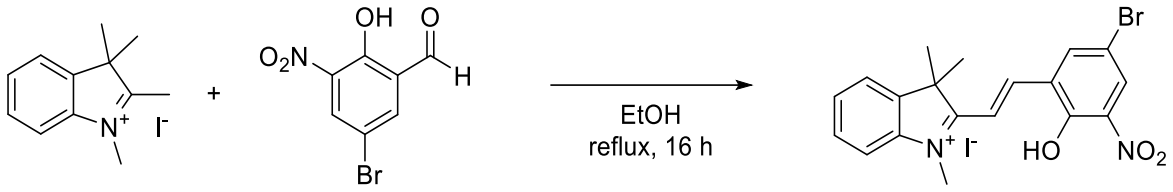

33 **35** **38**

Under argon atmosphere, indolium **33** (1.51 g, 5.00 mmol, 1.0 eq.) and salicylic aldehyde **35** (1.23 g, 5.00 mmol, 1.0 eq.) were suspended in dry EtOH (20 mL) and heated to reflux. After 16 h, full conversion was confirmed by TLC. The solution was cooled to ambient temperature and the precipitated product was filtered of and dried under reduced pressure. Indolium iodide **38** was obtained as a red solid in 82 % (2.16 g, 4.08 mmol) yield.

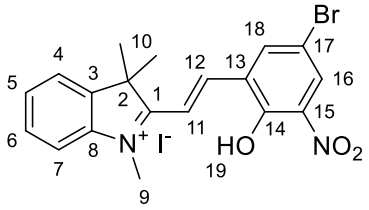

M($C_{19}H_{18}BrIN_2O_3$)**:** 529.17 $g \cdot mol^{-1}$.

Habitus: Red solid.

Yield: 2.16 g (4.08 mmol, 82 %).

Mp.: Turns dark >170 °C, melts at 198–199 °C.

^{1}H-NMR: (500 MHz, DMSO-d_6) δ [ppm] = 8.74 (d, $^{4}J_{H18-H16}$ = 2.5 Hz, 1H, H-18), 8.38 (d, $^{3}J_{H12-H11}$ = 16.5 Hz, 1H, H-12), 8.31 (d, $^{4}J_{H16-H18}$ = 2.5 Hz, 1H, H-16), 7.99 – 7.94 (m, 1H, H-7), 7.90 – 7.89 (m, 1H, H-4) 7.89 (d, $^{3}J_{H11-H12}$ = 16.5 Hz, 1H, H11), 7.70 – 7.64 (m, 2H, H-5, H-6), 4.18 (s, 3H, H-9), 1.77 (s, 6H, H-10, H-10').

^{13}C-NMR: (126 MHz, DMSO-d_6) δ [ppm] = 181.7 (C_q, 1C, C-1), 151.8 (C_q, 1C, C-14), 143.6 (C_q, 1C, C-3), 143.5 (CH_3, 1C, C-9) (CH_{Ar}, 1C, C-12), 141.8 (C_q, 1C, C-8), 139.3 (CH_{Ar}, 1C, C-15), 136.9 (CH_{Ar}, 1C, C-18), 131.0 (CH_{Ar}, 1C, C-16), 129.8 (CH_{Ar}, 1C, C-5), 129.1 (CH_{Ar}, 1C, C-6), 127.9 (CH_{Ar}, 1C, C-13), 122.9 (CH_{Ar}, 1C, C-4), 115.6 (CH_{Ar}, 1C, C-7), 115.5 (CH_{Ar}, 1C, C-11), 110.0 (C_q, 1C, C-17), 52.3 (C_q, 1C, C-2), 35.0 (CH_3, 1C, C-9), 25.4 (CH_{Ar}, 2C, C-10).

Spiropyran

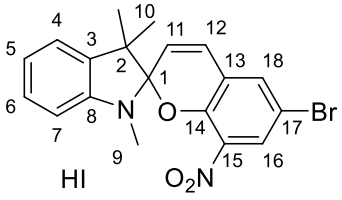

^{1}H-NMR: (500 MHz, DMSO-d_6) δ [ppm] = 7.92 (d, $^{4}J_{H-H}$ = 2.4 Hz, 1H, H16), 7.82 (d, $^{4}J_{H-H}$ = 2.4 Hz, 1H, H18), 7.17 (d, $^{3}J_{H12-H11}$ = 10.4 Hz, 1H, H-12), 7.15 – 7.10 (m, 2H, H-4, H-6), 6.81 (φtd, $^{3}J_{H5-H4, H5-H6}$ = 7.4 Hz, $^{4}J_{H5-H7}$ = 1.0 Hz, 1H, H-5), 6.61 (dd, $^{3}J_{H7-H6}$ = 8.2 Hz, $^{4}J_{H7-H5}$ = 1.0 Hz, 1H, H-7), 6.07 (d, $^{3}J_{H11-H12}$ = 10.4 Hz, 1H, H-11), 2.67 (s, 3H, H-9), 1.25 (s, 3H, H-10/H-10'), 1.11 (s, 3H, H-101/H-10').

^{13}C-NMR: (126 MHz, DMSO-d_6) δ [ppm] = 147.0 (C_q, 1C, C-8), 146.2 (C_q, 1C, C-14), 135.7 (C_q, 1C, C-3), 133.6 (CH_{Ar}, 1C, C-18), 127.7 (C_q, 1C, C-15), 127.6 (CH_{Ar}, 1C, C-6), 126.5 (CH_{Ar}, 1C, C-16), 123.3 (C_q, 1C, C-13), 122.4 (CH_{Ar}, 1C, C-11), 121.4 (CH_{Ar}, 1C, C-12), 119.5 (CH_{Ar}, 1C, C-5), 110.1 (C_q, 1C, C-17), 107.1 (CH_{Ar}, 1C, C-7), 106.7 (Cq, 1C, C-1), 51.9 (Cq, 1C, C-2), 28.5 (CH_3, 1C, C-9) 25.8 (CH_3, 1C, C-10/C-10'), 19.5 (CH_3, 1C, C-10/C-10').

C-10 and C-10' are barely visible in the ^{13}C-NMR but well detectable in the H,C-2D spectra

FT-IR (ATR): $\tilde{\nu}$ [cm^{-1}] = 3086 (w), 3013 (w), 2982 (w), 2926 (w), 1612 (w), 1595 (w), 1551 (w), 1528 (s), 1450 (m), 1410 (m), 1398 (m), 1302 (s), 1261 (m), 1236 (m), 1204 (w), 1157 (m), 1107 (w), 1088 (w), 1020 (w), 955 (m), 935 (w), 878 (m), 762 (s), 746 (s), 719 (s), 696 (m), 673 (m), 633 (m).

Synthesis of 6-bromo-1',3',3'-trimethyl-8-nitrospiro[chromene-2,2'-indoline]

[NIH_P309]

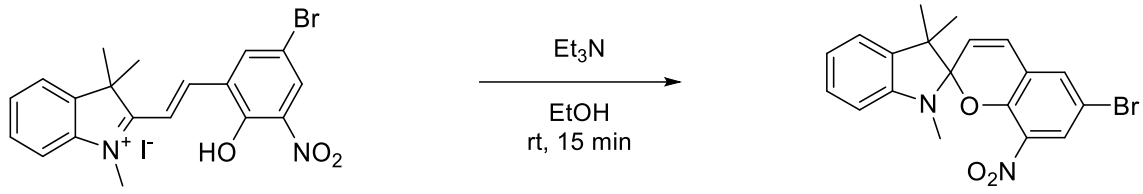

38 **9**

Indolium iodide **38** (1.06 g, 2.00 mmol, 1.0 eq.) and triethylamine (0.31 mL, 2.2 mmol, 1.1 eq.) were suspended in EtOH (7 mL, HPLC grade) and stirred for 15 min at ambient temperature. The solvent was removed under reduced pressure and the residue was refluxed for 15 min in water (25 mL). After cooling to ambient temperature, the solvent was filtered of and dried under reduced pressure. Spiropyran **9** was obtained as a dark blue solid in 95 % (0.76 g, 1.89 mmol) yield.

M($C_{19}H_{17}BrN_2O_3$)**:** 401.26 g·mol^{-1}.

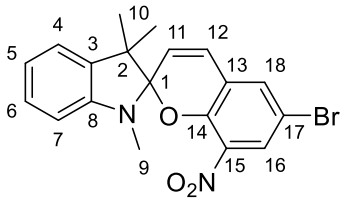

Habitus: Dark blue solid.

Yield: 0.76 g (1.89 mmol, 95 %).

Mp.: 126–129°C.

Spiropyran

^{1}H-NMR: (500 MHz, DMSO-d_6) δ [ppm] = 7.93 (d, $^4J_{H16\text{-}H18}$ = 2.5 Hz, 1H, H-16), 7.81 (d, $^4J_{H18\text{-}H16}$ = 2.5 Hz, 1H, H-18), 7.16 (d, $^3J_{H12\text{-}H11}$ = 10.5 Hz, 1H, H-12), 7.15 – 7.11 (m, 2H, H-4, H-6), 6.81 (td, $^3J_{H5\text{-}H4,\ H5\text{-}H6}$ = 7.4 Hz, $^4J_{H5\text{-}H7}$ 1.0 Hz, 1H, H-5), 6.62 (d, $^3J_{H7\text{-}H6}$ =

7.5 Hz, 1H, H-7), 6.07 (d, $^{3}J_{H11\text{-}H12}$ = 10.5 Hz, 1H, H-11), 2.67 (s, 3H, H-9), 1.25 (s, 3H, H-10/H-10'), 1.11 (s, 3H, H-10/H-10').

^{13}C-NMR: (126 MHz, DMSO-d_6) δ [ppm] = 147.0 (C_q, 1C, C-8), 146.2 (C_q, 1C, C-14), 137.3 (C_q, 1C, C-15), 135.7 (C_q, 1C, C-3), 133.6 (C_q, 1C, C-18), 127.7 (CH_{Ar}, 1C, C-12), 127.6 (CH_{Ar}, 1C, C-6), 126.5 (C_q, 1C, C-16), 123.3 (C_q, 1C, C-13), 122.4 (CH_{Ar}, 1C, C-11), 121.4 (CH_{Ar}, 1C, C-4), 119.5 (CH_{Ar}, 1C, C-5), 110.1 (C_q, 1C, C-17), 107.1 (CH_{Ar}, 1C, C-7), 106.8 (C_q, 1C, C-1), 51.9 (C_q, 1C, C-2), 28.4 (CH_3, 1C, C-9), 25.8 (CH_3, 1C, C-10/C-10'), 19.5 (CH_3, 1C, C-10/C-10').

FT-IR (ATR): $\tilde{\nu}$ [cm^{-1}] = 3057 (w), 2974 (w), 2953 (w), 2870 (w), 1605 (w), 1530 (s), 1487 (s), 1456 (s), 1423 (m), 1358 (s), 1308 (m), 1267 (s), 1219 (m), 1175 (s), 1159 (m), 1101 (s), 1022 (s), 993 (m), 910 (s), 897 (s), 878 (s), 827 (m), 816 (s), 741 (s), 723 (s), 698 (s), 646 (m).

HRMS (ESI): $^{m}/_{z}$ calcd. for $C_{19}H_{17}BrN_2O_3$: 401.0495315 $[M+H]^+$;
found: 401.04956.
$^{m}/_{z}$ calcd. for $C_{19}H_{17}BrN_2O_3$: 423.0314762 $[M+Na]^+$;
found: 423.03156.

UV/Vis: $\tilde{\nu}$ [nm]: λ_{max} (MeOH, 0.025 mM): MC = 554, 365, 245, 218; SP = 361, 284, 242.

Synthesis of 1',3',3'-trimethyl-8-nitrospiro[chromene-2,2'-indoline]

[NIH_P311]

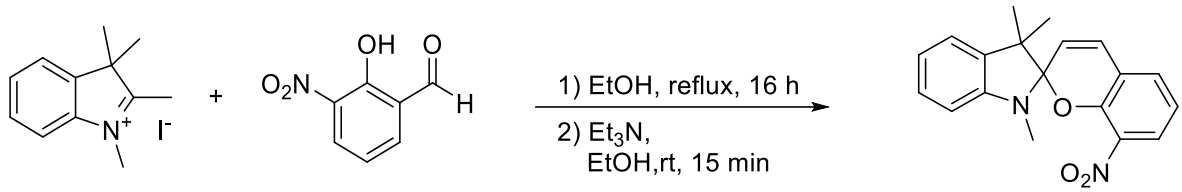

33 **36** **32**

Under argon atmosphere, indolium **33** (903 mg, 3.00 mmol, 1.0 eq.) and salicylic aldehyde **36** (501 mg, 3.00 mmol, 1.0 eq.) were suspended in EtOH (10 mL, HPLC grade) and heated to reflux. After 16 h, the reaction was cooled to ambient temperature and the precipitated was filtered of and dried under reduced pressure. The hydroiodide salt of **32** was obtained as a red solid in 90 % (1.22 g, 2.71 mmol). The salt was suspended in EtOH (10 mL) and triethylamine (0.41 mL, 3.0 mmol, 1.1 eq.) were added. After stirring for 15 min at ambient temperature, the purple solution was concentrated to dryness under reduced pressure. The residue was recrystallised from water and spiropyran **32** was obtained as colourless solid in 81 % (785 mg, 2.44 mmol) yield.

M($C_{19}H_{18}N_2O_3$)**:** 322.26 g·mol^{-1}.

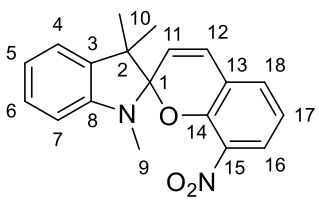

Habitus: Colourless solid.

Yield: 785 mg (2.44 mmol, 81 %).

Mp.: Slowly turns blue >127°C, melts at 147–149 °C.

^{1}H-NMR: (500 MHz, DMSO-d_6) δ [ppm] = 7.70 (dd, $^3J_{H16\text{-}H17}$ = 8.2 Hz, $^4J_{H16\text{-}H18}$ = 1.5 Hz, 1H, H-16), 7.54 (dd, $^3J_{H18\text{-}H17}$ = 7.5 Hz, $^4J_{H18\text{-}H16}$ = 1.5 Hz, 1H, H-18), 7.17 (d, $^3J_{H12\text{-}H11}$ = 10.4 Hz, 1H, H-12), 7.00 (dd, $^3J_{H17\text{-}H16}$ = 8.2 Hz, $^3J_{H17\text{-}H18}$ = 7.5 Hz, 1H, H-17) 7.14 – 7.10 (m, 2H, H-4, H-6), 6.80 (td, $^3J_{H5\text{-}H4,\ H5\text{-}H6}$ = 7.4 Hz, $^4J_{H5\text{-}H7}$ 1.0 Hz, 1H, H-5), 6.63 – 6.57 (m, 1H, H-7), 5.97 (d, $^3J_{H11\text{-}H12}$ = 10.4 Hz, 1H, H-11), 2.67 (s, 3H, H-9), 1.26 (s, 3H, H-10/H-10'), 1.11 (s, 3H, H-10/H-10').

^{13}C-NMR: (126 MHz, DMSO-d_6) δ [ppm] = 147.2 (C_q, C1, C-8), 147.0 (C_q, C1, C-14), 136.7 (C_q, C1, C-15), 135.8 (C_q, C1, C-3), 131.5 (CH_{Ar}, 1C, C-18), 128.6 (CH_{Ar}, 1C, C-12), 127.5 (CH_{Ar}, 1C, C-

4/6), 124.7 (CH_{Ar}, 1C, C-16), 121.4 (CH_{Ar}, 1C, C-4/6), 121.3 (C_q, C1, C-13), 121.0 (CH_{Ar}, 1C, C-11), 119.8 (CH_{Ar}, 1C, C-17), 119.4 (CH_{Ar}, 1C, C-5), 107.0 (CH_{Ar}, 1C, C-7), 106.2 (C_q, 1C, C-1), 51.8 (C_q, 1C, C-2), 28.5 (CH_3, 1C, C-9), 25.8 (CH_3, 1C, C-10/C-10'), 19.6 (CH_3, 1C, C-10/C-10').

FT-IR (ATR): $\tilde{\nu}$ [cm^{-1}] = 2963 (w), 2866 (w), 1653 (w), 1607 (w), 1522 (m), 1454 (m), 1362 (m), 1302 (m), 1265 (s), 1177 (w), 1103 (m), 1074 (m), 1022 (m), 991 (w), 912 (s), 804 (s), 737 (s), 623 (w).

HRMS (ESI): $^{m}/_{z}$ calcd. for $C_{19}H_{18}N_2O_3$: 323.1390190 $[M+H]^+$;
found: 323.13858.
$^{m}/_{z}$ calcd. for $C_{19}H_{18}N_2O_3$: 345.1209636 $[M+Na]^+$;
found: 345.12058.

UV/Vis: $\tilde{\nu}$ [nm]: λ_{max} (MeOH, 0.025 mM): MC = 543, 364, 245; SP = 353, 281, 245.

Synthesis of 8-bromo-1',3',3'-trimethylspiro[chromene-2,2'-indoline]

[NIH_P296]

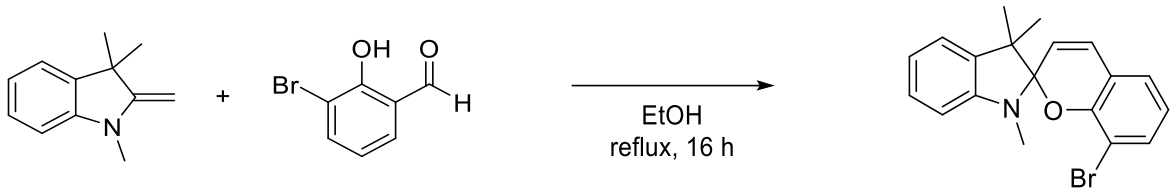

43 **44** **40**

Under argon atmosphere, indole **43** (1.06 mL, 6.00 mmol, 1.2 eq.) and salicylic aldehyde **44** (1.05 g, 5.00 mmol, 1.0 eq.) were dissolved in EtOH (10 mL, HPLC grade) and heated to reflux. After 16 h, full conversion was confirmed by TLC. The solvent was removed under reduced pressure and the crude product was purified by column chromatography over silica gel (30:1, *c*Hex:EtOAc). Spiropyran **40** was obtained as colourless solid in 93 % (1.66 g, 4.66 mmol) yield.

M($C_{19}H_{18}BrNO$)**:** 356.26 g·mol^{-1}.

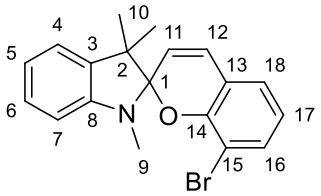

Habitus: Colourless solid.

Yield: 1.66 g (4.66 mmol, 93 %).

R_f: 0.53 (30:1, *c*Hex:EtOAc).

Mp.: Slowly turns purple >125 °C, melts at 139–140 °C.

^{1}H-NMR: (500 MHz, DMSO-d_6) δ [ppm] = 7.37 (dd, $^3J_{H16\text{-}H17}$ = 7.9 Hz, $^4J_{H16\text{-}H18}$ = 1.6 Hz, 1H, H-16), 7.20 (dd, $^3J_{H18\text{-}H17}$ = 7.5 Hz, $^4J_{H18\text{-}H16}$ = 1.6 Hz, 1H, H-18), 7.13 – 7.08 (m, 2H, H-4, H-6), 7.03 (d, $^3J_{H12\text{-}H11}$ = 10.2 Hz, 1H, H-12), 6.83 – 6.76 (m, 2H, H-5, H-17), 6.59 (d, $^3J_{H7\text{-}H8}$ = 7.6 Hz, 1H, H-7), 5.83 (d, $^3J_{H11\text{-}H12}$ = 10.2 Hz, 1H, H-11), 2.65 (s, 3H, H-9), 1.23 (s, 3H, H-10/H-10'), 1.10 (s, 3H, H-10/H-10').

^{13}C-NMR: (126 MHz, DMSO-d_6) δ [ppm] = 150.0 (C_q, 1C, C-14), 147.5 (C_q, 1C, C-8), 136.1 (C_q, 1C, C-3), 132.7 (CH_{Ar}, 1C, C-16), 128.9 (CH, 1C, C-12), 127.5 (CH_{Ar}, 1C, C-4/C-6), 126.3 (CH_{Ar}, 1C, C-18), 121.4 (CH_{Ar}, 2C, C-17, C-4/C-6), 120.5 (CH, 1C, C-11), 120.4 (C_q, 1C, C-13), 119.1 (CH_{Ar}, 1C, C-5), 108.1 (C_q, 1C, C-15), 106.8 (C_q, 1C, C-7), 105.2 (C_q, 1C, C-1), 51.5 (C_q, 1C, C-2),

28.5 (CH_3, 1C, C-9), 25.6 (CH_3, 1C, C-10/C-10'), 20.0 (CH_3, 1C, C-10/C-10').

FT-IR (ATR): $\tilde{\nu}$ [cm^{-1}] = 3057 (w), 2963 (w), 2924 (w), 2868 (w), 1651 (w), 1607 (w), 1487 (m), 1443 (s), 1362 (w), 1302 (m), 1260 (m), 1209 (w), 1130 (w), 1103 (m), 1065 (w), 1022 (m), 966 (s), 876 (s), 858 (m), 795 (m), 743 (s), 718 (s), 619 (w).

HRMS (ESI): $^{m}/_{z}$ calcd. for $C_{19}H_{18}BrNO$: 356.0644534 $[M+H]^+$;
found: 356.06430.
$^{m}/_{z}$ calcd. for $C_{19}H_{18}BrNO$: 378.0463980 $[M+Na]^+$;
found: 378.04631.

UV/Vis: $\tilde{\nu}$ [nm]: λ_{max} (MeOH, 0.025 mM): MC = 566, 385, 293; SP = 293 231.

Synthesis of 6-bromo-1',3',3'-trimethylspiro[chromene-2,2'-indoline]

[NIH_P298]

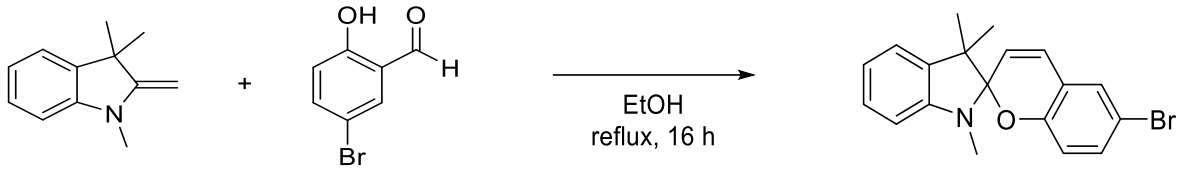

43 **41** **41**

Under argon atmosphere, indole **43** (1.06 mL, 6.00 mmol, 1.2 eq.) and salicylic aldehyde **41** (1.05 g, 5.00 mmol, 1.0 eq.) were dissolved in EtOH (10 mL, HPLC grade) and heated to reflux. After 16 h, full conversion was confirmed by TLC. The solvent was removed under reduced pressure and the crude product was purified by column chromatography over silica gel (50:1, *c*Hex:EtOAc). Spiropyran **41** was obtained as colourless solid in 90 % (1.59 g, 4.46 mmol) yield.

M($C_{19}H_{18}BrNO$)**:** 356.26 g·mol^{-1}.

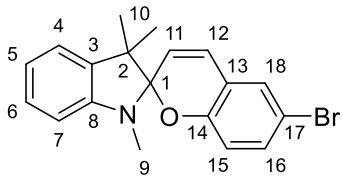

Habitus: Colourless solid.

Yield: 1.59 g (4.46 mmol, 90 %).

R_f: 0.35 (50:1, *c*Hex:EtOAc).

Mp.: 90–93 °C.

^{1}H-NMR: (500 MHz, DMSO-*d*$_6$) δ [ppm] = 7.42 (d, $^4J_{H18\text{-}H16}$ = 2.5 Hz, 1H, H-18), 7.23 (dd, $^3J_{H16\text{-}H15}$ = 8.6 Hz, $^4J_{H16\text{-}H18}$ = 2.5 Hz, 1H, H-16), 7.13 – 7.08 (m, 2H, H-4, H-6), 7.02 (d, $^3J_{H12\text{-}H11}$ = 10.2 Hz, 1H, H-12), 6.78 (t, $^3J_{H5\text{-}H4;\ H5\text{-}H6}$ = 7.3 Hz, 1H, H-5), 6.65 (d, $^3J_{H15\text{-}H16}$ = 8.6 Hz, 1H, H-15), 6.57 (d, $^3J_{H7\text{-}H6}$ = 7.7 Hz, 1H, H-7), 5.85 (d, $^3J_{H11\text{-}H12}$ = 10.2 Hz, 1H, H-11), 2.65 (s, 3H, H-9), 1.21 (s, 3H, H-10/H-10'), 1.09 (s, 3H, H-10/H-10').

^{13}C-NMR: (126 MHz, DMSO-*d*$_6$) δ [ppm] = 153.2 (C_q, 1C, C-14), 147.7 (CH_{Ar}, 1C, C-8), 136.1 (CH_{Ar}, 1C, C-3), 132.0 (CH_{Ar}, 1C, C-16), 129.1 (CH_{Ar}, 1C, C-18), 128.3 (CH_{Ar}, 1C, C-12), 127.5 (CH_{Ar}, 1C, C-6), 121.5 (CH_{Ar}, 1C, C-4), 120.9 (C_q, 1C, C-13), 120.7 (CH_{Ar}, 1C, C-11), 119.1 (CH_{Ar}, 1C, C-5), 116.6 (CH_{Ar}, 1C, C-15), 111.2 (C_q, 1C, C-17), 106.8 (CH_{Ar}, 1C, C-7), 104.3 (CH_{Ar}, 1C, C-1),

51.5 (C_q, 1C, C-2), 28.5 (CH_3, 1C, C-9), 25.6 (CH_3, 1C, C-10/H-10'), 19.8 (CH_3, 1C, C-10/H-10').

FT-IR (ATR): $\tilde{\nu}$ [cm^{-1}] = 3049 (w), 2963 (w), 2924 (w), 2866 (w), 2808 (w), 1639 (w), 1607 (w), 1474 (s), 1464 (s), 1420 (w), 1356 (m), 1298 (m), 1256 (s), 1213 (w), 1177 (m), 1124 (m), 1115 (m), 1103 (m), 1065 (w), 1020 (m), 951 (s), 924 (m), 874 (s), 829 (s), 814 (s), 746 (s), 710 (s), 677 (s), 621 (w).

HRMS (ESI): $^{m}/_{z}$ calcd. for $C_{19}H_{18}BrNO$: 356.0644534 $[M+H]^+$;
found: 356.06438.

UV/Vis: $\tilde{\nu}$ [nm]: λ_{max} (MeOH, 0.025 mM): MC = 526, 353, 265; SP = 337, 265, 242.

Synthesis of 1',3',3'-trimethyl-6-nitrospiro[chromene-2,2'-indoline]

[NIH_P146, **VAG_02**]

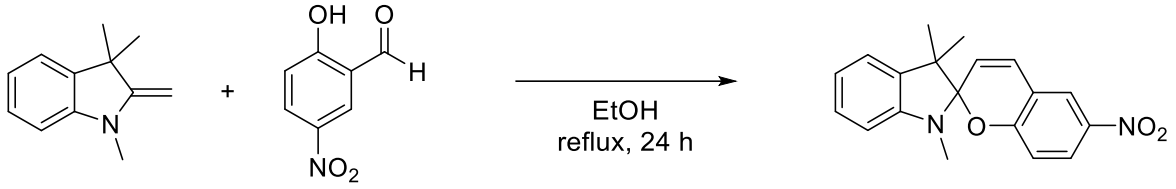

43 **29** **7**

Under argon atmosphere, salicylic aldehyde **29** (3.40 g, 20.3 mmol, 1.0 eq.) and Fischer base **43** (3.60 mL, 20.3 mmol, 1.0 eq.) were dissolved in dry EtOH (100 mL) and the solution was heated to reflux. After 24 h, the solution was cooled to ambient temperature and concentrated under reduced pressure to approximately 25 mL. The mixture was cooled to 0 °C, the precipitated solid was filtered off and washed with cold EtOH. After recrystallisation from EtOH, spiropyran **7** was obtained as a yellow solid in 83 % (5.46 g, 16.9 mmol) yield.

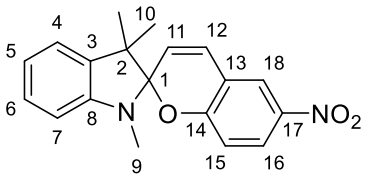

M($C_{19}H_{18}N_2O_3$)**:** 322.36 g·mol^{-1}.

Habitus: Yellow solid.

Yield: 5.46 g (16.9 mmol, 83 %).

Mp.: Turns blue >169 °C, melts at 176–179 °C, Lit.:[134] 182–183 °C.

^{1}H-NMR: (500 MHz, DMSO-d_6) δ [ppm] = 8.23 (d, $^4J_{H18\text{-}H16}$ = 2.8 Hz, 1H, H-18), 8.00 (dd, $^3J_{H16\text{-}H15}$ = 9.0 Hz, $^4J_{H16\text{-}H18}$ = 2.8 Hz, 1H, H-16), 7.23 (d, $^3J_{H12\text{-}H11}$ = 10.4 Hz, 1H, H-12), 7.14 (m, 2H, H-4, H-6)), 6.89 (d, $^3J_{H15\text{-}H16}$ = 9.0 Hz, 1H, H-15), 6.82 (td, $^3J_{H5\text{-}H4,\ H5\text{-}H6}$ = 7.5 Hz, $^4J_{H5\text{-}H7}$ = 1.0 Hz, 1H, H-5), 6.62 (br, d, $^3J_{H7\text{-}H6}$ = 7.5 Hz, 1H, H-7), 6.00 (d, $^3J_{H11\text{-}H12}$ = 10.4 Hz, 1H, H-11), 2.68 (s, 3H, H-9), 1.22 (s, 3H, H-10/H-10'), 1.12 (s, 3H, H-10/H-10').

^{13}C-NMR: (126 MHz, DMSO-d_6) δ [ppm] = 159.4 (C_q, 1C, C-14), 147.4 (C_q, 1C, C-8), 140.5 (C_q, 1C, C-17), 135.8 (C_q, 1C, C-3), 128.3 (CH_{Ar}, 1C, C-12), 127.7 (CH_{Ar}, 1C, C-4/C-6), 125.7 (CH_{Ar}, 1C, C-16), 122.8 (CH_{Ar}, 1C, C-18), 121.5 (CH_{Ar}, 1C, C-4/C-6), 121.4 (CH_{Ar}, 1C, C-11), 119.4 (CH_{Ar}, 1C, C-5), 118.9 (C_q, 1C, C-13), 115.4 (CH_{Ar}, 1C, C-15), 107.0 (CH_{Ar}, 1C, C-7), 106.1 (C_q, 1C, C-1),

51.9 (C_q, 1C, C-2), 28.5 (CH_3, 1C, C-9), 25.7 (CH_3, 1C, C-10/C-10'), 19.7 (CH_3, 1C, C-10/C-10').

FT-IR (ATR): $\tilde{\nu}$ [cm^{-1}] = 2963 (w), 2866 (w), 2816 (w), 1655 (w), 1609 (w), 1574 (w), 1508 (m), 1487 (m), 1477 (m), 1443 (m), 1423 (w), 1364 (w), 1331 (s), 1298 (m), 1269 (s), 1223 (w), 1184 (m), 1123 (m), 1088 (s), 1069 (w), 1015 (m), 1015 (m), 949 (s), 912 (s), 837 (m), 806 (s), 781 (m), 748 (s), 716 (m), 681 (m), 627 (w).

HRMS (ESI): $^{m}/_{z}$ calcd. for $C_{19}H_{18}N_2O_3$: 323.1390190 $[M+H]^+$;
found: 323.13872.
$^{m}/_{z}$ calcd. for $C_{19}H_{18}N_2O_3$: 345.1209636 $[M+Na]^+$;
found: 345.12097.

UV/Vis: $\tilde{\nu}$ [nm]: λ_{max} (MeOH, 0.025 mM): MC = 529, 352, 307, 266, 243; SP = 339, 298, 266, 242.

Synthesis of 8-bromo-1',3',3'-trimethyl-6-nitrospiro[chromene-2,2'-indoline]

[NIH_P171]

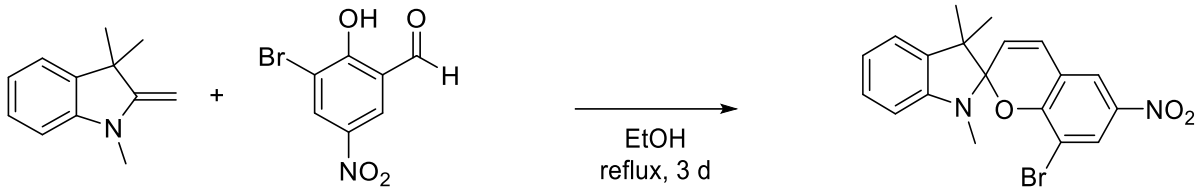

43 **46** **9**

Under argon atmosphere, Fischer Base **43** (0.59 mL, 3.3 mmol, 1.0 eq.) and salicylic aldehyde **46** (0.82 g, 3.3 mmol, 1.0 eq.) were dissolved in dry EtOH (60 mL) and heated to reflux. After three days, the reaction was cooled to ambient temperature and the precipitated solid was filtered off and washed with cold EtOH. Spiropyran **9** was obtained as green crystals in 88 % (1.2 g, 2.9 mmol) yield.

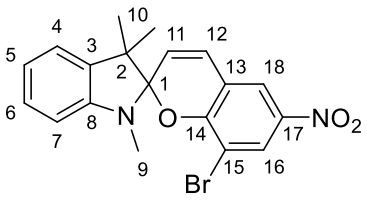

M($C_{19}H_{17}BrN_2O_3$)**:** 401.26 g·mol^{-1}.

Habitus: Green crystals.

Yield: 1.2 g (2.9 mmol, 88 %).

Mp.: Turns purple upon heating >240°C, melts at 253–254 °C.

^{1}H-NMR: (500 MHz, DMSO-d_6) δ [ppm] = 8.28 – 8.25 (m, 2H, H-16, H-18), 7.25 (d, $^3J_{H12\text{-}H11}$ = 10.4 Hz, 1H, H-12), 7.17 – 7.10 (m, 2H, H-4, H-6), 6.83 (td, $^3J_{H5\text{-}4,\ H5\text{-}H6}$ = 7.4 Hz, $^4J_{H5\text{-}H7}$ = 1.0 Hz, 1H, H-5), 6.65 (dd, $^3J_{H7\text{-}H6}$ = 8.1 Hz, $^3J_{H7\text{-}H5}$ = 1.0 Hz, 1H, H-7), 6.06 (d, $^3J_{H11\text{-}H12}$ = 10.4 Hz, 1H, H-11), 2.68 (s, 3H, H-9), 1.23 (s, 3H, H-10/H-10'), 1.13 (s, 3H, H-10/H-10').

^{13}C-NMR: (126 MHz, DMSO-d_6) δ [ppm] = 155.5 (C_q, 1C, C-14), 147.1 (C_q, 1C, C-8), 140.6 (C_q, 1C, C-17), 135.7 (C_q, 1C, C-3), 128.1 (CH_{Ar}, 1C, C-12), 128.0 (CH_{Ar}, 1C, C-16), 127.7 (CH_{Ar}, 1C, C-4/C-6), 122.2 (CH_{Ar}, 1C, C-11), 122.0 (CH_{Ar}, 1C, C-18), 121.5 (CH_{Ar}, 1C, C-4/C-6), 119.9 (C_q, 1C, C-13), 119.6 (CH_{Ar}, 1C, C-5), 108.4 (C_q, 1C, C-15), 107.8 (C_q, 1C, C-1), 107.1 (CH_{Ar}, 1C, C-7), 52.0 (C_q, 1C, C-2), 28.5 (CH_3, 1C, C-9), 25.7 (CH_3, 1C, C-10/C-10'), 19.7 (CH_3, 1C, C-10/C-10').

FT-IR (ATR): $\tilde{\nu}$ [cm^{-1}] = 3087 (w), 3051 (w), 3018 (w), 2980 (w), 2937 (w), 1587 (m), 1519 (s), 1434 (m), 1398 (m), 1323 (s), 1233 (s), 1116 (s),1069 (m), 1019 (m), 970 (m), 850 (m), 754 (s), 721 (m).

HRMS (ESI): $^{m}/_{z}$ calcd. for $C_{19}H_{17}BrN_2O_3$: 401.0495315 $[M+H]^+$;
found: 401.04996.
$^{m}/_{z}$ calcd. for $C_{19}H_{17}BrN_2O_3$: 423.0314762 $[M+Na]^+$;
found: 423.03187.

UV/Vis: $\tilde{\nu}$ [nm]: λ_{max} (MeOH, 0.025 mM): MC = 523, 367, 265, 229; SP = 330, 272, 242.

Synthesis of 1',3',3'-trimethyl-6,8-dinitrospiro[chromene-2,2'-indoline]

[NIH_P172]

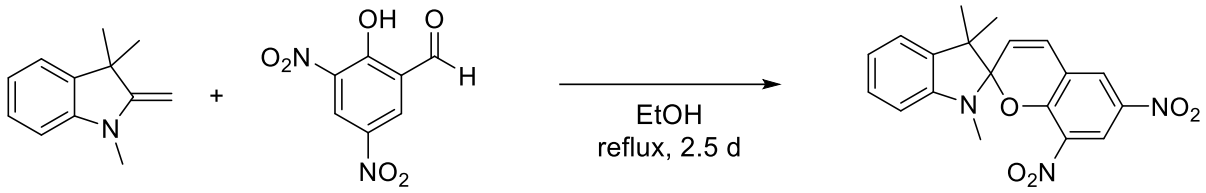

43 **47** **19**

Under argon atmosphere, salicylic aldehyde **47** (2.12 g, 10.0 mmol, 1.0 eq.) and Fischer-Base **43** (1.77 mL, 10.0 mmol, 1.0 eq.) were dissolved in 100 mL EtOH and heated to reflux. After 2.5 d, the reaction was cooled to ambient temperature. The precipitated product was filtered of washed with cold EtOH. The filtrate was concentrated to approximately 30 mL and the precipitated solid was filtered off and washed with cold EtOH. The solids were combined and spiropyran **19** was obtained as a dark, green solid in 66 % (2.44 g, 6.64 mmol) yield.

M($C_{19}H_{17}N_3O_5$)**:** 367.36 $g \cdot mol^{-1}$.

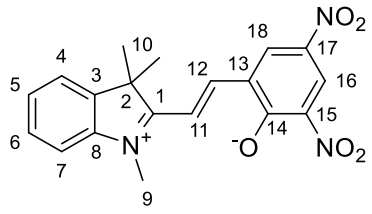

Habitus: Green solid.

Yield: 2.44 g (6.64 mmol, 66 %).

Mp.: Turns dark red >175 °C,
decomp. at 248–250 °C, Lit.:[50] >220 °C.

^{1}H-NMR: (500 MHz, DMSO-d_6) δ [ppm] = 8.90 (d, $^{4}J_{H16-H18}$ = 3.3 Hz, 1H, H-16), 8.57 (d, $^{4}J_{H18-H16}$ = 3.3 Hz, 1H, H-18), 8.53 (d, $^{3}J_{H11-H12}$ = 15.8 Hz, 1H, H-11), 8.40 (d, $^{3}J_{H12-H11}$ = 15.8 Hz, 1H, H-12), 7.87 – 7.79 (m, 2H, H-4, H-7), 7.59 (td, $^{3}J_{H6-H5,\ H6-H7}$ = 7.5 Hz, $^{4}J_{H6-H4}$ = 1.5 Hz, 1H, H-6), 7.55 (td, $^{3}J_{H5-H6,\ H5-H4}$ = 7.5 Hz, $^{4}J_{H5-H7}$ = 1.1 Hz, 1H, H-5), 3.98 (s, 3H, H-9), 1.77 (s, 6H, H-10).

^{13}C-NMR: (126 MHz, DMSO-d_6) δ [ppm] = 182.5 (C_q, 1C, C-1), 169.5 (C_q, 1C, C-14), 151.8 (CH_{Ar}, 1C, C-12), 143.3 (C_q, 1C, C-3), 141.9 (C_q, 1C, C-8), 140.9 (C_q, 1C, C-15), 134.6 (CH_{Ar}, 1C, C-16), 128.8 (CH_{Ar}, 1C, C-6), 128.5 (CH_{Ar}, 1C, C-5), 128.2 (C_q, 1C, C-17), 126.3 (C_q, 1C, C-13), 125.3 (CH_{Ar}, 1C, C-18), 122.7 (C_q, 1C, C-4), 114.5 (C_q, 1C, C-7), 110.9 (CH_{Ar}, 1C, C-11), 51.5 (C_q, 1C, C-2), 33.7 (CH_3, 1C, C-9), 25.9 (CH_3, 2C, C-10, C-10').

FT-IR (ATR): $\tilde{\nu}$ [cm^{-1}] = 3041 (w), 3023 (w), 2996 (w), 1623 (m), 1549 (w), 1522 (s), 1453 (m), 1438 (s), 1414 (m), 1281 (s), 1236 (s), 1164 (m), 1078 (s), 1024 (m), 978 (s), 927 (m), 855 (w), 777 (s), 743 (w).

HRMS (ESI): $^{m}/_{z}$ calcd. for $C_{19}H_{17}N_3O_5$: 368.1240971 $[M+H]^+$;
found: 368.12396.
$^{m}/_{z}$ calcd. for $C_{19}H_{17}N_3O_5$: 390.1060418 $[M+Na]^+$;
found: 390.10612.

UV/Vis: $\tilde{\nu}$ [nm]: λ_{max} (MeOH, 0.025 mM): MC = 507, 378, 360, 302, 263; SP = 339, 255.

The analytic data are in agreement with the literature[50]

6.4 Derivatisation of the Indole

Synthesis of 2,3,3-Trimethyl-5-methoxy-3*H*-indole

[NIH_P225, **NIH_P250**]

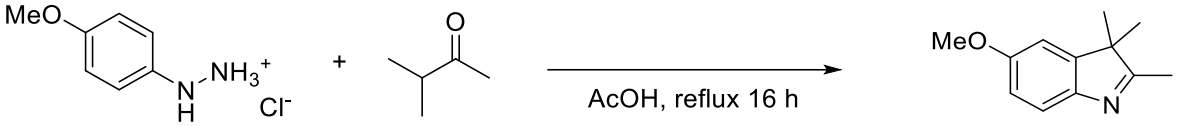

125 **126** **52**

Under argon atmosphere, 4-methoxy-phenylhydrazine hydrochloride (**125**) (8.73 g, 50.0 mmol, 1.00 eq.) and 3-methyl-2-butanone (**126**) (6.4 mL, 60 mmol, 1.2 eq.) were dissolved in 50 mL acetic acid. The reaction was refluxed overnight. After full conversion was indicated by TLC, the mixture was cooled to ambient temperature and concentrated under reduced pressure. Water (30 mL) and DCM (50 mL) were added to the residue. The mixture was neutralised with sat. Na_2CO_3 solution stirring vigorously. The phases were separated and the aqueous phase was extracted with DCM (3x30 mL). The combined organic phases were washed with brine (30 mL) and dried over Na_2SO_4. After filtration, the solvent was removed under reduced pressure and indole **52** was obtained as a brown solid in 96 % (9.07 g, 47.9 mmol) yield and was used without further purification.

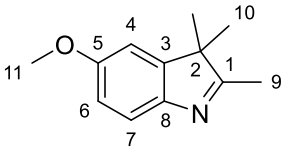

M($C_{12}H_{15}NO$)**:** 189.26 g·mol^{-1}.

Habitus: Brown solid.

Yield: 9.07 g (47.9 mmol, 96 %).

R_f: 0.33 (2:3, *c*Hex:EtOAc).

Mp.: 50–51 °C, Lit.:[135] 53–56 °C.

^{1}H-NMR: (500 MHz, DMSO-d_6) δ [ppm] = 7.31 (d, $^3J_{H7\text{-}H6}$ = 8.4 Hz, 1H, H-7), 7.03 (d, $^4J_{H4\text{-}H6}$ = 2.5 Hz, 1H, H-4), 6.81 (dd, $^3J_{H6\text{-}H7}$ = 8.4, $^4J_{H6\text{-}H4}$ = 2.6 Hz, 1H, H-6), 3.76 (s, 3H, H-11), 2.16 (s, 3H, H-9), 1.22 (s, 6H, H-10).

^{13}C-NMR: (126 MHz, DMSO-d_6) δ [ppm] = 185.2 (C_q, 1C, C-1), 157.4 (C_q, 1C, C-5), 147.5 (C_q, 1C, C-3), 147.1 (C_q, 1C, C-8), 119.5 (CH_{Ar}, 1C, C-7), 112.1 (CH_{Ar}, 1C, C-6), 108.1 (CH_{Ar}, 1C, C-4), 55.4

(CH_3, 1C, C-11), 53.3 (C_q, 1C, C-2), 22.6 (CH_3, 2C, C-10), 14.6 (CH_3, 1C, C-9).

FT-IR (ATR): $\tilde{\nu}$ [cm^{-1}] = 2995 (w), 2961 (w), 2930 (w), 2833 (w), 1713 (w), 1686 (w), 1612 (w), 1578 (m), 1510 (m), 1462 (s), 1431 (s), 1377 (w), 1337 (w), 1288 (s), 1271 (s), 1246 (s), 1211 (s), 1198 (s), 1179 (s), 1144 (w), 1069 (s), 1030 (s), 943 (w), 866 (w), 824 (s), 735 (m), 698 (w), 615 (m).

GC-MS: τ_R = 11.64 min; $^m/_z$ (%) = 189.1 $[M]^{\cdot+}$ (100), 188.1 $[M, -H]^{\cdot+}$ (19), 174.1 $[M, -CH_3]^{\cdot+}$, 159.1 $[M, 2x -CH_3]^{\cdot+}$ (19), 146.1 $[M, 3x -CH_3]^{\cdot+}$, 131.1 (33), 115.2 (21), 77.0 $[C_6H_5]^{\cdot+}$ (21), 51.1 $[C_4H_3]^{\cdot+}$ (16).

The analytic data are in agreement with the literature[135, 136]

Synthesis of 5-methoxy-1,2,3,3-tetramethyl 3*H*-indolium iodide

[NIH_P252]

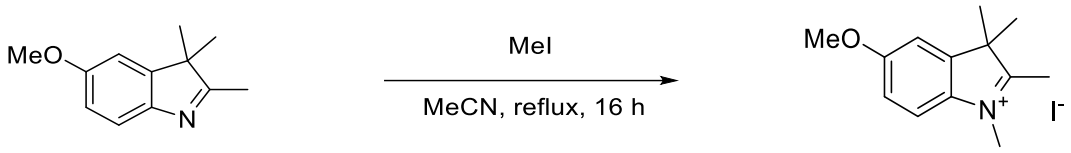

52 **56**

Under argon atmosphere, indole **52** (9.00 g, 48.0 mmol, 1.0 eq.) was dissolved in MeCN (60 mL, HPLC grade). Iodomethane (15.0 mL, 240 mmol, 5.0 eq.) was added and the reaction was refluxed overnight. After full conversion was confirmed by TLC, the reaction was cooled to ambient temperature. The precipitated product was filtered off and washed with Et_2O. The indolium iodide **56** was obtained as pale-red crystals in 66 % (10.5 g, 32.0 mmol) yield. By concentration of the filtrate and subsequent filtration, another 1.21 g of product could be obtained.

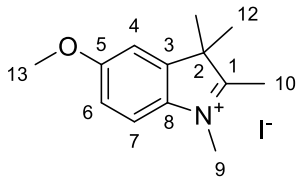

M($C_{13}H_{18}INO$)**:** 331.20 g·mol^{-1}.

Habitus: Pale-red crystals.

Yield: 11.7 g (35.4 mmol, 74 %).

Mp.: 260-263 °C, decomp, Lit.:[135] 226–228 °C.

^{1}H-NMR: (500 MHz, DMSO-d_6) δ [ppm] = 7.83 (d, $^3J_{H7\text{-}H6}$ = 8.8 Hz, 1H, H-7), 7.50 (d, $^4J_{H4\text{-}H6}$ = 2.5 Hz, 1H, H-4), 7.15 (dd, $^3J_{H6\text{-}H7}$ = 8.8, $^4J_{H6H4}$ = 2.5 Hz, 1H, H-6), 3.96 (s, 3H, H-9), 3.87 (s, 3H, H-13), 2.74 (s, 3H, H-10), 1.53 (s, 6H, H-12).

^{13}C-NMR: (126 MHz, DMSO-d_6) δ [ppm] = 193.0 (C_q,1C, C-1), 160.5 (C_q, 1C, C-5), 143.6 (C_q, 1C, C-3), 135.3 (C_q, 1C, C-8), 116.0 (CH_{Ar}, 1C, C-7), 114.1 (CH_{Ar}, 1C, C-6), 109.2 (CH_{Ar}, 1C, C-4), 56.1 (CH_3, 1C, C-13), 53.7 (C_q, 1C, C-2), 34.8 (CH_3, 1C, C-9), 21.8 (CH_3 2C, C-12), 14.0 (CH_3, 1C, C-10).

FT-IR (ATR): $\tilde{\nu}$ [cm^{-1}] = 3011 (w), 2974 (w), 1618 (m), 1599 (m), 1481 (m), 1456 (m), 1441 (m), 1389 (m), 1364 (w), 1346 (w), 1290 (s), 1217 (s), 1184 (m), 1157 (m), 1065 (m), 1020 (s), 988 (w), 959 (w), 935 (w), 880 (s), 860 (s), 820 (s), 781 (w), 746 (m), 708 (m).

The analytic data are in agreement with the literature[135]

Synthesis of 8-bromo-5'-methoxy-1',3',3'-trimethyl-6-nitrospiro-[chromene-2,2'-indoline]

[NIH_P255]

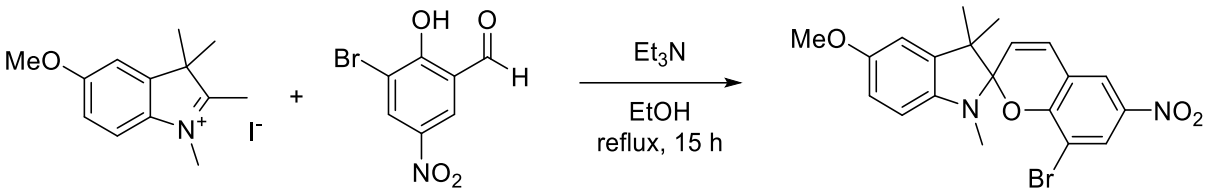

56 **46** **51**

Under argon atmosphere, indolium **56** (3.31 g, 10.0 mmol, 1.0eq.) and salicylic aldehyde **46** (2.71 g, 11.0 mmol, 1.1 eq.) were suspended in dry EtOH (60 mL) and heated to reflux. After 15 h, full conversion was confirmed via TLC. After cooling to ambient temperature, the precipitate was filtered off and washed with Et_2O. After drying under reduced pressure, spiropyran **51** was obtained as black powder in 99 % (4.28 g, 9.92 mmol) yield.

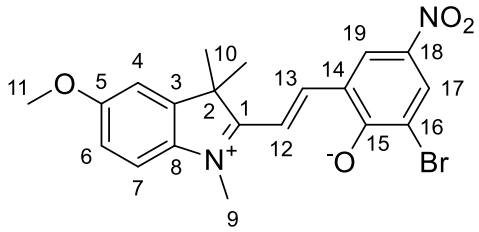

M($C_{20}H_{19}BrN_2O_4$)**:** 431.29 g·mol^{-1}.

Habitus: Black powder.

Yield: 4.28 g (9.92 mmol, 99 %).

Mp.: 239–241 °C.

^{1}H-NMR: (600 MHz, DMSO-*d*$_6$) δ [ppm] = 8.70 (d, $^4J_{H19\text{-}H17}$ = 3.0 Hz, 1H, H-19), 8.42 (d, $^3J_{H12\text{-}H13,trans}$ = 15.6 Hz, 1H, H-12), 8.32 (d, $^3J_{H13\text{-}H12,trans}$ = 15.6 Hz, 1H, H-13), 8.24 (d, $^4J_{H17\text{-}H19}$ = 3.0 Hz, 1H, H17), 7.69 (d, $^3J_{H7\text{-}H6}$ = 8.8 Hz, 1H, H-7), 7.46 (d, $^4J_{H6\text{-}H4}$ = 2.5 Hz, 1H, H-4), 7.10 (dd, $^3J_{H6\text{-}H7}$ = 8.8 Hz, $^4J_{H4\text{-}H6}$ = 2.5 Hz, 1H, H-6), 3.91 (s, 3H, H-9), 3.87 (s, 3H, H-11), 1.75 (s, 6H, H-10).

^{13}C-NMR: (126 MHz, DMSO-*d*$_6$) δ [ppm] = 180.2 (C_q, 1C, C-1), 173.3 (C_q, 1C, C-15), 159.9 (C_q, 1C, C-5), 152.1 (CH, 1C, C-13), 145.0 (C_q, 1C, C-3), 135.3 (C_q, 1C, C-8), 132.2 (CH_{Ar}, 1C, C-19), 130.6 (C_q, 1C, C-18), 129.4 (CH_{Ar}, 1C, C-17), 120.5 (C_q, 1C, C-14), 119.5 (C_q, 1C, C-16), 115.0 (CH_{Ar}, 1C, C-7), 114.2 (CH_{Ar}, 1C, C-6), 109.0 (CH, 1C, C-12), 108.7 (CH_{Ar}, 1C, C-4), 56.0 (CH_3, 1C, C-11), 51.1 (C_q, 1C, C-2), 33.3 (CH_3, 1C, C-9), 26.2 (CH_3, 2C, C-10).

Spiropyran:

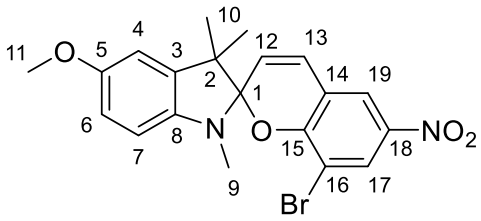

^{1}H-NMR: (600 MHz, DMSO-d_6) δ [ppm] = 8.26 (d, $^{4}J_{H17\text{-}H19}$ = 2.7 Hz, 1H, H-17), 8.25 (d, $^{4}J_{H19\text{-}H17}$ = 2.8 Hz, 1H, H-19), 7.24 (d, $^{3}J_{H13\text{-}H12}$ = 10.4 Hz, 1H, H-13), 6.81 (d, $^{4}J_{H4\text{-}H6}$ = 2.6 Hz, 1H, H-4), 6.70 (dd, $^{3}J_{H6\text{-}H7}$ = 8.4 Hz, $^{4}J_{H6\text{-}H4}$ = 2.6 Hz, 1H, H-6), 6.56 (d, $^{3}J_{H7\text{-}H6}$ = 8.4 Hz, 1H, H-7), 6.04 (d, $^{3}J_{H12\text{-}H13}$ = 10.3 Hz, 1H, H-12), 3.71 (s, 3H, H-11), 2.61 (s, 3H, H-9), 1.22 (s, 3H, H-10/H10'), 1.14 (s, 3H, H-10/H10').

^{13}C-NMR: (126 MHz, DMSO-d_6) δ [ppm] = 155.7 (C_q, 1C, C-15), 153.8 (C_q, 1C, C-5), 141.2 (C_q, 1C, C-8), 140.5 (C_q, 1C, C-18), 137.3 (C_q, 1C, C-3), 128.1 (CH_{Ar}, 1C, C-12), 128.0 (CH_{Ar}, 1C, C-17), 122.1 (CH_{Ar}, 1C, C-19), 122.0 (CH_{Ar}, 1C, C-13), 119.9 (C_q, 1C, C-14), 111.5 (CH_{Ar}, 1C, C-6), 109.2 (CH_{Ar}, 1C, C-4), 108.5 (C_q, 1C, C-1), 108.4 (C_q, 1C, C-16), 107.4 (CH_{Ar}, 1C, C-7), 55.4 (CH_3, 1C, C-11), 52.1 (C_q, 1C, C-2), 28.8 (CH_3, 1C, C-9), 25.5 (CH_3, 1C, C-10/C10'), 19.6 (CH_3, 1C, C-10/C10').

FT-IR (ATR): $\tilde{\nu}$ [cm^{-1}] = 3078 (w), 3054 (w), 2997 (w), 2981 (w), 2970 (w), 2900 (w), 2836 (w), 1607 (m), 1586 (m), 1532 (s), 1431 (m), 1397 (w), 1297 (s), 1277 (s), 1238 (s), 1219 (s), 1137 (m), 1045 (w), 1018 (m), 846 (m), 742 (m).

HRMS (ESI): $^{m}/_{z}$ calcd. for $C_{20}H_{19}BrN_2O_4$: 431.0600962 $[M+H]^+$;
found: 431.06046.
$^{m}/_{z}$ calcd. for $C_{20}H_{19}BrN_2O_4$: 453.0420409 $[M+Na]^+$;
found: 453.04249.

UV/Vis: $\tilde{\nu}$ [nm]: λ_{max} (MeOH, 0.025 mM): MC = 521, 382, 320, 280, 272; SP = 346, 317, 272, 243.

Synthesis of 5-carboxy-2,3,3-trimethyl-3*H*-indole

[NIH_P239, **NIH_P242**]

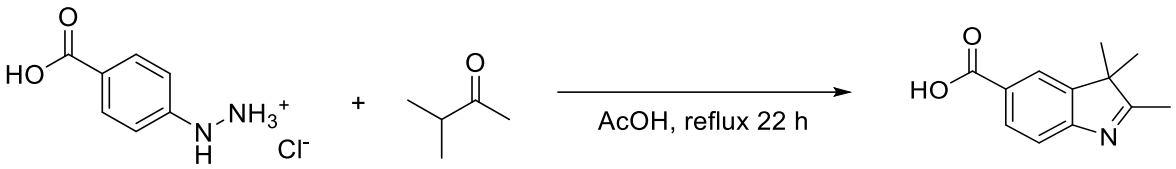

127 **126** **53**

Under argon atmosphere, 5-carboxy-phenylhydrazine hydrochloride (127) (6.2 g, 41 mmol, 1.0 eq.) and 3-methyl-2-butanone (126) (6.0 g, 70 mmol, 1.5 eq.) were dissolved in 50 mL acetic acid. The reaction was refluxed overnight. After full conversion was indicated by TLC, the mixture was cooled to ambient temperature and concentrated under reduced pressure. Water (30 mL) and DCM (50 mL) were added to the residue. The mixture was neutralised with sat. Na_2CO_3 solution while it was stirred vigorously. The phases were separated and the aqueous phase was extracted with DCM (3x60 mL). The combined organic phases were washed with brine (30 mL) and dried over Na_2SO_4. After filtration, the solvent was removed under reduced pressure and the crude product was recrystallised from EtOH. The product was filtered off and washed with Et_2O. Indole **53** was obtained as a pale orange solid in 86 % (7.4 g, 36 mmol) yield.

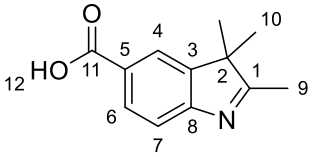

M($C_{12}H_{13}NO_2$)**:** 203.24 g·mol^{-1}.

Habitus: Pale orange solid.

Yield: 7.4 g (36 mmol, 96 %).

R_f: 0.15 (100 %, EtOAc).

Mp.: 209–212 °C, Lit.:[136] 208–210 °C.

^{1}H-NMR: (500 MHz, DMSO-d_6) δ [ppm] = 12.82 (s, br, 1H, H-12), 8.00 (d, $^4J_{H4\text{-}H5}$ = 1.7 Hz, 1H, H-4), 7.92 (dd, $^3J_{H6\text{-}H7}$ = 8.0, $^4J_{H6\text{-}H4}$ = 1.7 Hz, 1H, H-6), 7.51 (d, $^3J_{H7\text{-}H6}$ = 8.0 Hz, 1H, H-7), 2.26 (s, 3H, H-9), 1.29 (s, 6H, H-10).

^{13}C-NMR: (126 MHz, DMSO-d_6) δ [ppm] = 191.7 (C_q, 1C, C-1), 167.5 (C_q, 1C, C-11), 157.4 (C_q, 1C, C-8), 146.1 (C_q, 1C, C-3), 129.6 (CH_{Ar}, 1C, C-6), 127.3 (C_q, 1C, C-5), 122.7 (CH_{Ar}, 1C, C-4), 119.1

(CH_{Ar}, 1C, C-7), 53.5 (C_q, 1C, C-2), 22.3 (CH_3, 2C, C-10), 15.4 (CH_3, 1C, C-9).

FT-IR (ATR): $\tilde{\nu}$ [cm^{-1}] = 2968 (w), 2930 (br, w), 2536 (br, w), 1682 (s), 1616 (w), 1582 (m), 1570 (m), 1464 (w), 1420 (m), 1344 (w), 1296 (s), 1275 (m), 1256 (m), 1231 (s), 1211 (s), 1152 (w), 1111 (w), 995 (w), 943 (m), 905 (w), 891 (w), 843 (m), 791 (m), 779 (m), 758 (m), 748 (m), 669 (m).

The analytic data are in agreement with the literature[136, 137]

6.3 Synthesis of 5-carboxy-1,2,3,3-tetramethyl-3*H*-indolium iodide

[NIH_P248, **NIH_P251**]

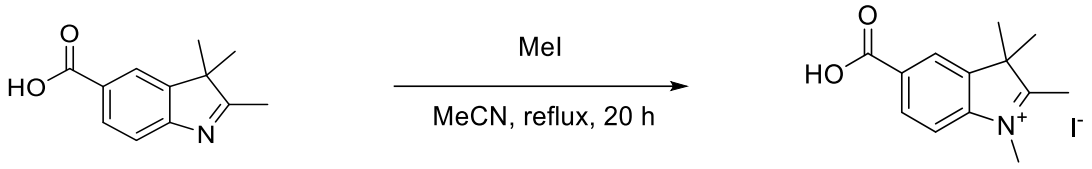

53 **57**

Under argon atmosphere, indole **53** (2.03 g, 10.0 mmol, 1.0 eq.) was dissolved in MeCN (100 mL, HPLC grade). Iodomethane (5.0 mL, 80 mmol, 8.0 eq.) was added and the reaction was refluxed overnight. After full conversion was confirmed by TLC, the reaction was cooled to ambient temperature. The precipitated product was filtered off and washed with Et_2O. The indolium iodide **57** was obtained as colourless solid in 70 % (2.4 g, 7.0 mmol) yield. By concentration of the filtrate and subsequent filtration, additional 1.0 g of product could be obtained.

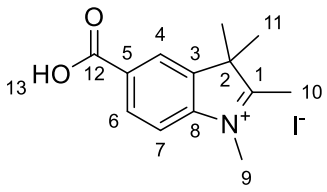

M($C_{13}H_{16}INO_2$)**:** 354.18 $g \cdot mol^{-1}$.

Habitus: Beige solid.

Yield: 3.4 g (9.7 mmol, 97 %).

R_f: 0.33 (100 %, EtOAc).

Mp.: 232–234 °C; >235 °C decomp.

^{1}H-NMR: (500 MHz, DMSO-d_6) δ [ppm] = 13.13 (s, br, 1H, H-13), 8.38 (s, 1H, H-4), 8.19 (d, $^3J_{H6\text{-}H7}$ = 8.2 Hz, 1H, H-6), 8.03 (d, $^3J_{H7\text{-}H6}$ = 8.4

Hz, 1H, H-7), 4.00 (s, 3H, H-9), 2.82 (s, 3H, H-10), 1.58 (s, 6H, H-11).

^{13}C-NMR: (126 MHz, DMSO-d_6) δ [ppm] = 199.0 (C_q, 1C, C-1), 166.5 (C_q, 1C, C-12), 145.2 (C_q, 1C, C-8), 141.9 (C_q, 1C, C-3), 131.6 (C_q, 1C, C-5), 130.4 (CH_{Ar}, 1C, C-6), 124.2 (CH_{Ar}, 1C, C-4), 115.4 (CH_{Ar}, 1C, C-7), 54.2 (C_q, 1C, C-2), 35.0 (CH_3, 1C, C-9), 21.5 (CH_3, 2C, C-11), 14.6 (CH_3, 1C, C-10).

FT-IR (ATR): $\tilde{\nu}$ [cm^{-1}] = 2972 (w), 2876 (br, m), 2716 (br, w), 1715 (s), 1620 (m), 1593 (w), 1468 (w), 1433 (m), 1364 (s), 1333 (w), 1207 (s), 1169 (s), 1107 (m), 943 (m), 818 (s), 766 (m), 718 (s).

The analytic data are in agreement with the literature[138]

Synthesis of 8-bromo-5'-carboxy-1',3',3'-trimethyl-6-nitrospiro[chromene-2,2'-indoline]

[NIH_P254]

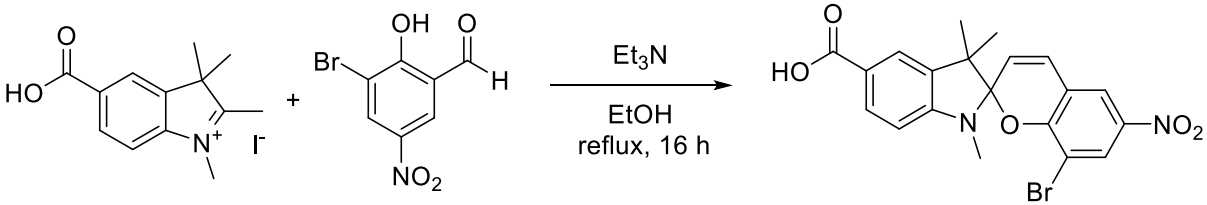

57 **46** **48**

Under argon atmosphere, indolium **57** (1.50 g, 4.3 mmol, 1.0 eq.) was suspended in dry EtOH (40 mL). Triethylamine (0.67 mL, 4.8 mmol, 1.1 eq.) and salicylaldehyde **46** (1.18 g, 4.8 mmol, 1.1 eq.) were added and the reaction was refluxed overnight. After full conversion was confirmed by TLC, the reaction as cooled to ambient temperature and the precipitated product was filtered off. After drying, spiropyran **48** was obtained as a yellow solid in 98 % (1.88 g, 4.2 mmol) yield.

M($C_{20}H_{17}BrN_2O_5$)**:** 445.27 g·mol^{-1}.

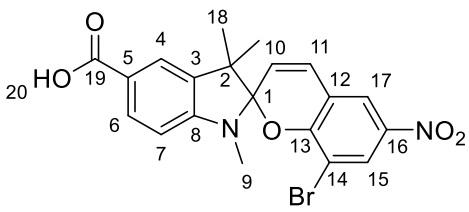

Habitus: Yellow solid.

Yield: 1.88 g (4.2 mmol, 98 %).

Mp.: Slowly turns dark >235°C, melts at 268–271 °C.

^{1}H-NMR: (500 MHz, DMSO-d_6) δ [ppm] = 12.44 (s, br, 1H, H-20), 8.28 (s, 2H, H15, H17), 7.83 (dd, $^{3}J_{H6-H7}$ = 8.2, $^{4}J_{H6-H4}$ = 1.8 Hz, 1H, H-6), 7.70 (d, $^{4}J_{H4-H6}$ = 1.8 Hz, 1H, H-4), 7.29 (d, $^{3}J_{H11-H10}$ = 10.4 Hz, 1H, H-11), 6.74 (d, $^{3}J_{H7-H6}$ = 8.2 Hz, 1H, H-7), 6.10 (d, $^{3}J_{H10-H11}$ = 10.4 Hz, 1H, H-10), 2.77 (s, 3H, H-9), 1.26 (s, 3H, H18/H18'), 1.15 (s, 3H, H18/H18').

^{13}C-NMR: (126 MHz, DMSO-d_6) δ [ppm] = 167.4 (C_q, 1C, C-19), 155.2 (C_q, 1C, C-13), 151.0 (C_q, 1C, C-8), 140.8 (C_q, 1C, C-16), 135.8 (C_q, 1C, C-3), 130.9 (CH_{Ar}, 1C, C-6), 128.4 (CH_{Ar}, 1C, C-11), 128.1 (CH_{Ar}, 1C, C-15/C-17), 122.9 (CH_{Ar}, 1C, C-4), 122.1 (CH_{Ar}, 1C, C-17/C-15), 121.8 (C_q, 1C, C-5), 121.7 (CH_{Ar},1C, C-10), 119.8 (C_q, 1C, C-12), 108.4 (C_q, 1C, C-14), 107.5 (C_q, 1C, C-1), 106.4 (CH_{Ar}, 1C, C-7), 51.7 (C_q, 1C, C-2), 28.4 (CH_3, 1C, C-9), 25.4 (CH_3, 1C, C18/C18'), 19.6 (CH_3, 1C, C18/C18').

FT-IR (ATR): $\tilde{\nu}$ [cm^{-1}] = 3092 (w), 2965 (w), 2874 (w), 2816 (br, w), 2639 (br, w), 1668 (m), 1609 (m), 1512 (s), 1439 (m), 1366 (m), 1333 (s), 1290 (s), 1258 (s), 1090 (s), 1055 (m), 1024 (m), 968 (s), 918 (s), 860 (s), 758 (s), 743 (s), 721 (s).

HRMS (ESI): $^{m}/_{z}$ calcd. for $C_{20}H_{17}BrN_2O_5$: 445.0393607 $[M+H]^+$;
found: 445.03983.

UV/Vis: $\tilde{\nu}$ [nm]: λ_{max} (MeOH, 0.025 mM): MC = 541, 371, 320, 271; SP= 332, 278, 228.

Synthesis of 2,3,3,5-tetramethyl-3*H*-indole

[OC-WP, Kimia Niazkar]

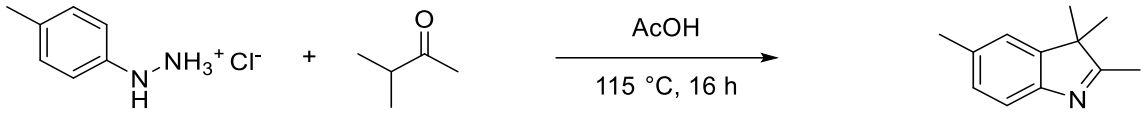

128 **126** **55**

Under argon atmosphere, 5-metyl-phenylhydrazine hydrochloride (**128**) (6.51 g, 41.0 mmol, 1.0 eq.) and 3-methyl-2-butanone (**126**) (7.50 mL, 70.5 mmol, 1.7 eq.) were dissolved in AcOH (50 mL) and heated to 16 h. After 16 h, full conversion was confirmed by TLC. The solvent was partially removed under reduced pressure and the remaining solution was neutralised with sat. Na_2CO_3 solution. The phases were separated and the aqueous phases was extracted DCM (3x60 mL, 2x20 mL). The combined organic phases were washed with brine (40 mL) and dried over Na_2SO_4. After filtration, the solvent was removed under reduced pressure and indole **55** was obtained as a dark red liquid in 90 % (6.37 g, 36.8 mmol) yield.

M($C_{12}H_{15}N$)**:** 173.26 g·mol^{-1}.

Habitus: Dark red liquid.

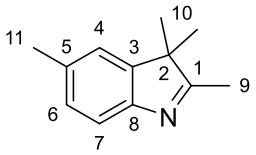

Yield: 6.37 g (36.8 mmol, 90 %).

R_f: 0.30(2:1, *c*Hex:EtOAc).

^{1}H-NMR: (500 MHz, $CDCl_3$) δ [ppm] = 7.41 (d, $^3J_{H7\text{-}H6}$ = 7.7 Hz, 1H, H-7), 7.12 – 7.06 (m, 2H, H-4, H-6), 2.39 (s, 3H, H-11), 2.25 (s, 3H, C-9), 1.28 (s, 6H, C-10, C-10').

^{13}C-NMR: (126 MHz, $CDCl_3$) δ [ppm] = 187.1 (C_q, 1C, C-1), 151.6 (C_q, 1C, C-8), 145.9 (C_q, 1C, C-3), 134.9 (C_q, 1C, C-5), 128.2 (CH_{Ar}, 1C, C-4), 122.2 (CH_{Ar}, 1C, C-6), 119.5 (CH_{Ar}, 1C, C-7), 53.5 (C_q, 1C, C-2), 23.3 (CH_3, 2C, C-10, C-10'), 21.5 (CH_3, 1C, C-11), 15.4 (CH_3, 1C, C-9).

FT-IR (ATR): $\tilde{\nu}$ [cm^{-1}] = 2961 (w), 2924 (w), 2862 (w), 1578 (m), 1460 (s), 1429 (m), 1377 (w), 1360 (w), 1248 (w), 1202 (w), 1140 (w), 1034 (w), 943 (w), 880 (w), 820 (s), 635 (w), 615 (w).

GC-MS: τ_R = 10.21 min; $^m/_z$ (%) = 173.1 $[M]^{\cdot+}$ (80), 158.1 [M, –CH_3] (100), 115.1 (37), 91.1 $[C_7H_7]^{\cdot+}$ (20), 77.0 $[C_6H_5]^{\cdot+}$ (8), 51.1 $[C_4H_3]^{\cdot+}$ (8).

The analytic data are in agreement with the literature[139]

Synthesis of 1,2,3,3,5-pentamethyl-3*H*-indol-1-ium iodide

[OC-WP, Kimia Niazkar]

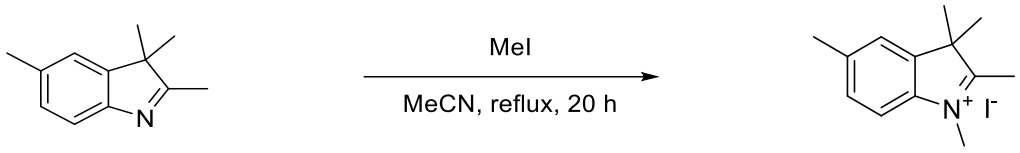

55 **59**

Under argon atmosphere, indole **55** (1.73 g, 10.0 mmol, 1.0 eq.) and iodomethane (1.20 mL, 19.2 mmol, 1.9 eq.) were dissolved in acetonitrile (50 mL) and heated to reflux. After 20 h, full conversion was confirmed by TLC. The solvent was removed under reduced pressure and the residue was recrystallised from ethanol. Indolium **59** was obtained a light-brown solid in 91 % (1.91 g, 6.34 mmol) yield.

M($C_{13}H_{18}IN$)**:** 315.20 g·mol^{-1}.

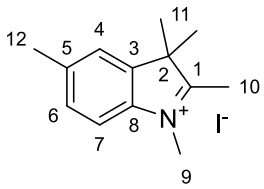

Habitus: Light-brown solid.

Yield: 1.91 g (6.34 mmol, 91 %).

Mp.: Turns dark >220°C, melts at 227-229 °C, Lit.:[140] 214–215 °C.

^{1}H-NMR: (500 MHz, DMSO-*d*$_6$) δ [ppm] = 7.78 (d, $^3J_{H7\text{-}H\text{-}6}$ = 8.2 Hz, 1H, H-7), 7.64 (d, $^4J_{H4\text{-}H6}$ = 1.5 Hz, 1H, H-4), 7.43 (dd, $^3J_{H6\text{-}H7}$ = 8.2 Hz, $^4J_{H6\text{-}H4}$ = 1.5 Hz, 1H, H-6), 3.94 (s, 3H, H-9), 2.73 (s, 3H, H-10), 2.44 (s, 3H, H-12), 1.50 (s, 6H, H-11, H-11').

^{13}C-NMR: (126 MHz, DMSO-*d*$_6$) δ [ppm] = δ 194.8 (C_q, 1C, C-1), 141.7 (C_q, 1C, C-3), 140.0 (C_q, 1C, C-8), 139.5 (C_q, 1C, C-5), 129.2 (CH_{Ar}, 1C, C-6), 123.7 (CH_{Ar}, 1C, C-4), 114.7 (CH_{Ar}, 1C, C-7), 53.6 (C_q, 1C, C-2), 34.6 (CH_3, 1C, C-9), 21.8 (CH_3, 2C, C-11, C-11'), 21.0 (CH_3, 1C, C-12), 13.9 (CH_3, 1C, C-10).

FT-IR (ATR): $\tilde{\nu}$ [cm^{-1}] = 3024 (w), 2967 (w), 2930 (w), 2864 (w), 1632 (w), 1612 (w), 1597 (w), 1481 (m), 1464 (m), 1427 (w), 1391 (m), 1331 (w), 1236 (w), 1163 (w), 1144 (w), 1094 (w), 1036 (w), 991 (w), 947 (m), 876 (w), 818 (s), 704 (m).

GC-MS: τ_R = 10.61 min; $^m/_z$ (%) = 187.2 [M, –HI]$^{\cdot+}$ (35), 172.1 [M, –HI, –CH_3]$^{\cdot+}$ (100), 157.1 [M, –HI, –2XCH_3]$^{\cdot+}$ (15), 115.1 (10), 91.1 [C_7H_7]$^{\cdot+}$ (7).

The analytic data are in agreement with the literature[140]

Synthesis of 8-bromo-1',3',3',5'-tetramethyl-6-nitrospiro[chromene-2,2'-indoline]

[OC-WP, Kimia Niazkar]

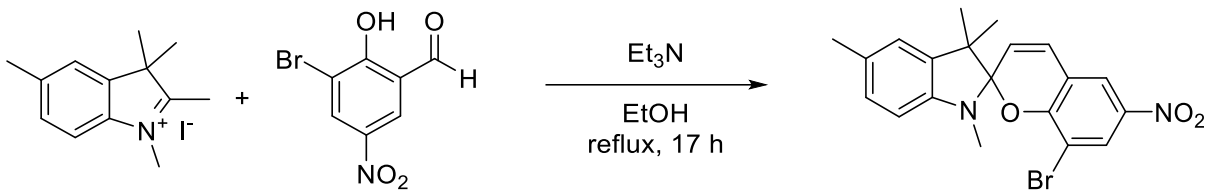

59 **46** **59**

Under argon atmosphere, indolium **59** (600 mg, 2.00 mmol, 1.0 eq.), salicylic aldehyde **46** (490 mg, 2.20 mmol, 1.1 eq.) and triethylamine (0.30 mL, 2.2 mmol, 1.1 eq.) were dissolved in dry EtOH (50 mL) and heated to reflux. After 17 h, the solution was cooled to ambient temperature and the precipitated solid was filtered off and dried. Spiropyran **59** was obtained as a green solid in 98 % (820 mg, 1.96 mmol) yield.

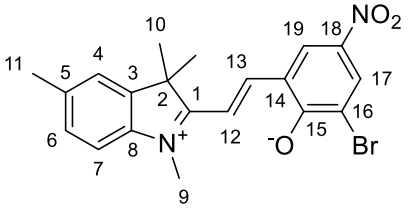

M($C_{20}H_{19}BrN_2O_3$)**:** 415.29 g·mol^{-1}.

Habitus: Green solid.

Yield: 820 mg (1.96 mmol, 98 %).

Mp.: Turns dark purple upon heating >230 °C, melts at 245–248 °C.

^{1}H-NMR: (500 MHz, DMSO-d_6) δ [ppm] = 8.72 (d, $^4J_{H17\text{-}H19}$ = 3.1 Hz, 1H, H-17), 8.44 (d, $^3J_{H12\text{-}H13}$ = 15.5 Hz, 1H, H-12), 8.37 (d, $^3J_{H13\text{-}H12}$ = 15.5 Hz, 1H, H-13), 8.32 – 8.20 (m, 1H, H-19), 7.65 (d, $^3J_{H7\text{-}H6}$ =

8.3 Hz, 1H, H-7), 7.61 (d, $^4J_{H4-H6}$ = 1.6 Hz, 1H, H-4), 7.37 (dd, $^3J_{H6-H7}$ = 8.3 Hz, $^4J_{H6-H4}$ = 1.6 Hz, 1H, H-6), 3.90 (s, 3H, H-9), 2.44 (s, 3H, H-11), 1.74 (s, 6H, H-10, H-10').

^{13}C-NMR: (126 MHz, DMSO-d_6) δ [ppm] = 181.2 (C_q, 1C, C-1), 173.4 (C_q, 1C, C-15), 153.2 (CH_{Ar}, 1C, C-13), 143.1 (C_q, 1C, C-3), 139.9 (C_q, 1C, C-8), 138.0 (C_q, 1C, C-5), 132.6 (CH_{Ar}, 1C, C-17), 130.8 (C_q, 1C, C-18), 129.5 (CH_{Ar}, 1C, C-19), 129.1 (CH_{Ar}, 1C, C-6), 123.2 (CH_{Ar}, 1C, C-4), 120.5 (C_q, 1C, C-16), 119.6 (C_q, 1C, C-14), 113.6 (CH_{Ar}, 1C, C-7), 108.8 (CH_{Ar}, 1C, C-12), 50.9 (C_q, 1C, C-2), 33.2 (CH_3, 1C, C-9), 26.2 (CH_3, 2C, C-10, H-10'), 21.1 (CH_3, 1C, C-11).

C-17 is barely visible in the ^{13}C-NMR but well noticeable in the H,C-2D spectra

Spiropyran

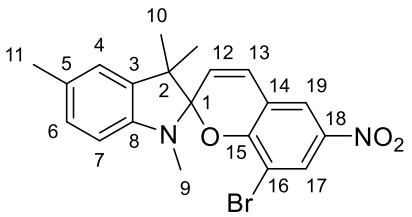

^{1}H-NMR: (500 MHz, DMSO-d_6) δ [ppm] = 8.28 – 8.21 (m, 2H, H-19, H-17), 7.24 (d, $^3J_{H13-H14}$ = 10.4 Hz, 1H, H-13), 6.97 (s, 1H, H-4), 6.95 – 6.93 (m, 1H, H-6), 6.54 (d, $^3J_{H7-H6}$ = 7.8 Hz, 1H, H-7), 6.05 (d, $^3J_{H12-H13}$ = 10.3 Hz, 1H, H-12), 2.64 (s, 3H, H-9), 2.26 (s, 3H, H-11), 1.22 (s, 3H, H-10/H-10'), 1.12 (s, 3H, H-10/H-10').

^{13}C-NMR: (126 MHz, DMSO-d_6) δ [ppm] = 155.6 (C_q, 1C, C-15), 145.0 (C_q, 1C, C-8), 140.5 (C_q, 1C, C-18), 135.8 (C_q, 1C, C-3), 128.2 (C_q, 1C, C-5), 128.1 (CH_{Ar}, 1C, C-13), 128.0 (CH_{Ar}, 1C, C-17), 127.8 (CH_{Ar}, 1C, C-6), 122.3 (CH_{Ar}, 1C, C-4), 122.2 (CH_{Ar}, 1C, C-12), 122.0 (CH_{Ar}, 1C, C-19), 119.9 (C_q, 1C, C-14), 108.4 (C_q, 1C, C-16), 108.1 (C_q, 1C, C-1), 106.9 (CH_{Ar}, 1C, C-7), 52.0 (C_q, 1C, C-2), 28.6 (CH_3, 1C, C-9), 25.7 (CH_3, 1C, C-10/C-10'), 20.7 (CH_3, 1C, C-11), 19.8 (CH_3, 1C, C-10/C-10').

FT-IR (ATR): $\tilde{\nu}$ [cm^{-1}] = 3087 (w), 3055 (w), 2984 (w), 2973 (w), 2932 (w), 1586 (m), 1519 (s), 1432 (m), 1397 (m), 1355 (w), 1301 (m), 1276 (s), 1232 (s), 1167 (m), 1136 (w), 1119 (s), 1070 (m), 970 (m), 847 (m), 742 (m), 696 (m).

HRMS (ESI): $^{m}/_{z}$ calcd. for $C_{20}H_{19}BrN_2O_3$: 415.0651816 $[M+H]^+$;
found: 415.06537.
$^{m}/_{z}$ calcd. for $C_{20}H_{19}BrN_2O_3$: 437.0471263 $[M+Na]^+$;
found: 437.04736.

UV/Vis: $\tilde{\nu}$ [nm]: λ_{max} (MeOH, 0.025 mM): MC = 521, 382, 318. 270; SP= 334, 307, 273, 243.

Synthesis of 5-bromo-2,3,3-trimethyl-3*H*-indole

[OC-WP, Rebecca Maier]

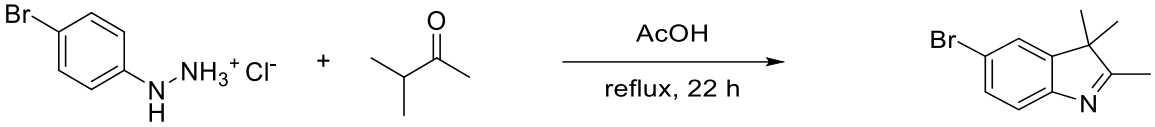

129 **126** **54**

Under argon atmosphere, (4-bromophenyl)hydrazine hydrochloride (**129**) (9.20 g, 41.0 mmol, 1.0 eq.) and 3-methyl-2-butanone (**126**) (6.00 g, 70.0 mmol, 1.7 eq.) were dissolved in acetic acid (50 mL) and heated to reflux. After 22 h, full conversion was confirmed by TLC. The mixture was cooled to ambient temperature and concentrated under reduced pressure. Water (30 mL) and DCM (50 mL) were added to the residue and the mixture was neutralised with sat. Na_2CO_3 solution. The phases were separated and the aqueous phase was extracted with DCM (4x60 mL). The combined organic phases were dried over $MgSO_4$ and filtered. After the solvent was removed under reduced pressure, indole **54** was obtained as dark yellow oil in 98 % (9.53 g, 40.0 mmol) yield.

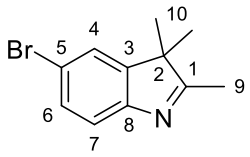

M($C_{11}H_{12}BrN$)**:** 238.13 g·mol^{-1}.

Habitus: Dark yellow oil.

Yield: 9.53 g (40.0 mmol, 98 %).

^{1}H-NMR: (500 MHz $CDCl_3$) δ [ppm] = 7.50 – 7.31 (m, 3H, H-4, H-6, H-7), 2.26 (s, 3H, H-9), 1.30 (s, 6H, H-10, H-10').

^{13}C-NMR: (126 MHz, $CDCl_3$) δ [ppm] = 188.6 (C_q, 1C, C-9), 152.8 (C_q, 1C, C-8), 148.0 (C_q, 1C, C-3), 130.8 (CH_{Ar}, 1C, C-6), 125.0 (CH_{Ar}, 1C, C-4/C-7), 121.4 125.0 (CH_{Ar}, 1C, C-4/C-7), 119.0 (C_q, 1C,

C-5), 54.3 (C_q, 1C, C-2), 23.1 (CH_3, 2C, C-10, C-10'), 15.6 (CH_3, 2C, C-9).

FT-IR (ATR): $\tilde{\nu}$ [cm^{-1}] = 2963 (w), 2926 (w), 2868 (w), 1690 (w), 1605 (w), 1574 (m), 1531 (w), 1462 (s), 1445 (s), 1427 (m), 1416 (m), 1362 (m), 1314 (w), 1256 (m), 1244 (m), 1219 (m), 1198 (m), 1148 (w), 1117 (w), 1084 (m), 1051 (w), 1007 (w), 937 (w), 874 (m), 820 (s), 808 (s), 760 (w), 706 (m), 677 (m), 633 (m).

GC-MS: τ_R = 11.36 min; $^m/_z$ (%) = 239.1 [M, $^{81}Br]^{\cdot+}$ (92), 237.0 [M, $^{79}Br]^{\cdot+}$ (100), 224.0 [M, ^{81}Br, $-CH_3]^{\cdot+}$ (73), 222.0 [M, ^{79}Br, $-CH_3]^{\cdot+}$ (73), 158.1 [M, $-Br]^{\cdot+}$ (34), 143.1 [M,–Br, $-CH_3]^{\cdot+}$ (41), 115.1 (97), 102.1 (29), 91.1 (23), 75.1 (21).

The analytic data are in agreement with the literature[141]

Synthesis of 5-bromo-1,2,3,3-tetramethyl-3*H*-indol-1-ium iodide

[OC-WP, Rebecca Maier]

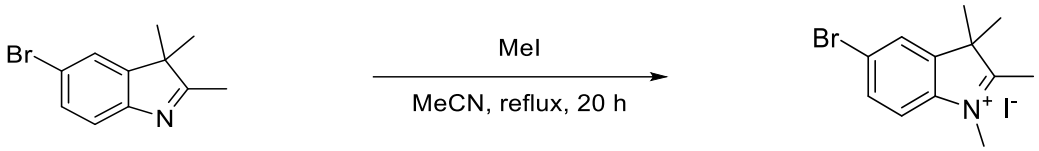

54 **58**

Under argon atmosphere, indole **54** (2.38 g, 10.0 mmol, 1.0 eq.) and iodomethane (5.0 mL, 80.0 mmol, 8.0 eq.) were dissolved in acetonitrile (100 mL) and heated to reflux. After 20 h, full conversion was confirmed by TLC. The mixture was cooled to ambient temperature, and the precipitate solid was filtered off and washed with diethyl ether. Indolium **58** was obtained as a beige solid in 72 % (2.75 g, 7.24 mmol) yield.

M($C_{12}H_{15}BrNO$)**:** 380.07 g·mol^{-1}.

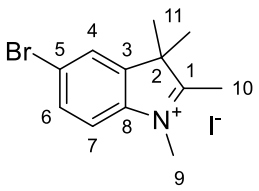

Habitus: Beige solid.

Yield: 2.75 g (7.24 mmol, 72 %).

Mp.: 235–236 °C, Lit.: [141] 245 °C.

^{1}H-NMR: (500 MHz, DMSO-d_6) δ [ppm] = 8.17 (d, $^{4}J_{H4-H6}$ = 1.8 Hz, 1H, H-4), 7.88 (d, $^{3}J_{H7-H6}$ = 8.5 Hz, 1H), 7.85 (dd, $^{3}J_{H6-H7}$ = 8.5 Hz, $^{4}J_{H6-H4}$ 1.8 Hz, 1H), 3.96 (s, 3H, H-9), 2.76 (s, 3H), 1.54 (s, 6H).

^{13}C-NMR: (126 MHz, DMSO-d_6) δ [ppm] = 196.5 (C_q, 1C, C-1), 143.8 (C_q, 1C, C-3), 141.4 (C_q, 1C, C-8), 131.7 (CH_{Ar}, 1C, C-6), 126.7 (CH_{Ar}, 1C, C-4), 122.6 (C_q, 1C, C-5), 117.1 (CH_{Ar}, 1C, C-7), 54.2 (C_q, 1C, C-2), 34.9 (CH_3, 1C, C-9), 21.5 (CH_3, 2C, C-11, C-11'), 14.3 (CH_3, 1C, C-10).

FT-IR (ATR): $\tilde{\nu}$ [cm^{-1}] = 3040 (w), 3013 (w), 2967 (w), 2913 (w), 2868 (w), 1628 (w), 1607 (w), 1582 (w), 1466 (m), 1450 (m), 1406 (m), 1337 (w), 1319 (w), 1254 (w), 1233 (w), 1169 (w), 1134 (m), 1078 (m), 1036 (w), 1035 (m), 880 (w), 824 (s), 795 (m), 638 (w).

GC-MS: τ_R =12.02 min; $^{m}/_{z}$ (%) = 253.0 [M, ^{81}Br, –HI]$^{\cdot+}$ (44), 251.1 [M, ^{79}Br, –HI]$^{\cdot+}$ (45), 238.0 [M, ^{81}Br, -HI, –CH_3]$^{\cdot+}$ (95), 236.0 [M, ^{79}Br, -HI, –CH_3]$^{\cdot+}$ (100), 157.1 [M, –HI,– CH_3, –Br]$^{\cdot+}$ (45), 143.1 [M,–Br, –CH_3]$^{\cdot+}$ (41), 142.1 (15), 128.1 (23), 115.1 (27).

The analytic data are in agreement with the literature[141]

Synthesis of 5',8-dibromo-1',3',3'-trimethyl-6-nitrospiro[chromene-2,2'-indoline]

[OC-WP, Rebecca Maier]

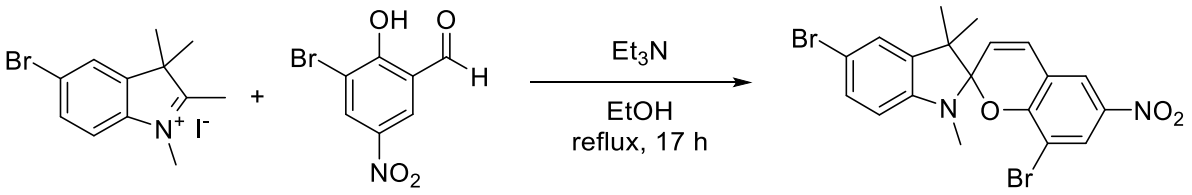

54 **46** **58**

Under argon atmosphere, indolium **54** (1.14 g, 3.00 mmol, 1.0 eq.), salicylic aldehyde **46** (0.86 g, 3.50 mmol, 1.2 eq.) and triethylamine (0.44 mL, 3.2 mmol, 1.1 eq.) were suspended in dry EtOH (50 mL) and the mixture was heated to reflux. After 17 h, the mixture was cooled to ambient temperature and the precipitated solid was filtered off and washed with cold EtOH. After drying under reduced pressure, spiropyran **58** was obtained as a dark-grey solid in 79 % (1.3 g, 2.7 mmol) yield.

M($C_{19}H_{16}Br_2N_2O_3$)**:** 480.16 g·mol^{-1}.

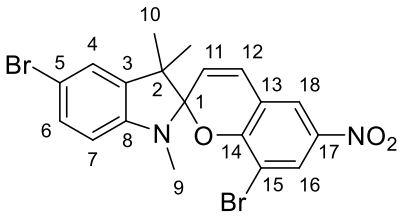

Habitus: Dark-grey solid.

Yield: 1.3 g (2.7 mmol, 79 %).

Mp.: 249°C, Lit.:[141] 252 °C.

^{1}H-NMR: (500 MHz, DMSO-d_6) δ [ppm] = 8.28 (d, $^4J_{H16\text{-}H18}$ = 2.7 Hz, 1H, H-16), 8.27 (d, $^4J_{H18\text{-}H16}$ = 2.7 Hz, 1H, H-18), 7.35 (d, $^4J_{H4\text{-}H6}$ = 2.1 Hz, 1H, H-4), 7.30 (dd, $^3J_{H6\text{-}H7}$ = 8.3, $^4J_{H6\text{-}H4}$ = 2.1 Hz, 1H, H-6), 7.27 (d, $^3J_{H12\text{-}H11}$ = 10.4 Hz, 1H, H-12), 6.64 (d, $^3J_{H7\text{-}H6}$ = 8.3 Hz, 1H, H-7), 6.06 (d, $^3J_{H11\text{-}H12}$ = 10.4 Hz, 1H, H-11), 2.67 (s, 3H, H-9), 1.23 (s, 3H, H-10/H-10'), 1.14 (s, 3H, H-10/H-10').

^{13}C-NMR: (126 MHz, DMSO-d_6) δ [ppm] = 155.3 (C_q, 1C, C-14), 146.5 (C_q, 1C, C-8), 140.7 (C_q, 1C, C-16), 138.5 (C_q, 1C, C-3), 130.2 (CH_{Ar}, 1C, C-6), 128.4 (CH_{Ar}, 1C, C-12), 128.1 (CH_{Ar}, 1C, C-16), 124.7 (CH_{Ar}, 1C, C-4), 122.1 (C_q, 1C, C-18), 121.7 (CH_{Ar}, 1C, C-11), 119.8 (C_q, 1C, C-13), 110.7 (C_q, 1C, C-5), 109.1 (CH_{Ar}, 1C, C-7), 108.4, 107.6 (C_q, 1C, C-1), 52.1 (C_q, 1C, C-2), 28.5 (CH_3, 1C, C-9), 25.2 (CH_3, 1C, C-10/C-10'), 19.4 (CH_3, 1C, C-10/C-10').

FT-IR (ATR): $\tilde{\nu}$ [cm^{-1}] = 3102 (w), 2983 (w), 2936 (w), 1598 (m), 1511 (s), 1441 (m), 1399 (m), 1291 (s), 1204 (s), 1167 (m), 1120 (m), 1081 (s), 960 (m), 823 (m), 745 (w), 730 (m).

HRMS (ESI): $^m/_z$ calcd. for $C_{19}H_{16}Br_2N_2O_3$: 433.9749659 $[M+H]^+$;
found: 433.97533.
$^m/_z$ calcd. for $C_{19}H_{16}Br_2N_2O_3$: 500.9419888 $[M+Na]^+$;
found: 500.94274.

UV/Vis: $\tilde{\nu}$ [nm]: λ_{max} (MeOH, 0.025 mM): MC = 532, 371, 320, 273, 239; SP= 335, 313, 271, 247.

The analytic data are in agreement with the literature[141]

Synthesis of 1,2,3,3-tetramethyl-3H-indol-1-ium iodide

[NIH_P267]

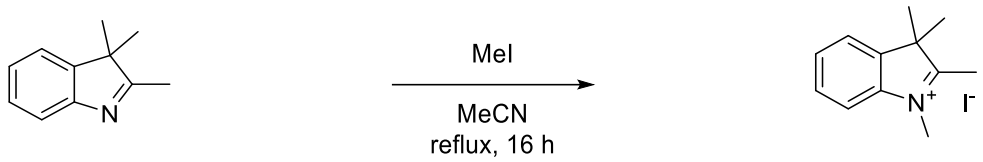

25 **33**

Under argon atmosphere, indole **25** (15.9 g, 100 mmol, 1.0 eq.) and iodomethane (18.7 mL, 300 mmol, 3.0 eq.) were dissolved in MeCN (80 mL, HPLC grade) and refluxed for 16 h. After cooling to ambient temperature, the precipitate was filtered off and washed with Et_2O. Indolium **33** was obtained as beige solid in 93 % (27.9 g, 92.5 mmol) yield.

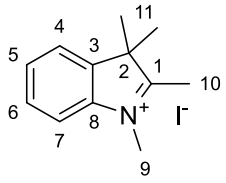

M($C_{12}H_{16}IN$)**:** 301.17 g·mol^{-1}.

Habitus: Beige solid.

Yield: 27.9 g (92.5 mmol, 93 %).

Mp.: decomp. >248 °C, Lit.:[142] decomp. >245 °C.

^{1}H-NMR: (500 MHz, DMSO-d_6) δ [ppm] = 7.94 – 7.90 (m, 1H, H-7), 7.86 – 7.82 (m, 1H, H-4), 7.66 – 7.60 (m, 2H, H-5, H-6), 3.98 (s, 3H), 2.78 (s, 3H), 1.54 (s, 6H).

^{13}C-NMR: (126 MHz, DMSO-d_6) δ [ppm] = 196.0 (C_q, 1C, C-1), 142.1 (C_q, 1C, C-8), 141.6 (C_q, 1C, C-3), 129.3 (CH_{Ar}, 1C, C-5), 128.8 (CH_{Ar}, 1C, C-6), 123.3 (CH_{Ar}, 1C, C-4), 115.1 (CH_{Ar}, 1C, C-7), 53.9 (C_q, 1C, C-1), 34.7 (CH_3, 1C, C-9), 21.7 (CH_3, 2C, C-11), 14.2 (CH_3, 1C, C-10).

FT-IR (ATR): $\tilde{\nu}$ [cm^{-1}] = 3026 (w), 2974 (w), 2965 (w), 2928 (w), 2864 (w), 1630 (w), 1595 (w), 1481 (m), 1456 (m), 1393 (w), 1356 (w), 1325 (w), 1296 (w), 1263 (w), 1236 (w), 1173 (w), 1092 (w), 989 (w), 937 (m), 883 (w), 818 (w), 777 (s), 768 (s).

GC-MS: τ_R= min 10.18; $^m/_z$ (%) = 171.6 (33), 156.5 (100), 141.4 (17) 113.2 (13).

The analytic data are in agreement with the literature[142]

Synthesis of 2,3,3-trimethyl-5-nitro-3H-indole

[NIH_P273, **NIH_P290**]

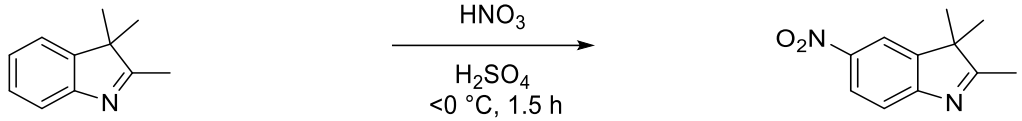

25 **60**

Indole **25** (9.6 mL, 60 mmol, 1.0 eq.) was added in small portions to conc. sulfuric acid (40 mL) which was cooled to –10 °C. While addition the temperature was kept below 10 °C. After the temperature was back at –10 °C, a solution of conc. nitric acid (6.1 mL, 72 mmol, 1.2 eq.) in conc. sulfuric acid (40 mL) was added over 1.5 h while the temperature was kept below 0 °C. The solution was stirred for further 1.5 h before it was poured onto ice (150 g). The pH of the solution was adjusted to eight by addition of conc. NaOH while keeping the temperature below 15 °C. The precipitated solid was filtered of and washed with water. The wet product was dissolved in EtOH and dried over Na_2SO_4. After the solvent was removed under reduced pressure, indole **60** was obtained a yellow solid in 87 % (10.6 g, 51.9 mmol) yield.

M($C_{11}H_{12}N_2O_2$)**:** 204.23 g·mol^{-1}.

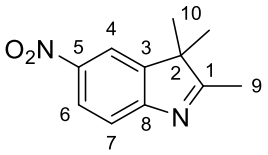

Habitus: Yellow solid.

Yield: 10.6 g (51.9 mmol, 87 %).

R_f: 0.36 (1:2, *c*Hex:EtOAc).

Mp.: 129–130 °C, Lit.:[120] 130–131 °C.

^{1}H-NMR: (500 MHz, $CDCl_3$) δ [ppm] = 8.25 (dd, $^3J_{H6\text{-}H7}$ = 8.4 Hz, $^3J_{H6\text{-}H4}$ = 2.3 Hz, 1H, H-6), 8.15 (d, $^3J_{H4\text{-}H6}$ = 2.3 Hz, 1H, H-4), 7.61 (d, $^3J_{H7\text{-}J6}$ = 8.5 Hz, 1H, H-7), 2.35 (s, 3H, H-9), 1.36 (s, 6H, H-10, H-10').

^{13}C-NMR: (126 MHz, $CDCl_3$) δ [ppm] = 194.2 (C_q, 1C, C-1), 159.1 (C_q, 1C, C-8), 146.8 (C_q, 1C, C-3), 145.8 (C_q, 1C, C-5), 124.7 (CH_{Ar}, 1C, C-6), 120.2 (CH_{Ar}, 1C, C-7), 117.3 (CH_{Ar}, 1C, C-4), 54.6 (C_q, 1C, C-2), 22.9 (CH_3, 2C, C-10, C-10'), 16.1 (CH_3, 1C, C-9).

FT-IR (ATR): $\tilde{\nu}$ [cm^{-1}] = 3094 (w), 3032 (w), 2976 (w), 1599 (w), 1564 (m), 1514 (s), 1464 (w), 1450 (w), 1420 (m), 1389 (w), 1335 (s), 1315 (s), 1288 (m), 1240 (m), 1206 (m), 1152 (w), 1111 (m), 1055 (w),

1036 (w), 997 (w), 945 (w), 912 (m), 899 (w), 847 (s), 802 (s), 773 (m), 739 (s), 710 (w), 681 (w), 635 (w).

GC-MS: τ_R = 12.35 min; $^m/_z$ (%) = 204.1 $[M]^+$ (100), 189.0 [M, $-CH_3]^{\cdot+}$ (81), 174.1 [M, $2x-CH_3]^{\cdot+}$ (31), 159.1 [M, $NO_2]^{\cdot+}$ (33), 143.1 (36), 115.1 (78), 91.1 (34), 77.0 $[C_6H_5]^{\cdot+}$ (17).

The analytic data are in agreement with the literature[120]

Synthesis of 1,2,3,3-tetramethyl-5-nitro-3H-indol-1-ium iodide

[**NIH_P275**, NIH_P291]

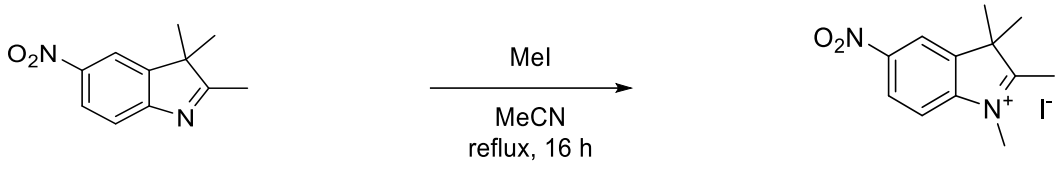

60 **63**

Under argon atmosphere, indole **60** (4.43 g, 22.0 mol, 1.0 eq.) and iodomethane (4.1 mL, 66 mmol, 3.0 eq.) were suspended in MeCN (40 mL, HPLC grade) and heated to reflux. After 16 h, the solvent and excess iodomethane were removed under reduced pressure. The residue was suspended in Et_2O and filtered. Indolium **63** was obtained as a beige powder in 91 % (7.1 g, 20 mmol) yield.

M($C_{12}H_{15}IN_2O_2$)**:** 346.17 g·mol^{-1}.

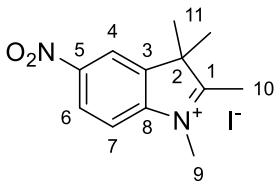

Habitus: Beige powder.

Yield: 7.1 g (20 mmol, 91 %).

Mp.: Turns dark >180°C, melts at 198–200 °C, Lit.:[120] 205–208 °C.

^{1}H-NMR: (500 MHz, CD_3CN) δ [ppm] = 8.59 (d, $^4J_{H4\text{-}H6}$ = 2.2 Hz, 1H, H-4), 8.50 (dd, $^3J_{H6\text{-}H7}$ = 8.8 Hz, $^3J_{H6\text{-}H4}$ = 2.3 Hz, 1H, H-6), 7.94 (d, $^3J_{H7\text{-}H6}$ = 8.8 Hz, 1H, H-7), 3.99 (s, 3H, H-9), 2.80 (s, 3H, H-10), 1.63 (s, 6H, H-11, H-11').

^{13}C-NMR: (126 MHz, CD_3CN) δ [ppm] = 202.4 (C_q, 1C, C-1), 149.7 (C_q, 1C, C-5), 147.1 (C_q, 1C, C-8), 143.9 (C_q, 1C, C-3), 126.3 (CH_{Ar}, 1C, C-6), 120.1 (CH_{Ar}, 1C, C-4), 117.2 (CH_{Ar}, 1C, C-7), 56.2 (C_q, 1C,

C-2), 36.6 (CH_3, 1C, C-9), 22.1 (CH_3, 1C, C-10), 16.0 (CH_3, 2C, C-11, C-11').

C-1, C-5 and C8 are barely visible in the ^{13}C-NMR but well noticeable in the H,C-2D spectra

FT-IR (ATR): $\tilde{\nu}$ [cm^{-1}] = 3464 (w), 3092 (w), 3067 (w), 3028 (w), 2978 (w), 2947 (w), 1632 (w), 1595 (w), 1530 (s), 1474 (m), 1462 (m), 1341 (s), 1265 (w), 1113 (w), 1053 (w), 984 (w), 945 (w), 920 (w), 824 (w), 781 (s), 733 (m).

GC-MS: τ_R = 13.54 min; $^m/_z$ (%) = 218.1 $[M]^{\cdot+}$ (59), 203.0 $[M, -CH_3]^{\cdot+}$ (100), 197.9 $[M, 2x-CH_3]^{\cdot+}$ (13), 173.0 $[M, 3x-CH_3]^{\cdot+}$ (20), 157.1 $[M, -CH_3, -NO_2]^{\cdot+}$ (73), 115.1 (27), 91.1 $[C_7H_7]^{\cdot+}$ (17), 77.0 $[C_6H_5]^{\cdot+}$ (22), 51.1 $[C_4H_3]^{\cdot+}$ (27).

The analytic data are in agreement with the literature[46, 120]

Synthesis of 8-bromo-1',3',3'-trimethyl-5',6-dinitrospiro[chromene-2,2'-indoline]

[NIH_P278]

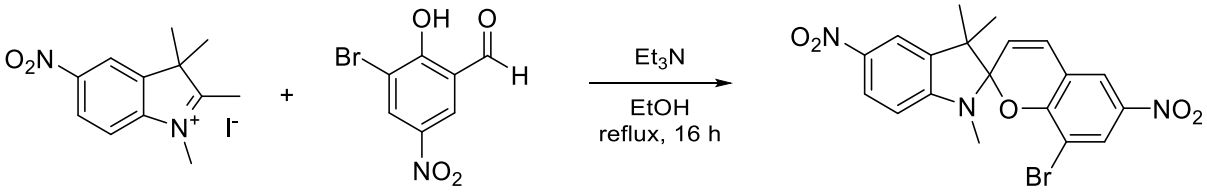

63 **46** **61**

Under argon atmosphere, indolium **63** (0.69 mg, 2.0 mmol, 1.0 eq.) and salicylic aldehyde **46** (0.54 g, 2.2 mmol, 1.1 eq.) were suspended in EtOH (10 mL, HPLC grade) and heated to reflux. After 16 h, the solution was cooled to ambient temperature and the precipitated product was filtered of and washed with Et_2O. Spiropyran **61** was obtained a yellow solid in 85 % (0.75 g, 1.7 mmol) yield.

M($C_{19}H_{16}BrN_3O_5$)**:** 446.26 g·mol^{-1}.

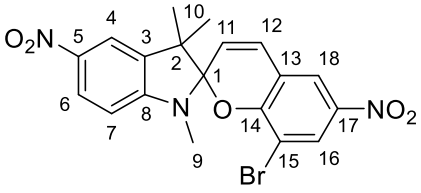

Habitus: Yellow solid.

Yield: 0.75 g (1.7 mmol, 85 %).

Mp.: Slowly turns dark >190 °C, melts at 222–224 °C.

^{1}H-NMR: (500 MHz, DMSO-d_6) δ [ppm] = 8.31 (s, 2H, H-16, H-18), 8.17 (dd, $^{3}J_{H6-H7}$ = 8.7 Hz, $^{4}J_{H6-H4}$ = 2.4 Hz, 1H, H-6), 8.08 (d, $^{4}J_{H4-H6}$ = 2.4 Hz, 1H, H-4), 7.32 (d, $^{3}J_{H13-H12}$ = 10.4 Hz, 1H, H-12), 6.87 (d, $^{3}J_{H7-H6}$ = 8.7 Hz, 1H, H-7), 6.12 (d, $^{3}J_{H12-H13}$ = 10.4 Hz, 1H, H-11), 2.85 (s, 3H, H-9), 1.31 (s, 3H, H-10/H-10'), 1.19 (s, 3H, H-10/H-10').

^{13}C-NMR: (126 MHz, DMSO-d_6) δ [ppm] = 154.7 (C_q, 1C, C-14), 152.7 (C_q, 1C, C-8), 141.1 (C_q, 1C, C-17), 140.1 (C_q, 1C, C-7), 136.8 (C_q, 1C, C-3), 128.6 (CH_{Ar}, 1C, C-12), 128.2 (CH_{Ar}, 1C, C-15), 126.2 (CH_{Ar}, 1C, C-6), 122.2 (CH_{Ar}, 1C, C-18), 121.1 (CH_{Ar}, 1C, C-11), 119.7 (C_q, 1C, C-13), 118.1 (CH_{Ar}, 1C, C-4), 108.5 (C_q, 1C, C-15), 107.2 (C_q, 1C, C-1), 106.3 (CH_{Ar}, 1C, C-7), 51.7 (C_q, 1C, C-2), 28.5 (CH_3, 1C, C-9), 25.0 (CH_3, 1C, C-10/C-10'), 19.3 (CH_3, 1C, C-10/C-10').

FT-IR (ATR): $\tilde{\nu}$ [cm^{-1}] = 3078 (w), 2968 (w), 2938 (w), 1603 (m), 1516 (s), 1491 (s), 1441 (m), 1312 (s), 1287 (s), 1269 (s), 1260 (s), 1225 (m), 1206 (w), 1177 (m), 1123 (m), 1107 (s), 1090 (s), 1051 (m), 1020 (s), 968 (s), 930 (s), 905 (s), 868 (s), 843 (m), 814 (s), 772 (m), 760 (m), 719 (s).

HRMS (ESI): $^{m}/_{z}$ calcd. for $C_{19}H_{16}BrN_3O_5$: 446.0346097 $[M+H]^+$;
found: 446.03503.
$^{m}/_{z}$ calcd. for $C_{19}H_{16}BrN_3O_5$: 468.0165544 $[M+Na]^+$;
found: 468.01708.

UV/Vis: $\tilde{\nu}$ [nm]: λ_{max} (MeOH, 0.025 mM): MC = 559, 370, 245; SP= 365, 246. 226.

Synthesis of 2,3,3-trimethyl-3H-indol-5-amine

[NIH_P284]

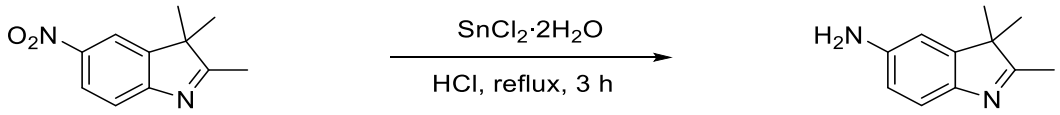

60 **64**

Indole **60** (3.65 g, 17.9 mmol, 1.0 eq.) and tin(II)chloride dihydrate (22.2 g, 98.4 mmol, 5.5 eq.) were suspended in 6 M HCl (40 mL) and heated to reflux. After 3 h, full conversion was confirmed by TLC. The solution was cooled to 0 °C and neutralised (pH 7) with conc. NaOH-solution. After extraction with EtOAc (3x100 mL), the combined organic phases were dried over Na_2SO_4 and filtered. The solvent was removed under reduced pressure and indole **64** was obtained a beige solid in 88 % (2.76 g, 15.8 mmol) yield.

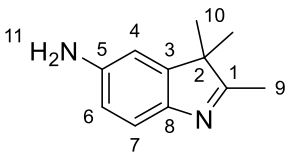

M($C_{11}H_{14}N_2$)**:** 174.25 g·mol^{-1}.

Habitus: Beige solid.

Yield: 2.76 g (15.8 mmol, 88 %).

R_f: 0.30 (1:3, *c*Hex:EtOAc).

Mp.: 182–185°C.

^{1}H-NMR: (500 MHz, DMSO-d_6) δ [ppm] = 7.06 (d, $^3J_{H7\text{-}H6}$ = 8.1 Hz, 1H, H-7), 6.57 (d, $^4J_{H4\text{-}H6}$ = 2.2 Hz, 1H, H-4), 6.44 (dd, $^3J_{H6\text{-}H4}$ = 8.1 Hz, $^3J_{H6\text{-}H7}$ = 2.2 Hz, 1H, H-6), 4.97 (s, 2H, H-11), 2.10 (s, 3H, H-9), 1.16 (s, 6H, H-10, H-10').

^{13}C-NMR: (126 MHz, DMSO-d_6) δ [ppm] = 181.5 (C_q, 1C, C-1), 147.1 (C_q, 1C, C-3), 146.5 (C_q, 1C, C-5), 143.9 (C_q, 1C, C-8), 119.3 (CH_{Ar}, 1C, C-7), 112.1 (CH_{Ar}, 1C, C-6), 107.7 (CH_{Ar}, 1C, C-4), 52.5 (C_q, 1C, C-2), 23.0 (CH_3, 2C, C-10, C-10'), 14.7 (CH_3, 1C, C-9).

FT-IR (ATR): $\tilde{\nu}$ [cm^{-1}] = 3333 (w), 3194 (m), 2959 (m), 2922 (w), 2862 (w), 1651 (w), 1616 (m), 1589 (m), 1576 (m), 1476 (s), 1460 (s), 1422 (m), 1377 (m), 1346 (m), 1306 (m), 1288 (m), 1248 (w), 1223 (w), 1196 (m), 1115 (m), 1063 (w), 945 (w), 860 (s), 822 (s), 768 (m), 708 (s), 679 (s), 613 (s).

GC-MS: τ_R = 11.74 min; $^m/_z$ (%) = 174.1 $[M]^{\cdot+}$ (100), 159.1 [M, $-CH_3]^{\cdot+}$ (88), 132.1 (12), 91.1 (9), 77.0 $[C_6H_5]^{\cdot+}$ (9).

Synthesis of *N,N,N*,1,3,3-hexamethyl-2-methyleneindolin-5-aminium iodide

[NIH_P285]

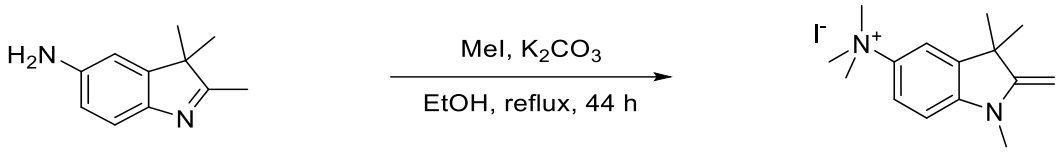

64 **65**

Under argon atmosphere, indole **64** (1.74 g, 10.0 mmol, 1.0 eq.), iodomethane (2.80 mL, 45.0 mmol, 4.5 eq.) and K_2CO_3 (6.22 g, 45.0 mmol, 4.5 eq.) were suspended in dry EtOH (90 mL) and heated to reflux. After 18 h and after 38 h, additional iodomethane (2x2.8 mL, 20 mmol, 2.0 eq.) was added to the reaction. The reaction was stopped after in total 44 h. The reaction mixture was filtered and the solution was washed with water (100 mL). The organic phase was dried over Na_2SO_4, filtered and the solvent was removed under reduced pressure. The crude product was purified by column chromatography over silica gel (7:1→5:1, DCM:MeOH). Indolium **65** was obtained as a red solid in 29 % (0.76 g, 2.9 mmol) yield.

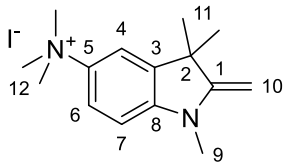

M($C_{15}H_{23}IN_2$)**:** 385.27 g·mol^{-1}.

Habitus: Red solid.

Yield: 0.76 g (2.0 mmol, 20 %).

R_f: 0.23 (5:1, DCM:MeOH).

Mp.: decomp. >110°C.

^{1}H-NMR: (500 MHz, DMSO-d_6) δ [ppm] = 7.86 (d, $^4J_{H4\text{-}H6}$ = 2.9 Hz, 1H, H-4), 7.64 (dd, $^3J_{H6\text{-}H7}$ = 8.8 Hz, $^4J_{H6\text{-}H4}$ = 2.8 Hz, 1H, H-6), 6.81 (d, $^3J_{H7\text{-}H6}$ = 8.8 Hz, 1H, H-7), 4.03 – 3.94 (m, 2H, H-10), 3.57 (s, 9H, H-12), 3.06 (CH_3, 1C, H-9), 1.34 (s, 6H, H-11, H-11').

^{13}C-NMR: (126 MHz, DMSO-d_6) δ [ppm] = 161.2 (C_q, 1C, C-1), 146.6 (C_q, 1C, C-8), 138.8 (C_q, 1C, C-5), 138.6 (C_q, 1C, C-3), 119.9 (CH_{Ar}, 1C, C-6), 114.6 (CH_{Ar}, 1C, C-4), 104.7 (CH_{Ar}, 1C, C-7), 76.3 (CH_2, 1C, C-10), 56.8 (CH_3, 3C, C-12), 43.8 (C_q, 1C, C-2), 29.5 (CH_3, 2C, C-11, C-11'), 28.8 (CH_3, 1C, C-9).

FT-IR (ATR): $\tilde{\nu}$ [cm^{-1}] = 3406 (m), 3011 (w), 2957 (w), 2922 (w), 2899 (w), 2864 (w), 1655 (m), 1611 (s), 1495 (s), 1470 (s), 1460 (s), 1385 (s), 1364 (m), 1344 (m), 1304 (s), 1285 (m), 1238 (m), 1227 (m), 1161 (w), 1140 (m), 1119 (s), 1099 (s), 1061 (m), 937 (s), 918 (s), 874 (s), 864 (s), 797 (s), 762 (s), 706 (m), 681 (m), 650 (s), 619 (s), 606 (s).

GC-MS: τ_R = 13.05 min; $^m/_z$ (%) = 230.2 $[M–HI]^{\cdot+}$ (73), 215.2 [M, –HI, $–CH_3]^{\cdot+}$ (100), 200.2 [M, –HI, 2x$–CH_3]^{\cdot+}$ (31), 188.1 (15), 173.2 [M, $–INMe_3]^{\cdot+}$ (14), 115.1 (13), 77.1 $[C_6H_5]^{\cdot+}$ (10).

Synthesis of 8-bromo-*N*,*N*,*N*,1',3',3'-hexamethyl-6-nitrospiro-[chromene-2,2'-indolin]-5'-aminium iodide

[NIH_P287]

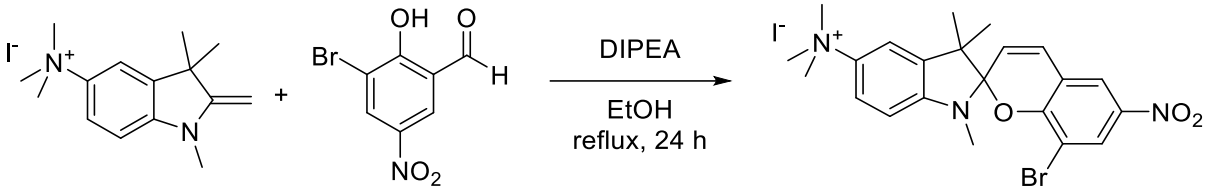

65 **46** **62**

Under argon atmosphere, indole **65** (500 mg, 1.40 mmol, 1.0 eq.), salicylic aldehyde **46** (615 mg, 2.50 mmol, 1.8 eq.) and diisopropylethylamine (0.40 mL, 2.3 mmol, 1.6 eq.) were suspended in EtOH (15 mL, HPLC grade) and heated to reflux. Full conversion was confirmed by TLC after 24 h. All volatile components were removed under reduced pressure and the residue was recrystallised from EtOH. Spiropyran **62** was obtained as a pale red solid in 71 % (609 mg, 1.04 mmol) yield.

M($C_{22}H_{25}BrIN_3O_3$)**:** 586.27 g·mol^{-1}.

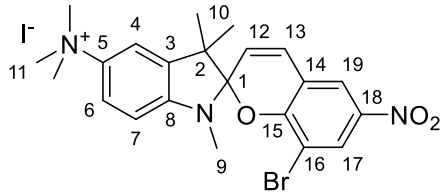

Habitus: Pale red solid.

Yield: 609 mg (1.04 mmol, 71 %).

Mp.: turns dark >160 °C, melts at 196–198 °C.

^{1}H-NMR: (500 MHz, DMSO-*d*$_6$) δ [ppm] = 8.30 (s, 2H, H-17, H-19), 7.83 (d, $^4J_{H4\text{-}H6}$ = 2.8 Hz, 1H, H-4), 7.70 (dd, $^3J_{H6\text{-}H7}$ = 8.7 Hz, $^4J_{H6\text{-}H4}$ = 2.8 Hz, 1H, H-6), 7.29 (d, $^3J_{H13\text{-}H12}$ = 10.3 Hz, 1H, H-13), 6.81 (d, $^3J_{H7\text{-}H6}$ = 8.8 Hz, 1H, H-7), 6.08 (d, $^3J_{H12\text{-}H13}$ = 10.3 Hz, 1H, H-12), 3.58 (s, 9H, H-11), 2.75 (s, 3H, H-9), 1.30 (s, 3H, H-10/H-10'), 1.17 (s, 3H, H-10/H-10').

^{13}C-NMR: (126 MHz, DMSO-*d*$_6$) δ [ppm] = 155.5 (C_q, 1C, C-15), 148.2 (C_q, 1C, C-8), 141.4 (C_q, 1C, C-18), 140.7 (C_q, 1C, C-5), 137.8 (C_q, 1C, C-3), 128.8 (CH_{Ar}, 1C, C-13), 128.6 (CH_{Ar}, 1C, C-17), 122.6 (CH_{Ar}, 1C, C-19), 122.1 (CH_{Ar}, 1C, C-12), 120.6 (CH_{Ar}, 1C, C-6), 120.3 (C_q, 1C, C-14), 114.9 (CH_{Ar}, 1C, C-4), 108.8 (C_q, 1C, C-16), 107.8 (C_q, 1C, C-1), 107.0 (CH_{Ar}, 1C, C-7), 57.2 (CH_3, 3C, C-11), 52.7 (C_q, 1C, C-2), 28.9 (CH_3, 1C, C-9), 26.0 (CH_3, 1C, C-10/C-10'), 20.1 (CH_3, 1C, C-10/C-10').

FT-IR (ATR): $\tilde{\nu}$ [cm^{-1}] = 3080 (w), 3007 (w), 2963 (w), 1655 (w), 1614 (w), 1589 (w), 1520 (s), 1497 (m), 1449 (w), 1437 (w), 1375 (w), 1341 (s), 1312 (m), 1275 (m), 1206 (w), 1092 (m), 1022 (w), 972 (m), 951 (w), 924 (w), 862 (s), 806 (w), 743 (m), 721 (m), 696 (w), 679 (w).

HRMS (ESI): $^m/_z$ calcd. for $C_{22}H_{25}BrIN_3O_3$: 458.1073808 [M, –I]$^+$;
found: 458.10800.

UV/Vis: $\tilde{\nu}$ [nm]: λ_{max} (MeOH, 0.025 mM): MC = 544, 376, 309, 250; SP = 388, 336, 252.

Synthesis of 5-hydroxy-2,3,3-trimethyl-3H-indole

[NIH_P240]

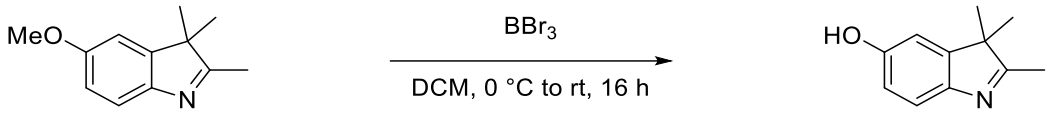

52 **70**

Indole **52** (1.70 g, 9.00 mmol, 1.0 eq.) was dissolved in dry DCM (40 mL) and cooled to 0 °C. A solution of BBr_3 in heptane (1 M, 10 mL, 10 mmol,1.1 eq.) was added over a period of 10 min. After the addition was completed, the reaction was stirred for further 30 min at 0 °C and then warmed to ambient temperature. After 16 h, full conversion was confirmed by TLC. Water (60 mL) was added to the solution and pH~6 was adjusted by the addition of a sat. solution of Na_2CO_3. The phases were separated, the aqueous solution was extracted with DCM (2x50 mL) and the combined organic phases were dried over Na_2SO_4. After filtration, the solvent was removed under reduced pressure and indole **70** was obtained as a pale brown solid in 88 % (1.4 g, 7.88 mmol) yield.

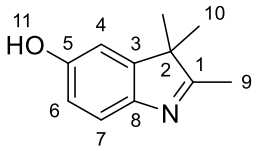

M($C_{11}H_{13}NO$)**:** 175.21 g·mol^{-1}.

Habitus: Pale brown solid.

Yield: 1.38 g (7.88 mmol, 88 %).

R_f: 0.29 (1:3, *c*Hex:EtOAc).

Mp.: 175–177 °C.

^{1}H-NMR: (500 MHz, DMSO-d_6) δ [ppm] = 9.29 (s, 1H, H11), 7.19 (d, $^3J_{H7\text{-}H6}$ = 8.2 Hz, 1H, H7), 6.79 (d, $^3J_{H4\text{-}H6}$ = 2.4 Hz, 1H, H-4), 6.65 (dd, $^3J_{H6\text{-}H7}$ = 8.2, $^4J_{H6\text{-}H4}$ = 2.4 Hz, 1H, H6), 2.14 (s, 3H, H9), 1.20 (s, 6H, H10).

^{13}C-NMR: (126 MHz, DMSO-d_6) δ [ppm] = 184.2 (C_q, 1C, C-1), 155.4 (C_q, 1C, C-5), 147.4 (C_q, 1C, C-3), 145.5 (C_q, 1C, C-8), 119.4 (CH_{Ar}, 1C, C-4), 113.5 (CH_{Ar}, 1C, C-6), 109.2 (CH_{Ar}, 1C, C-7), 53.1 (C_q, 1C, C-2), 22.8 (CH_3, 2C, C-10), 14.8 (CH_3, 1C, C-9).

FT-IR (ATR): $\tilde{\nu}$ [cm^{-1}] = 3022 (w), 2967 (w), 2928 (w), 2837 (w), 2681 (w), 2631 (w), 2561 (w), 1620 (w), 1582 (m), 1460 (s), 1429 (m),

1387 (s), 1358 (s), 1292 (s), 1269 (m), 1190 (s), 1111 (w), 1061 (m), 945 (w), 847 (m), 816 (s), 764 (m), 621 (w).

Synthesis of 5-(2-(2-(2-methoxyethoxy)ethoxy)ethoxy)-2,3,3-tri-methyl-3H-indole

[**NIH_P232**, NIH_P246]

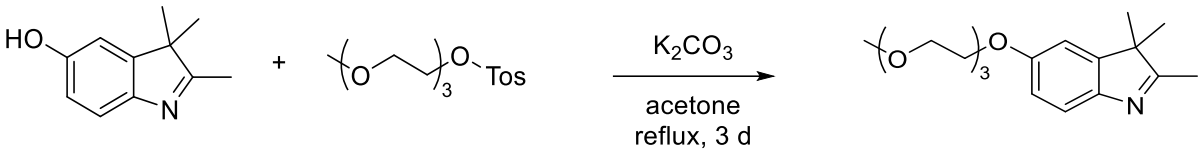

70 **72** **71**

Under argon atmosphere, indole **70** (0.28 g, 1.6 mmol, 1.0 eq.) and K_2CO_3 (0.66 g, 4.8 mmol, 3.0 eq.) were dissolved in acetone (20 mL, HPLC grade). Tosylate **72** (*m*PEG3-Tos) (0.61 g, 1.9 mmol, 1.2 eq.) was added and the reaction was heated to reflux. After 3 d, the reaction was cooled to ambient temperature. Water (25 mL) was added and the phases were separated. After extraction with DCM (4x50 mL) the combined organic phases were washed with brine (1x50 mL) and dried over Na_2SO_4. The solvent was removed under reduced pressure and the crude product was purified by column chromatography over silica gel (1:3, *c*Hex:EtOAc). Indole **71** was obtained as an orange resin in 75 % (0.38 g, 1.2 mmol) yield.

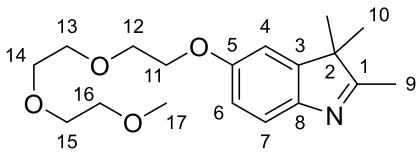

M($C_{18}H_{27}NO_4$)**:** 321.42 g·mol^{-1}.

Habitus: Orange resin.

Yield: 0.38 g (1.2 mmol, 75 %).

R_f: 0.11 (1:3, *c*Hex:EtOAc).

^{1}H-NMR: (500 MHz, $CDCl_3$) δ [ppm] 7.42 (d, $^3J_{H6\text{-}H7}$ = 8.4 Hz, 1H, H-7), 6.88 (d, $^4J_{H4\text{-}H6}$ = 2.4 Hz, 1H, H-4), 6.83 (dd, $^3J_{H6\text{-}H7}$ = 8.4, $^4J_{H6\text{-}H4}$ = 2.4 Hz, 1H, H-6), 4.15 (m, 2H, H1-1), 3.91 – 3.84 (m, 2H, H-12), 3.75 (m, 2H, H-13), 3.69 (m, 2H, H-14), 3.66 (m, 2H, H-15), 3.55 (m, 2H, H-16), 3.38 (s, 3H, H-17), 2.26 (s, 3H, H-9), 1.28 (s, 6H, H-10, H-10').

^{13}C-NMR: (126 MHz, $CDCl_3$) δ [ppm] = 186.2 (C_q, 1C, C-1), 157.4 (C_q, 1C, C-5), 147.2 (C_q, 2C, C3, C-8), 120.1 (CH_{Ar}, 1C, C-7), 112.9 (CH_{Ar}, 1C, C-4), 109.2 (CH_{Ar}, 1C, C-6), 72.1 (CH_2, 1C, C-16), 71.0 (CH_2, 1C, C-13), 70.8 (CH_2, 1C, C-14), 70.7 (CH_2, 1C, C-15), 70.0 (CH_2, 1C, C-12), 68.1 (CH_2, 1C, C-11), 59.2 (CH_3, 1C, C-17), 53.9 (C_q, 1C, C-2), 23.3 (CH_3, 2C ,C-10), 15.4 (CH_3, 1C, C-9).

FT-IR (ATR): $\tilde{\nu}$ [cm^{-1}] = 2959 (w), 2866 (w), 1612 (w), 1593 (w), 1578 (w), 1460 (s), 1435 (w), 1377 (w), 1287 (m), 1248 (w), 1196 (s), 1105 (s), 1070 (s), 1030 (m), 995 (w), 957 (m), 932 (m), 849 (m), 822 (m), 758 (w).

GC-MS: τ_R = 15.97 min; $^m/_z$ (%) = 321.3 $[M]^{\cdot+}$, 175.1 [M, $-(CH_2CH_2O)_2CH_3$, $+H]^{\cdot+}$ (81), 174.2 [M, $-(CH_2CH_2O)_2CH_3]^{\cdot+}$ (27), 160.1 [M,$-(CH_2CH_2O)_2CH_3$, $-CH_3$, $+H]^{\cdot+}$ (47), 147.1 (26) 131.1 (15), 115.2 (23), 77.0 $[C_6H_5]^{\cdot+}$ (11), 59.1 $[C_3H_7O]^{\cdot+}$ (93).

Synthesis of 5-(2-(2-(2-methoxyethoxy)ethoxy)ethoxy)-1,2,3,3-tetramethyl-3H-indol-1-ium iodide

[NIH_P234, **NIH_P253**]

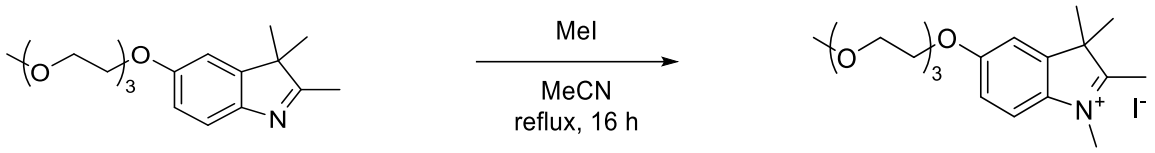

71 **73**

Under argon atmosphere, indole **71** (0.72 g, 2.2 mmol,1.0 eq.) was dissolved in MeCN (10 mL, HPLC grade). Iodomethane (0.65 mL, 11 mmol, 5.0 eq.) was added and the reaction was heated to reflux. After 16 h full conversion was confirmed by TLC and the reaction was cooled to ambient temperature. Solvent and excess iodomethane were removed under reduced pressure. Iodolium **73** was obtained as a brown solid in quantitative (1.0 g, 2.2 mmol) yield.

M($C_{19}H_{30}INO_4$)**:** 463.36 g·mol^{-1}.

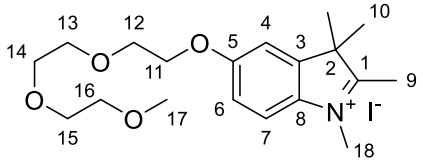

Habitus: Brown solid.

Yield: 1.0 g (2.2 mmol, quant.).

^{1}H-NMR: (500 MHz, DMSO-d_6) δ [ppm] = 7.80 (d, $^3J_{H7-H6}$ = 8.8 Hz, 1H, H7), 7.49 (d, $^4J_{H4-H6}$ = 2.5 Hz, 1H, H4), 7.16 (dd, $^3J_{H6-H7}$ = 8.8, $^4J_{H6-H4}$ = 2.5 Hz, 1H, H6), 4.23 – 4.16 (m, 2H, H11), 3.93 (s, 3H, H18), 3.84 – 3.73 (m, 2H, H12), 3.60 (dd, $^3J_{H13-H14}$ = 5.9 Hz, $^4J_{H13-H12}$ 3.5 Hz, 2H, H13), 3.56 – 3.48 (m, 4H, H14, H15), 3.45 – 3.41 (m, 2H, H16), 3.23 (s, 3H, H17), 2.69 (s, 3H, H9), 1.50 (s, 6H, H10).

^{13}C-NMR: (126 MHz, DMSO-d_6) δ [ppm] = 193.1 (C_q, 1C, C-1), 159.8 (C_q, 1C, C-5), 143.6 (C_q, 1C, C-3), 135.4 (C_q, 1C, C-8), 116.0 (CH_{Ar}, 1C, C-7), 114.4 (CH_{Ar}, 1C, C-6), 109.9 (CH_{Ar}, 1C, C-4), 71.3 (CH_2, 1C, C-16), 70.0 (CH_2, 1C, C-13), 69.8 (CH_2, 1C, C-14), 69.6 (CH_2, 1C, C-15), 68.8 (CH_2, 1C, C-12), 68.0 (CH_2, 1C, C-11), 58.1 (CH_3, 1C, C-17), 53.7 (C_q, 1C, C-2), 34.6 (CH_3, 1C, C-18), 21.8 (CH_3, 2C, C-10), 13.7 (CH_3, 1C, C-9).

HRMS (ESI): $^m/_z$ calcd. for $C_{19}H_{30}INO_4$: 336.2169349 [M–I]$^+$;
found: 336.21663.

Synthesis of 8-bromo-5'-(2-(2-(2-methoxyethoxy)ethoxy)ethoxy)-1',3',3'-trimethyl-6-nitrospiro[chromene-2,2'-indoline]

[NIH_P274]

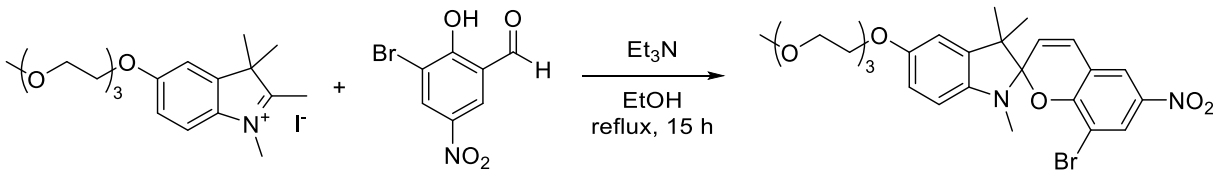

73 **46** **69**

Under argon atmosphere, indolium **73** (0.91 g, 2.7 mmol, 1.0 eq.), salicylic aldehyde **46** (1.1 g, 3.0 mmol, 1.1 eq.) and triethylamine (0.42 mL, 3.0 mmol, 1.1 eq.) were suspended in EtOH (20 mL, dry) and heated to reflux. After 16 h, full conversion

was confirmed by TLC and all volatile components were removed under reduced pressure. The crude mixture was dissolved in DCM (100 mL) and water (70 mL) under vigorous stirring. The phases were separated and the aqueous phase was extracted with DCM (2x40 mL). The combined organic phases were dried over Na_2SO_4, filtered and the solvent was removed under reduced pressure. The crude product was recrystallised from EtOH and spiropyran **69** was obtained as a black powder in 40 % (0.61 g,1.1 mmol) yield.

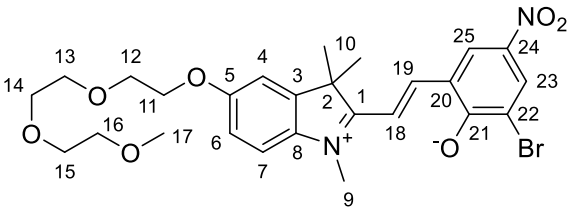

M($C_{26}H_{31}BrN_2O_7$)**:** 563.45 g·mol^{-1}.

Habitus: Black powder.

Yield: 0.61 g (1.1 mmol, 40 %).

Mp.: 115–117 °C.

^{1}H-NMR: (500 MHz, DMSO-d_6) δ [ppm] = 8.69 (d, $^4J_{H23\text{-}H25}$ = 3.0 Hz, 1H, H-23), 8.41 (d, $^3J_{H19\text{-}H18}$ = 15.6 Hz, 1H), 8.31 (d, $^3J_{H18\text{-}H19}$ = 15.5 Hz, 1H), 8.24 (d, $^4J_{H25\text{-}H24}$ = 3.0 Hz, 1H, H-25), 7.68 (d, $^3J_{H7\text{-}H6}$ = 8.8 Hz, 1H, H-7), 7.48 (d, $^4J_{H4\text{-}H6}$ = 2.5 Hz, 1H), 7.11 (dd, $^3J_{H6\text{-}H7}$ = 8.8 Hz, $^4J_{H6\text{-}H4}$ = 2.4 Hz, 1H, H-6), 4.26 – 4.17 (m, 2H, H-11), 3.90 (s, 3H, H-9), 3.81 – 3.72 (m, 2H, H-12), 3.60 (dd, $^3J_{H13\text{-}H14}$ = 5.9 Hz, $^4J_{H13\text{-}H12}$ =3.4 Hz, 2H, H-13), 3.58 – 3.50 (m, 4H, H-14, H-15,), 3.45 – 3.41 (m, 2H, H-16), 3.24 (s, 3H, H-17), 1.74 (s, 6H, H-10, H10').

^{13}C-NMR: (126 MHz, DMSO-d_6) δ [ppm] = 180.2 (C_q, 1C, C-1), 173.3 (C_q, 1C, C-21), 159.0 (C_q, 1C, C-5), 152.1 (CH_{Ar}, 1C, C-18), 145.0 (CH_{Ar}, 1C, C-3), 135.3 (CH_{Ar}, 1C, C-8), 132.3 (CH_{Ar}, 1C, C-23), 130.6 (CH_{Ar}, 1C, C-24), 129.4 (CH_{Ar}, 1C, C-18), 120.5 (CH_{Ar}, 1C, C-20), 119.5 (CH_{Ar}, 1C, C-22), 115.0 (CH_{Ar}, 1C, C-7), 114.6 (CH_{Ar}, 1C, C-6), 109.3 (CH_{Ar}, 1C, C-4), 109.1 (CH_{Ar}, 1C, C-19), 71.3 (CH_2, 1C, C-16), 70.0 (CH_2, 1C, C-13), 69.8 (CH_2, 1C, C-14/C-15), 69.6 (CH_2, 1C, C-14/C-15), 68.9 (CH_2, 1C, C-12), 68.0 (CH_2, 1C, C-11), 58.1 (CH_3, 1C, C-17), 51.1 (C_q, 1C, C-2), 33.3 (CH_3, 1C, C-9), 26.2 (CH_3, 2C, C-10, C-10').

Spiropyran

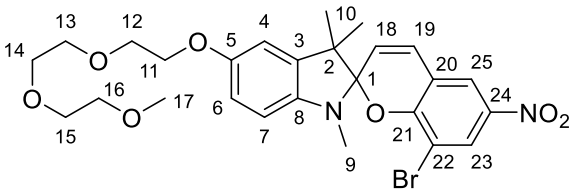

^{1}H-NMR: (500 MHz, DMSO-d_6) δ [ppm] = 8.26 (d, $^{4}J_{H23\text{-}H25}$ = 3.0 Hz, 1H, H-23), 8.25 (d, $^{4}J_{H25\text{-}H23}$ = 3.1 Hz, 1H, H-25), 7.24 (d, $^{3}J_{H19\text{-}H18}$ = 10.3 Hz, 1H, H-19), 6.84 (d, $^{4}J_{H4\text{-}H6}$ = 2.5 Hz, 1H, H-4), 6.71 (dd, $^{3}J_{H6\text{-}H7}$ = 8.4 Hz, $^{4}J_{H6\text{-}H4}$ = 2.5 Hz, 1H, H-6), 6.55 (d, $^{3}J_{H7\text{-}H6}$ = 8.3 Hz, 1H, H-7), 6.04 (d, $^{3}J_{H18\text{-}H19}$ = 10.3 Hz, 1H, H-18), 4.03 (t, $^{3}J_{H11\text{-}H12}$ = 4.7 Hz, 2H, H-11), 3.73 (t, $^{3}J_{H12\text{-}H11}$ = 4.7 Hz, 2H, H-12), 3.63 – 3.57 (m, 2H, H-13), 3.57 – 3.41 (m, 6H, H-14, H-15, H-16), 3.25 (s, 3H, H-17), 2.61 (s, 3H, H-9), 1.22 (s, 3H, H-10/H-10'), 1.14 (s, 3H, H-10/H-10').

^{13}C-NMR: (126 MHz, DMSO-d_6) δ [ppm] = 155.7 (C_q, 1C, C-21), 152.9 (C_q, 1C, C-5), 141.2 (C_q, 1C, C-8), 140.5 (C_q, 1C, C-24), 137.3 (C_q, 1C, C-3), 128.1 (CH_{Ar}, 1C, C-18), 128.0 (CH_{Ar}, 1C, C-23), 122.1 (CH_{Ar}, 1C, C-25), 122.0 (CH_{Ar}, 1C, C-19), 119.9 (C_q, 1C, C-20), 112.0 (CH_{Ar}, 1C, C-6), 109.9 (CH_{Ar}, 1C, C-4), 108.5 (C_q, 1C, C-1), 108.4 (C_q, 1C, C-22), 107.4 (CH_{Ar}, 1C, C-7), 71.3 (CH_2), 70.0 (CH_2), 69.8 (CH_2), 69.6 (CH_2, 1C, C-13), 69.2 (CH_2, 1C, C-12), 67.5 (CH_2, 1C, C-11), 58.1 (CH_3, 1C, C-17), 52.1 (C_q, 1C, C-2), 28.8 (CH_3, 1C, C-9), 25.1 (CH_3, 1C, C-10/C10'), 19.6 (CH_3, 1C, C-10/C10').

FT-IR (ATR): $\tilde{\nu}$ [cm^{-1}] = 3078 (w), 2972 (w), 2868 (w), 1585 (s), 1522 (s), 1481 (m), 1437 (s), 1398 (m), 1369 (m), 1271 (s), 1234 (s), 1206 (s), 1171 (s), 1123 (s), 1086 (s), 1069 (s), 1024 (s), 961 (s), 926 (s), 889 (s), 866 (s), 849 (s), 799 (s), 773 (s), 745 (s), 725 (s), 692 (s), 629 (m).

HRMS (ESI): $^{m}/_{z}$ calcd. for $C_{26}H_{31}BrN_2O_7$: 563.1387404 $[M+H]^+$;
found: 563.13864.
$^{m}/_{z}$ calcd. for $C_{26}H_{31}BrN_2O_7$: 585.1206850 $[M+Na]^+$;
found: 585.12071.

6.5 Substitution at the Geminal Methyl Groups

Synthesis of dimethoxydiphenylmethane

[NIH_P191; **NIH_P199**]

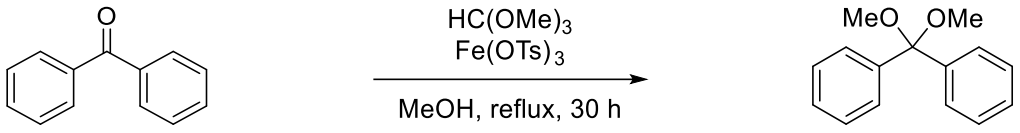

76 **77**

Under argon atmosphere, benzophenone (**76**) (18.2 g, 100 mmol, 1.00 eq.) and $Fe(OTs)_3$ (1.7 g, 3.0 mmol, 0.03 eq.) were dissolved in 500 mL dry MeOH. Trimethyl orthoformate (32.8 mL, 300 mmol, 3.00 eq.) were added and the reaction was refluxed for 30 h. After cooling down to ambient temperature, the solution was concentrated to 150 mL under reduced pressure. After adding saturated $NaHCO_3$ solution (200 mL) the mixture was extracted with Et_2O (3x200 mL) and the combined organic phases were washed with brine (1x100 mL) and dried over Na_2SO_4. After filtration, the solvent was removed under reduced pressure and ketal **77** was obtained as colourless crystals in 97 % yield (22.2 g, 97.2 mmol).

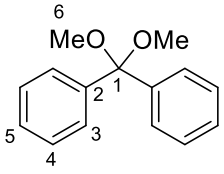

Habitus: Colourless crystals.

M($C_{15}H_{16}O_2$): 228.29 g·mol^{-1}.

Yield: 22.2 g (97.2 mmol, 97 %) Lit.: 99 %[124].

Mp.: 107–108 °C, Lit.: 106 °C[143].

^{1}H-NMR: (500 MHz, $CDCl_3$) δ [ppm] = 7.53 – 7.46 (m, 4H, H-3), 7.32 – 7.24 (m, 4H, H-4), 7.23 – 7.18 (m, 2H, H-5), 3.12 (s, 6H, H-6).

^{13}C-NMR: (75 MHz, $CDCl_3$) δ [ppm] = 142.4 (C_q, 2C, C-2), 128.0 (C_{Ar}, 2C, C-4), 127.4 (C_{Ar}, 2C, C-5), 126.9 (C_{Ar}, 2C, C-3), 49.3 (CH_3, 2C, C-6).

FT-IR (ATR): $\tilde{\nu}$ [cm^{-1}] = 3082 (w), 3065 (w), 3022 (w), 2959 (w), 2936 (w), 2889 (w), 2828 (w), 1487 (w), 1450 (w), 1431 (w), 1312 (w), 1288 (w), 1240 (w), 1213 (m), 1186 (w), 1171 (m), 1084 (m), 1059 (s), 1028 (m), 991 (s), 908 (w), 772 (m), 745 (s), 694 (s), 652 (m), 642 (m), 617 (w).

GC-MS: τ_R=11.69 min; $^m/_z$ (%) = 197.1 [M, –OMe]$^{\cdot+}$ (100), 151.1 [M, –C_6H_5]$^{\cdot+}$ (23), 105.0 [PhCO]$^{\cdot+}$ (43), 77.1 [C_6H_5]$^{\cdot+}$ (44), 51.1 (15).

The analytic data are in agreement with the literature[124, 143]

Synthesis of diethyl 2,2-diphenyl-1,3-dioxane-5,5-dicarboxylate

[NIH_P202]

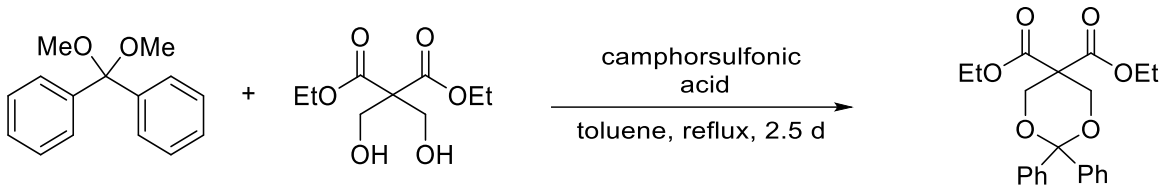

77 **78** **79**

Under argon atmosphere, dimethyl ketal **77** (14.8 g, 65.0 mmol, 1.10 eq.), diethyl malonate **78** (13.0 g, 59.0 mmol, 1.00 eq.) and camphor sulfonic acid (1.37 g, 5.90 mmol, 0.10 eq.) were dissolved in 300 mL dry toluene and heated to reflux. After 2.5 d, the rection mixture was cooled down, washed with sat. $NaHCO_3$ solution (3x150 mL) and brine (1x150 mL) and dried over Na_2SO_4. After filtration, the solvent was removed under reduced pressure and dioxane **79** was obtained as colourless solid in 90 % yield (20.3 g, 52.8 mmol).

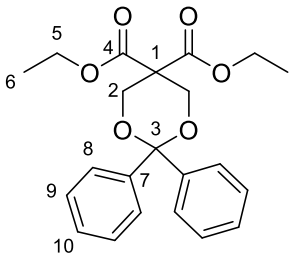

Habitus: Colourless solid.

M($C_{12}H_{24}O_6$): 384.43 g·mol^{-1}.

Yield: 20.3 g (52.8 mmol, 90 %).

R_f: 0.14 (20:1, *c*Hex/EtOAc).

Mp.: 102–105 °C.

^{1}H-NMR: (500 MHz, $CDCl_3$) δ [ppm] = 7.45 – 7.41 (m, 4H, H-8), 7.36 – 7.30 (m, 4H, H-9), 7.30 – 7.25 (m, 2H, H-10), 4.38 (s, 4H, H-2), 4.22 (q, $^3J_{H5\text{-}H6}$ = 7.1 Hz, 4H, H-5), 1.25 (t, $^3J_{H5\text{-}H6}$ = 7.1 Hz, 6H, H-6).

^{13}C-NMR: (75 MHz, $CDCl_3$) δ [ppm] = 167.6 (C_q, 2C, C-4), 140.6 (C_q, 2C, C-7), 128.4 (C_{Ar}, 2C, C-9), 128.3 (C_{Ar}, 2C, C-10), 126.9 (C_{Ar}, 2C,

C-8), 101.7 (C_q, 1C, C-3), 64.0 (CH_2, 2C, C-2), 62.0 (CH_2, 2C, C-5), 53.5 (C_q, 1C, C-1), 14.0 (CH_3, 2C, C-6).

FT-IR (ATR): $\tilde{\nu}$ [cm^{-1}] = 3059 (w), 3030 (w), 2986 (w), 2941 (w), 2903 (w), 2866 (w), 1749 (m), 1728 (s), 1487 (w), 1476 (w), 1452 (m), 1387 (w), 1366 (w), 1317 (w), 1271 (w), 1248 (s), 1217 (s), 1198 (s), 1148 (s), 1109 (s), 1055 (s), 1026 (s), 999 (s), 974 (s), 947 (m), 937 (m), 908 (m), 866 (w), 851 (m), 827 (w), 773 (s), 748 (s), 708 (s), 694 (s), 631 (m), 588 (w).

GC-MS: τ_R=16.47 min; $^m/_z$ (%) = 355.2 [M, –Et]$^{\cdot+}$ (3), 339.2 [M, –OEt]$^{\cdot+}$ (4), 307.1 [M, –C_6H_5]$^{\cdot+}$ (100), 182.1 [Ph_2CO]$^{\cdot+}$ (12), 105.1 [PhCO]$^{\cdot+}$ (67).

Synthesis of 2,2-diphenyl-1,3-dioxane-5,5-dicarboxylic acid

[NIH_P179; **NIH_P206**]

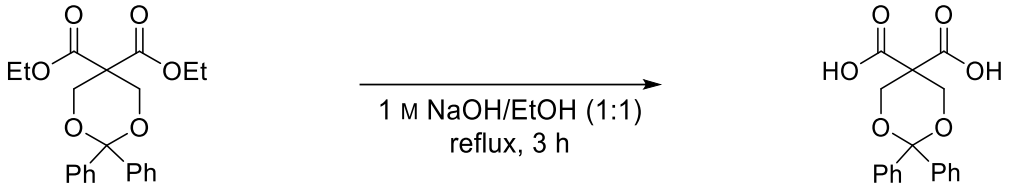

79 **80**

Diethyl dicarboxylate **79** (20.0 g, 52.0 mmol, 1.00 eq.) was suspended in 300 mL 1 M NaOH and 300 mL water and heated to reflux. After 3 h, full conversion was indicated by TLC. The ethanol was removed under reduced pressure and the solution was acidified to pH 3–4. The mixture was extracted wit Et_2O (3x150 mL) and the combined organic phases were washed with brine (1x150 mL), dried over Na_2SO_4 and filtered. After removing the solvent under reduced pressure, dicarboxylic acid **80** was obtained as a colourless solid in quantitative yield (17.0 g, 51.8 mmol).

Habitus: Colourless solid.

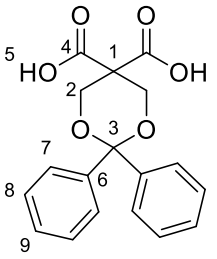

M($C_{18}H_{16}O_6$): 328.32 g·mol^{-1}.

Yield: 17.0 g (51.8 mmol, quant.).

Mp.: 141–143 °C.

^{1}H-NMR: (500 MHz, DMSO-d_6) δ [ppm] = 7.47 – 7.41 (m, 4H, H-7), 7.40 – 7.32 (m, 4H, H-8), 7.32 – 7.24 (m, 2H, H-9), 4.24 (s, 4H, H-2).

^{13}C-NMR: (75 MHz, DMSO-d_6) δ [ppm] = 169.0 (C_q, 2C, C-4), 141.1 (C_q, 2C, C-6), 128.4 (C_{Ar}, 2C, C-8), 128.0 (C_{Ar}, 2C, C-9), 126.0 (C_{Ar}, 2C, C-7), 100.4 (C_q, 1C, C-3), 63.6 (CH_2, 2C, C-2), 52.8 (C_q, 1C, C-1).

FT-IR (ATR): $\tilde{\nu}$ [cm^{-1}] = 3474 (w, br), 2889 (w, br), 2615 (w, br), 1699 (s), 1452 (m), 1248 (s), 1198 (s), 1163 (m), 1113 (s), 1059 (m), 1030 (m), 999 (s), 976 (m), 951 (m), 932 (s), 908 (m), 791 (w), 773 (m), 735 (s), 706 (s), 692 (s), 646 (m), 621 (m)

GC-MS: Not detected. Only decomposition to benzophenone observed.

Synthesis of 2,2-diphenyl-1,3-dioxane-5-carboxylic acid

[NIH_P180; **NIH_P198**; NIH_P208]

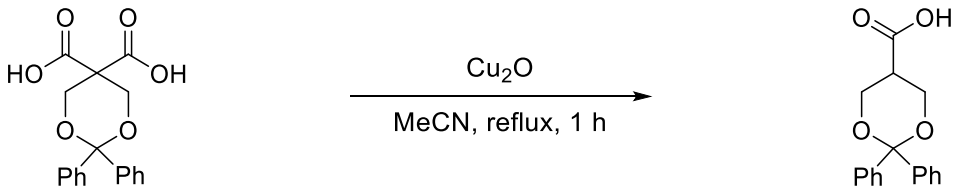

80 **81**

Under argon atmosphere, dicarboxylic acid **80** (4.13 g, 12.6 mmol, 1.00 eq.) was dissolved in 60 mL MeCN. After the addition of Cu_2O (0.09 g, 0.63 mmol, 0.05 eq.), the reaction as refluxed resulting in a blue solution. Full conversion was indicated by TLC after one hour. The reaction was cooled to ambient temperature and the solvent was removed under reduced pressure. The residue was suspended in 150 mL water and 150 mL Et_2O. A few drops of conc. HCl were added until pH 2 was obtained. The phases were separated, the aqueous phase was extracted with Et_2O (3x150 mL) and the combined organic phases were dried over Na_2SO_4. After filtration, the solvent of the blue solution was removed under reduced pressure and the residue was suspended in 200 mL Et_2, 20 mL water and 0.01 mL pyridine. After separation, the organic phase was dried over Na_2SO_4 and filtered. The solvent of the colourless

solution was removed under reduced pressure and carboxylic acid **81** was obtained as a colourless solid in 81 % yield (2.92 g, 10.2 mmol).

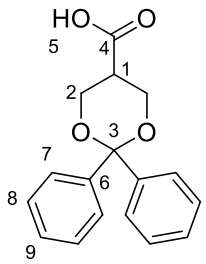

M($C_{17}H_{16}O_4$): 284.31 g·mol^{-1}.

Habitus: Colourless solid.

Yield: 2.92 g (10.2 mmol, 81 %).

Mp.: 203–206 °C.

^{1}H-NMR: (500 MHz, DMSO-d_6) δ [ppm] = 12.71 (br, s, 1H, H-5), 7.51 – 7.41 (m, 4H; H-7, H-7'), 7.41 – 7.31 (m, 4H, H-8, H-8'), 7.31 – 7.23 (m, 2H, H-9, H-9'), 4.11 (dd, $^2J_{H2eq-H2ax}$ = 11.5 Hz, $^3J_{H2eq-H1}$ = 4.5 Hz, 2H, H-2$_{eq}$), 4.06 (dd, $^2J_{H2ax-H2eq}$ = 11.4 Hz, $^3J_{H2ax-H1}$ = 6.9 Hz, 2H, H-2$_{ax}$), 2.81 (tt, $^3J_{H1-H2ax}$ = 7.0 Hz, $^3J_{H1-H2eq}$ = 4.5 Hz, 1H, H-1).

^{13}C-NMR: (75 MHz, DMSO-d_6) δ [ppm] = 172.0 (C_q, 1C, C-4), 142.0 (C_q, 1C, C-6/C-6'), 141.5 (C_q, 1C, C-6/C-6'), 128.4(7) (C_{Ar}, 1C, C-8/C-8'), 128.3 (C_{Ar}, 1C, C-8/C-8'), 127.7(4) (C_{Ar}, 1C, C-9/C-9'), 127.7(0) (C_{Ar}, 1C, C-9/C-9'), 126.1 (C_{Ar}, 1C, C-7/C-7'), 125.8 (C_{Ar}, 1C, C-7/C-7'), 100.1 (C_q, 1C, C-3), 61.6 (CH_2, 2C, C-2), 39.1 (CH, 1C, C-1).

FT-IR (ATR): $\tilde{\nu}$ [cm^{-1}] = 3022 (w), 2945 (w), 2886 (w), 1697 (s), 1487 (w), 1449 (w), 1423 (w), 1294 (m), 1256 (w), 1246 (w), 1194 (s), 1171 (w), 1146 (w), 1130 (w), 1096 (s), 1086 (s), 1026 (m), 1015 (w), 997 (s), 966 (m), 955 (m), 937 (m), 922 (m), 908 (m), 899 (m), 853 (w), 814 (w), 772 (s), 746 (s), 696 (s), 675 (m), 650 (m), 637 (w), 619 (w).

GC-MS: Not detected. Only decomposition to benzophenone observed.

Synthesis of *N*-methoxy-*N*-methyl-2,2-diphenyl-1,3-dioxane-5-carboxamide

[**NIH_P182**; NIH_P209]

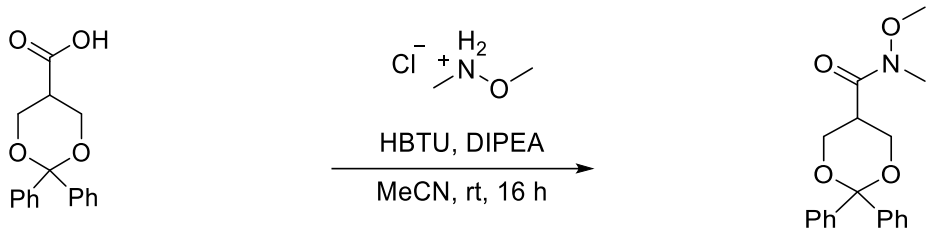

81 **82**

Carboxylic acid **81** (0.91 g, 3.2 mmol, 1.0 eq.) and diisopropylethylamine (1.7 mL, 9.9 mmol, 3.1 eq.) were dissolved in 35 mL MeCN. After the addition of HBTU (1.46 g, 3.85 mmol, 1.20 eq.), the reaction was stirred for five minutes at ambient temperature before *N*,*O*-dimethyl hydroxylamine hydrochloride (0.34 g, 3.5 mmol, 1.1 eq.) were added. After stirring for 16 h the reaction was concentrated and purified by column chromatography over silica gel (10:1, DCM/MeOH). The obtained product was still contaminated with DIPEA and tetramethyl urea. Therefore, the residue was dissolved in DCM and water and acidified with conc. HCl until pH 4 was obtained. The phases were separated, the organic phase was dried over Na_2SO_4 and filtered. After purification by column chromatography over silica (100 %, DCM), the Weinreb amid **82** was obtained as a colourless solid in 70 % yield (0.74g 2.3 mmol).

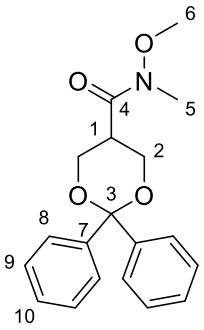

Habitus: Colourless solid.

M($C_{19}H_{21}NO_4$): 327.38 g·mol^{-1}.

Yield: 0.74 g (2.3 mmol, 70 %).

R_f: 0.26 (100 %, DCM).

Mp.: 114-115 °C.

^{1}H-NMR: (300 MHz, DMSO-d_6) δ [ppm] = 7.53 – 7.39 (m, 6H, H-8, H-8‘, H-9/H-9‘), 7.36 – 7.19 (m, 4H, H-10, H-10‘, H-9/H-9‘), 4.13 (dd, $^2J_{H2eq-H2ax}$ = 11.5 Hz, $^2J_{H2eq-H1}$ 4.7 Hz, 2H, H-2$_{eq}$), 3.92 (br, φt, $^2J_{H2ax-H2eq}$ = 11.5 Hz, $^3J_{H2ax-H1}$ = 11.5 Hz, 2H, H-2$_{ax}$), 3.73 (s, 3H), 3.45 – 3.33 (m, 1H, H-1), 3.05 (s, 3H).

^{13}C-NMR: (75 MHz, DMSO) δ [ppm] = 174.6 (C_q, 1C, C-4), 144.0 (C_q, 1C, C-7/C-7‘), 139.7 (C_q, 1C, C-7/C-7‘), 129.0 (CH_{Ar}, 2C, C-9/C-9‘/C-

8/C-8'), 127.9(1) (CH_{Ar}, 1C, C-10/C-10'), 127.8(8) (CH_{Ar}, 2C, C-9/C-9'), 127.6 (CH_{Ar}, 1C, C-10/C-10'), 126.8 (CH_{Ar}, 2C, C-8/C-8'), 125.0 (CH_{Ar}, 2C, C-8/C-8'), 100.1 (C_q, 1C, C-3), 62.1 (CH_2, 2C, C-2), 61.5 (CH_3, 1C, C-6), 37.4 (CH, 1C, C-1), 31.5 (CH_3, 1C, C-5).

FT-IR (ATR): $\tilde{\nu}$ [cm^{-1}] = 3379 (w), 3063 (w), 2968 (w), 2941 (w), 2884 (w), 2868 (w), 1651 (s), 1489 (w), 1450 (m), 1423 (m), 1393 (w), 1377 (m), 1356 (w), 1298 (w), 1242 (m), 1204 (s), 1175 (m), 1153 (s), 1119 (m), 1096 (s), 1072 (s), 1022 (s), 984 (s), 964 (s), 955 (m), 912 (m), 905 (m), 833 (m), 772 (s), 756 (s), 696 (s), 669 (s), 640 (m), 613 (m)

GC-MS: τ_R = 16.15 min; $^m/_z$ (%) = 250.1 [M, $-C_6H_5]^{\cdot+}$ (99), 182.0 $[PhCOPh]^{\cdot+}$ (20), 105.1 $[PhCO]^{\cdot+}$ (100), 77.1 $[C_6H_5]^{\cdot+}$ (67), 55.1 (33)

Synthesis of 1-(2,2-diphenyl-1,3-dioxan-5-yl)ethanone

[NIH_P183]

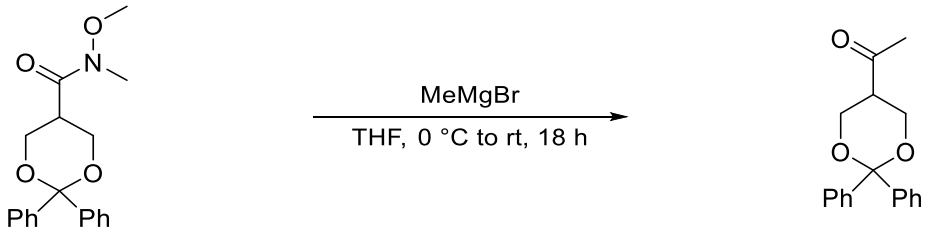

82 **15**

Under argon atmosphere, Weinreb amide **82** (0.70 g, 2.1 mmol, 1.0 eq.) was dissolved in 15 mL dry THF and cooled to 0 °C. A 3 M solution of MeMgBr in Et_2O (1.1 mL 3.2 mmol, 1.5 eq.) was added and the reaction was stirred for one hour at 0 °C. The solution was then allowed to warm to ambient temperature and stirred for 18 h. The reaction mixture was cooled to 0 °C again and 30 mL Et_2O and 50 mL of sat. NH_4Cl solution were added. The phases were separated and the aqueous phase was extracted with Et_2O (3x30 mL). The combined organic phases were washed with brine (1x30 mL), dried over Na_2SO_4 and filtered. After the solvent was removed under reduced pressure, ketone **15** was obtained as a colourless solid in quantitative yield (0.60 g, 2.1 mmol).

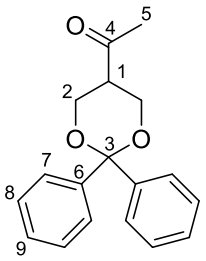

Habitus: Colourless solid.

M($C_{18}H_{18}O_3$): 282.34 g·mol^{-1}.

Yield: 0.60 g (2.1 mmol, quant.).

^{1}H-NMR: (500 MHz, $CDCl_3$) δ [ppm] = 7.57 – 7.46 (m, 4H, H-7, H-7'), 7.43 – 7.32 (m, 4H, H-8, H8'), 7.32 – 7.26 (m, 2H, H-9, H-9'), 4.26 (dd, $^2J_{H2eq-H2ax}$ = 11.6, $^3J_{H2eq-H1}$ = 4.5 Hz, 2H, H-2$_{eq}$), 4.17 (dd, $^2J_{H2ax-H2eq}$ = 11.6 Hz, $^3J_{H2ax-H1}$ = 8.0 Hz, 2H, H-2$_{ax}$), 2.94 (tt, $^3J_{H1-H2ax}$ = 8.1 Hz, $^3J_{H1-H2eq}$ = 4.5 Hz, 1H, H-1), 2.23 (s, 3H).

^{13}C-NMR: (75 MHz, $CDCl_3$) δ [ppm] = 206.6 (C_q, 1C, C-4) 140.4 (C_q, 2C, C-6), 128.7 (CH_{Ar}, 2C, C-7/C-8/C-7'/C-8'), 128.3 (CH_{Ar}, 2C, C-7/C-8/C-7'/C-8'), 128.1 (CH_{Ar}, 2C, C-9/C-9'), 128.0 (CH_{Ar}, 2C, C-9/C-9'), 126.8 (CH_{Ar}, 2C, C-7/C-8/C-7'/C-8'), 126.0 (CH_{Ar}, 2C, C-7/C-8/C-7'/C-8'), 101.2 (C_q, 1C, C-3) 62.2 (CH_2, 2C, C-2), 47.9 (CH_3, 1C, C-1), 29.0 (CH_3, 1C, C-5).

C-3 and C-4 are not detectable by ^{13}C-NMR but well detectable in the H,C-2D spectra.

Synthesis of Boc-isonipecotic acid

[NIH_P188]

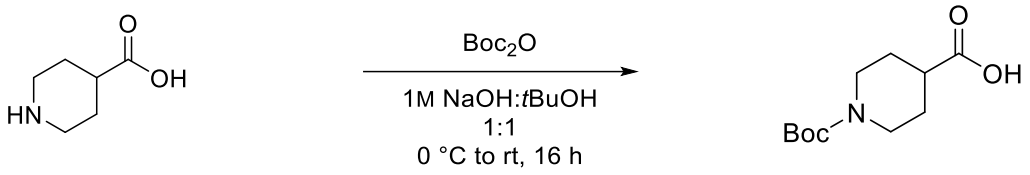

88 **89**

Isonipecotic acid (**88**) (12.9 g, 100 mmol, 1.00 eq.) was dissolved a mixture of 120 mL *t*BuOH and 120 mL 1M NaOH and cooled to 0 °C. Boc_2O (24.0 g, 110 mmol. 1.10 eq.) was added and the reaction was stirred for 30 min at 0 °C and then at ambient temperature. After stirring for 16 h, the solution was concentrated to 40–50 % under reduced pressure. The remaining solution was acidified with 10 % HCl until pH 4 was obtained and the formed precipitated was filtered off. After drying the solid in a desiccator over $CaCl_2$, Boc-Inp-OH **89** was obtained with 97 % yield (22.2 g 97.0 mmol) as colourless powder.

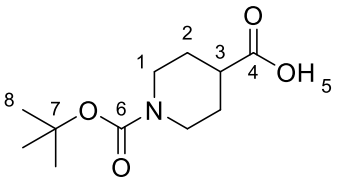

M($C_{11}H_{19}NO_4$): 229.28 g·mol^{-1}.

Habitus: Colourless powder.

Yield: 22.2 g (97.0 mmol, 97 %) Lit.: 98 %[144].

Mp.: 150–151 °C, Lit.: 149–152 °C[145].

^{1}H-NMR: (500 MHz, DMSO-d_6) δ [ppm] = 12.23 (s, 1H, H-5), 3.83 (d, $^2J_{H1\text{-}H1}$ = 13.2 Hz, 2H, H-1, H-1'), 2.81 (s, 2H, H-1, H-1')), 2.40 (tt, $^3J_{H3\text{-}H2ax}$ = 11.0 Hz, $^3J_{H3\text{-}H2ax}$ = 3.8 Hz, 1H, H-3), 1.89 – 1.68 (m, 2H, H-2, H-2'), 1.43 – 1.34 (m, 2H, H-2, H-2'), 1.39 (s, 9H, H-8).

^{13}C-NMR: (75 MHz, DMSO-d_6) δ [ppm] = 175.6 (C_q, 1C, C-4), 153.9 (C_q, 1C, C-6), 78.6 (C_q, 1C, C-7), 42.8 (br, CH_2, 2C, C-1, C-1'), 40.1 (CH, 1C, C-3), 28.1 (CH_3, 3C, C-8), 27.8 (CH_2, 2C, C-2, C-2').

FT-IR (ATR)**:** $\tilde{\nu}$ [cm^{-1}] = 3188 (w), 2972 (w), 2930 (w), 2860 (w), 1732 (s), 1655 (m), 1472 (w), 1429 (s), 1391 (w), 1366 (m), 1279 (m), 1240 (m), 1206 (w), 1153 (s), 1130 (s), 1107 (m), 1078 (m), 1032 (s), 945 (w), 922 (m), 860 (m), 831 (m), 816 (m), 764 (m), 721 (m), 646 (w), 631 (w). **The analytic data are in agreement with the literature[144]**

Synthesis of 1-(*tert*-butoxycarbonyl)piperidine-4-carboxylic acid

[NIH_P189]

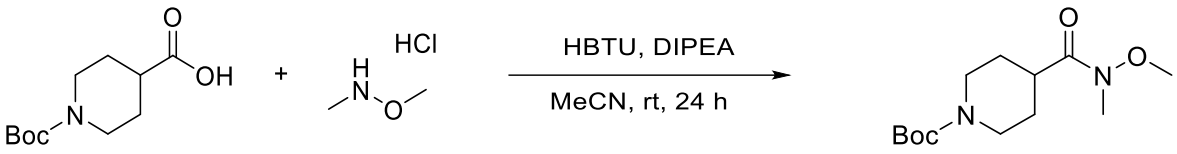

89 **130** **90**

Boc-Inp-OH **89** (16.3 g, 71.0 mmol, 1.00 eq.) and DIPEA (38.3 mL, 220 mmol, 3.10 eq.) were dissolved in 500 mL acetonitrile. After the addition of HBTU (32.3 g, 85.2 mmol, 1.20 eq.) the reaction was stirred for 5 min at ambient temperature before *N*,*O*-dimethyl hydroxylamine hydrochloride (**130**) (7.77 g, 78.1 mmol, 1.10 eq.) was added. Full conversion was obtained after 1 d indicated by TLC. The solvent was removed under reduced pressure. The residue was dissolved in 150 mL water and 200 mL DCM. The mixture was stirred vigorously and the pH was adjusted to four by the addition of HCl. The phases were separated, the aqueous phase was extracted with DCM (3x100 mL) and the combined organic phases were dried over Na_2SO_3. After filtration and removal of the solvent under reduced pressure, the crude residue was purified by column chromatography over silica gel (1:1, *c*hex:EtOAc). Since the product was obtained HOBT impurities, it was dissolved in 100 mL DCM and 100 mL water and the pH was adjusted to 9–10 by the addition of sat. Na_2CO_3 solution. The aqueous phase was extracted with DCM (2x75 mL) and the combined organic phases were washed with brine (1x100 mL) and dried over Na_2SO_4. The drying agent was filtered off and the solvent was removed under reduced pressure. The obtained oil slowly crystallised overnight and Weinreb amide **90** was obtained with 81 % yield (15.7 g, 57.6 mmol) as a colourless solid.

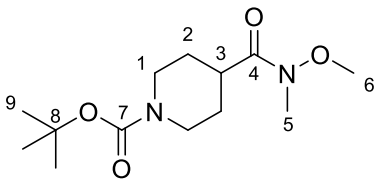

M($C_{13}H_{24}N_2O_4$): 272.35 g·mol^{-1}.

Habitus: Colourless solid.

Yield: 15.7 g (57.6 mmol, 81 %).

Mp.: 65–68 °C, Lit.: 68–72 °C[146].

^{1}H-NMR: (500 MHz, $CDCl_3$) δ [ppm] = 4.15 (d, $^2J_{H1\text{-}H1}$ = 12.9 Hz, 2H, H-1, H-1'), 3.72 (s, 3H, H-6), 3.19 (s, 3H, H-5), 2.93 – 2.70 (m, 3H, H-3, H-1, H-1'), 1.83 – 1.61 (m, 4H, H-2, H-2'), 1.46 (s, 9H, H-9).

^{13}C-NMR: (75 MHz, $CDCl_3$) δ [ppm] = 175.6 (C_q, 1C, C-4), 154.7 (C_q, 1C, C-7), 79.4 (C_q, 1C, C-8), 61.5 (CH_3, 1C, C-6), 43.2 (CH_2, 2C, C-1, C-1'), 38.1 (CH, 1C, C-3), 32.2 (CH_3, 1C, C-5), 28.4 (CH_3, 3C, C-9), 27.9 (CH_2, 2C, C-2, C-2').

FT-IR (ATR): $\tilde{\nu}$ [cm^{-1}] = 2974 (w), 2961 (w), 2932 (w), 2901 (w), 1684 (s), 1651 (s), 1452 (m), 1420 (s), 1387 (m), 1354 (m), 1287 (m), 1231 (s), 1163 (s), 1128 (s), 1074 (s), 1057 (m), 1032 (m), 1001 (s), 978 (s), 937 (m), 870 (m), 816 (w), 766 (m), 712 (w), 629 (w).

GC-MS: τ_R=13.84 min; $^m/_z$ (%) = 215.3 [M, –*t*Bu]$^{\cdot+}$ (21), 199.3 [M, –*t*BuO]$^{\cdot+}$ (17), 171.2 [M, –Boc]$^{\cdot+}$ (100), 141.2 [M, –Boc, –MeO]$^{\cdot+}$ (35), 112.1 [M, –Boc, –MeONMe]$^{\cdot+}$ (34), 82.2 [tetrahydropyridine, –H]$^{\cdot+}$ (99), 57.1 [*t*Bu]$^{\cdot+}$ (71).

The analytic data are in agreement with the literature[146]

Synthesis of 4-acetylpiperidine-1-(*tert*-butyl-carboxylate

[NIH_P190]

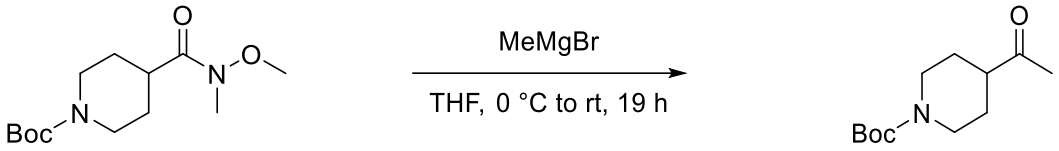

90 **91**

Under argon atmosphere, Weinreb-amide **90** (13.6 g, 50.0 mmol, 1.00 eq.) was dissolved in 50 mL dry THF and cooled to 0 °C. A solution 3M of MeMgBr (25 mL, 75 mmol, 1.5 eq.) in Et_2O was added dropwise over 30 min. After full addition, the solution was stirred for additional 30 min at 0 °C and then stirred at ambient temperature. After 19 h, full conversion was indicated by TLC. The solution was cooled to 0 °C and 100 mL Et_2O were added. The reaction was quenched with sat. NH_4Cl solution (100 mL). The phases were separated and the aqueous phase was extracted with Et_2O (2x100 mL). The combined organic phases were washed with brine (1x100 mL), dried over Na_2SO_4 and filtered. After removing the solvent under reduced pressure, ketone **91** was obtained in 96 % yield (10.9 g, 47.9 mmol) as slightly yellow oil.

M($C_{12}H_{21}NO_3$): 227.30 g·mol^{-1}.

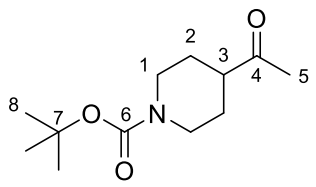

Habitus: Slightly yellow oil.

Yield: 10.9 g (47.9 mmol, 96 %).

R_f: 0.37 (1:1, *c*hex:EtOAc).

^{1}H-NMR: ^{1}H NMR (500 MHz, $CDCl_3$) δ [ppm] = 4.10 (br, d, $^2J_{H1eq-H1ax}$ = 13.2 Hz, 2H, H-1$_{eq}$, H-1'$_{eq}$), 2.78 (td, $^2J_{H1ax-H1eq}$ = 13.3 Hz, $^3J_{H1ax-H2ax}$ = 12.8 Hz, $^3J_{H1ax-H2ax}$ = 2.8 Hz, 2H, H-1$_{ax}$, H-1'$_{ax}$), 2.46 (tt, $^3J_{H3-H2ax}$ = 11.6 Hz, $^3J_{H3-H2eq}$ = 3.7 Hz, 1H, H-3), 2.16 (s, 3H, H-5), 1.83 (br, d, $^2J_{H2eq-H2ax}$ = 12.5 Hz, H-2$_{eq}$, H-2'$_{eq}$), 1.52 (dtd, $^2J_{H2ax-H2eq}$ = 13.4 Hz, $^3J_{H2ax-H3}$ = 11.6 Hz, ^3J = 4.4 Hz, 2H, H-2$_{ax}$, H-2'$_{ax}$), 1.46 (s, 9H, H-8).

^{13}C-NMR: (75 MHz, $CDCl_3$) δ [ppm] = 210.1 (C_q, 1C, C-4), 49.2 (CH, 1C, C-3), 43.2 (CH_2, 2C, C-1, C-1'), 28.4 (CH_3, 3C, C-8), 27.9 (CH_3, 1C, C-5), 27.4 (CH_2, 2C, C-2).

FT-IR (ATR): $\tilde{\nu}$ [cm^{-1}] = 2974 (w), 2932 (w), 2857 (w), 1686 (s), 1447 (w), 1418 (s), 1364 (m), 1354 (w), 1306 (w), 1277 (m), 1236 (s), 1157 (s), 1124 (s), 1084 (w), 1030 (m), 961 (w), 930 (w), 889 (w), 862 (w), 768 (w), 640 (w).

GC-MS: τ_R = 12.22 min; $^m/_z$ (%) = 170.1 [M, –*t*Bu]$^{\cdot+}$ (31), 154.2 [M, –*t*BuO]$^{\cdot+}$ (22), 126.2 [M, –Boc]$^{\cdot+}$ (10), 84.1 [piperidine, –H]$^{\cdot+}$ (28), 57.1 [*t*Bu]$^{\cdot+}$ (100).

Synthesis of 4-acetylpiperidine hydrochloride

[NIH_P196]

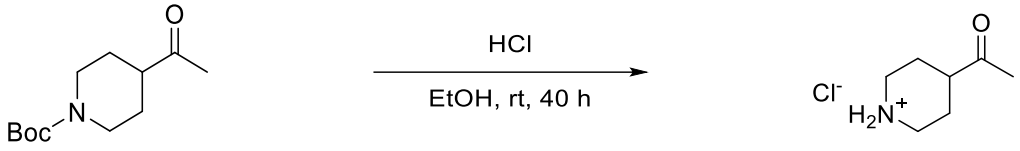

91 **94**

Boc-protected piperidine **10** (1.0 g, 4.4 mmol, 1.0 eq.) was dissolved in 15 mL EtOH and 1 mL conc. HCl (~12M, 12 mmol, 2.7 eq.) was added. After 24 h still traces of substrate were detected by TLC. Therefore, 1 mL conc. HCl was added. After further 16 h full conversion was indicated by TLC. The solvent was removed under reduced pressure and hydrochloride **13** was obtained in quantitative yield (725 mg, 4.4 mmol) as beige solid.

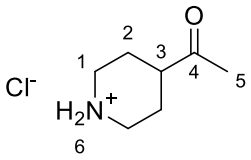

M($C_7H_{14}ClNO$): 163.65 g·mol^{-1}.

Habitus: Beige solid.

Yield: 725 mg (4.4 mmol, quant.).

^{1}H-NMR: (500 MHz, DMSO-d_6) δ [ppm] = 9.38 (s, 1H), 9.15 (s, 1H), 3.27 – 3.12 (m, 2H, H-1$_{ax}$, H-1'$_{ax}$), 2.87 (br, m, 2H, H-1$_{eq}$), 2.69 (tt, $^3J_{H3\text{-}H2ax}$ = 11.2 Hz, $^3J_{H3\text{-}H2eq}$ = 3.7 Hz, 1H, H-3), 2.14 (s, 3H, H-5), 2.06 – 1.86 (m, 2H, H-2), 1.72 – 1.62 (m, 2H, H-2).

^{13}C-NMR: (126 MHz, DMSO) δ [ppm] = 209.2 (C_q, 1C, C-4), 45.3 (CH, 1C, C-3), 42.2 (CH_2, 2C, C-1), 27.8 (CH_3, 1C, C-5), 23.7 (CH_2, 2C, C-2).

FT-IR (ATR): $\tilde{\nu}$ [cm^{-1}] = 2938 (w), 2930 (w), 2793 (m), 2766 (m), 2720 (m), 2629 (w), 2563 (w), 2492 (w), 1697 (s), 1611 (w), 1595 (w), 1454 (m), 1437 (m), 1420 (w), 1396 (w), 1358 (m), 1315 (m), 1265 (m), 1188 (m), 1144 (w), 1074 (w), 1036 (w), 991 (w), 955 (w), 920 (w), 899 (w), 611 (m).

GC-MS: τ_R = 8.88 min; $^m/_z$ (%) = 127.0 [M, –HCl]$^{\cdot+}$ (16), 91 (18), 84.1 [M, –HCl, –$COCH_3$]$^{\cdot+}$ (35), 77.8 (35), 68.3 (24), 55.1 (100).

6.6 Peptide Synthesis

Synthesis of Fmoc-Pro-Cys(trt)-OMe

[NIH_P003]

100 **101** **102**

H_2N-Cys(trt)-OMe **101** (10.2 g, 26.9 mmol, 1.0 eq.) was dissolved in DMF (150 mL) and DIPEA (10.0 mL, 56.8 mmol, 2.1 eq.) and HBTU (12.3 g, 32.3 mmol, 1.2 eq.) were added subsequently. After 5 min, Fmoc-*N*-Pro-OH **100** (9.99 g, 29.6 mmol. 1.1 eq.) was added and the reaction was stirred at ambient temperature. After 2 d full conversion of H_2N-Cys(trt)-OMe **101** was observed *via* TLC. Water (150 mL), EtOAc (150 mL) and brine (50 mL) were added and the phases were separated. The aqueous phase was extracted with EtOAc (3x150 mL) and the combined organic phases were washed with brine (100 mL), dried over $MgSO_4$ and filtered. After removing the solvent under reduced pressure, a dark oil containing a significant amount of DMF was obtained. Et_2O (100 mL), water (100 mL) and brine (100 mL) were added and the phases were separated. After extraction with Et_2O (3x100 mL) the combined organic phases were dried over $MgSO_4$ and filtered. The after the solvent was removed under reduced pressure, the remaining residue was purified by column chromatography over silica gel (3:1 → 1:1, *c*Hex:EtOAc). The desired dipeptide **102** was obtained as a colourless solid in 75 % (14.0 g, 14.1 mmol) yield.

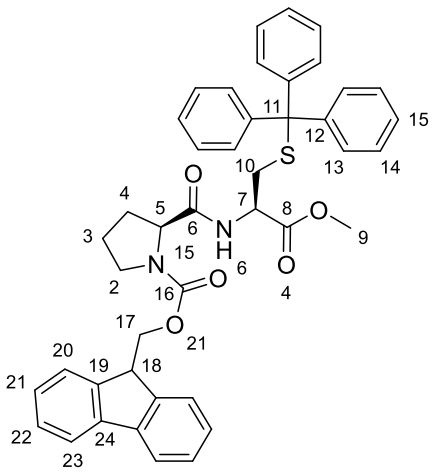

Habitus: Colourless, foam-like solid

M($C_{43}H_{40}N_2O_5S$)**:** 696.86 g·mol^{-1}.

Yield: 14.0 g (14.0 mmol, 75 %).

R_f: 0.62 (1:1, *c*Hex:EtOAc).

Mp.: 92–93°C.

^{1}H-NMR: (500 MHz, DMSO-d_6) δ [ppm] =8.66 (d, *J* = 8.1 Hz, 1H, NH), 8.40 (d, *J* = 7.7 Hz, 0.5H, NH_{minor}), 7.91 (d, *J* = 7.5 Hz, 1H, $Fmoc_{minor}$), 7.87 (d, *J* = 7.5 Hz, 2H, $Fmoc_{major}$), 7.67 (t, ^{3}J = 7.5 Hz, 2H, $Fmoc_{major}$), 7.54 (d, *J* = 7.5 Hz, 1H, $Fmoc_{minor}$), 7.45 – 7.37 (m, 3H, $Fmoc_{major+minor}$), 7.37 – 7.09 (m, 26H, $Fmoc_{major+minor,}$ $trt_{major+minor}$), 4.44 (dd, *J* = 8.7, 3.2 Hz, 1H, H-5_{major}), 4.32 – 4.20 (m, 4H, H-$5_{minor,}$ H-17, H-18), 4.15 (t, *J* = 7.6 Hz, 2H, H-18, H-7), 3.96 (dd, *J* = 10.1, 8.1 Hz, 1H, H-17), 3.53 (s, 2H, H-9_{minor}), 3.49 (s, 3H, H-9_{major}), 3.48 – 3.32 (m, 3H, H-$2_{major+minor}$), 2.58 – 2.52 (m, 1.5H, $H10_{major+minor}$), 2.43 – 2.32 (m, 1.5H, $H10'_{major+minor}$) 2.24 (dq, *J* = 11.8, 8.4 Hz, 1H, C-8/H-9), 2.13 – 1.78 (m, 6H, H-$8_{major+minor}$, H-$9_{major+minor}$).

^{13}C-NMR: (126 MHz, DMSO-d_6) δ [ppm] = 172.3 (Cq 1C, C-8/C-6), 170.6 (Cq 1C, C-8/C-6), 153.8 (Cq 1C, C-16), 143.9(9) (Cq, 1C, Fmoc), 143.9 (Cq, 3C, C-12, 143.5 (Cq, 1C, Fmoc), 140.7(4) (Cq, 1C, Fmoc), 140.7(2) (Cq, 1C, Fmoc), 128.9 (CH_{Ar}, 6C, C-13/C-14) , 127.9 (CH_{Ar}, 6C, C-13/C-14), 127.6 (CH_{Ar}, Fmoc), 127.1 (CH_{Ar}, 2C, C-15), 125.7 (CH_{Ar}, Fmoc), 125.1 (CH_{Ar}, Fmoc), 120.0 (CH_{Ar}, Fmoc), 67.1, 66.2, 59.2 (CH, 1C, C-5), 52.1 (CH_3, 1C, C-9), 51.5, 47.1 (CH_2, 1C, C-2), 46.6, 32.5 (CH_{Ar}, 1C, C-10), 31.2 (CH_{Ar}, 1C, C-3/C-4), 22.9 (CH_{Ar}, 1C, C-3/C-4).

Full assignment was not possible due to the superimposition of the signals of the isomers. For the ^{13}C-NMR only the signals of the major isomer are reported

FT-IR (ATR): $\tilde{\nu}$ [cm^{-1}] = 3300 (br, w), 3049 (w), 2972 (w), 2949 (w), 2886 (w), 2876 (w), 1744 (w), 1676 (m), 1593 (w), 1508 (w), 1489 (w), 1477 (w), 1443 (m), 1412 (m), 1348 (m), 1335 (m), 1319 (w), 1240 (w), 1198 (m), 1175 (m), 1115 (m), 1086 (m), 1032 (w), 986 (w), 939 (w), 918 (w), 885 (w), 872 (w), 849 (w), 758 (m), 739 (s), 698 (s), 675 (m), 621 (m).

GC-MS: Not detectable.

Synthesis of Fmoc-Cys(trt)-Pro-Cys(trt)-OMe

[NIH_P008]

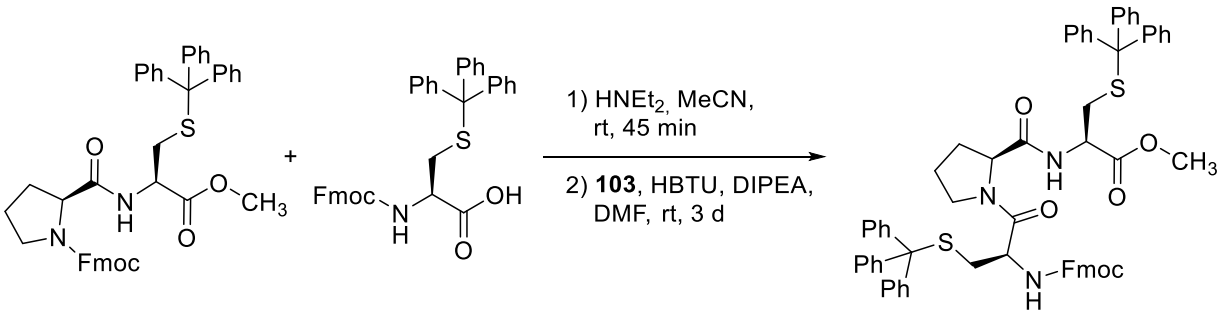

102 **103** **99**

Dipeptide **102** (3.00 g, 4.30 mmol, 1.00 eq.) was dissolved in MeCN (20 mL) and diethylamine (5.00 mL, 48.3 mmol, 11.2 eq.) was added. After 45 min full conversion was indicated by TLC. The solvent was removed under reduced pressure and the residue was dissolved in 50 mL MeCN and DIPEA (1.53 mL, 9.00 mmol, 2.1 eq.) and HBTU (1.97 g, 5.20 mmol, 1.2 eq.) were added subsequently. After 5 min, Fmoc-Cys(trt)-OH **103** (2.77 g, 4.70 mmol, 1.1 eq.) was added and the reaction was stirred at ambient temperature. After 3 d full conversion was indicated *via* TLC. The reaction mixture was concentrated under reduced pressure and the residue was dissolved in Et_2O (100 mL), water (50 mL) and brine (100 mL). The phases were separated and the aqueous phases was extracted with Et_2O (2x100 mL). The combined organic phases were washed with water (100 mL) and brine (100 mL). The solvent was removed under reduced pressure. The pale-brown solid was purified by column chromatography over silica gel (3:1 → 1:1; *c*Hex:EtOAc) to give 3.72 g of tripeptide as a white solid. Since the NMR and TLC still indicated impurities, the product was again purified by column chromatography over silica gel (*c*Hex → 1:1 *c*Hex:EtOAc) to give the desired tripeptide **99** as a colourless solid in 73 % (3.27 g, 3.14 mmol) yield.

Yield: 3.27 g (3.14 mmol, 73 %).

See next procedure for analytic data

One-Pot Synthesis of Fmoc-*N*-Cys(trit)-Pro-Cys(trt)-OMe

[NIH_P013]

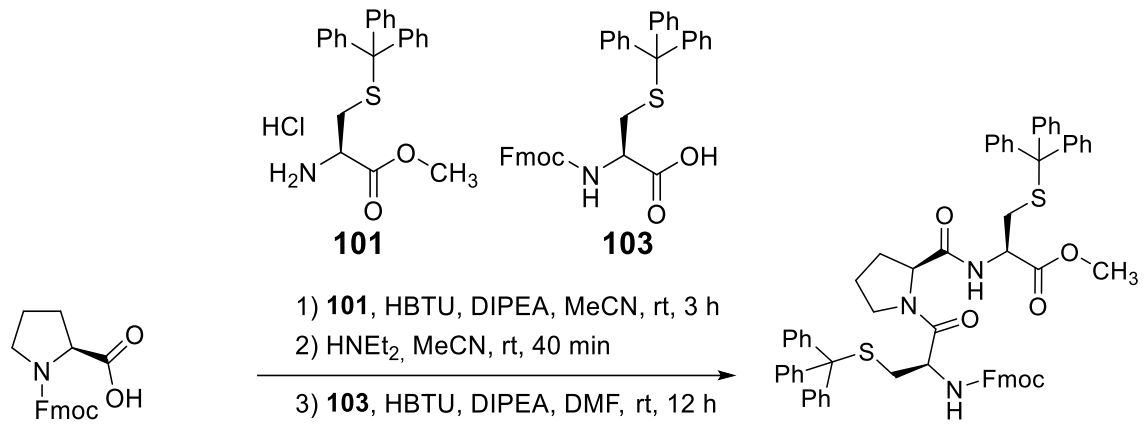

Fmoc-Pro-OH **100** (815 mg, 2.42 mmol, 1.0 eq.) and DIPEA (0.83 mL, 7.50 mmol, 3.1 eq.) were dissolved in MeCN (20 mL). HBTU (1.10 g, 2.90 mmol, 1.2 eq.) was added and the mixture was stirred for 5 min before H_2N-Cys(trt)-OMe hydrochloride **101** (1.00 g, 2.42 mmol, 1.0 eq.) was added. After stirring for 4 h at ambient temperature, full conversion was observed *via* TLC. Diethylamine (2.00 mL, 19.3 mmol, 8.0 eq.) was added and the reaction was stirred ambient temperature. The conversion was monitored by TLC. After 40 min full conversion was obtained. All volatiles were removed under reduced pressure and the residue was dissolved in 20 mL MeCN. HBTU (1.10 g, 2.90 mmol, 1.2 eq.) and DIPEA (0.83 mL, 7.5 mmol, 3.1 eq.) were added and the mixture was stirred for 5 min at ambient temperature before Fmoc-Cys(trt)-OH **103** (1.55 g, 2.66 mmol, 1.1 eq.) was added. After stirring for 12 h at ambient temperature, all volatiles were removed. The residue was purified by column chromatography over silica gel (10:1→1:1, *c*Hex:EtOAc) and tripeptide **99** was obtained as colourless solid in 61 % (1.55 g, 1.48 mmol) yield.

Habitus: Colourless, foam-like solid

Yield: 1.55 g (1.48 mmol, 61 %).

M($C_{65}H_{59}N_3O_6S_2$)**:** 1042.32 g·mol^{-1}.

R_f: 0.63 (1:1, *c*Hex:EtOAc).

^{1}H-NMR: (500 MHz, DMSO-d_6) δ [ppm] = 8.20 (d, J = 7.7 Hz, 1H, NH), 7.88 (dd, J = 8.3, 4.7 Hz, 4H, Fmoc), 7.74 (dd, J = 7.7, 3.3 Hz, 2H, Fmoc), 7.43 – 7.19 (m, 32H, Fmoc+ trt), 4.37 – 4.19 (m, 4H, H-7, H-26, H-27), 4.19 – 4.08 (m, 2H, H-10, H-2), 3.50 (s, 3H, H-12), 3.21 – 3.11 (m, 1H, H-4), 2.79 (dt, J = 9.6, 5.8 Hz, 1H, H-4), 2.72 (dd, ^{2}J = 12.7 Hz, ^{3}J = 10.1 Hz, 1H, H-13/H-19), 2.43 – 2.33 (m, 3H, H, H-13/H-19), 1.96 – 1.88 (m, 1H, H-6), 1.79 – 1.65 (m, 3H, H-6, H-5).

^{13}C-NMR: (75 MHz, DMSO-d_6) δ [ppm] = 171.3 (C_q, 2C, CO), 168.1 (C_q, 1C, CO), 155.8 (C_q, 1C, C-25), 144.3 (C_q, 3C, C-21/C-15), 144.0 (C_q, 3C, C-21/C-15), 143.7 (C_q, 2C, C-33/C-28), 140.7 (C_q, 2C, C-33/C-28), 129.2 (C_{Ar}, 4C, C-16/C-17/C-22/C-23), 129.0 (C_{Ar}, 4C, C-16/C-17/C-22/C-23), 128.1 (C_{Ar}, 4C, C-16/C-17/C-22/C-23), 128.0 (C_{Ar}, 4C, C-16/C-17/C-22/C-23), 127.6(C_{Ar}, 2C, Fmoc), 127.0 (C_{Ar}, 2C, Fmoc), 126.8 (C_{Ar}, 2C, C-18/C-14), 126.7 (C_{Ar}, 2C, C-18/C-14), 125.3 (C_{Ar}, 2C, Fmoc), 120.0 (C_{Ar}, 2C, Fmoc), 66.4 (C_q, 1C, C-14/C-20), 66.3 (C_q, 1C, C-14/C-20), 65.7 (CH_2, 1C, C-26), 59.0 (CH, 1C, C-7), 52.5 (CH, 1C, C-2/C-10), 52.0 (CH_3, 1C, C-12), 51.4 (CH, 1C, C-2/C-10), 46.6 (CH, 1C, C-27), 46.3 (CH_2, 1C, C-4), 32.8 (CH_2, 1C, C-13/C-19), 32.6 (CH_2, 1C, C-13/C-19), 28.9 (CH_2, 1C, C-6), 24.0 (CH_2, 1C, C-5).

LR-ESI-MS: m/z: 1064.3 $[M+Na]^+$.

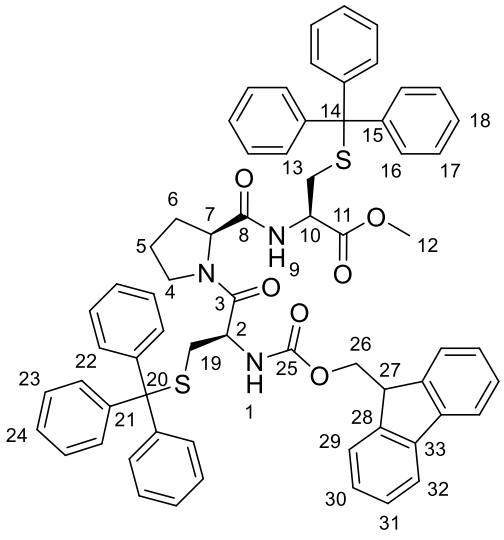

Synthesis of H_2N-Cys(*t*Bu)-OH hydrochloride

[NIH_P053]

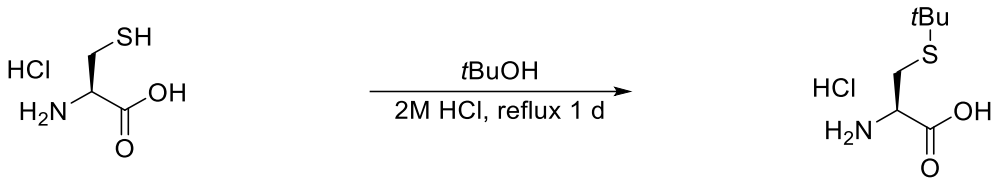

95 **96**

Cysteine hydrochloride (**95**) (20.0 g 127 mmol, 1.0 eq.) and tertiary butanol (15.5 mL, 165 mmol, 1.3 eq.) were dissolved in 60 mL 2 M HCl and refluxed. After 1 d, full conversion was observed *via* TLC. After removing the solvent and excessive tertiary butanol under reduced pressure, protected cysteine **96** was obtained as a colourless solid in 96 % (25.9 g, 121 mmol) yield.

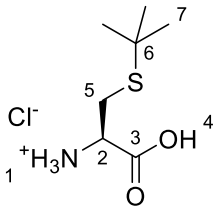

Habitus: Colourless solid.

Yield: 25.9 g (121 mmol, 96 %, lit.:[130] 90 %).

M($C_7H_{16}ClNO_2S$): 213.72 g·mol^{-1}.

Mp.: 197–200 °C, lit.:[130] 204 °C.

^{1}H-NMR: (300 MHz, MeOD-*d*$_4$) δ [ppm] = 4.20 (dd, $^3J_{H2\text{-}H5b}$ = 7.4, $^3J_{H2\text{-}H5a}$ = 4.3 Hz, 1H, H-2), 3.21 (dd, $^2J_{H5a\text{-}H5b}$ = 13.8, $^3J_{H5a\text{-}H2}$ = 4.3 Hz, 1H, H-5a), 3.07 (dd, $^2J_{H5b\text{-}H5a}$ = 13.8, $^3J_{H5b\text{-}H2}$ = 7.4 Hz, 1H, H-5b), 1.39 (s, 9H, H-7).

^{13}C-NMR: (75 MHz, MeOD-*d*$_4$) δ [ppm] = 170.2 (C_q, 1C, C-3), 54.2 (CH, 1C, C-2), 44.3 (C_q, 1C, C-6), 31.1 (CH_2, 1C, C-5), 29.5 (CH_3, 3C, C-7).

FT-IR (ATR): $\tilde{\nu}$ [cm^{-1}] = 3086 (w, br), 2967 (m), 2953 (m), 2926 (m), 2891 (m), 2862 (m), 2752 (w), 2693 (w), 1736 (s), 1595 (w), 1485 (s), 1468 (m), 1437 (m), 1410 (m), 1366 (m), 1346 (m), 1312 (w), 1223 (s), 1190 (s), 1161 (m), 1144 (m), 1098 (m), 1049 (m), 966 (w), 881 (m), 841 (m), 806 (m), 758 (m), 696 (w), 604 (w).

GC-MS: Not detectable.

The analytic data are in agreement with the literature[130]

Synthesis of Boc-Cys(*t*Bu)-OH

[NIH_P056]

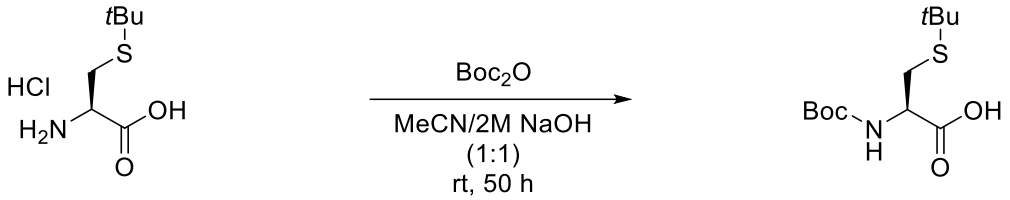

96 **97**

Cysteine hydrochloride **96** (12.8 g, 60 mmol, 1.0 eq.) was dissolved in 100 mL MeCN and 100 mL of 2 M NaOH. Boc_2O (17.0 g, 78 mmol, 1.3 eq.) was added and the reaction was tired for 50 h at ambient temperature. The MeCN was removed under reduced pressure and the solution was cooled to 0 °C. After adjusting the pH to 3–4 with conc. HCl, 100 mL brine and 100 mL DCM were added. The phases were separated and the aqueous phase was extracted with DCM (2x100 mL). The residue was dissolved in 200 mL Et_2O and 200 mL water. The phases were separated, the aqueous phase was extracted with Et_2O (2x100 mL) and the combined organic phases were dried over Na_2SO_4 and filtered. After removing the solvent under reduced pressure, double protected cysteine **97** was obtained as colourless, honey-like oil in 68% (11.25 g, 41 mmol) yield. The NMR showed traces of solvent which might prevent the product from solidifying.

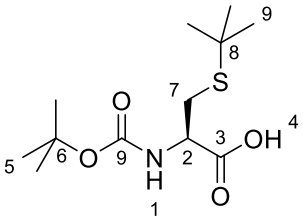

Yield: 11.25 g (41 mmol, 68%).

Habitus: Colourless oil.

M($C_{12}H_{23}NO_4S$): 277.38 g·mol^{-1}.

^{1}H-NMR: (300 MHz, $CDCl_3$) δ [ppm] = 11.31 (s, 1H, H-4), 5.37 (d, *J* = 8.0 Hz, 1H, H-1), 4.59 (dt, *J* = 8.8, 5.1 Hz, 1H, H-2f)), 3.01 (m, 2H, H-7), 1.44 (s, 9H, H-5/H-9), 1.31 (s, 9H, H-5/H-9).

^{13}C-NMR: (75 MHz, $CDCl_3$) δ [ppm] = 175.5 (C-3), 155.4 (C-9), 80.4 (C-6), 53.1 (C-2), 42.7 (C-8), 30.8 (C-5/C-9), 30.5 (C-7), 28.3 (C-5/C-9).

LR-ESI-MS: m/z: 276.1 [M, –H]$^-$, 312.0 [M+Cl]$^-$.

FT-IR: 3327 (w, br), 2972 (w), 2932 (w), 2901 (w), 2866 (w), 1717 (m, br), 1506 (m), 1458 (w), 1395 (m), 1368 (m), 1337 (w), 1300 (w),

1248 (w), 1215 (w), 1161 (s), 1053 (w), 1026 (w), 934 (w), 858 (w), 777 (w).

Synthesis of Boc-Cys(*t*Bu)-Pro-OMe

[NIH_P077]

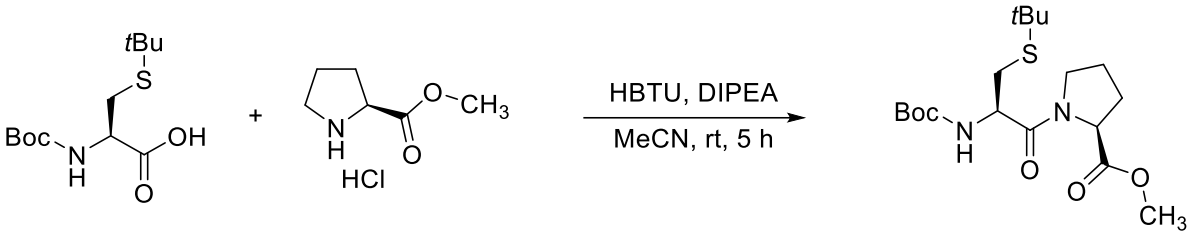

97 **98** **94**

Cysteine **97** (11.4 g, 41.0 mmol, 1.0 eq.) and DIPEA (22.1 mL, 127 mmol, 3.1 eq.) were dissolved in 150 mL MeCN. HBTU (18.7 g, 49.2 mmol, 1.2 eq.) was added and the reaction mixture was stirred for 5 min before proline **98** (7.47 g, 45.1 mmol, 1.1 eq.) was added. Full conversion was observed by TLC after 24 h and the reaction mixture was concentrated. After purification by column chromatography over silica (5:1, *c*Hex/EtOAc), dipeptide **94** was obtained as a colourless oil in 73 % (12.6 g, 32.4 mmol) yield.

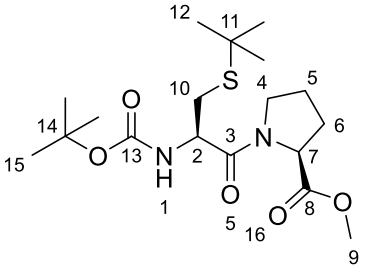

Habitus: Colourless solid.

Yield: 12.6 g (32.4 mmol, 73 %).

M($C_{18}H_{32}N_2O_5S$): 388.52 g·mol^{-1}.

Mp.: 75–76 °C.

^{1}H-NMR: (500 MHz, DMSO-d_6) δ [ppm] = 7.15 (d, ^3J = 8.4 Hz, 1H, NH), 4.36 – 4.17 (m, 2H, H-7, H-2), 3.69 – 3.54 (m, 2H, H-4), 3.61 (s, 3H, H-9), 2.74 (dd, $^2J_{H10\text{-}H10'}$ = 13.0 Hz, $^3J_{H10\text{-}H2}$ = 5.6 Hz, 1H, H-10), 2.64 (dd, $^2J_{H10'\text{-}H10}$ = 13.0 Hz, $^3J_{H10'\text{-}H2}$ = 8.2 Hz, 1H, H-10'), 2.21 – 2.12 (m, 1H, H-5/H-6), 1.97 – 1.79 (m, 3H, H-5/H-6), 1.37 (s, 9H, H-15), 1.27 (s, 9H, H-12).

^{13}C-NMR: (75 MHz, DMSO-d_6) δ [ppm] = 172.1 (C_q, 1C, C-8), 169.2 (C_q, 1C, C-3), 155.2 (C_q, 1C, C-13), 78.2 (C_q, 1C, C-14), 58.6 (CH,

1C, C-7), 52.7 (CH, 1C, C-2), 51.7 (CH_3, 1C, C-9), 46.5 (CH_2, 1C, C-4), 41.9 (C_q, 1C, C-11), 30.7 (CH_3, 3C, C-12), 29.3 (CH_2, 1C, C-10), 28.5 (CH_2, 1C, C5/C-6) 28.2 (CH_3, 3C, C-15), 24.6 (CH_2, 1C, C5/C-6).

FT-IR (ATR): $\tilde{\nu}$ [cm^{-1}] = 3385 (w), 2978 (w), 2959 (w), 2940 (w), 2897 (w), 1749 (m), 1707 (s), 1639 (s), 1508 (s), 1433 (s), 1391 (w), 1362 (m), 1337 (w), 1319 (w), 1304 (m), 1281 (m), 1238 (m), 1198 (m), 1157 (s), 1096 (w), 1063 (w), 1042 (w), 1018 (m), 997 (w), 901 (m), 868 (w), 849 (w), 766 (m), 752 (w), 729 (w), 706 (w), 667 (w), 602 (m).

LR-ESI-MS: m/z: 411.1 $[M, +Na]^+$.

Synthesis of Boc-Pro-OH

[NIH_P074]

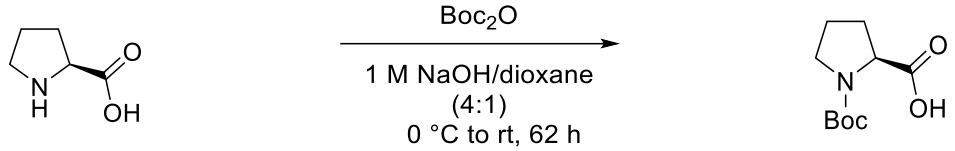

118 **105**

Proline (**118**) (15.0 g, 130 mmol, 1.0 eq.) was dissolved in 260 mL 1 M NaOH and 65 mL dioxane and the solution was cooled to 0 °C. Boc_2O (34.0 g, 156 mmol, 1.2 eq.) was added in small portions. After complete addition, the solution was stirred at 0 °C for 30 min and then at ambient temperature over the weekend. After 62 h full conversion was observed by TLC. The dioxane was removed under reduced pressure and the solution was cooled to 0 °C. The pH was adjusted to 4–5 by adding conc. HCl and 150 mL EtOAc and 100 mL brine were added to the solution. The phases were separated and the aqueous phase was extracted with EtOAc (3x100 mL). The combined organic phases were washed with brine (1x100 mL), dried over Na_2SO_4 and filtered. After removing the solvent under reduced pressure, protected proline **105** was obtained as a colourless solid in 75 % (20.87 g, 97 mmol) yield.

Yield: 20.87 g (97 mmol, 75 %).

Habitus: Colourless solid.

M($C_{10}H_{17}NO_4$): 215.25 g·mol^{-1}.

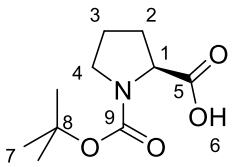

Mp.: 132–134 °C, lit.:[19] 133–135 °C.

^{1}H-NMR: (300 MHz, $CDCl_3$) δ [ppm] =11.53 (s, 1H, H-6), 4.29 (dd, $^3J_{H1\text{-}H2}$ = 8.5 Hz, $^3J_{H1\text{-}H2'}$ = 3.9 Hz, 1H, H-1), 3.66 – 3.27 (m, 2H, H-4), 2.41 – 1.79 (m, 4H, H-3, H-2), 1.44 (s, 9H, H-7).

^{13}C-NMR: **Major:** (75 MHz, $CDCl_3$) δ [ppm] = 178.8 (C_q, 1C, C-5), 153.9 (C_q, 1C, C-9), 80.3 (C_q, 1C, C-8), 59.0 (CH, 1C, C-1), 46.3 (CH_2, 1C, C-4), 30.8 (CH_2, 1C, C-2), 28.3 (CH_3, 3C, C-7), 23.6 (CH_2, 1C, C-3).

^{13}C-NMR: **Minor:** (75 MHz, $CDCl_3$) δ [ppm] = 176.1 (C_q, 1C, C-5), 155.9 (C_q, 1C, C-9), 81.0 (C_q, 1C, C-8), 59.0 (CH, 1C, C-1), 46.9 (CH_2, 1C, C-4), 29.0 (CH, 1C, C-2), 28.4 (CH_3, 3C, C-7), 24.3 (CH_2, 1C, C-3).

FT-IR (ATR): $\tilde{\nu}$ [cm^{-1}] = 2968 (w), 2932 (w), 2895 (w), 2884 (w), 1734 (s), 1632 (s), 1477 (m), 1423 (s), 1410 (s), 1389 (m), 1362 (m), 1333 (w), 1269 (w), 1254 (w), 1242 (w), 1207 (s), 1186 (m), 1159 (s), 1128 (s), 1088 (m), 1057 (w), 1032 (w), 978 (w), 897 (m), 853 (m), 829 (w), 791 (w), 773 (m), 760 (w), 729 (w), 640 (w).

Synthesis of Boc-Pro-Cys(trt)-OMe

[NIH_P061]

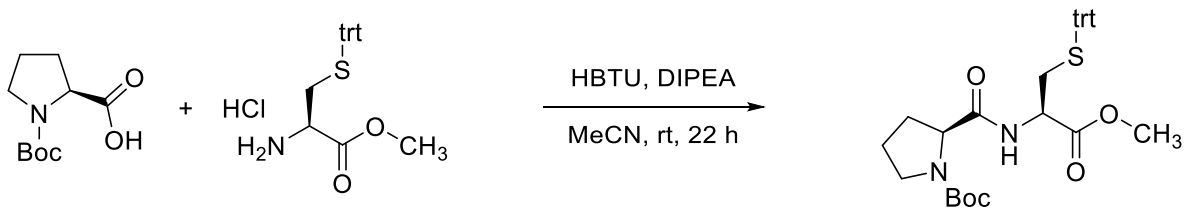

105 **101** **106**

Protected proline **105** (2.37 g, 11.0 mmol, 1.1 eq.) was dissolved in 40 mL MeCN and DIPEA (5.4 mL, 31 mmol, 3.1 eq.) and HBTU (4.55 g, 12.0 mmol, 1.2 eq.) was added. The solution as stirred for 5 min at ambient temperature before cysteine **101** (4.14 g, 10.0 mmol, 1.0 eq.) was added. After 22 h, full conversion was observed by TLC. The reaction mixture was concentrated and purified by column chromatography over silica (2:1, *c*Hex/EtOAc). Dipeptide **106** was obtained as a colourless solid in 90 % (5.17 g, 9.0 mmol) yield.

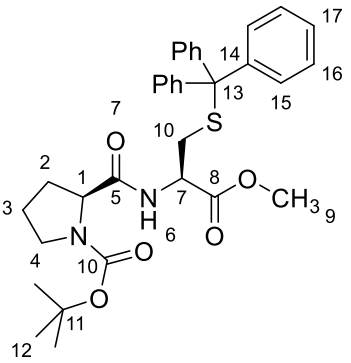

Habitus: Colourless solid.

Yield: 5.17 g (9.0 mmol, 90 %).

M($C_{14}H_{23}N_2O_5S$): 574.74 g·mol^{-1}.

Mp.: 59–60 °C.

^{1}H-NMR: (500 MHz, DMSO-*d*$_6$) δ [ppm] = 8.34 (d, *J* = 8.1 Hz, 1H, H-6), 7.42 – 7.18 (m, 15H, H-15, H-16, H-17), 4.20 – 4.13 (m, 1H, H-1), 4.10 – 4.03 (m, 1H, H-7), 3.54 (s, 3H, H-9), 3.42 – 3.34 (m, 1H, H-4), 3.30 – 3.19 (m, 1H, H-4'), 2.60 (dd, $^2J_{H10\text{-}H10'}$ = 12.3 Hz, $^3J_{H10\text{-}H7}$ = 8.8 Hz, 1H), 2.42 (dd, $^2J_{H10'\text{-}H10}$= 12.4, $^3J_{H10'\text{-}H7}$ = 5.8 Hz, 1H- H-10'), 2.20 – 1.98 (m, 1H, H-3/H-2), 1.90 – 1.66 (m, 3H, H-2, H-3), 1.28 (s, 9H, H-12).

^{13}C-NMR: (126 MHz, DMSO-*d*$_6$) δ = 172.5 (C_q, 1C, C-5), 170.6 (C_q, 1C, C-8), 153.3 (C_q, 1C, C-10), 144.1 (C_q, 3C, C-14), 129.0 (CH_{Ar}, 6C, C-15/C-16), 128.1 (CH_{Ar}, 6C, C-15/C-16), 126.8 (CH_{Ar}, 3C, C-17), 78.4 (C_q, 1C, C-11), 66.3 (C_q, 1C, C-13), 59.3 (CH, 1C, C-7), 52.1 (CH_3, 1C, C-9), 51.3 (CH, 1C, C-1), 46.4 (CH_2, 1C,

C-4), 32.6 (CH_2, 1C, C-10), 30.9 (CH_2, 1C, C-2/C-3), 28.0 (CH_3, 1C, C-12), 22.9 (CH_2, 1C, C-2/C-3).

LR-ESI-MS: m/z: 597.2 $[M, +Na]^+$.

FT-IR (ATR): $\tilde{\nu}$ [cm^{-1}] = 3294 (br, w), 3055 (w), 2976 (w), 2928 (w), 1746 (w), 1670 (m), 1489 (w), 1443 (w), 1391 (m), 1366 (m), 1319 (w), 1244 (w), 1206 (m), 1161 (m), 1121 (m), 1086 (w), 1034 (w), 984 (w), 920 (w), 885 (w), 853 (w), 766 (w), 743 (m), 698 (s), 675 (m), 617 (m).

Synthesis of Boc-Pro-Cys(trt)-OH hydrochloride

[NIH_P065]

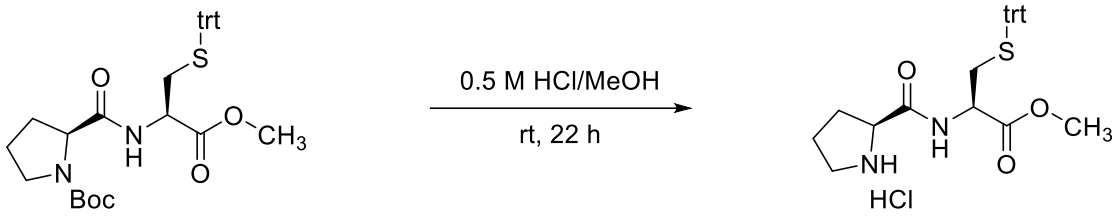

106 **108**

Dipeptide **106** (2.87 g, 5.0 mmol, 1.0 eq.) was dissolved in 0.5 M HCl in MeOH (20 mL, 10 mmol, 2.0 eq.) and stirred at ambient temperature. Full conversion was observed by TLC after 8 h. The solvent was removed under reduced pressure and dipeptide **108** was obtained as a colourless solid in quantitative yield (2.55 g, 5.0 mmol) yield.

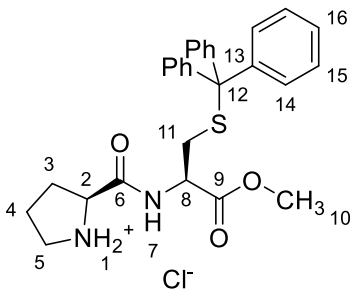

Habitus: Colourless solid.

Yield: 2.55 g (5.0 mmol, quant.).

M($C_9H_{16}ClN_2O_3S$): 511.08 g·mol^{-1}.

Mp.: 119–121 °C.

^{1}H-NMR: (500 MHz, MeOD-d_4) δ [ppm] = 7.39 – 7.35 (m, 6H, H-14), 7.31 – 7.26 (m, 6H, H-15), 7.25 – 7.19 (m, 3H, H-16), 4.33 (dd, $^3J_{H2\text{-}H3}$ = 8.8 Hz, $^3J_{H2\text{-}H3}$ = 6.0 Hz, 1H, H-2), 4.22 (dd, $^3J_{H8\text{-}H11}$ = 8.9 Hz,

$^{3}J_{H8\text{-}H11'}$ = 4.9 Hz, 1H, H-8), 3.61 (s, 3H, H-10), 3.41 – 3.32 (m, 3H, H-5), 2.72 (dd, $^{2}J_{H11'\text{-}H11}$ = 12.9 Hz, $^{3}J_{H11\text{-}H8}$ = 8.9 Hz, 1H, H-11), 2.61 (dd, $^{2}J_{H11\text{-}H11'}$ = 12.9 Hz, $^{3}J_{H11\text{-}H8}$ = 4.9 Hz, 1H, H-11), 2.49 – 2.38 (m, 1H, H-3), 2.09 – 1.94 (m, 3H, H-3, H-4).

^{13}C-NMR: (75 MHz, MeOD-d_4) δ [ppm] = 171.6 (C_q, 1C, C-9), 169.7 (C_q, 1C, C-6), 145.6 (C_q, 3C, C-13), 130.6 (CH_{Ar}, 6C, C-14), 129.0 (CH_{Ar}, 6C, C-15), 128.0 (CH_{Ar}, 3C, C-16), 68.2 (C_q, 1C, C-12), 60.8 (CH, 1C, C-2), 53.6 (CH, 1C, C-8), 53.0 (CH_3, 1C, C-10), 47.5 (CH2, 1C, C-5), 34.0 (CH_2, 1C, C-11), 31.0 (CH_2, 1C, C-3), 24.9 (CH_2, 1C, C-4).

FT-IR (ATR): $\tilde{\nu}$ [cm^{-1}] = 3181 (w, br), 3055 (w), 2972 (w), 2951 (w), 2891 (w), 2822 (w), 1736 (w), 1676 (m), 1593 (w), 1535 (w), 1489 (w), 1443 (m), 1387 (w), 1341 (w), 1317 (w), 1213 (m), 1180 (m), 1113 (w), 1082 (w), 1034 (w), 1001 (w), 976 (w), 847 (w), 743 (m), 698 (s), 675 (m), 615 (m).

Synthesis of Boc-Cys(trt)-Pro-Cys(trt)-OMe

[NIH_P085, **NIH_P159**]

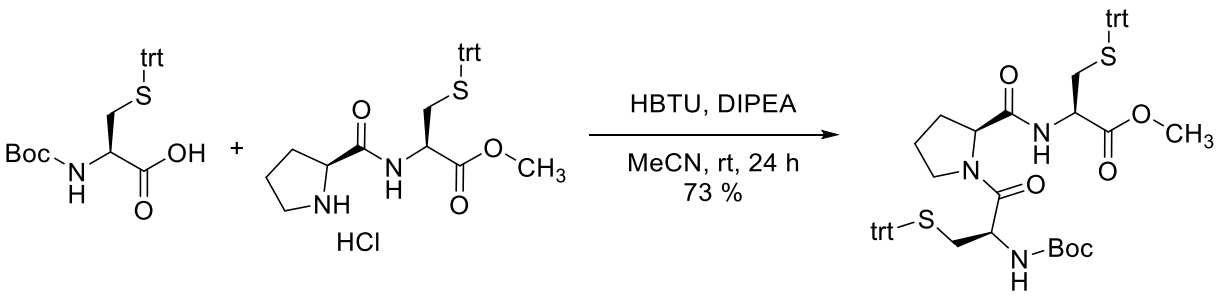

107 **108** **104**

Dipeptide **108** (7.67 g. 15.0 mmol, 1.0 eq.) and DIPEA (8.10 mL, 46.5 mmol, 3.1 eq.) were dissolved in MeCN (250 mL). HBTU (6-83 g, 18.0 mmol, 1.2 eq.) was added and the solution was stirred for five minutes at ambient temperature. After cysteine **107** (7.65 g. 16.5 mmol, 1.1 eq.) was added, the solution was stirred for 24 h at ambient temperature. The solvent was removed under reduced pressure and the product was purified by column chromatography over silica gel (2:1→1:1, *c*Hex:EtOAc). After the solvent was removed under reduced pressure, tripeptide **104** was obtained as a colourless solid in 73 % (11.0 mmol, 10.1 g).

M($C_{55}H_{57}N_3O_6S_2$)**:** 919.37.17 g·mol^{-1}.

Habitus: Colourless solid.

Yield: 10.1 g (11.0 mmol, 73 %).

Mp.: 95–96 °C

^{1}H-NMR: (500 MHz, DMSO-d_6) δ [ppm] = 8.18 (d, J = 7.6 Hz, 1H, NH), 7.47 – 7.21 (m, 30H, H-16, H-17, H-21, H-22, H-22, H-23), 4.33 – 4.20 (m, 1H, H-7), 4.18 – 3.95 (m, 2H, H10, H-2), 3.50 (s, 3H, H-12), 3.20 – 3.10 (m, 1H, H-4), 2.75 – 2.65 (m, 1H, H-4'), 2.59 (dd, $^2J_{H19\text{-}H19'}$ = 12.7 Hz, $^3J_{H19\text{-}H2}$ = 9.8 Hz, 1H, H-19), 2.46 (dd, $^2J_{H13\text{-}H13'}$ = 12.4 Hz, $^3J_{H13\text{-}H10}$ = 8.1 Hz, 1H, H-13), 2.35 (dd, $^2J_{H13'\text{-}H13}$ = 12.4 Hz, $^3J_{H13'\text{-}H10}$ = 5.4 Hz, 1H, H-13'), 2.30 (dd, $^2J_{H19'\text{-}H19}$ = 12.7 Hz, $^3J_{H19'\text{-}H2}$ = 4.5 Hz, 1H, H-19), 1.97 – 1.65 (m, 4H, H-5, H 6), 1.38 (s, 9H, H-27).

^{13}C-NMR: (126 MHz, DMSO-d_6) δ [ppm] = 171.4 (C_q, 1C, C-8), 170.6 (C_q, 1C, C-11), 168.3 (C_q, 1C, C-3), 155.2 (C_q, 1C, C-24), 144.4 (C_q, 3C, C-15/C-21), 144.0 144.4 (C_q, 3C, C-15/C-21), 129.2 144.4 (CH_{Ar}, 6C, C-H16/C-17/C-22/C-23), 129.0 (CH_{Ar}, 6C, C-H16/C-17/C-22/C-23), 128.1 (CH_{Ar}, 6C, C-H16/C-17/C-22/C-23), 128.0 (CH_{Ar}, 6C, C-H16/C-17/C-22/C-23), 126.8 (CH_{Ar}, 6C, C-H18/C-24), 126.7 (CH_{Ar}, 6C, C-H18/C-24), 78.2 (C_q, 1C, C-26), 66.4 (C_q, C1, C-14/C-20), 66.3 (C_q, C1, C-14/C-20), 58.9 (CH, 1C, C-7), 52.3 (CH, 1C, C-2/C-10), 52.0 (CH_3, 1C, C-12), 51.4 (CH, 1C, C-2/C-10), 46.2 (CH_2, 1C, C-4), 32.6 (CH_2, 2C, C-13, C-19), 28.9 (CH_2, 1C, C-5/C-6), 28.2 (CH_3, 3C, C-27), 24.1 (CH_2, 1C, C-5/C-6).

FT-IR (ATR): $\tilde{\nu}$ [cm^{-1}] = 3412 (w, br), 3296 (w, br), 3055 (w), 2974 (w), 2949 (w), 2928 (w), 2874 (w), 1744 (w), 1686 (w), 1649 (m), 1595 (w), 1582 (w), 1489 (m), 1441 (m), 1391 (w), 1366 (w), 1344 (w), 1317 (w), 1304 (w), 1246 (w), 1206 (w), 1161 (s), 1082 (w), 1032 (w), 1001 (w), 922 (w), 883 (w), 853 (w), 741 (s), 696 (s), 675 (m), 617 (m), 604 (w).

HRMS (ESI): m/z calcd. for $C_{55}H_{57}N_3O_6S_2$: 920.3761543 $[M+H]^+$;
found: 920.37676.
m/z calcd. for $C_{55}H_{57}N_3O_6S_2$: 942.3580990 $[M+Na]^+$;
found: 942.35879.

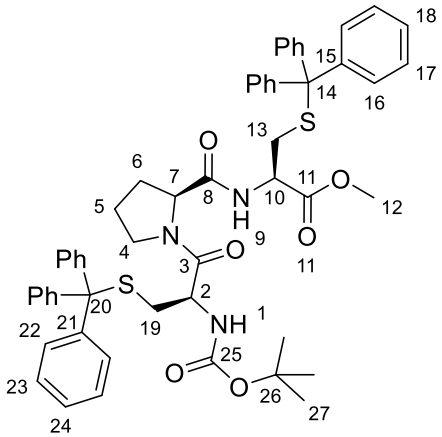

Synthesis of H_2N-Cys(Bzl)-OMe hydrochloride

[NIH_P040]

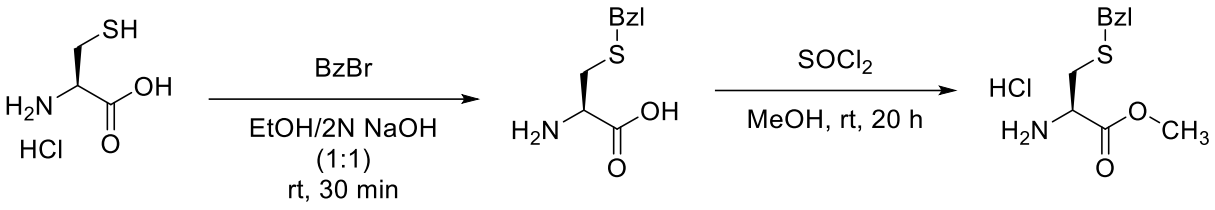

112 **113** **110**

Cysteine hydrochloride (**112**) (12.61 g, 80 mmol, 1.0 eq.) was dissolved in 150 mL EtOH and 75 mL 2 N NaOH and benzyl bromide (9.50 mL,80 mmol, 1.0 eq.) was added under vigorous stirring. After full addition, the reaction was stirred for further 30 min before neutralisation by the addition of conc. HCl. The precipitate was filtered off, washed with water, EtOH and Et_2O and dried under reduced pressure to yield benzyl protected cysteine **113** as a colourless solid which was directly used without further purification.

Benzyl protected cysteine was suspended in 150 mL MeOH and thionyl chloride (8.7 mL, 120 mmol, 1.5 eq.) was slowly added over a dropping funnel. After stirring for 4 h, additional thionyl chloride (2.9 ml, 40 mmol, 0.5 eq.) was added and the reaction was stirred overnight. After full conversion as detected *via* TLC, all volatile parts were removed under reduced pressure to yield 12.52 g (48 mmol, 60 %) of hydrochloride **110** as colourless solid.

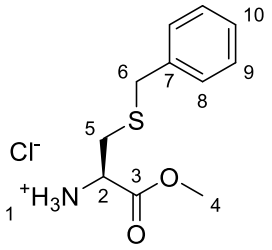

Yield: 12.52 g (48 mmol, 60 %, lit.:[131] 85 %).

Habitus: Colourless solid.

M($C_{11}H_{14}ClNO_3S$): 261.76 g·mol^{-1}.

Mp.: 147–149 °C, lit.:[131] 148–150 °C.

^{1}H-NMR: (500 MHz, MeOD-*d*$_4$) δ [ppm] = 7.40 – 7.35 (m, 2H, H-8), 7.33 (t, $^3J_{H9\text{-}H8,\ H9\text{-}H10}$ = 7.5 Hz, 2H, H-9), 7.29 – 7.23 (m, 1H, H-10), 4.22 (dd, $^3J_{H2\text{-}H5}$ = 7.9 Hz, $^3J_{H2\text{-}H5'}$ = 4.5 Hz, 1H, H-2), 3.83 (s, 2H, H-6), 3.82 (s, 3H, H-4), 3.05 (dd, $^2J_{H5\text{-}H5'}$ = 14.8 Hz, $^3J_{H5\text{-}H2}$ = 4.5 Hz, 1H, H-5), 2.93 (dd, $^2J_{H5'\text{-}H5}$ = 14.8 Hz, $^3J_{H5'\text{-}H2}$ =7.9 Hz, 1H, H-5).

^{13}C-NMR: (75 MHz, MeOD-*d*$_4$) δ [ppm] = 169.6 (C_q, 1C, C-3), 138.6 (C_q, 1C, C-7), 130.2 (CH_{Ar}, 2C, C-8), 129.7 (CH_{Ar}, 2C, C-9), 128.4

(CH_{Ar}, 1C, C-10), 53.9 (CH_3, 1C, C-4), 53.3 (CH, 1C, C-2), 36.8 (CH_2, 1C, C-6), 32.0 (CH_2, 1C, C-5).

FT-IR (ATR): $\tilde{\nu}$ [cm^{-1}] = 3130 (w), 2999 (w), 2860 (w), 2801 (m), 2752 (w), 2720 (w), 2669 (w), 2639 (w), 2567 (w), 2494 (w), 1736 (s), 1578 (w), 1493 (m), 1445 (m), 1418 (w), 1383 (m), 1287 (w), 1234 (s), 1200 (m), 1182 (m), 1153 (m), 1101 (m), 1069 (w), 1038 (m), 1003 (w), 937 (m), 912 (w), 839 (m), 756 (w), 702 (s), 658 (w).

LR-ESI-MS: m/z: 226.0 $[M, +H]^+$, 248.0 $[M, +Na]^+$.

The analytic data are in agreement with the literature[131]

Synthesis of Boc-Cys(Bzl)-OH

[NIH_P042]

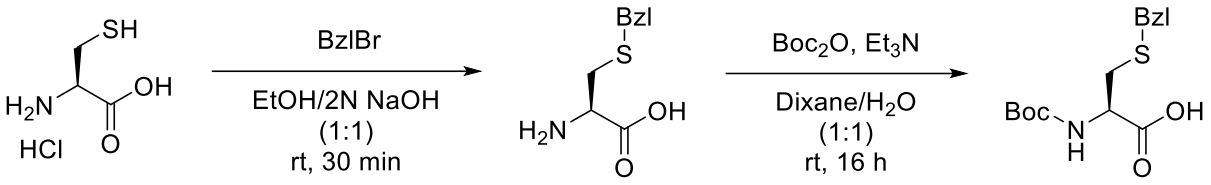

112 **113** **111**

Cysteine hydrochloride (**112**) (12.61 g, 80 mmol, 1.0 eq.) was dissolved in 150 mL EtOH and 75 mL 2 N NaOH and benzyl bromide (9.50 mL,80 mmol, 1.0 eq.) was slowly added over a dropping funnel under vigorous stirring. After full addition, the reaction was stirred for further 30 min before neutralisation by the addition of conc. HCl. The precipitate was filtered off, washed with water, EtOH and Et_2O and dried under reduced pressure to yield 14.78 g (70 mmol, 86%) of benzyl protected cysteine **113** as a colourless solid which was directly used without further purification. Benzyl protected cysteine was dissolved in 140 mL dioxane/water (1:1) and Et_3N (16.7 mL, 120 mmol, 1.5 eq.). Boc_2O (17.46 g, 80 mmol, 1.0 eq.) were added and the reaction was stirred for 16 h. The major part of dioxane was removed under reduced pressure and the reaction was cooled to 0 °C. After adjusting the pH to 4-5, the solution was extracted with EtOAc (3x100 mL), dried over Na_2SO_4 and filtrated. After drying for more than 7 d, double protected cysteine **111** was obtained in 78 % yield (19.52 g, 62.7 mmol) as a colourless oil containing traces of solvent.

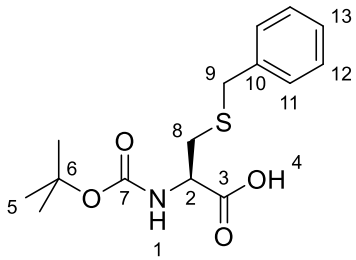

Habitus: Colourless oil.

Yield: 19.52 g (62.7 mmol, 78 %, lit.:[16] 93 %).

M($C_{15}H_{19}NO_5S$): 325.38 g·mol^{-1}.

^{1}H-NMR: (300 MHz, $CDCl_3$) δ [ppm] = 10.78 (s, 1H, H-4), 7.33 – 7.20 (m, 5H, H-Ph), 5.37 (d, *J* = 7.8 Hz, 1H, H-1), 4.50 (d, *J* = 6.8 Hz, 1H, H-2), 3.73 (s, 2H, H-9), 2.92 (dd, *J* = 14.0, 4.8 Hz, 1H, H-8), 2.84 (dd, *J* = 14.2, 5.9 Hz, 1H, H-8), 1.44 (s, 9H, H-5).

^{13}C-NMR: (75 MHz, $CDCl_3$) δ [ppm] = 175.6 (C-3), 155.5 (C-7), 137.7 (C-10), 129.0 (C-11/C-12), 128.6 (C-11/C-12), 127.2 (C-13), 53.2 (C-2), 36.7 (C-9), 33.4 (C-8), 28.3 (C-5).

Synthesis of Fmoc-Pro-Cys(Bzl)-OMe

[NIH_P044]

100 **110** **114**

Fmoc-Pro-OH **100** (2.84 g, 8.4 mmol, 1.1 eq.) was dissolved in 40 mL MeCN and DIPEA (4.1 mL, 23.7 mmol, 3.1 eq.). After the addition of HBTU (3.48 g, 9.2 mmol, 1.2 eq.), the reaction mixture was stirred for 5 min before double protected cysteine hydrochloride **110** was added. After stirring at ambient temperature for 6 h, full conversion was observed *via* TLC. All volatile parts were removed and the reaction mixture was purified by column chromatography over silica gel (1:1, *c*Hex/EtOAc). Dipeptide **114** was obtained as a colourless oil in 90 % (3.74 g, 6.9 mmol) yield.

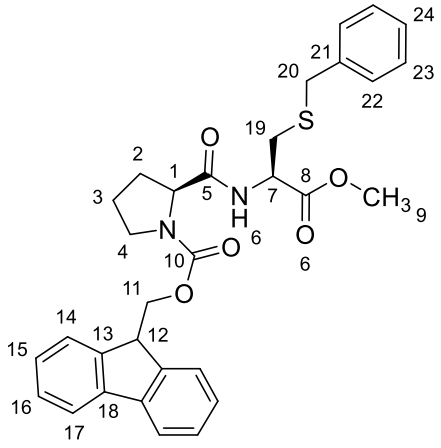

Yield: 3.74 g (6.9 mmol, 90 %).

Habitus: Colourless oil.

M($C_{31}H_{30}N_2O_6S$): 558.65 g·mol^{-1}.

^{1}H-NMR: (500 MHz, $CDCl_3$) δ [ppm] = 7.75 (d, *J* = 7.5 Hz, 2H), 7.61 – 7.50 (m, 2H), 7.38 (t, *J* = 7.5 Hz, 2H), 7.32 – 7.17 (m, 7H), 4.76 (dt, *J* = 7.8, 5.6 Hz, 1H, H-7), 4.50 – 4.29 (m, 3H), 4.29 – 4.18 (m, 1H), 3.70 (s, 2H), 3.65 (s, 2H, H-20), 3.63 – 3.41 (m, 3H), 2.92 (dd, *J* = 13.8, 4.9 Hz, 1H, H-19), 2.84 – 2.70 (m, 1H, H-19), 2.41 – 1.79 (m, 4H, H, H-2, H-3).

^{13}C-NMR: 13C NMR (75 MHz, CDCl3) δ 171.6, 171.1, 143.8, 141.3, 137.6 129.0, 128.6, 127.8, 127.3, 127.1, 125.2, 125.2, 120.1, 67.9, 60.5, 52.7, 51.9 (C-7), 47.3, 47.1, 36.5 (C-20), 33.4 (C-19), 24.7.

Could not be assigned properly due to superimposed signals of isomers

FT-IR (ATR): $\tilde{\nu}$ [cm^{-1}] = 3314 (w, br), 3063 (w), 3028 (w), 2951 (w), 2884 (w), 1744 (w), 1674 (m), 1518 (w), 1450 (m), 1414 (m), 1350 (m), 1335 (m), 1240 (w), 1204 (m), 1175 (m), 1115 (m), 1088 (m), 1030 (w), 986 (w), 908 (m), 878 (w), 758 (m), 727 (s), 702 (m), 646 (w).

Synthesis of Boc-Cys(Bzl)-Pro-Cys(Bzl)-OMe

[NIH_P055]

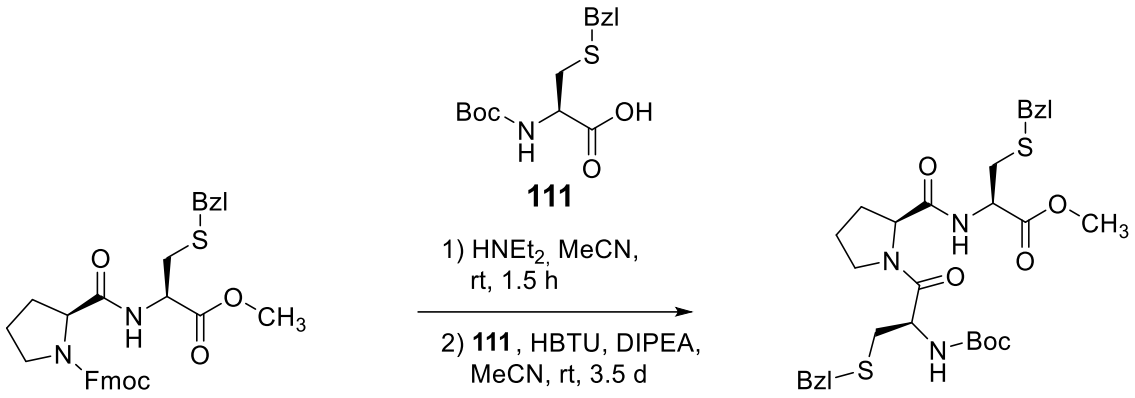

114 **109**

Fmoc-Pro-Cys(Bzl)-OMe **114** (3.75 g, 6.9 mmol, 1.0 eq.) was dissolved in 30 mL MeCN and diethylamine (7.1 mL, 69 mmol, 10 eq.) was added. After stirring for 1.5 h complete cleavage of the Fmoc-protecting group was observed *via* TLC. The Solvent and excess diethylamine were removed under reduced pressure and the crude residue was dissolved in 30 mL MeCN. Boc-Cys(Bzl)-OH **111** (2.72 g, 8.7 mmol, 1.5 eq.) was dissolved in 30 mL MeCN and DIPEA (3.8 mL, 21.8 mmol, 3.2 eq.). HBTU (3.93 g, 10.4 mmol, 1.5 eq.) was added and the reaction was stirred for 5 min at ambient temperature before the solution of dipeptide was added. After 3.5 d, the solution was concentrated under reduced pressure and 100 mL DCM and 100 mL water were added. After adjusting the pH to 3–4, the phases were separated and the aqueous phase was extracted with DCM (2x100 mL). The combined organic phases were washed with brine (1x100 mL), dried over Na_2SO_4 and filtered. The crude product was purified by column chromatography over silica (10:1 to 1:1, *c*Hex/EtOAc). Tripeptide **109** was obtained as a slightly yellow tare in 62% (2.62 g, 4.3 mmol) yield. The NMR showed impurities which could not be removed by column chromatography.

Habitus: Slightly yellow tare.

Yield: Crude: 2.62 g (4.3 mmol, 62 %).

M($C_{31}H_{41}N_3O_6S_2$): 615.80 g·mol^{-1}.

Synthesis of H_2N-Pro-OMe hydrochloride

[NIH_P060]

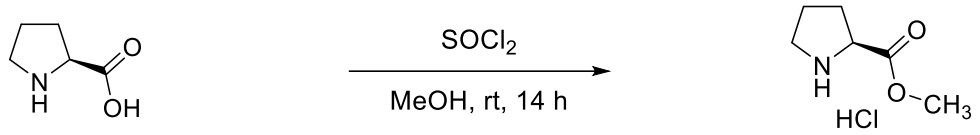

118 **119**

Proline 1**18** (5.76 g, 50 mmol, 1.0 eq.) was dissolved in 50 mL MeOH and cooled to 0 °C. Thionyl chloride (7.3 mL, 100 mmol, 2.0 eq.) was slowly added over a dropping funnel. The reaction was warmed up to ambient temperature. After 14 h full conversion was observed by TLC and MeOH and excessive thionyl chloride were removed under reduced pressure. Proline methyl ester hydrochloride 1**19** was obtained as colourless solid in 98 % (8.11 g, 49 mmol) yield.

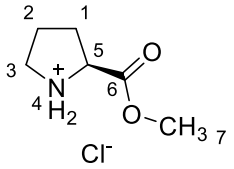

Habitus: Colourless solid.

Yield: 8.11 g (49 mmol, 98 %).

M($C_6H_{12}ClNO_2$): 165.62 g·mol^{-1}.

Mp.: 72–75 °C.

^{1}H-NMR: (300 MHz, MeOD-*d*$_4$) δ [ppm] = 3.18 (dd, *J* = 8.7, 6.9 Hz, 1H, H-5), 2.57 (d, *J* = 0.6 Hz, 3H, H-7), 2.21 – 2.04 (m, 2H, H-3), 1.22 – 1.05 (m, 2H, H-1), 0.97 – 0.71 (m, 3H, H-1, H-2).

^{13}C-NMR: (75 MHz, MeOD-*d*$_4$) δ [ppm] = 169.0 (C_q, 1C, C-6), 59.2 (CH, 1C, C-5), 52.5 (CH_3, 1C, C-7), 45.7 (CH_2, 1C, C-3), 27.8 (CH_2, 1C, C-1), 23.1 (CH_2, 1C, C-2).

FT-IR (ATR): $\tilde{\nu}$ [cm^{-1}] = 2862 (m, br), 2812 (m), 2727 (m), 2668 (m), 2615 (w), 2558 (m), 2465 (w), 2440 (w), 1744 (s), 1447 (m), 1422 (w), 1389 (w), 1369 (m), 1352 (m), 1321 (m), 1304 (w), 1248 (s), 1207 (s), 1157 (w), 1088 (m), 1059 (m), 1038 (m), 1005 (m), 959 (w), 918 (m), 889 (m), 692 (w).

LR-ESI-MS: m/z: 130.1 [M, +H, –Cl]$^+$.

Synthesis of Boc-Cys(trt)-Pro-OMe

[**NIH_P067,** NIH_P061]

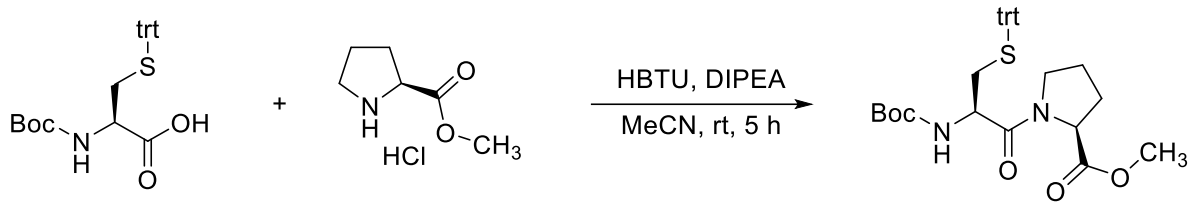

107 **119** **120**

Cysteine **107** (1.29 g, 2.8 mmol, 1.1 eq.) were dissolved in 40 mL MeCN and DIPEA (1.35 mL, 7.8 mmol, 3.1 eq.). HBTU (1.14 g, 3.0 mmol, 1.2 eq.) was added and the solution was stirred for 5 min before proline 1**19** (414 mg, 2.6 mmol, 1.0 eq.) was added. After stirring for 5 h at ambient temperature, full conversion was observed by TLC. The Reaction mixture was concentrated under reduced pressure and purified by column chromatography over silica (5:1 to 1:1, *c*Hec:EtOAc). Dipeptide 1**20** was obtained as colourless solid in 88 % (1.42 g, 2.5 mmol) yield. The NMR-spectra shows two rotamers and traces of EtOAc.

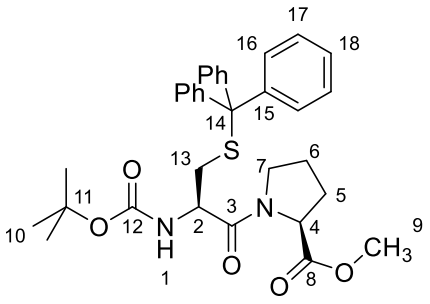

Habitus: Colourless, foam-like solid.

Yield: 1.42 g (2.5 mmol, 88 %).

M($C_{14}H_{23}N_2O_5S$): 574.74 g·mol^{-1}.

Mp.: 60–62 °C.

^{1}H-NMR: **Major:** (500 MHz, $CDCl_3$) δ [ppm] = 7.47 – 7.34 (m, 6H, H-16), 7.31 – 7.23 (m, 6H, H-17), 7.23 – 7.16 (m, 3H, H-18), 5.05 (d, *J* = 9.1 Hz, 1H, H-1), 4.43 (dd, *J* = 8.4, 3.9 Hz, 1H, H-4), 4.34 – 4.26 (m, 1H, H-2), 3.62 (s, 3H, H-9), 3.51 – 3.40 (m, 1H, H-7), 3.15 – 3.05 (m, 1H, H-7), 2.50 (d, *J* = 6.8 Hz, 2H, H-13), 1.57 – 1.33 (s, 9H, H-10).

^{13}C-NMR: **Major:** (75 MHz, $CDCl_3$) δ [ppm] = 172.1 (C_q, 1C, C-8), 169.6 (C_q, 1C, C-3), 155.3 (C_q, 1C, C-12), 144.63 (C_q, 3C, C-15), 129.8 (CH_{Ar}, 6C, C-16), 128.0 (CH_{Ar}, 6C, C-17), 126.8 (CH_{Ar}, 3C, C-18), 79.9 (C_q, 1C, C-11), 67.2 (C_q, 1C, C-14), 59.0 (CH, 1C, C-4), 52.2 (CH_3, 1C, C-9), 51.7 (CH, 1C, C-2), 46.7 (CH_2, 1C,

C-7), 34.2 (CH_2, 1C, C-13), 29.0 (CH_2, 1C, C-5), 28.4 (CH_3, 3C, C-10), 24.9 (CH_2, 1C, C-6).

^{13}C-NMR: **Minor:** (75 MHz, $CDCl_3$) δ [ppm] = 172.3 (C_q, 1C, C-8), 169.2 (C_q, 1C, C-3), 155.3 (C_q, 1C, C-12), 144.6 (C_q, 3C, C15), 129.8 (CH_{Ar}, 6C, C-16), 128.0 (CH_{Ar}, 6C, C-17), 126.8 (CH_{Ar}, 3C, C-18), 79.9 (C_q, 1C, C-11), 67.2 (C_q, 1C, C-14), 59.1 (CH, 1C, C-4), 52.3 (CH_3, 1C, C-9), 51.4 (CH, 1C, C-2), 46.9 (CH_2, 1C, C-7), 34.6 (CH_2, 1C, C-13), 29.1 (CH_2, 1C, C-5), 28.4 (CH_3, 3C, C-10), 24.7 (CH_2, 1C, C-6).

FT-IR (ATR): $\tilde{\nu}$ [cm^{-1}] = 3412 (w, br), 3298 (w, br), 3055 (w), 2976 (w), 2953 (w), 2930 (w), 2882 (w), 1746 (m), 1709 (m), 1647 (m), 1489 (m), 1443 (m), 1366 (m), 1341 (w), 1277 (w), 1248 (m), 1167 (s), 1043 (w), 1022 (w), 910 (w), 866 (w), 766 (w), 733 (s), 700 (s).

Synthesis of Boc-Cys(trt)-Pro-OH

[NIH_P073]

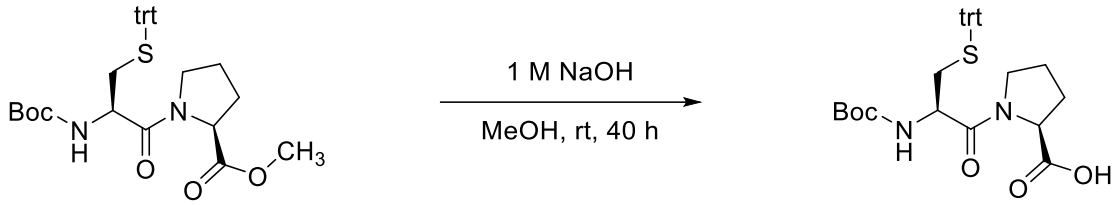

120 **116**

Dipeptide **120** (1.42 g, 2.5 mmol, 1.0 eq.) was dissolved in 30 mL MeCN and 1 m NaOH (25 mL, 25 mmol, 10 eq.) was added. The reaction was stirred at ambient temperature. After 40 h full conversion was observed by TLC. The MeCN was removed under reduced pressure and 50 mL water were added. The pH was adjusted to 3–4 by adding conc. HCl. The solution was extracted with EtOAc (3x50 mL) and the combine organic phases were dried over Na_2SO_4. After column chromatography over silica (20:1, DCM/MeOH), dipeptide 1**16** was obtained as a colourless solid in 64% (875 mg, 1.6 eq.) yield.

Habitus: Colourless, foam-like solid.

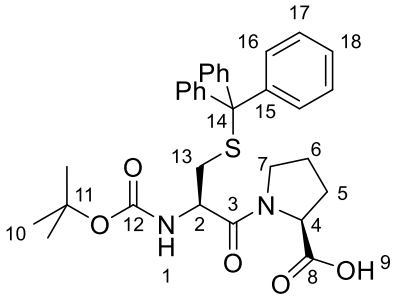

Yield: 875 mg (1.6 mmol, 64%).

M($C_{13}H_{21}N_2O_5S$): 560.71 g·mol^{-1}.

Mp.: Brought range.

^{1}H-NMR: **Major:** (500 MHz, $CDCl_3$) δ [ppm] = 7.49 – 7.33 (m, 6H, H-16), 7.29 – 7.25 (m, 6H, H-17), 7.22 – 7.17 (m, 3H, H-18), 5.13 (d, *J* = 8.6 Hz, 1H, H-1), 4.48 (dd, $^3J_{H4\text{-}H5}$ = 8.4 Hz, $^3J_{H4\text{-}H5'}$ = 3.5 Hz, 1H, H-4), 4.26 (dd, $^3J_{H2\text{-}H13'}$ = 14.8 Hz, $^3J_{H2\text{-}H13}$ = 7.4 Hz, 1H, H-2), 3.51 – 3.40 (m, 1H, H-7), 3.06 (dt, *J* = 10.5 Hz, *J* = 6.0 Hz, 1H. H-7), 2.52 – 2.42 (m, 2H, H-13), 2.24 – 2.11 (m, 1H, H-5), 2.05 – 1.97 (m, 1H, H-5), 1.94 – 1.80 (m, 2H, H-6), 1.41 (s, 9H, H-10).

^{1}H-NMR: **Minor:** (500 MHz, $CDCl_3$) δ [ppm] = 7.49 – 7.33 (m, 6H, H-16), 7.29 – 7.25 (m, 6H, H-17), 7.22 – 7.17 (m, 3H, H-18), 5.22 (d, *J* = 8.7 Hz, 1H,H-1), 4.44 (dd, $^3J_{H4\text{-}H5}$ = 8.2 Hz, $^3J_{H4\text{-}H5'}$ = 3.2 Hz, 1H, H-4), 4.38 – 4.32 (m, 1H, H-2), 3.64 – 3.52 (m, 1H, H-7), 3.18 – 3.09 (m, 1H, H-7), 2.44 (dd, $^2J_{H13\text{-}H13'}$ = 13.0 Hz, $^2J_{H13\text{-}H2}$ = 6.9 Hz, 2H, H-13), 2.25 – 2.08 (m, 1H, H-5), 2.05 – 1.97 (m, 1H, H-5), 11.94 – 1.84 (m, 2H, H-6), 1.39 (s, 9H, H-9).

^{13}C-NMR: (75 MHz, $CDCl_3$) δ [ppm] = 173.8 (C_q, 1C, C-8), 171.7 (C_q, 1C, C-3), 155.3 (C_q, 1C, C-12), 144.5 (C_q, 3C, C-15), 129.7 (CH_{Ar}, 6C, C-16), 128.1 (CH_{Ar}, 6C, C-17), 127.0 (CH_{Ar}, 3C, C-18), 80.3 (C_q, 1C, C-11), 67.4 (C_q, 1C, C-14), 59.8 (CH, 1C, C-4), 51.7 (CH, 1C, C-2), 47.3 (CH_2, 1C, C-7), 34.0 (CH_2, 1C, C-13), 28.4 (CH_3, 3C, C-10), 27.9 (CH_2, 1C, C-5), 24.8 (CH_2, 1C, C-6).

FT-IR: $\tilde{\nu}$ [cm^{-1}] = 3420 (w, br), 3296 (w, br), 3055 (w), 3011 (w), 2976 (w), 2930 (w), 2884 (w), 1711 (m), 1645 (w), 1618 (w), 1489 (w), 1443 (m), 1393 (w), 1368 (w), 1346 (w), 1319 (w), 1298 (w), 1271 (w), 1246 (w), 1217 (w), 1161 (m), 1034 (w), 1022 (w), 862 (w), 854 (w), 743 (s), 700 (s), 675 (w), 665 (w), 621 (w).

GC-MS: Not detectable.

Synthesis of H_2N-Cys(Acm)-OME hydrochloride

[NIH_P066]

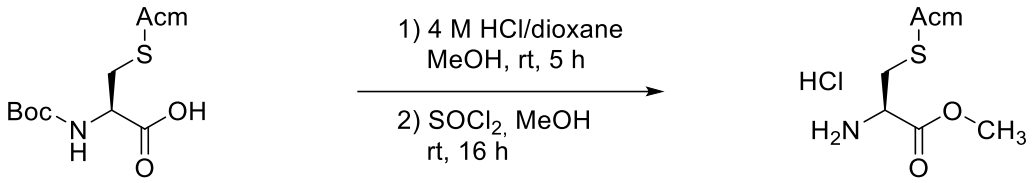

121 **122**

A 4 M Solution of HCl in dioxane (24 mL, 96 mmol, 6.4 eq.) was added to protected cysteine **121** (4.39 g, 15 mmol, 1.0 eq.) and stirred for 3 h at ambient temperature. Due to the bad solubility, additional 4 M HCl in dioxane (6 mL, 24 mmol, 1.6 eq.) and 60 mL MeOH were added. After 2 h full conversion was observed and the reaction mixture was concentrated to dryness. The residue was dissolved in 50 mL MeOH and cooled to 0 °C. Thionyl chloride (3.6 mL, 30 mmol, 2.0 eq.) was slowly added and the reaction was warmed to ambient temperature. After 16 h full conversion was observed and the reaction mixture was dissolved to dryness. The product was purified by column chromatography over silica (10:1, DCM/MeOH). Protected cysteine **122** was obtained as colourless solid in 66% (2.45 g, 10 mmol) yield.

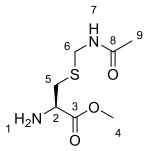

Habitus: Colourless solid.

Yield: 2.45 g (10 mmol, 66%).

M($C_7H_{15}ClN_2O_3S$): 242.72 g·mol^{-1}.

Mp.: 131–133 °C, lit.:[] 130–132 °C.

^{1}H-NMR: (300 MHz, MeOD-d_4) δ [ppm] = 4.49 (d, J = 13.9 Hz, 1H, H-6), 4.40 (dd, J = 8.0, 4.6 Hz, 1H, H-2), 4.28 (d, J = 13.8 Hz, 1H, H-6), 3.87 (s, 3H, H-4), 3.41 – 3.21 (m, 1H, H-5), 3.07 (dd, J = 14.9, 8.0 Hz, 1H, H-5), 2.01 (s, 3H, H-9).

^{13}C-NMR: (75 MHz, MeOD-d_4) δ [ppm] = 53.9 (CH_3, 1C, C-4), 53.7 (CH, 1C, C-2), 41.7 (CH_2, 1C, C-6), 31.8 (CH_2, 1C, C-5), 22.6 (CH_3, 1C, C-9).

C-3 and C-8 were not detected.

FT-IR (ATR): $\tilde{\nu}$ [cm^{-1}] = 3385 (w, br), 3244 (w, br), 2953 (w), 2930 (w), 2855 (w), 2621 (w),1746 (s), 1638 (s), 1530 (s), 1437 (m), 1418 (m), 1373 (m), 1250n (s), 1084 (m), 1005 (w), 934 (w), 708 (w).

LR-ESI-MS: m/z: 207.0 $[M, +H, -Cl]^+$, 229.0 $[M, +Na, -Cl]^+$.

Synthesis of Boc-Phe-Pro-Cys(Acm)-OMe

[NIH_P072, NIH_P140]

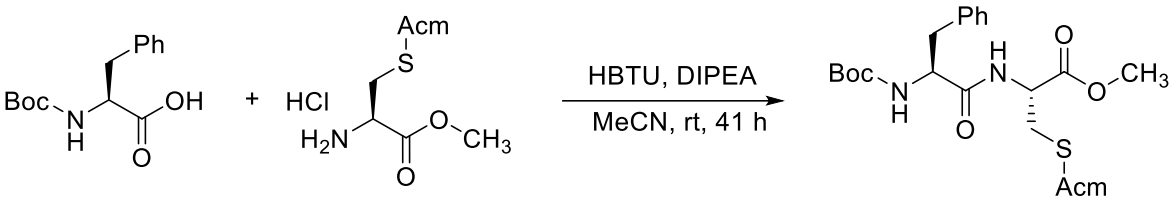

123 **122** **124**

Phenylalanine **123** (1.46 g, 5.5 mmol, 1.1 eq.) was dissolved in 30 mL MeCN and DIPEA (2.70 mL, 15.5 mmol, 3.1 eq.), before HBTU (2.28 g, 6.0 mmol, 1.2 eq.) was added. After stirring for 5 min at ambient temperature, cysteine **122** (1.21 g, 5 mmol, 1.0 eq.) was added and the reaction was stirred over the weekend. Full conversion was obtained after 41 h by TLC. The reaction was concentrated and purified by column chromatography over silica (1:1 to 1:2 to 0:1, *c*Hex/EtOAc). Dipeptide **124** was obtained as a colourless solid in 76% (1.72 g, 3.79 mmol) yield.

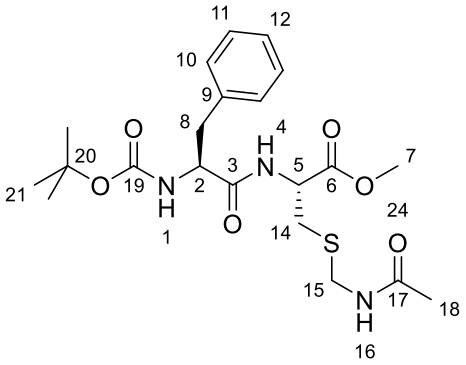

Habitus: Colourless solid.

Yield: 1.72 g (3.79 mmol, 76%).

M($C_{21}H_{31}N_3O_6S$): 453.55 g·mol^{-1}.

Mp.: 100–102 °C, lit.:[] 99–102 °C.

^{1}H-NMR: (500 MHz, $CDCl_3$) δ [ppm] = 7.63 – 7.41 (m, 1H, H-4), 7.31 – 7.25 (m, 2H, H-11), 7.23 (m, 3H, H-10, H-12), 5.45 – 5.28 (m, 1H, H-1), 4.78 (q, *J* = 6.4 Hz, 1H, H_5), 4.46 (q, *J* = 7.3 Hz, 1H, H-2), 4.38 – 4.26 (m, 2H, H-15), 3.79 – 3.67 (m, 3H, H-7), 3.18

(dd, *J* = 13.9, 5.9 Hz, 1H), 3.09 – 2.97 (m, 2H), 2.92 (dd, *J* = 14.6, 6.9 Hz, 1H), 2.05 – 2.00 (m, 3H), 1.43 – 1.34 (m, 9H).

^{13}C-NMR: (75 MHz, $CDCl_3$) δ [ppm] = 172.0 (C_q, 1C, C-3), 170.9 (C_q, 1C, C-17), 170.7 (C_q, 1C, C-6), 155.6 (C_q, 1C, C-19), 136.6 (C_q, 1C, C-9), 129.4 (CH_{Ar}, 2C, C-10), 128.6 (CH_{Ar}, 2C, C-11), 126.9 (CH_{Ar}, 1C, C-12), 80.2 (C_q, 1C, C-20), 55.9 (CH, 1C, C-2), 53.2 (CH, 1C, C-5), 52.8 (CH_3, 1C, C-7), 42.2 (CH_2, 1C, C-15), 38.3, (CH_2, 1C, C-8), 33.4 (CH_2, 1C, C-14), 28.3 (CH_3, 3C, C-21), 23.2 (CH_3, 1C, C-18).

FT-IR (ATR): $\tilde{\nu}$ [cm^{-1}] = 3345 (w), 3250 (w), 3032 (w), 2990 (w, br), 2909 (w, br), 2889 (w), 2803 (w), 2760 (w), 2642 (w), 2588 (w), 1734 (s), 1645 (s), 1537 (s), 1481 (s), 1456 (m), 1429 (s), 1404 (m), 1368 (m), 1356 (m), 1344 (m), 1321 (m), 1310 (s), 1271 (m), 1234 (s), 1221 (s), 1207 (s), 1192 (s), 1159 (m), 1126 (w), 1109 (m), 1086 (m), 1045 (m), 1024 (m), 995 (s), 984 (m), 959 (m), 947 (m), 885 (m), 768 (m), 741 (s), 727 (s), 704 (s), 675 (m), 627 (w), 602 (m)

GC-MS: Not detectable.

Synthesis of H_2N-Phe-Cys(Acm)-OMe

[NIH_P083]

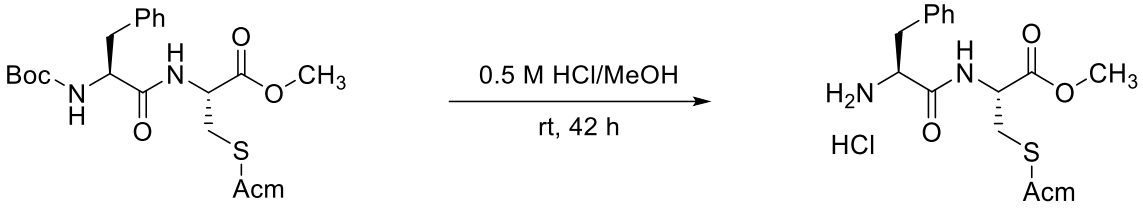

124 **117**

Dipeptide **124** (1.72 g, 3.8 mmol, 1.0 eq.) was dissolved in 0.5 M HCl in MeOH (30 mL, 15 mmol, 4.0 eq.) and stirred at ambient temperature. Full conversion was observed by TLC after 42 h. The solvent was removed under reduced pressure and dipeptide **117** was obtained as a colourless solid in 95 % (1.43 g, 3.6 mmol) yield.

Habitus: Colourless solid.

Yield: 1.43 g (3.6 mmol, 95%).

M($C_{16}H_{24}ClN_3O_4S$): 389.90 g·mol^{-1}.

Mp.: 166–168 °C.

^{1}H-NMR: (500 MHz, MeOD-d_4) δ [ppm] = 7.44 – 7.21 (m, 5H, H-10, H-11, H-12), 4.77 (dd, $^3J_{H5\text{-}H14}$ = 7.7 Hz, $^3J_{H5\text{-}NH}$ = 4.9 Hz, 1H, H-5), 4.46 (d, $^2J_{H15a\text{-}H15b}$ = 13.8 Hz, 1H, H-15a), 4.27 – 4.13 (m, 2H, H-15b), 3.73 (s, 3H, H-7), 3.35 – 3.26 (m, 1H, H-8), 3.13 – 3.03 (m, 2H, H,-8, H-14), 2.94 (dd, $^2J_{H14a\text{-}H14b}$ = 14.3 Hz, $^3J_{H14\text{-}H5}$ = 7.7 Hz, 1H, H-14), 1.99 (s, 3H, H-18).

^{13}C-NMR: (75 MHz, MeOD-d_4) δ [ppm] = 173.6 (C_q, 1C, C-17), 171.7 (C_q, 1C, C-6), 169.7 (C_q, 1C, C-3), 135.5 (C_q, 1C, C-9), 130.6 (CH_{Ar}, 2C, C-10), 130.1 (CH_{Ar}, 2C, C-11), 128.8 (CH_{Ar}, 1C, C-12), 55.6 (CH, 1C, C-2), 54.3 (CH, 1C, C-5), 53.0 (CH_3, 1C, C-7), 42.0 (CH_2, 1C, C-15), 38.5 (CH_2, 1C, C-8), 32.7 (CH_2, 1C, C-14), 22.7 (CH_3, 1C, C-18).

FT-IR (ATR): $\tilde{\nu}$ [cm^{-1}] = 3345 (w), 3250 (w), 3032 (w), 2988 (w), 2957 (w), 2882 (w), 2795 (w), 2691 (w), 1734 (m), 1647 (s), 1597 (w), 1537 (s), 1481 (m), 1456 (w), 1429 (m), 1404 (m), 1368 (m), 1356 (m), 1344 (m), 1310 (m), 1271 (w), 1234 (m), 1221 (m), 1209 (m), 1194 (m), 1159 (m), 1109 (m), 1088 (w), 1026 (m), 995 (m), 984 (w), 947 (m), 885 (w), 864 (w), 829 (w), 768 (m), 743 (m), 727 (m), 704 (s), 675 (m), 602 (m).

LR-ESI-MS: m/z: 354.1 [M, +H, –Cl]$^+$.

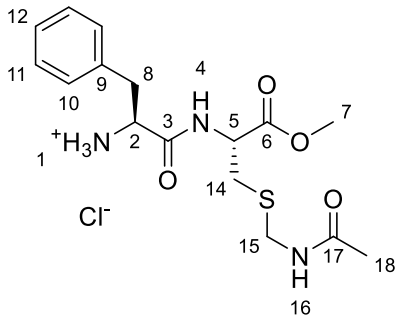

Synthesis of Boc-Cys(trt)-Pro-Phe-Cys(Acm)-OMe

[NIH_P084]

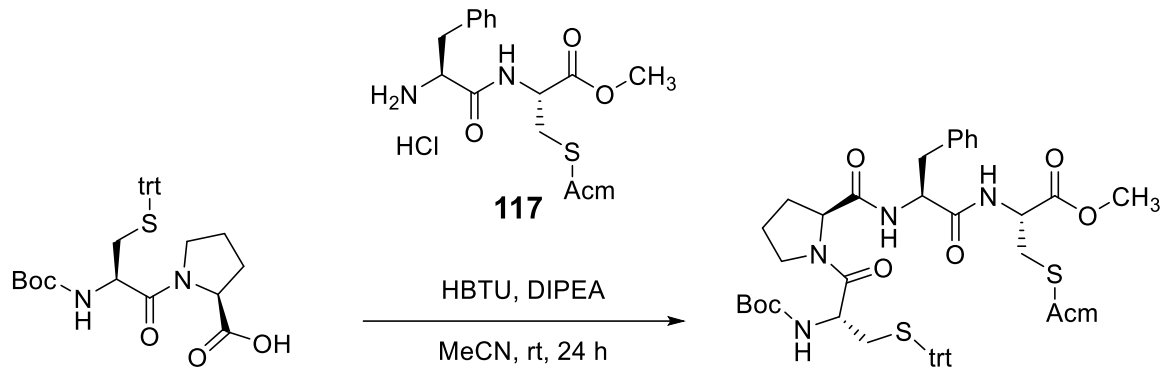

Dipeptide **116** (817 mg, 1.50 mmol, 1.0 eq.) and DIPEA (0.81 mL, 4.65 mmol, 3.1 eq.) were dissolved in 30 mL MeCN. After the addition of HBTU (683 mg, 1.80 mmol, 1.2 eq.), the reaction was stirred for 5 min before dipeptide **117** was added. The reaction was stirred for 24 h and then solvent was removed under reduced pressure. The crude product was purified by column chromatography over silica. The product **115** was obtained as colourless solid in 49 % (650 mg, 0.73 mmol) yield

Habitus: Colourless, glassy solid.

Yield: 650 mg (0.73 mmol, 49 %).

M($C_{48}H_{57}N_5O_8S_2$): 896.13 g·mol^{-1}.

^{1}H-NMR: (500 MHz, DMSO-d_6) δ [ppm] = ^{1}H NMR (500 MHz, DMSO-d_6) δ 8.52 (t, *J* = 6.5 Hz, 1H), 8.41 (d, *J* = 7.8 Hz, 1H), 7.38 – 7.14 (m, 20H, H_{Trt}, H_{Ph}), 4.47 (td, *J* = 8.3, 5.6 Hz, 2H, CH_{Cys}), 4.29 – 4.16 (m, 3H, CH_{Pro}, CH_{Acm}), 4.12 – 4.04 (m, 0.3 H, $H_{Cys,\ minor}$), 4.04 – 3.94 (m, 1H, 0.6 $H_{Cys,\ mayor}$), 3.62 (s, 3H, OMe), 3.31 – 2.28 (m, 8H, $CH_{2,\ Pro}$, $CH_{2,\ Phe}$ 2x$CH_{2,\ Cys}$) 1.85 (s, 3H), 1.91 – 1.53 (m, 4H, 2x$CH_{2,\ Pro}$), 1.37 (s, 3H, $CH_{3,\ Acm}$), 1.36 (s, 6H, $CH_{3,\ Boc}$).

^{13}C-NMR: (75 MHz, DMSO-d_6) δ [ppm] = 170.9, 170.8, 170.6, 169.5, 168.8, 164.6, 155.1, 144.4, 137.4, 129.2(3), 129.1(5), 128.1, 128.0, 126.7, 126.2, 78.2, 66.4, 59.4, 53.5, 52.4, 52.0, 46.3, 40.5, 37.4, 32.6, 31.4, 28.6, 28.2, 24.1, 22.6.

Full assignment was not possible. For all signals a major and a minor isomer could be observed. In the ^{13}C-NMR only the mayor peaks are depicted. The NMR-data agree with the literature[77]

FT-IR (ATR): $\tilde{\nu}$ [cm^{-1}] =3287 (w), 3057 (w), 3022 (w), 2974 (w), 2949 (w), 2934 (w), 2884 (w), 1744 (w), 1636 (s), 1508 (s), 1441 (m), 1410 (m), 1368 (m), 1304 (w), 1248 (m), 1209 (m), 1163 (s), 1084 (w), 1028 (m), 1001 (w), 941 (w), 914 (w), 854 (w), 743 (s), 698 (s), 675 (m), 646 (m), 615 (m).

HRMS (ESI): $^{m}/_{z}$ calcd. for $C_{48}H_{57}N_5O_8S_2$: 896.37211315 $[M+H]^+$;
found: 896.37369.
$^{m}/_{z}$ calcd. for $C_{48}H_{57}N_5O_8S_2$: 918.3540762 $[M+Na]^+$;
found: 918.35467.

7 References

[1] J. M. Berg, J. L. Tymoczko, G. J. Gatto jr., L. Stryer, *Stryer Biochemie,* Vol. 8, *Springer*, **2018**, 1151–1154.

[2] R. G. Matthews, R. Hubbard, P. K. Brown, G. Wald, “Tautomeric Forms of Metarhodopsin”, *J. Gen. Physiol.* **1963**, *47*, 215–240.

[3] H. Bouas-Laurent, H. Dürr, “Organic Photochromism (IUPAC Technical Report)”, *Pure Appl. Chem*. **2001**, 73, 639–665.

[4] J. Fritzsche, “Note sur les carbures d’hydrogène solides, tirés du gaudron de houille”, *C. R. Acad. Sci*. **1867**, *69*, 1035–1037.

[5] Y. Hirshberg, “Photochromy in the bianthrone series”, *C. R. Acad. Sci*. **1950**, *231*, 903–904.

[6] Y. M. Hirshberg, E. Fischer, “Photochromism and reversible multiple internal transitions in some spiropyrans at low temperatures. Part I”, *J. Chem. Soc.* **1954**, 297–303.

[7] R. Heiligman-Rim, Y. Hirshberg, E. Fischer, “Photochromism in Spiropyrans. Part V. On the Mechanism of Phototransformation”, *J. Phys. Chem.* **1962**, *66*, 2470–2477.

[8] S. Kobatake, *Photochromism*. In: Y. Ooyama, S. Yagi, *Progress in the Science of Functional Dyes*. Springer, Singapore, **2021**, 263–265.

[9] S. Helmy, F. A. Leibfarth, S. Oh, J. E. Poelma, C. J. Hawker, J. Read de Alaniz, “Photoswitching Using Visible Light: A New Class of Organic Photochromic Molecules”, *J. Am. Chem. Soc*. **2014**, *136*, 8169−8172.

[10] J. R. Hemmer, S. O. Poelma, N. Treat, Z. A. Page, N. D. Dolinski, Y. J. Diaz, W. Tomlinson, K. D. Clark, J. P. Hooper, C. Hawker, J. Read de Alaniz, “Tunable Visible and Near Infrared Photoswitches”, *J. Am. Chem. Soc*. **2016**, *138*, 13960–13966.

[11] M. Kathan, S. Hecht, “Photoswitchable molecules as key ingredients to drive systems away from the global thermodynamic minimum”, *Chem. Soc. Rev*. **2017**, 46, 5536–5550.

[12] Web of Science search for publications with the Keywords "photochromism", "photochrom" and "photochromic", URL: https://www.webofscience.com (07.05.2024)

[13] W. Yuan, L. Sun, H. Tang, Y. Wen, G. Jiang, W. Huang, L. Jiang, Y. Song, H. Tian, D. Zhu, “A novel thermally stable spironaphthoxazine and its application in rewritable high density optical data storage”, *Adv. Mater.* **2005**, *17*, 156–160.

[14] G. Berkovic, V. Krongauz, V. Weiss, “Spiropyrans and Spirooxazines for Memories and Switches”, *Chem. Rev.* **2000**, *100*, 1741–1754.

[15] S. Kawata, Y. Kawata, “Three-Dimensional Optical Data Storage Using Photochromic Materials”, *Chem. Rev.* **2000**,*100*,1777−1788

[16] A. A. Ali, R. Kharbash, Y. Kim, “Chemo- and biosensing applications of spiropyran and its derivatives - A review”, *Anal. Chim. Acta*. **2020**, *1110*, 199–223.

[17] R. Byrne, D. Diamond, “Chemo/bio-sensor networks”, *Nat. Mater*. **2006**, *5*, 421–424.

[18] J. Andersson, S. Li, P. Lincoln, J. Andréasson “Photoswitched DNA-Binding of a Photochromic Spiropyran”, *J. Am. Chem. Soc.* **2008**, *130*, 11836–11837.

[19] T. Sakata, Y. L. Yan, G. Marriott, “Optical switching of dipolar interactions on proteins”, *Proc. Natl. Acad. Sci. U. S. A*. **2005**, *102*, 4759–4764.

[20] Georgina K. Such, Richard A. Evans, and Thomas P. Davis, “Rapid Photochromic Switching in a Rigid Polymer Matrix Using Living Radical Polymerization”, Macromolecules 2006, 39, 4, 1391–1396.

[21] D. Kitagawa, S. Kobatake “Photoreversible current ON/OFF switching by the photoinduced bending of gold-coated diarylethene crystals.”, *Chem Commun,* **2015***,* *51*, 4421–4424.

[22] R. Klajn, “Spiropyran-based dynamic materials”, *Chem. Soc. Rev*. **2014**, *43*, 148–184.

[23] L. Kortekaas, W. R. Browne," The evolution of spiropyran: fundamentals and progress of an extraordinarily versatile photochrome", *Chem. Soc. Rev.* **2019**, *48*, 3406–3424.

[24] H. M. D. Bandara, S. C. Burdette, "Photoisomerization in different classes of azobenzene", *Chem. Soc. Rev.* **2012**, *41*, 1809–1825.

[25] S. Aiken, R. J. L. Edgar, C. D. Gabbutt, B. M. Heron, P. A. Hobson, "Negatively photochromic organic compounds: Exploring the dark side", *Dyes and Pigments*, **2018**, *149*, 92–121

[26] K. Matsuda, M. Irie, "Diarylethene as a photoswitching unit", *J. Photochem. Photobiol. C* **2004**, *5*, 169–182.

[27] S. Swansburg, E. Buncel, R. P. Lemieux, "Thermal Racemization of Substituted Indolinobenzospiropyrans:Evidence of Competing Polar and Nonpolar Mechanisms", *J. Am. Chem. Soc*. **2000**, *122*, 6594–6600.

[28] S. Chen, F. Jiang, Z. Cao, G. Wang, Z.-M. Dang, "Photo, pH, and thermo triple-responsive spiropyran-based copolymer nanoparticles for controlled release", *Chem. Commun*. **2015**, *51*, 12633–12636.

[29] S. Wan, Y. Zheng, J. Shen, W. Yang, M. Yin, ""On−off−on" Switchable Sensor: A Fluorescent Spiropyran Responds to Extreme pH Conditions and Its Bioimaging Applications", *Appl. Mater. Interfaces* **2014**, *6*, 19515−19519.

[30] J. T. C. Wojtyk, A. Wasey, N.-N. Xiao, P. M. Kazmaier, S. Hoz, C. Yu, R. P. Lemieux, E. Buncel, "Elucidating the Mechanisms of Acidochromic Spiropyran-Merocyanine Interconversion", *J. Phys. Chem. A* **2007**, *111*, 2511–2516.

[31] F. M. Raymo, S. Giordani, "Signal Processing at the Molecular Level", *J. Am. Chem. Soc*. **2001**, *123*, 4651–4652.

[32] K. Wagner, R. Byrne, M. Zanoni, S. Gambhir, L. Dennany, R. Breukers, M. Higgins, P. Wagner, D. Diamond, G. G. Wallace, D. L. Officer, "A Multiswitchable Poly(terthiophene) Bearing a Spiropyran Functionality: Understanding Photo- and Electrochemical Control", *J. Am. Chem. Soc.* **2011**, *133*, 5453–5462.

[33] D. A. Davis, A. Hamilton, J. L. Yang, L. D. Cremar, D. Van Gough, S. L. Potisek, M. T. Ong, P. V. Braun, T. J. Martinez, S. R. White, J. S. Moore N. R. Sottos, “Force-induced activation of covalent bonds in mechanoresponsive polymeric materials”, *Nature* **2009**, *459*, 68–72.

[34] D.Y. Hur, E.J. Shin, “A fluorescent chemosensor for Al_3^+, HSO_3^-, and CN^- based on a dyad bearing rhodamine and spiropyran units”, *Bull. Kor. Chem. Soc*. **2015**, *36*, 2027–2033.

[35] J.Q. Ren, H. Tian, “Thermally stable merocyanine form of photochromic spiropyran with aluminum ion as a reversible photo-driven sensor in aqueous Solution”, *Sensors* **2007**, *7*, 3166–3178.

[36] A. K. Bohaty, M. R. Newton and I. Zharov, “Light-controlled ion transport through spiropyran-modified nanoporous silica colloidal films”, *J. Porous Mater*. **2010**, *17*, 465–473.

[37] D. G. Weston, J. Kirkham and D. C. Cullen, “Photo-modulation of horseradish peroxidase activity via covalent attachment of carboxylated-spiropyran dyes”, *Biochim. Biophys. Acta* **1999**, *1428*, 463–467.

[38] F. Ciardelli, D. Fabbri, O. Pieroni and A. Fissi, “Photomodulation of Polypeptide Conformation by Sunlight in Spiropyran-Containing Poly(L-glutamic acid)”, *J. Am. Chem. Soc.* **1989**, *111*, 3470–3472.

[39] O. Brügner, T. Reichenbach, M. Sommer, M. Walter, „Substituent Correlations Characterized by Hammett Constants in the Spiropyran–Merocyanine Transition“, *J. Phys. Chem. A* **2017**, *121*, 2683–2687.

[40] L. Wimberger, S. K. K. Prasad, M. D. Peeks, J. Andréasson, T. W. Schmidt, J. E. Beves, “Large, Tunable, and Reversible pH Changes by Merocyanine Photoacids”, *J. Am. Chem. Soc*. **2021**, *143*, 20758−20768.

[41] C. Berton, D. M. Busiello, S. Zamuner, E. Solari, R. Scopelliti, F. Fadaei-Tirani, K. Severin, C. Pezzato, “Thermodynamics and kinetics of protonated merocyanine photoacids in water”, *Chem. Sci*. **2020**, *11*, 8457−8468.

[42] C. Hansch, A. Leo, R. W. Taft, “A Survey of Hammett Substituent Constants and Resonance and Field Parameters”, *Chem. Rev.* **1991**, *91*, 165–195.

[43] E. Berman, R. E. Fox, F. D. Thomson, “Photochromic Spiropyrans. I. The Effect of Substituents on the Rate of Ring Closure”, *J. Am. Chem. Soc*. **1959**, *21*, 5605–5608.

[44] R. W. Taft, “*Steric Effects in Organic Chemistry*”, ed. M. S. Newman, Wiley, New York, **1956**, chapter 13.

[45] N. L. Zaichenko, V. S. Marevtsev, V. D. Arsenov, M. I. Cherkashin, “Correlation Equation for the Activation free Energy of the Inversion of Configuration in the Closed Form of Indolinspiropyrans”, *Russ. Chem. Bull.* **1987**, *36*, 1518–1520.

[46] E. I. Balmond, B. K. Tautges, A. L. Faulkner, V. W. Or, B. M. Hodur, J. T. Shaw, A. Y. Louie, “Comparative Evaluation of Substituent Effect on the Photochromic Properties of Spiropyrans and Spirooxazines”, *J. Org. Chem*. **2016**, *81*, 8744−8758.

[47] K. A. Palasis, A. D. Abell, “Effect of indoline substitution on ring opening in 6-nitro BIPS spiropyran derivatives”, *Tetrahedron Lett.* **2024**, *138*, 154967

[48] A. V. Metelitsa, A. V. Chernyshev, N. A. Voloshin, E. V. Solov'eva, Y. S. Reutova, I. A. Rostovtseva, I. V. Dorogan, “Molecular platform for barochromic and dual-state photochromic compounds”, *Dyes and Pigments* **2024**, *228*, 112200.

[49] L. Eggers, V. Buss, “A Spiroindolinopyran with Switchable Optical Activity”, *Angew. Chem. Int. Ed.* **1997**, *36*, 881–883.

[50] A. Abdullah, T. G. Nevell, P. G. Sammes, C. J. Roxburgh, “Unusual thermo(photo)chromic properties of some mononitro- and dinitro- substituted 3’-alkyl indolospirobenzopyrans”, *Dyes and Pigments* **2015**, 121, 57–72.

[51] W. Tian, J. Tian, “An insight into the solvent effect on photo-, solvato-chromism of spiropyran through the perspective of intermolecular interactions”, *Dyes and Pigments* **2014**, *105*, 66–74.

[52] Y. Shiraishi, K. Yomo, T. Hirai, “Polarity-Driven Isomerization of a Hydroxynaphthalimide-Containing Spiropyran at Room Temperature”, *ACS Phys. Chem Au* **2023**, *3*, 290–298.

[53] H. Görner, “Photochromism of nitrospiropyrans: effects of structure, solvent and temperature”, *Phys. Chem. Chem. Phys*. **2001**, *3*, 416–423.

[54] K. Namba and S. Suzuki, “Photo-Control of Activity with a Photochromic Spiropyran Compound –Modicication of α-Amylase with Spiropyran Compound–”, *Chem. Lett.* **1975**, *9*, 947–950.

[55] M. Aizawa, K. Namba and S. Suzuki, “Photo Control of Enzyme Activity of *α*-Amylase” *Arch. Biochem. Biophys.* **1977**, *180*, 41–48.

[56] M. Aizawa, K. Namba and S. Suzuki, “Light-Induced Enzyme Activity Achanges associated with the Photoisomerisation of Bound Spiropyran”, *Arch. Biochem. Biophys.* **1977**, *182*, 305–310.

[57] I. Karube, S. Suzuki, Y. Nakamoto, M. Nishida, “Photocontrol of Trypsin Inhibition”, *J. Mol. Catal*, **1979**, *6*, 51–56.

[58] F. Ciardelli, D. Fabbri, O. Pieroni and A. Fissi, “Photomodulation of polypeptide conformation by sunlight in spiropyran-containing poly(L-glutamic acid)”, *J. Am. Chem. Soc.* **1989**, *111*, 3470–3472.

[59] A. Hrebonkin, S. Afonin, A. Nikitjuka, O. V. Borysov, G. Leitis, O. Babii, S. Koniev, T. Lorig, S. L. Grage, P. Nick, A. S. Ulrich, A. Jirgensons, I. V. Komarov, “Spiropyran-Based Photoisomerizable α-Amino Acid for Membrane-Active Peptide Modification”, *Chem. Eur. J*. **2024**, *30*, e202400066.

[60] I. Karube, S. Suzuki, Y. Nakamoto, M. Nishida, “Photocontrol of trypsin inhibition with immobilized inhibitor”, *Biotechnol. Bioeng*. **1977**, *19*, 1549–1552.

[61] T. Hirakura, Y. Nomura, Y. Aoyama, K. Akiyoshi, “Photoresponsive Nanogels Formed by the Self-Assembly of Spiropyrane-Bearing Pullulan That Act as Artificial Molecular Chaperones”, *Biomacromolecules* **2004**, *5*, 1804–1809.

[62] J Andersson, S. Li, P. Lincoln, J. Andéasson, “Photoswitched DNA-Binding of a Photochromic Spiropyran”, *J. Am. Chem. Soc. **2008***, *130*, 11836–11837.

[63] Z. Wu, J. Liu, X. Zhou, X. Zhang, J. Zhao, L. Jiang, C. Xie, Y. Liu, L. Zhang, “Molecular design of a solvent-free spiropyran-containing DNA material with

triple external stimuli-responsive behavior", *Dyes and Pigments* **2024**, *225*, 112092.

[64] S. S. Zimmerman, H. A. Scheraga, "Stability of *Cis*, *Trans*, and Nonplanar Peptide Groups", *Macromolecules* **1976**, *9*, 408–416.

[65] W. J. Wedemeyer, E. Welker, H. A. Scheraga, "Proline *Cis*-*Trans* Isomerization and Protein Folding", *Biochemistry* **2002**, *41*, 14637–14644.

[66] U. Reimer, G. Scherer, M. Drewello, S. Kruber, M. Schutkowski, G. Fischer, "Side-chain Effects on Peptidyl-prolyl *cis*/*trans* Isomerisation", *J. Mol. Biol*. **1998**, *279*, 449–460.

[67] W.-J. Wu, D. R. Raleigh, "Local Control of Peptide Conformation: Stabilization of *cis* Proline Peptide Bonds by Aromatic Proline Interactions", *Biopolymers* **1998**, *45*, 381–394.

[69] J. Egli, T. Schnitzer, J. C. B. Dietschreit, C. Ochsenfeld, H. Wennemers, "Why Proline? Influence of Ring-Size on the Collagen Triple Helix", *Org. Lett.* **2020**, *22*, 348−351.

[70] S. J. M. Verhoork, P. M. Killoran, C. R. Coxon, "Fluorinated Prolines as Conformational Tools and Reporters for Peptide and Protein Chemistry", *Biochemistry* **2018**, *57*, 6132−6143.

[71] A. K. Pandey, D. Naduthambi, K. M. Thomas, N. J. Zondlo, "Proline Editing: A General and Practical Approach to the Synthesis of Functionally and Structurally Diverse Peptides. Analysis of Steric versus Stereoelectronic Effects of 4-Substituted Prolines on Conformation within Peptides", *J. Am. Chem. Soc*. **2013**, *135*, 4333−4363.

[72] H. K. Ganguly, G. Basu, "Conformational landscape of substituted prolines", *Biophys. Rev.* **2020**, *12*, 25–39.

[73] S. C. R. Lummis, D. L. Beene, L. W. Lee, H. A. Lester, R. W. Broadhurst, D. A. Dougherty, "Cis–trans isomerization at a proline opens the pore of a neurotransmitter-gated ion channel", *Nature* **2005**, *438*, 248–252.

[74] C. Siebler, B. Maryasin, M. Kuemin, R. S. Erdmann, C. Rigling, C. Grünenfelder, C. Ochsenfeld, H. Wennemers, "Importance of dipole moments

and ambient polarity for the conformation of Xaa–Pro moieties – a combined experimental and theoretical study", *Chem. Sci*. **2015**, *6*, 6725–6730.

[75] G. Ivanova, B. Yakimova, S. Angelova, I. Stoineva, V. Enchev, "Influence of pH on the cis–trans isomerization of Valine-Proline dipeptide: An integrated NMR and theoretical investigation", *J. Mol. Struct*. **2010**, *975*, 330–334.

[76] A. Bröhl, B. Albrecht, Y. Zhang, E. Maginn, R. Giernoth, "Influence of Hofmeister Ions on the Structure of Proline-Based Peptide Models: A Combined Experimental and Molecular Modeling Study", *J. Phys. Chem. B* **2017**, *121*, 2062–2072.

[77] M. Bursch, J.-M. Mewes, A. Hansen, S. Grimme, "Best-Practice DFT Protocols for Basic Molecular Computational Chemistry", *Angew. Chem. Int. Ed*. **2022**, *61*, e202205735.

[78] R. A. Kendall, T. H. Dunning, Jr., R. J. Harrison, "Electron affinities of the first-row atoms revisited. Systematic basis sets and wave functions", *J. Chem. Phys*. **1992**, *96*, 6796–6806.

[79] D. E. Woon, T. H. Dunning, Jr., "Gaussian basis sets for use in correlated molecular calculations. IV. Calculation of static electrical response properties", *J. Chem. Phys.* **1994**, *100*, 2975–2988.

[80] B. P. Prascher, D. E. Woon, K. A. Peterson, T. H. Dunning, A. K. Wilson, "Gaussian basis sets for use in correlated molecular calculations. VII. Valence, core-valence, and scalar relativistic basis sets for Li, Be, Na, and Mg", *Theor. Chem. Acc*. **2011**, *128*, 69–82.

[81] D. E. Woon, T. H. Dunning, Jr., "Gaussian basis sets for use in correlated molecular calculations. III. The atoms aluminum through argon", *J. Chem. Phys*. **1993**, *98*, 1358–1371.

[82] N. B. Balabanov, K. A. Peterson, "Systematically convergent basis sets for transition metals. I. All-electron correlation consistent basis sets for the 3d elements Sc–Zn", *J. Chem. Phys*. **2005**, *123*, 064107.

[83] N. B. Balabanov, K. A. Peterson, "Basis set limit electronic excitation energies, ionization potentials, and electron affinities for the 3d transition metal atoms: Coupled cluster and multireference methods", *J. Chem. Phys*., **2006**, *125*, 074110.

[84] A. K. Wilson, D. E. Woon, K. A. Peterson, T. H. Dunning, “Gaussian basis sets for use in correlated molecular calculations. IX. The atoms gallium through krypton”, *J. Chem. Phys.* **1999**, *110*, 7667–7676.

[85] K. A. Peterson, C. Puzzarini, “Systematically convergent basis sets for transition metals. II. Pseudopotential-based correlation consistent basis sets for the group 11 (Cu, Ag, Au) and 12 (Zn, Cd, Hg) elements”, *Theor. Chem. Acc*. **2005**, *114*, 283–296.

[86] F. Weigend, “Accurate Coulomb-fitting basis sets for H to Rn”, *Phys. Chem. Chem. Phys*. **2006**, *8*, 1057–1065.

[87] F. Weigend, R. Ahlrichs, ”Balanced basis sets of split valence, triple zeta valence and quadruple zeta valence quality for H to Rn: Design and assessment of accuracy”, *Phys. Chem. Chem. Phys*. **2005**, *7*, 3297–3305.

[88] D. Rappoport, F. Furche, “Property-optimized Gaussian basis sets for molecular response calculations”, *J. Chem. Phys*. **2010**, *133*, 134105.

[89] P. G. Jambrina, J. Aldegunde, ”Chapter 20 – Computational Tools for the Study of Biomolecules”, *Comput. Aided Chem. Eng*. **2016**, *39*, 583–648.

[90] C. Kolano, K. Gomann, W. Sander, “Small Cyclic Disulfide Peptides: Synthesis in Preparative Amounts and Characterization by Means of NMR and FT-IR Spectroscopy*”, Eur. J. Org. Chem*. **2004**, *20*,4167–4176.

[91] C. Kolano, J. Helbing, G. Bucher, W. Sander, P. Hamm, “Intramolecular Disulfide Bridges as a Phototrigger To Monitor the Dynamics of Small Cyclic Peptides”, *J. Phys. Chem. B* **2007**, *111*, 11297–11302.

[92] F. Li, K. Bravo-Rodriguez, C. Phillips, R. W. Seidel, F. Wieberneit, R. Stoll, N. L. Doltsinis, E. Sanchez-Garcia, W. Sander, “Conformation and Dynamics of a Cyclic Disulfide-Bridged Peptide: Effects of Temperature and Solvent”, *J. Phys. Chem. B* **2013**, *117*, 3560−3570.

[93] F. Neese, “The ORCA program system”, *Wiley Interdiscip. Rev. Comput. Mol. Sci*. **2012**, *1*, 73–78.

[94] J. C. Zapata, L. K. McKemmish, “Computation of Dipole Moments: A Recommendation on the Choice of the Basis Set and the Level of Theory”, *J. Phys. Chem. A* **2020**, *124*, 7538–7548.

[95] J. -D. Chai, M. Head-Gordon, “Systematic optimization of long-range corrected hybrid density functionals”, *J. Chem. Phys*. **2008**, *128*, 084106.

[96] N. Mardirossian, M. Head-Gordon, “ωB97X-V: A 10-parameter, range-separated hybrid, generalized gradient approximation density functional with nonlocal correlation, designed by a survival-of-the-fittest strategy”, *Phys. Chem. Chem. Phys*. **2014**, *16*, 9904–9924.

[97] O. A. Vydrov, T. Van Voorhis, “Nonlocal van der Waals density functional: The simpler the better”, *J. Chem. Phys*. **2010**, *133*, 244103.

[98] W. Hujo, S. Grimme, “Performance of the van der Waals Density Functional VV10 and (hybrid) GGA Variants for Thermochemistry and Noncovalent Interactions”, *J. Chem. Theory Comput.,* **2011**, *7*, 3866–3871.

[99] A. D Becke, “A new mixing of Hartree–Fock and local density-functional theories”, *J. Chem. Phys.* **1993**, *98*, 1372−1377.

[100] P. J. Stephens, F. J. Devlin, C. F. Chabalowski, M. J. Frisch, “Ab Initio Calculation of Vibrational Absorption and Circular Dichroism Spectra Using Density Functional Force Fields”, *J. Phys. Chem.* **1994**, *98*, 11623−11627.

[101] Grimme, J. Antony, S. Ehrlich, H. Krieg, “A consistent and accurate ab initio parametrization of density functional dispersion correction (DFT-D) for the 94 elements H-Pu”, *J. Chem. Phys.* **2010**, *132*, 154104.

[102] S. Grimme, S. Ehrlich, L. Goerigk, “Effect of the damping function in dispersion corrected density functional theory”, *J. Comput. Chem*. **2011**, *32*, 1456–1465.

[103] N. Mardirossian, M. Head-Gordon, “Mapping the genome of meta-generalized gradient approximation density functionals: The search for B97M-V”, *J. Chem. Phys*. **2015**, *142*, 074111.

[104] Y. Zhao, D. G.; Truhlar, “A new local density functional for main-group thermochemistry, transition metal bonding, thermochemical kinetics, and noncovalent interactions”, *J. Chem. Phys.* **2006**, *125*, 194101.

[105] N. Mardirossian, M. Head-Gordon, “How Accurate Are the Minnesota Density Functionals for Noncovalent Interactions, Isomerization Energies, Thermochemistry, and Barrier Heights Involving Molecules Composed of Main-Group Elements?”, *J. Chem. Theory Comput.* **2016**, *12*, 4303–4325.

[106] Y. Zhao, D. G.; Truhlar, “The M06 suite of density functionals for main group thermochemistry, thermochemical kinetics, noncovalent interactions, excited states, and transition elements: two new functionals and systematic testing of

four M06-class functionals and 12 other functional", *Theor. Chem. Acc*. **2008**,*120*, 215–241.

[107] D. Nurok, R. M. Kleyle, P. Hajdu, B. Ellsworth, S. S. Myers, T. M. Brogan, Kenneth B. Lipkowitz, R. C. Glen, "Solvent-dependent regression equations for the prediction of retention in planar chromatography", *Anal. Chem*. **1995**, *67*, 4423–4430.

[108] D R. J. W. Le Fèvre, D. A. A. S. Narayana Rao, "The Dipole Moments of Bromobenzene, Methyl Iodide, and Iodobenzene as Vapours", *Aust. J. Chem.* **1955**, *8*, 140–142.

[109] L. G. Groves, S. Sugden, "221. The dipole moments of vapours. Part II", *J. Chem. Soc.* **1935**, 971–974.

[110] B. M. Ginzburg, Sh. Tuichiev, "Influence of the molecular structure on the phase transition temperatures of mononuclear aromatic compounds", *Russ. J. Appl. Chem.* **2009**, *82*, 1178–1187.

[111] S. V. Fedorov, I. G. Krivoruchka, A. M. Shulunova, L. V. Sherstyannikova, O. M. Trofimova, A. I. Vokin & V. K. Turchaninov, "Solvatochromism of Heteroaromatic Compounds: XXV. Effect of Bifurcate Hydrogen Bond with a Weak Intramolecular Component on the IR, NMR, and UV Spectra of 2,6-Dibromo-4-nitrophenol", *Russ. J. Gen. Chem.* **2005**, *75*, 100–110.

[112] K. Aparajithan, V. Baliah, "Detection of chelation by means of spectral and dipole moment measurments", *J. Indian Chem. Soc*. **1959**, *36*, 159–160.

[113] M. Levitus, G. Glasser, D. Neher, P. F. Aramendía, "Direct measurement of the dipole moment of a metastable merocyanine by electromechanical interferometry", *Chem. Phys. Lett*. **1997**, *277*, 118–124.

[114] D. Lapienis-Grochowska, M. Kryszewski, B. Nadolski, "Electronic structure of merocyanine form of indolinespirobenzopyrans determined by electronic spectroscopy and dielectric measurements", *J. Chem. Soc., Faraday Trans. 2*, **1979**, *75*, 312–316.

[115]: Y. Zhang, M. Cao, B. Yuan, T. Guo, W. Zhang, "RAFT synthesis and micellization of a photo-, temperature- and pH-responsive diblock copolymer based on spiropyran", *Polym. Chem.* **2017**, *8*, 7325–7332.

[116]: A. R. Tyler, A. Okoh Okoh, C. L. Lawrence, V. C. Jones, C Moffatt, R. B. Smith "*N*-Alkylated 2,3,3-trimethylindolenines and 2-methylbenzothiazoles. Potential

lead compounds in the fight against *Saccharomyces cerevisiae* infections", *Eur. J. Med. Chem.* **2013**, *64,* 222–227.

[117] D. E. Lynch, A. N. Kirkham, M. Z. H. Chowdhury, E. S. Wane, J. Heptinstall, "Water soluble squaraine dyes for use as colorimetric stains in gel electrophoresis", *Dyes and Pigments*, **2012**, *3*, 393–402.

[118]: W. Zhang, F. Huo, C. Yin, „Photocontrolled Single-/Dual-Site Alternative Fluorescence Probes Distinguishing Detection of H_2S/SO_2 in Vivo", *Org. Lett.* **2019**, *21*, 5277–5280.

[119]: J. Liu, W. Tang, L. Sheng, Z. Du, T. Zhang, X. Su, S. X. Zhang, „Effects of Substituents on Metastable-State Photoacids: Design, Synthesis, and Evaluation of their Photochemical Properties", *Chem. Asian J*. **2019**, *14*, 438–445.

[120] C. J. Roxburgh, P. G. Sammes, A. Abdullah, "Steric and substituent effects on the photoreversibility of novel indolospirobenzopyrans: Acid deuterolysis, UV and ^{1}H NMR spectroscopy", *Dyes and Pigments*, **2009**, *82,* 226–237.

[121] H. Gao, G. Liu, C. Cui, M. Wang, J. Gao, "Preparation and properties of a polyurethane film based on novel photochromic spirooxazine chain extension", *New J. Chem*. **2022**, *46*, 9128–9137.

[122] O. Demeter, A. Kormos, C. Koehler, G. Mező, K. Németh, E. Kozma, L. B. Takács, E. A. Lemke, P. Kele, "Bisazide Cyanine Dyes as Fluorogenic Probes for Bis-Cyclooctynylated Peptide Tags and as Fluorogenic Cross-Linkers of Cyclooctynylated Proteins", *Bioconjugate Chem*. **2017**, *28*, 1552–1559.

[123] M. Y. Berezin, K. Guo, B. Teng, W. B. Edwards, C. J. Anderson, O. Vasalatiy, A. Gandjbakhche, G. L. Griffiths, S. Achilefu, "Radioactivity-Synchronized Fluorescence Enhancement Using a Radionuclide Fluorescence-Quenched Dye", *J. Am. Chem. Soc*. **2009**, *131*, 9198–9200.

[124] H. Mansilla, M. M. Afonso, "Iron (III) Tosylate in the Preparation of Dimethyl and Diethyl Acetals from Ketones and β-Keto Enol Ethers from Cyclic β-Diketones" *Synth. Commun*., **2008**, *38*, 2607–2618.

[125] J. Ehrler, D. Seebach, "Enantioselektive Verseifungen substituierter, achiraler 3-Acyloxy-propylester mit Lipasen: Herstellung chiraler Derivate von ,,Tris(hydroxymethyl)methan"", *Justus Liebigs Ann. Chem.* **1990**, *4*, 379–388.

[126] K. Kubota, S. Osaki, M. Jin, H. Ito, "Copper(I)-Catalyzed Enantioselective Nucleophilic Borylation of Aliphatic Ketones: Synthesis of Enantioenriched

Chiral Tertiary α-Hydroxyboronates", *Angew. Chem. Int. Ed*. **2017**, *56*, 6646–6650.

[127] Y. Shiraishi, M. Itoh, T. Hirai, "Thermal isomerization of spiropyran to merocyanine in aqueous media and its application to colorimetric temperature indication", *Phys. Chem. Chem. Phys.* **2010**, *12*, 13737–13745.

[128] M. Eigen, "Methods for investigation of ionic reactions in aqueous solutions with half-times as short as 10–9 sec. Application to neutralization and hydrolysis reactions", *Discuss. Faraday Soc.* **1954**, *17*, 194–205.

[129] M. S.Vogt **2023**, "Untersuchungen zur Photochromoe substituierter Spiropyrane", Bachelor Thesis, University of Cologne, Institute of Organic Chemistry, Supervisor Prof. Dr. R. Giernoth.

[130] J. J. Pastuszak, A. Chimiak, "*tert*-Butyl group as thiol protection in peptide synthesis", *J. Org. Chem*. **1981**, *46*, 1868–1873.

[131] Y. Jia, X. Don, P. Zhou, X. Liu, L. Pan, H. Xin, Y Z. Zhu, Y. Wang, "The synthesis and biological evaluation of novel Danshensu–cysteine analog conjugates as cardiovascular-protective agents", *Eur. J. Med. Chem*, **2012**, *55*, 176–187.

[132] P. M. Killoran, G. S. M. Hanson, S. J. M. Verhoork, M. Smith, D. Del Gobbo, L.-Y. Lian, C. R. Coxon; "Probing Peptidylprolyl Bond cis/trans Status Using Distal ^{19}F NMR Reporters", *Chem. Eur. J*. **2023**, *29*, e202203017.

[133] Y. Yadav, A. Levitz, S. Dharma, R. Aneja, M. Henary, "Effects of heterocyclic *N*-alkyl chain length on cancer cell uptake of near infrared heptamethine cyanine dyes", *Dyes Pigm.* **2017**, *145*, 307–314.

[134] V. M. Breslin, M. A. Garcia-Garibay, "Transmission Spectroscopy and Kinetics in Crystalline Solids Using Aqueous Nanocrystalline Suspensions: The Spiropyran-Merocyanine Photochromic System", *Cryst. Growth Des.* **2017**, *17*, 637–642.

[135] P. Tannouri, K. M. Arafeh, J. M. Krahn, S. L. Beaupré, C. Menon, N. R. Branda, "A Photoresponsive Biomimetic Dry Adhesive Based on Doped PDMS Microstructures", *Chem. Mater*. **2014**, *15*, 4330–4333.

[135] E. A. Owens, H. Hyun, T. L. Dost, J. H. Lee, G. L. Park, D. H. Pham, M. H. Park, H. S. Choi, M. Henary, “Near-Infrared Illumination of Native Tissues for Image-GuidedSurgery”, *J. Med. Chem*. **2016**, *11*, 5311–5323.

[136] H. Wang, W.-R. Li, X.-F. Guo, H.-S. Zhang, “Spectrophotometric determination of total protein in serum using a novel near-infrared cyanine dye, 5,5′-dicarboxy-1, 1′-disulfobutyl-3,3,3′,3′-tetramethylindotricarbocyanine“, *Anal. Bioanal. Chem.* **2007**, 387, 2857–2862.

[137] M. Tomasulo, S. L. Kaanumal, S. Sortino, F. M. Raymo, “Synthesis and Properties of Benzophenone−Spiropyran and Naphthalene−Spiropyran Conjugates”, *J. Org. Chem.* **2007**, 2, 595−605.

[138] J. Cusido, S. S. Ragab, E. R. Thapaliya, S. Swaminathan, J. Garcia-Amorós, M. J. Roberti, B. Araoz, M. M. A. Mazza, S. Yamazaki, A. M. Scott, F. M. Raymo, M. L. Bossi, “A Photochromic Bioconjugate with Photoactivatable Fluorescence for Superresolution Imaging”, *J. Phys. Chem. C* **2016**, *23*, 12860–12870.

[139] O. Ivashenko, J. T. van Herpt, P. Rudolf, B. L. Feringaab, W. R. Browne, “Oxidative electrochemical aryl C–C coupling of spiropyrans”, *Chem. Commun.* **2013**, 49, 6737–6739.

[140] H. Li, Z.-J. Luan, G.-W. Zheng, J.-H Xu, “Efficient Synthesis of Chiral Indolines using an Imine Reductasefrom Paenibacillus lactis”, *Adv. Synth. Catal.* **2015**, 357, 1692–1696

[141] M. Schulz-Senft, P. J. Gates, F. D. Sönnichsen, A. Staubitz, “Diversely halogenated spiropyrans - Useful synthetic building blocks for a versatile class of molecular switches“, *Dyes and Pigments* **2017**, 136, 292–301.

[142] M. V. Kvach, A. V. Ustinov, I. A. Stepanova, A. D. Malakhov, M. V. Skorobogatyi, V. V. Shmanai, V. A. Korshun, “A Convenient Synthesis of Cyanine Dyes: Reagents for the Labeling of Biomolecules”, *Eur. J. Org. Chem.* **2008**, 2107–2117.

[143] M. Schmidt, J. Ungvaria, J. Glöde, B. Dobner, A. Langner, “New 1,3-dioxolane and 1,3-dioxane derivatives as effective modulators to overcome multidrug resistance“, *Bioorg. Med. Chem.* **2007**,*15* , 2283–2297.

[144] L. R. Mills, C. Zhou, E. Fung, S. A. L. Rousseaux," Ni-Catalyzed β-Alkylation of Cyclopropanol-Derived Homoenolates", *Org. Lett*. **2019**, *21*, 8805–8809.

[145] A. P. Silvestri, J. S. Oakdale, "Intermolecular cyclotrimerization of haloketoalkynes and internal alkynes: facile access to arenes and phthalides", *Chem. Commun*. **2020**, *56*, 13417–13420.

[146] D. Knez, N. Colettis, L. G. Iacovino, M. Sova, A. Pislar, J. Konc, S. Lesnik, J. Higgs, F. Kamecki, I. Mangialavori, A. Dolsak, S. Zakelj, J. Trontelj, J. Kos, C. Binda, M. Marder, S. Gobec, "Stereoselective Activity of 1-Propargyl-4-styrylpiperidine-like Analogues That Can Discriminate between Monoamine Oxidase Isoforms A and B", *J. Med. Chem*., **2020**, *63*, 1361–1387.

8 Appendix

8.1 Abbreviations

°C	degree celsius
A	absorption
abs.	absolute
Ac	acetyl
Acm	acetamidomethyl
ATR	attenuated total reflectance
a.u.	arbitrary unit
Boc	*tert*-butyloxycarbonyl
Bz	benzyl
conc.	concentration
cHex	cyclohexane
Cys	cysteine
d	day
D	debye
DCM	dichlormethane
DFT	density functional theory
DIPEA	*N,N*-diisopropylethylamine
DMF	dimethylformamide
DMSO	dimethyl sulfoxide
DNA	deoxyribonucleic acid
E	energy
eq.	equivalents
et al.	and others
ESI	electron spray ionisation
Fmoc	fluorenylmethoxycarbonyl
FT-IR	fourier-transform infrared spectroscopy
GGA	generalized gradient approximations
h	hour
HBTU	hexafluorophosphate benzotriazole tetramethyl uronium
Hz	Hertz
hv	photon energy

LDA	local-density approximation
Lit.	literature
MC	merocyanines
min	minute
Mp.	melting point
MS	mass spectrometry
nm	nano meter
NMR	nuclear magnetic resonance
Phe	phenylalanine
ppb	parts-per-billion
ppm	parts per million
Pro	proline
R	rest
R_f	retention factor
rt	room temperature
*t*Bu	*tert*-butyl
s	second
SP	spiropyran
TEG	triethylengycol
THF	tetrahydrofurane
TLC	thin layer chromatography
Tos	toluol sulfonyl
trt	trityl (triphenylmethane)
UV	ultraviolet
Val	valine
Vis	visible
W	watt

8.2 DFT-Calculations

Table 14: List of the calculated dipole moments for chromene substituted spiropyran and merocyanine isomers.

Substituents		Dipole Moments of the Isomers [D]				
Para	*Ortho*	Spiro	TTC	TTT	CTT	CTC
NMe_2	NMe_2	3.01	2.96	4.74	3.61	3.87
NMe_2	OMe	4.18	4.91	6.41	5.70	5.73
NMe_2	H	3.41	4.42	6.61	5.52	5.34
NMe_2	Br	4.34	6.89	8.80	7.81	7.71
NMe_2	COOH	7.16	12.53	14.06	13.30	12.76
NMe_2	CN	6.86	10.54	12.67	11.74	11.41
NMe_2	NO_2	6.70	10.61	12.84	11.76	11.52
OMe	NMe_2	1.68	2.50	5.20	2.49	4.66
OMe	OMe	2.64	4.64	7.37	4.86	4.89
OMe	H	2.49	5.71	5.70	4.70	4.57
OMe	Br	3.88	7.99	7.98	7.10	7.02
OMe	COOH	6.52	14.07	15.34	14.73	14.64
OMe	CN	6.79	10.15	13.48	11.22	12.43
OMe	NO_2	6.65	11.68	13.51	12.68	12.53
H	NMe_2	1.08	4.63	5.35	4.70	4.95
H	OMe	1.67	6.42	7.61	7.02	4.94
H	H	1.38	5.91	7.36	6.61	6.47
H	Br	2.64	8.40	9.80	9.10	8.98
H	COOH	5.30	14.43	13.97	15.17	14.96
H	CN	5.52	11.95	13.73	13.00	12.61
H	NO_2	5.37	12.82	13.97	13.77	12.78
Br	NMe_2	1.59	6.35	5.69	5.63	6.12
Br	OMe	2.51	8.20	7.64	7.57	5.72
Br	H	1.40	7.39	7.73	7.36	7.50
Br	Br	2.41	9.41	9.97	9.53	9.65
Br	COOH	4.35	15.36	16.10	15.73	15.73
Br	CN	5.07	12.64	13.84	13.31	13.10
Br	NO_2	5.02	13.57	14.61	14.13	13.32
COOH	NMe_2	5.03	6.89	8.37	7.41	8.66
COOH	OMe	5.83	8.58	8.58	9.10	8.39
COOH	H	4.39	9.46	11.72	8.28	7.72
COOH	Br	6.08	9.64	12.54	10.08	12.16
COOH	COOH	6.18	15.97	15.91	19.59	19.38
COOH	CN	7.98	12.54	16.20	13.23	15.39
COOH	NO_2	7.85	12.67	16.28	13.70	13.70
CN	NMe_2	5.09	10.27	8.58	8.91	9.74
CN	OMe	6.13	12.06	10.59	10.90	9.16
CN	H	4.87	11.15	10.24	10.33	10.88
CN	Br	5.07	12.74	12.20	12.19	12.62
CN	COOH	4.97	18.09	18.09	17.96	18.18
CN	CN	6.19	15.31	15.59	15.37	15.46
CN	NO_2	6.30	15.52	15.80	15.52	15.69
NO_2	NMe_2	5.37	11.28	9.55	9.91	10.74
NO_2	OMe	5.94	12.93	9.37	9.55	10.25
NO_2	H	5.17	12.18	11.23	11.35	11.89
NO_2	Br	5.30	13.64	13.07	13.08	13.49
NO_2	COOH	5.09	18.67	18.69	18.56	18.77
NO_2	CN	6.36	16.07	16.35	16.17	16.13
NO_2	NO_2	6.44	16.19	16.52	16.28	16.41

Table 15: List of the calculated dipole moments for indole substituted spiropyran and merocyanine isomers

Indol Sub	**Spiro**	**TTC**	**TTT**	**CTT**	**CTC**
NMe_3	24.25	34.40	37.72	38.74	38.70
NO_2	6.91	7.76	7.52	6.24	6.86
COOH	7.40	10.81	10.57	9.02	9.66
H	5.30	13.64	13.07	13.08	13.49
Br	3.04	11.72	11.19	10.96	11.42
OMe	6.60	16.14	15.49	15.15	15.58
OTEG	8.05	17.74	16.61	16.61	17.19
NMe_2	6.60	18.20	17.54	17.61	18.01

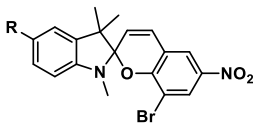

8.3 UV/Vis Analysis and Kinetics

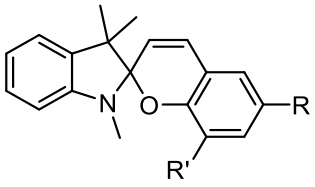

Table 16: Table with the absorption maxima of all chromene substituted spiropyrans and merocyanines.

R	R'	SP				MC					
H	**NO_2**	339	298	266	242	529	352		307	266	243
NO_2	**H**	353	281		245	543	364			245	
Br	**Br**	326	296	240	232	566	384		326	296	240
Br	**NO_2**	330	272		243	523	367			265	229
NO_2	**Br**	361	284		242	554	365			245	218
NO_2	**NO_2**	339		255		507	378	360	302	263	

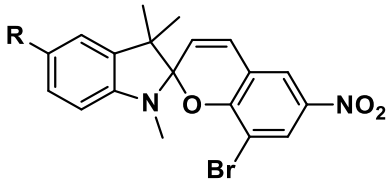

Table 17: Table with the absorption maxima of all indoles substituted spiropyrans and merocyanines.

R	SP				MC				
OMe	*346*	317	272	243	*521*	*382*	280	272	
Me	*334*	307	273	243	*521*	*371*	318	270	
H	*330*		272	243	*523*	*367*		265	229
Br	*335*	313	271	247	*532*	*371*	320	273	239
COOH	*332*		278	228	*541*	*371*	320	271	
NMe_3	*388*	336		252	*544*	*376*	309	250	
NO_2	*365*			246	*559*	*370*		245	

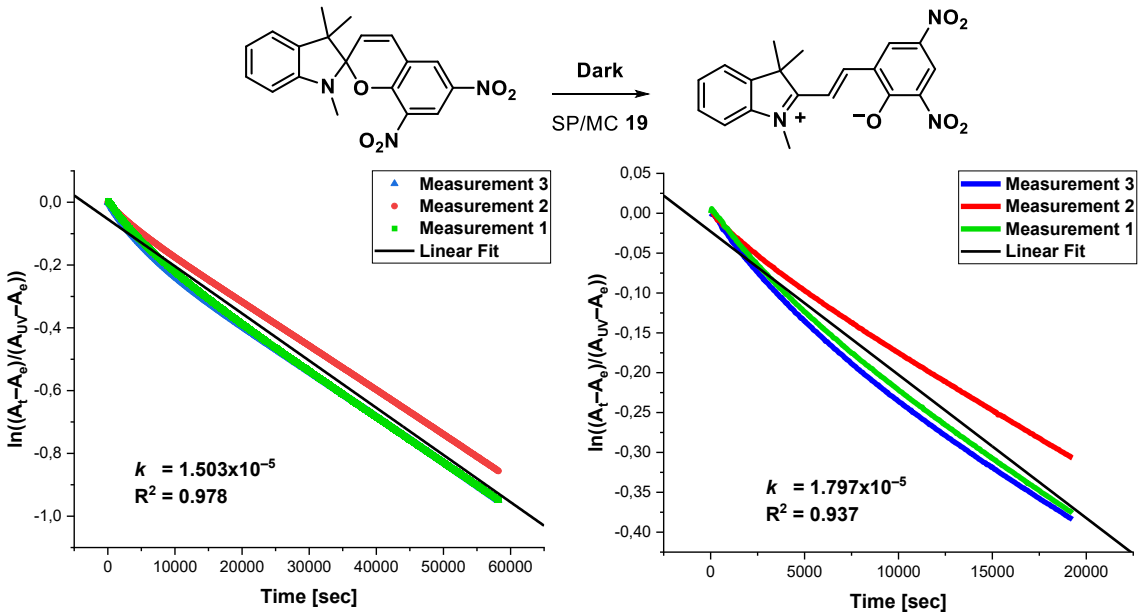

***Scheme 92*:** Comparison of the kinetics of system **19** using 60% conversion (left) and 30% conversion(right)

8.4 ^{1}H-NMR Ratios of SP/MC

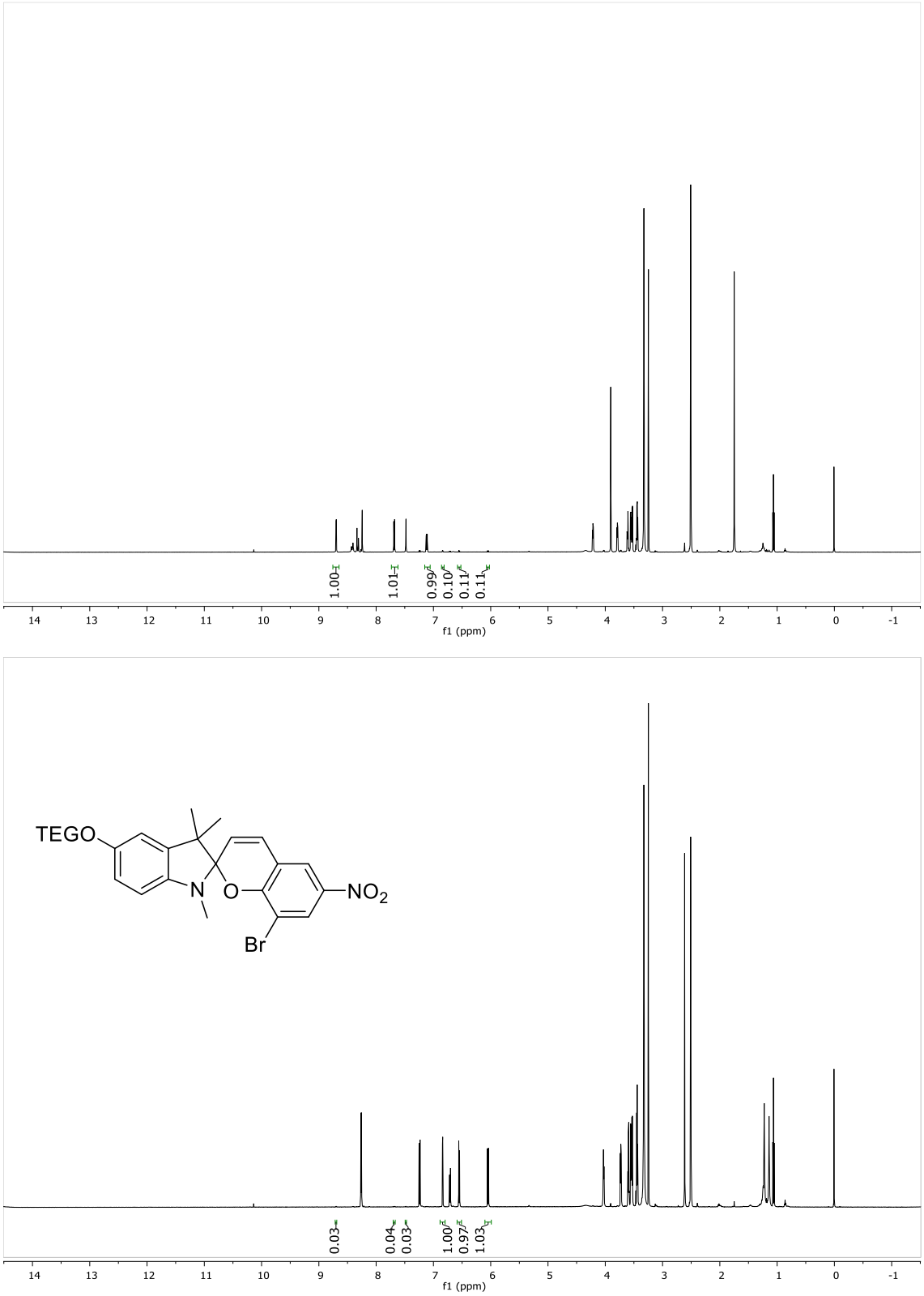

Scheme 93: ^{1}H-NMR-Spectra (600 MHz) of system **69** before (top) and after irradiation with visible light (bottom) in DMSO-d_6.

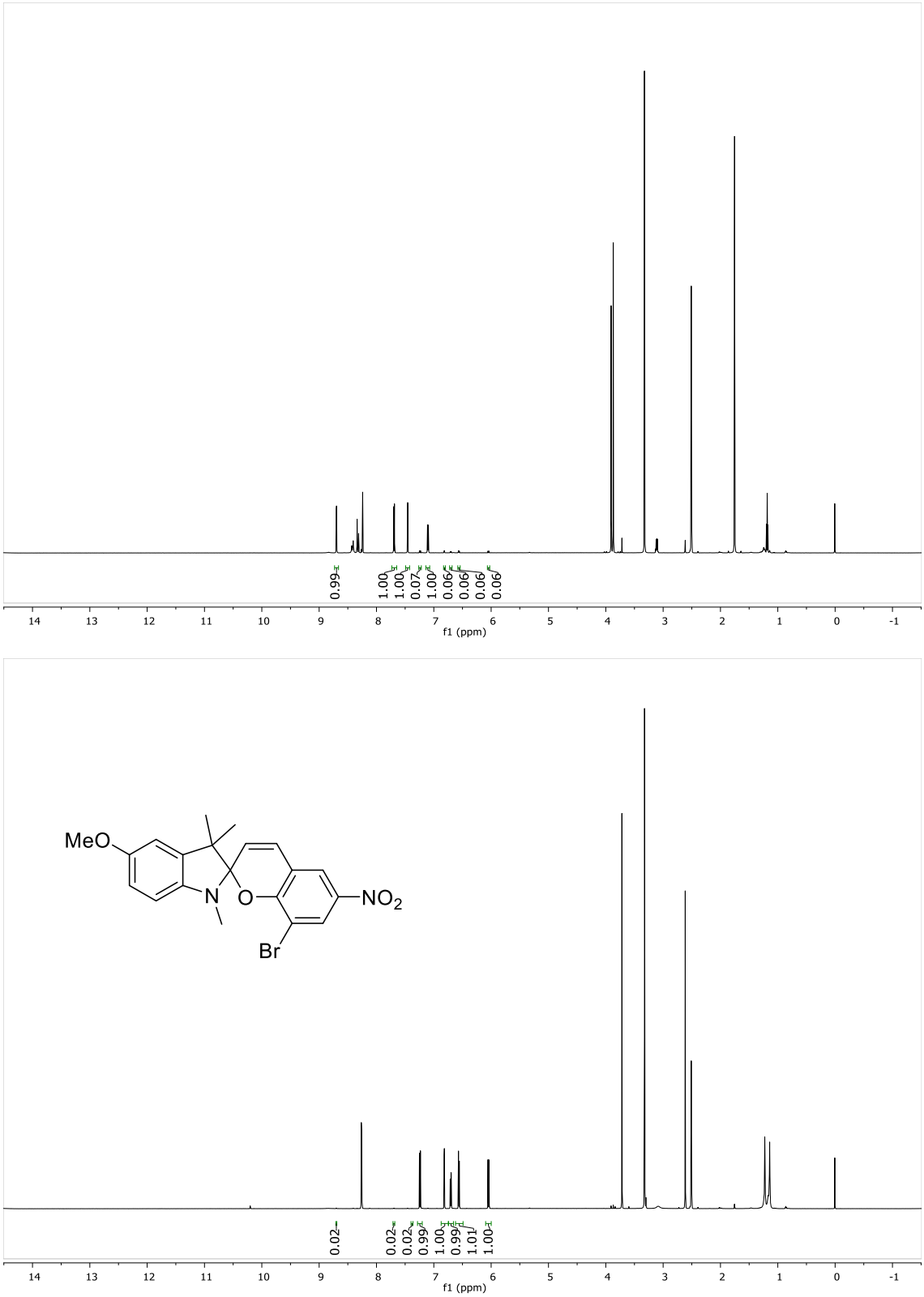

Scheme 94: ^{1}H-NMR-Spectra (600 MHz) of system **48** before (top) and after irradiation with visible light (bottom) in DMSO-d_6.

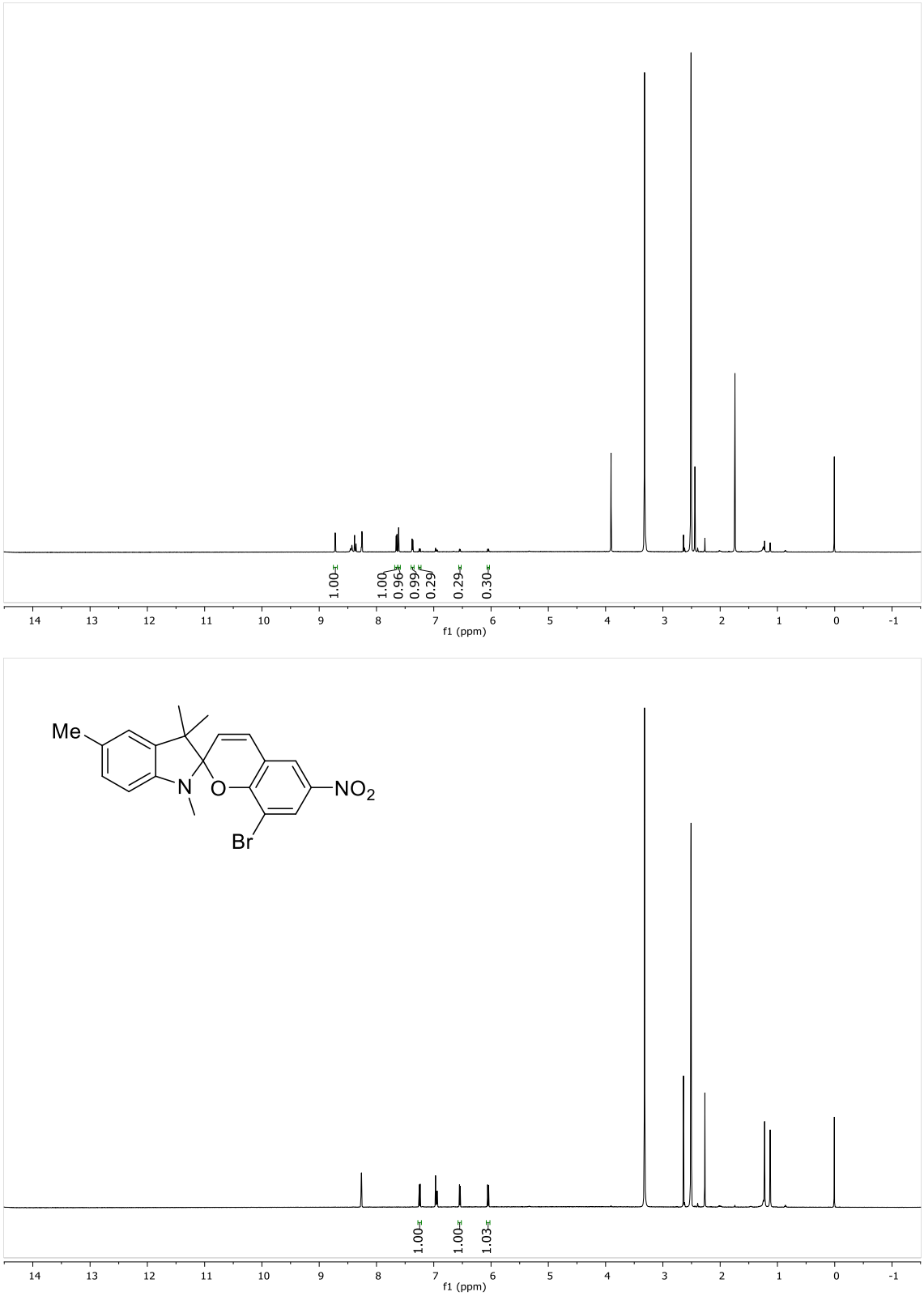

Scheme 95: ^{1}H-NMR-Spectra (600 MHz) of system **51** before (top) and after irradiation with visible light (bottom) in DMSO-d_6.

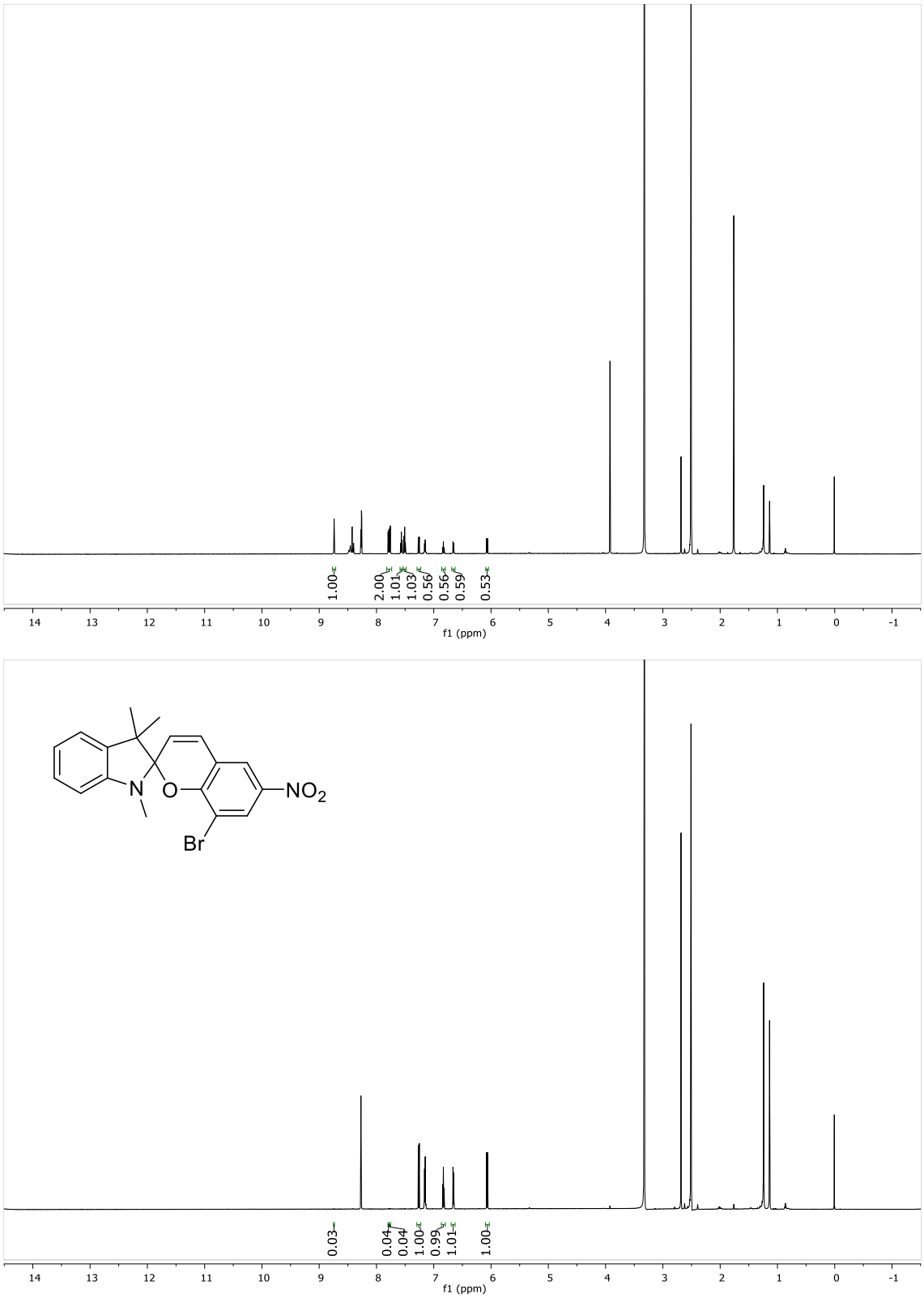

Scheme 96: ^{1}H-NMR-Spectra (600 MHz) of system **9** before (top) and after irradiation with visible light (bottom) in DMSO-d_6.

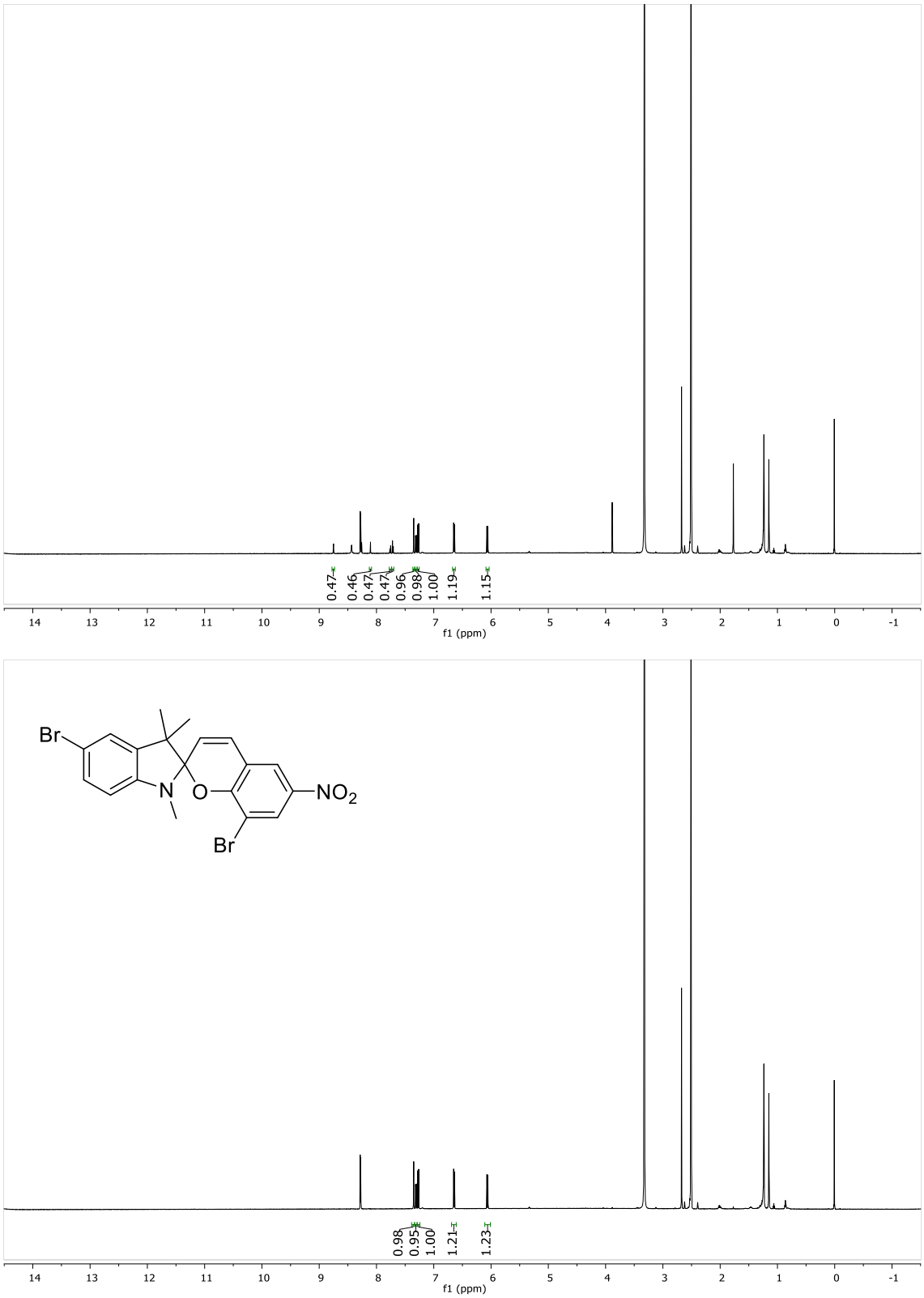

Scheme 97: ^{1}H-NMR-Spectra (600 MHz) of system **5** before (top) and after irradiation with visible light (bottom) in DMSO-d_6.

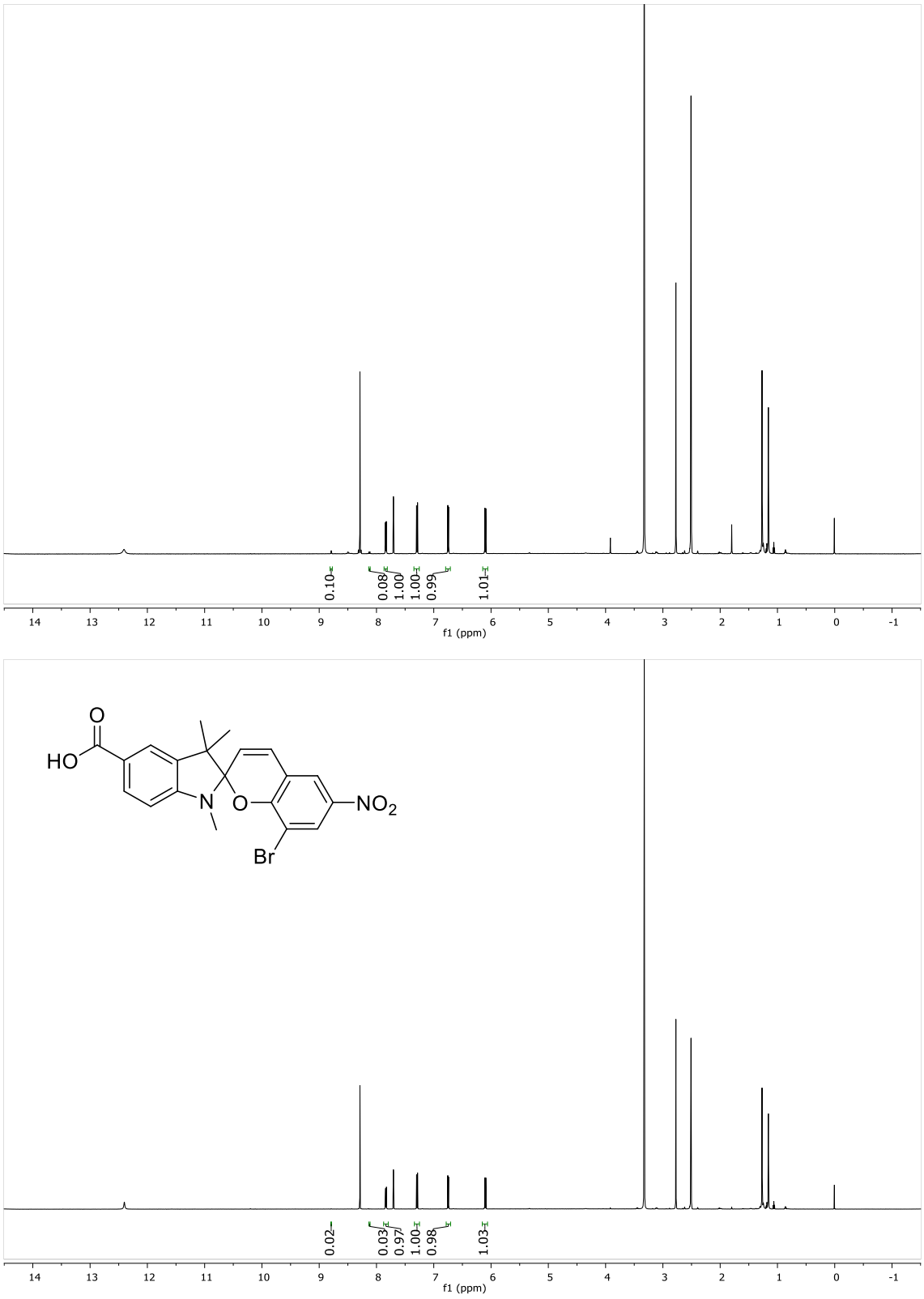

Scheme 98: ^{1}H-NMR-Spectra (600 MHz) of system **49** before (top) and after irradiation with visible light (bottom) in DMSO-d_6.

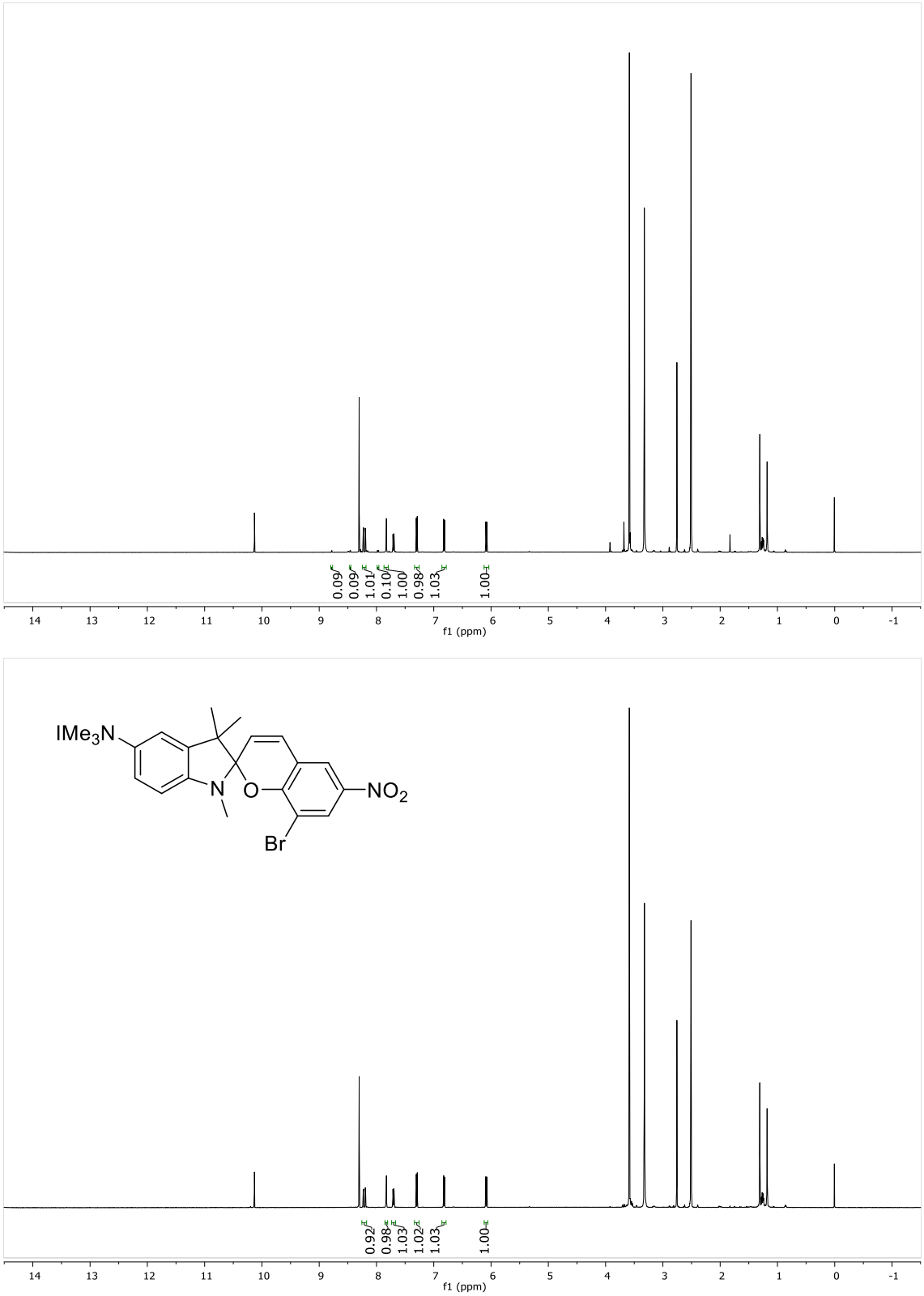

Scheme 99: ^{1}H-NMR-Spectra (600 MHz) of system **62** before (top) and after irradiation with visible light (bottom) in DMSO-d_6.

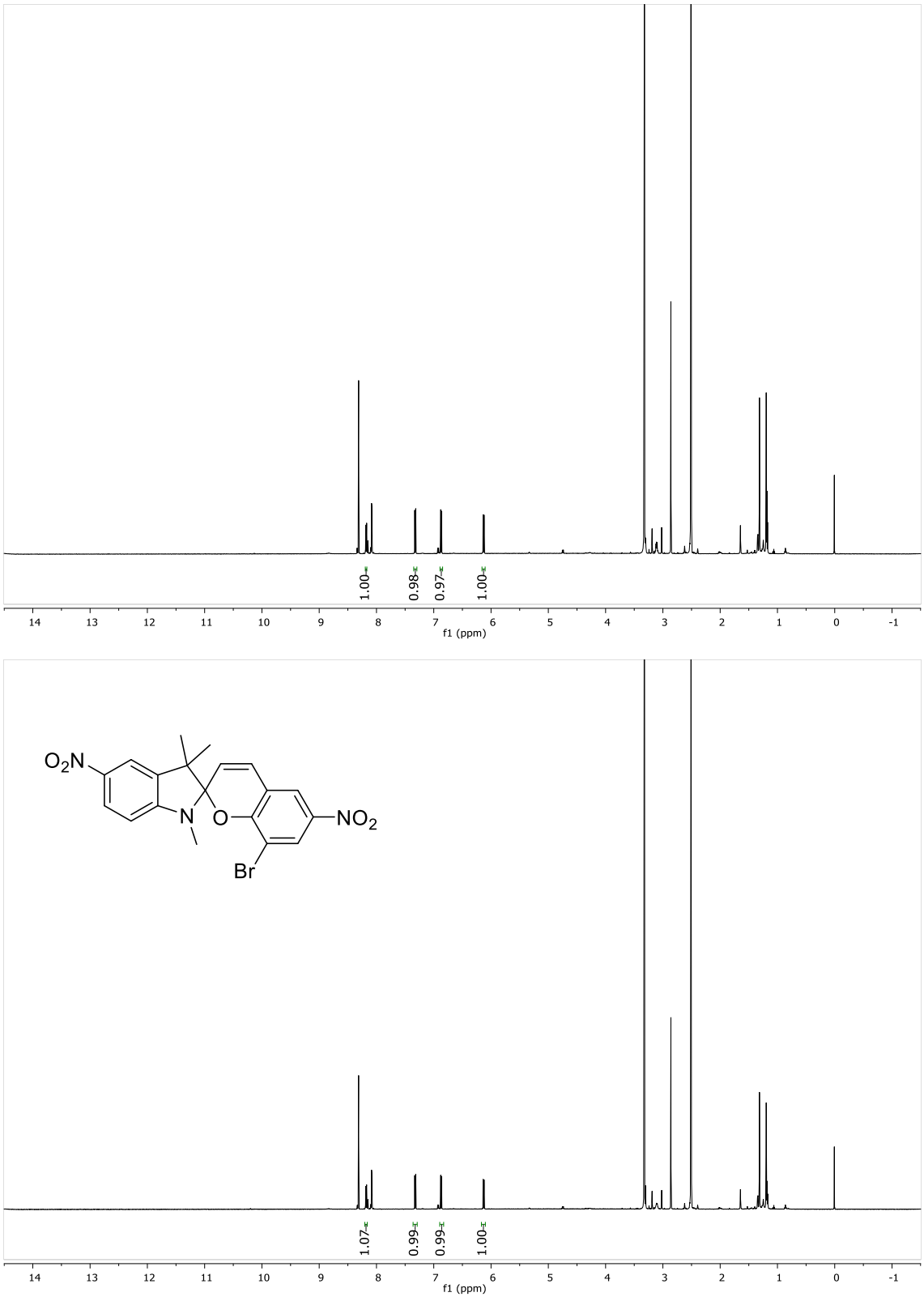

Scheme 100: ^{1}H-NMR-Spectra (600 MHz) of system **61** before (top) and after irradiation with visible light (bottom) in DMSO-d_6.

8.5 Peptide Experiments

In the following the ^{1}H-NMR-spectra described in chapter 4.6 are shown. A stock solution of SP/MC **69** in DMSO-d_6 was used at a concentration of 10 mM. This solution was kept in the dark for at least 72 h to ensure a proper equilibration. In the dark, 500 µL of the stock solution were used to directly dissolve 5 µmol of the respective peptide. After the ^{1}H-NMR of the sample was recorded (black), the same sample was irradiated with visible light until the decolourisation of the purple solution was observed (approximately 1 min). The second spectrum was recorded immediately after (red).

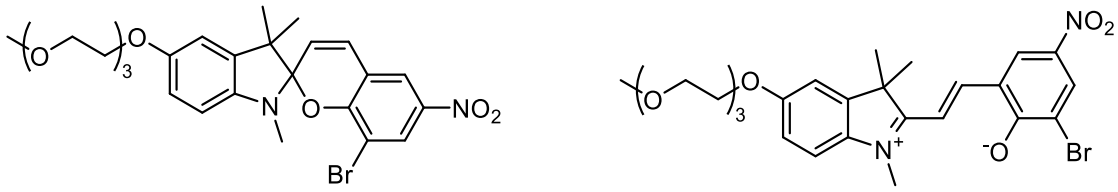

SP **69**

MC **69**

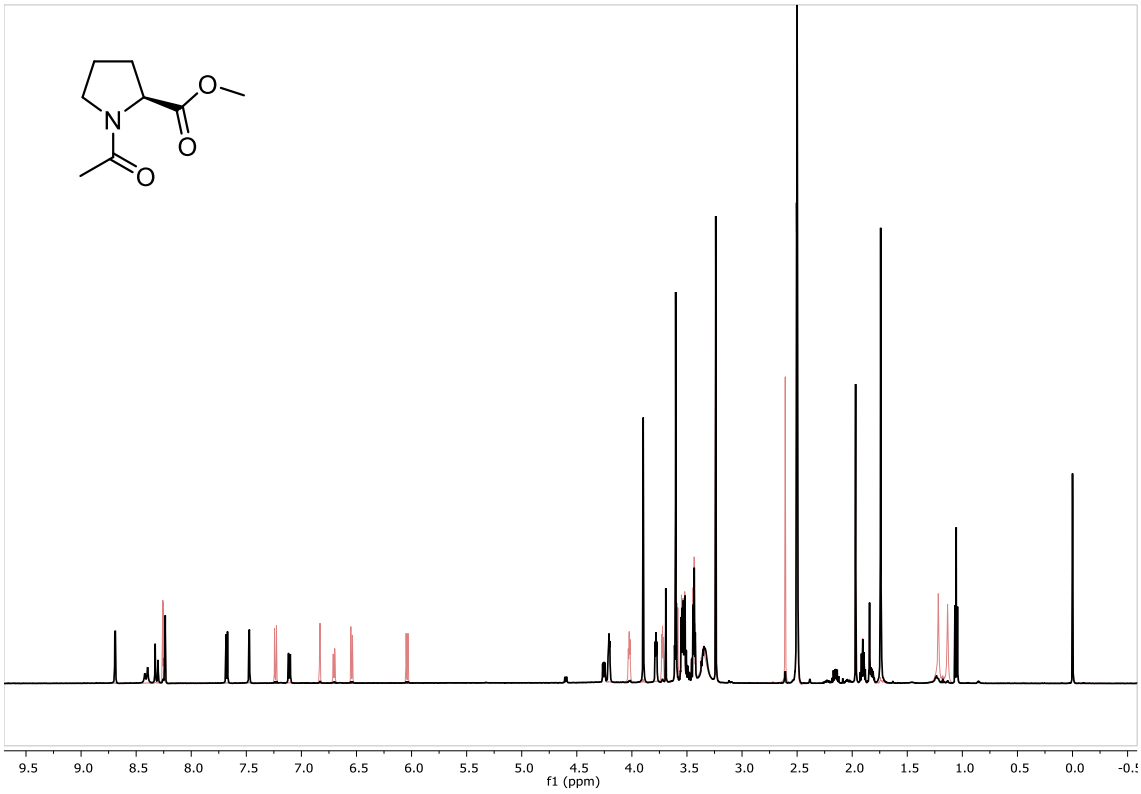

Scheme 102: ^{1}H-NMR (600 MHz) of Ac-Pro-OMe and photoswitch **69** in the dark (black) and after irradiation with visible light (red) in DMSO-d_6

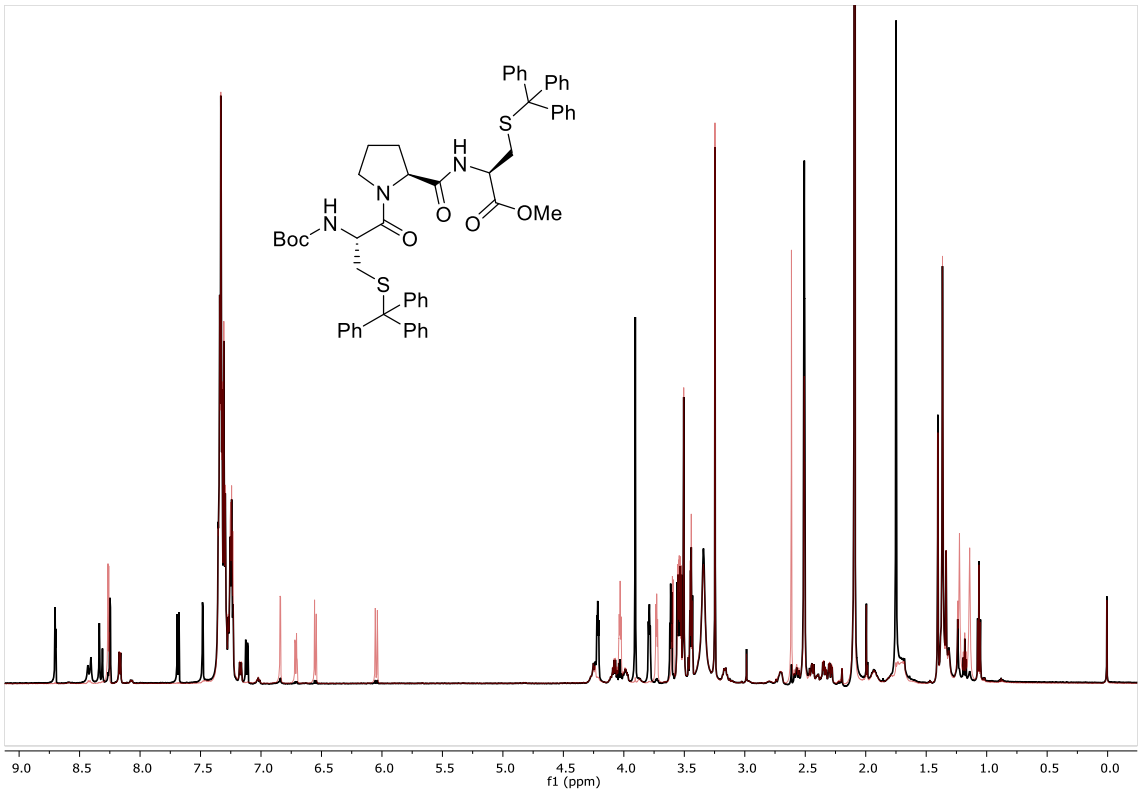

***Scheme 102*:** ^{1}H-NMR (600 MHz) of Boc-(Cys(trt)-Pro-Cys(trt)-OMe and photoswitch 69 in the dark (black) and after irradiation with visible light (red) in DMSO-d6.

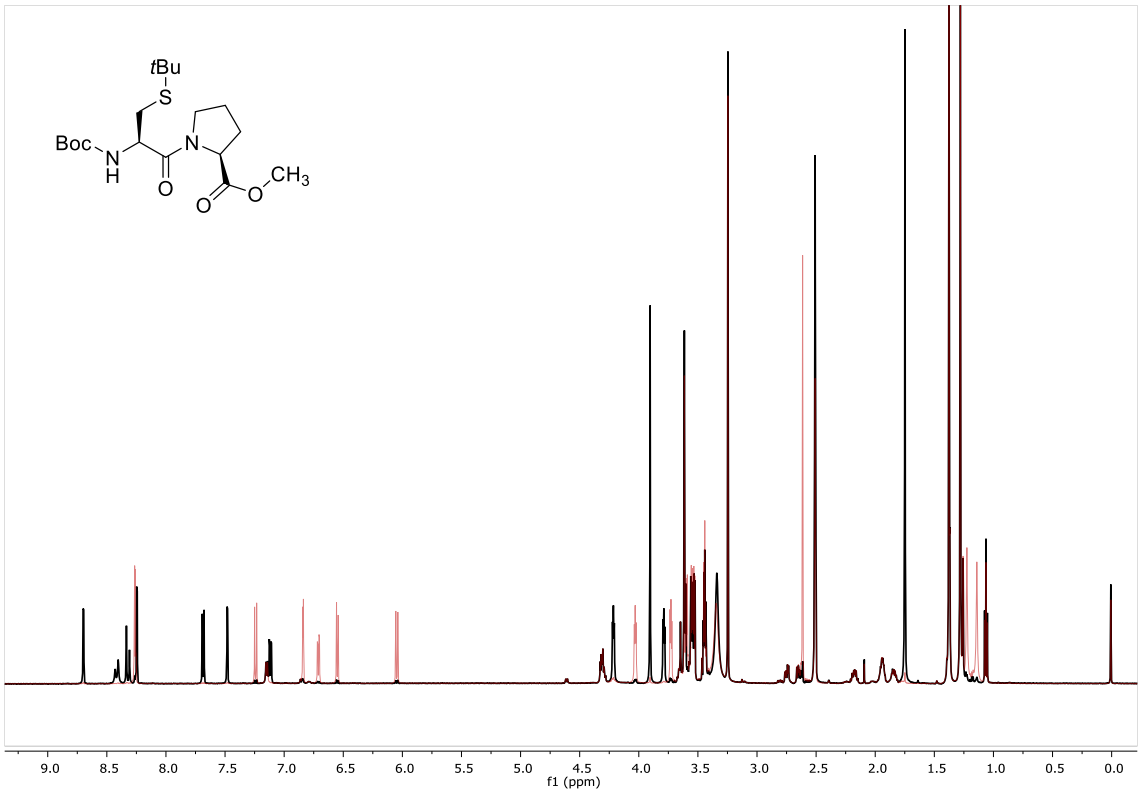

***Scheme 103*:** ^{1}H-NMR (600 MHz) of Boc-Cys(tBu)-Pro-OMe and photoswitch **69** in the dark (black) and after irradiation with visible light (red) in DMSO-d6.

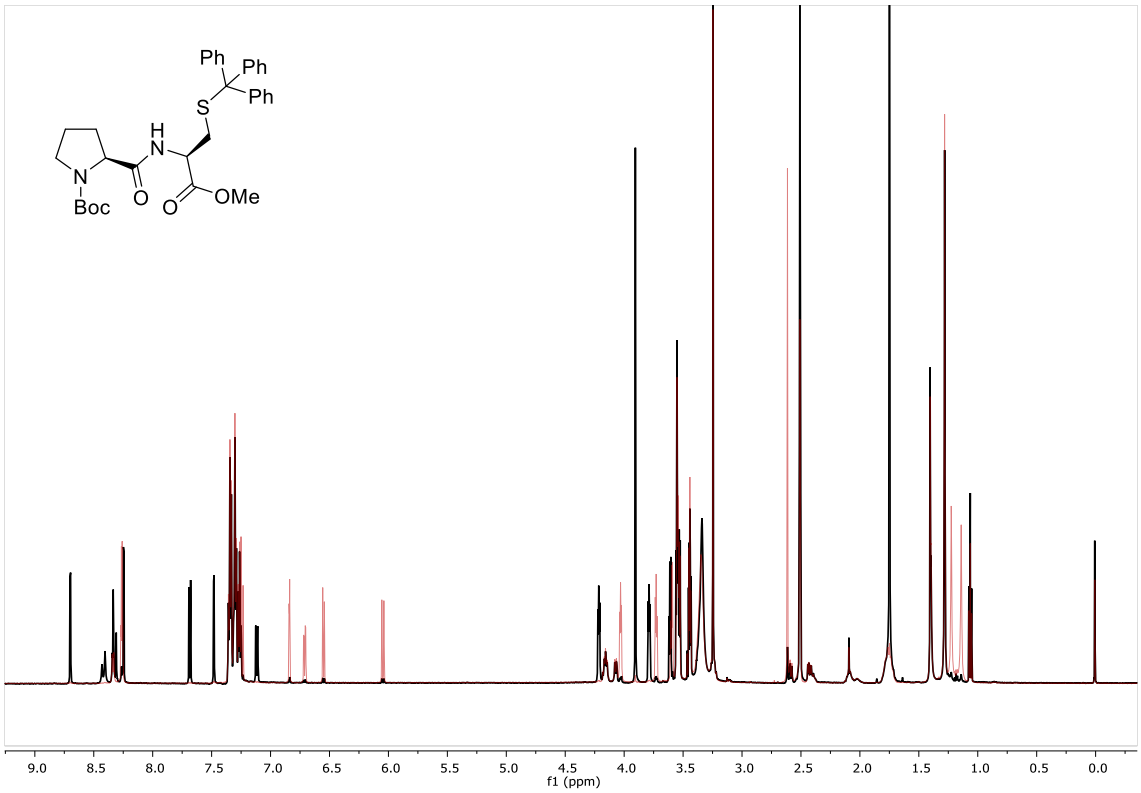

Scheme 104: ^{1}H-NMR (600 MHz) of Boc-Pro-Cys(trt)-OMe and photoswitch **69** in the dark (black) and after irradiation with visible light (red) in DMSO-d6.

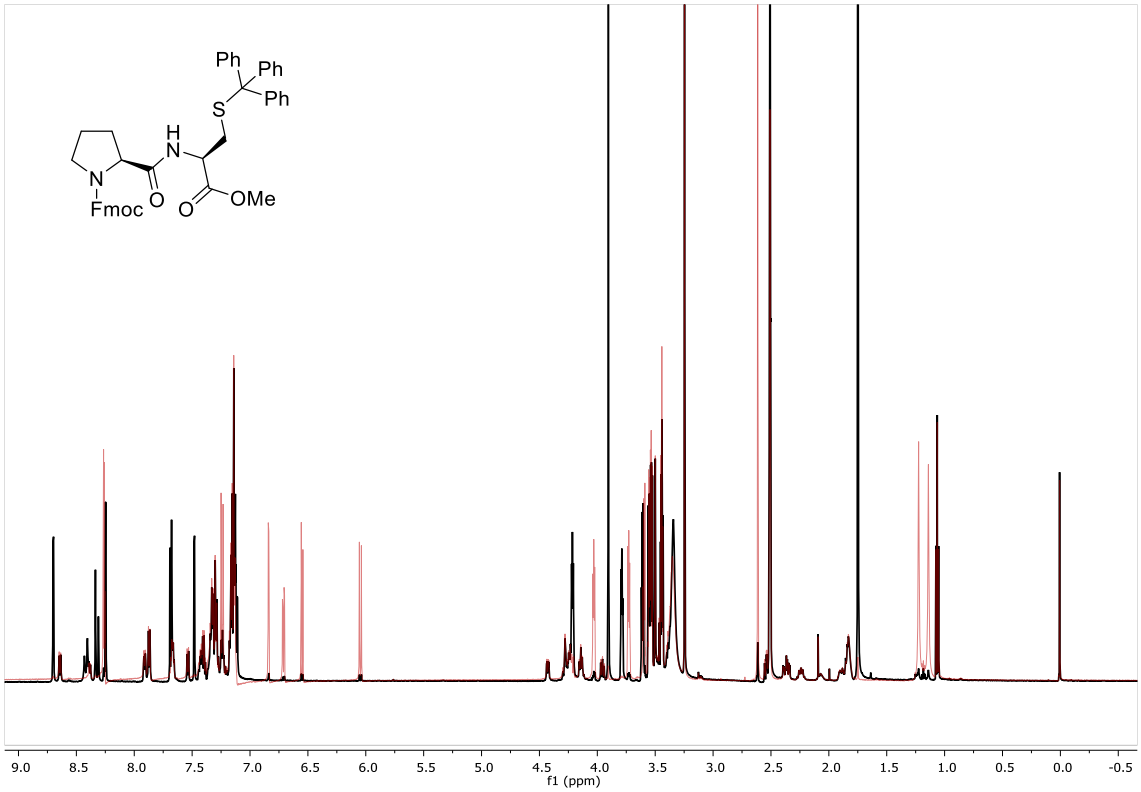

Scheme 105: ^{1}H-NMR (600 MHz) of Fmoc-Pro-Cys(trt)-OMe and photoswitch **69** in the dark (black) and after irradiation with visible light (red) in DMSO-d6.

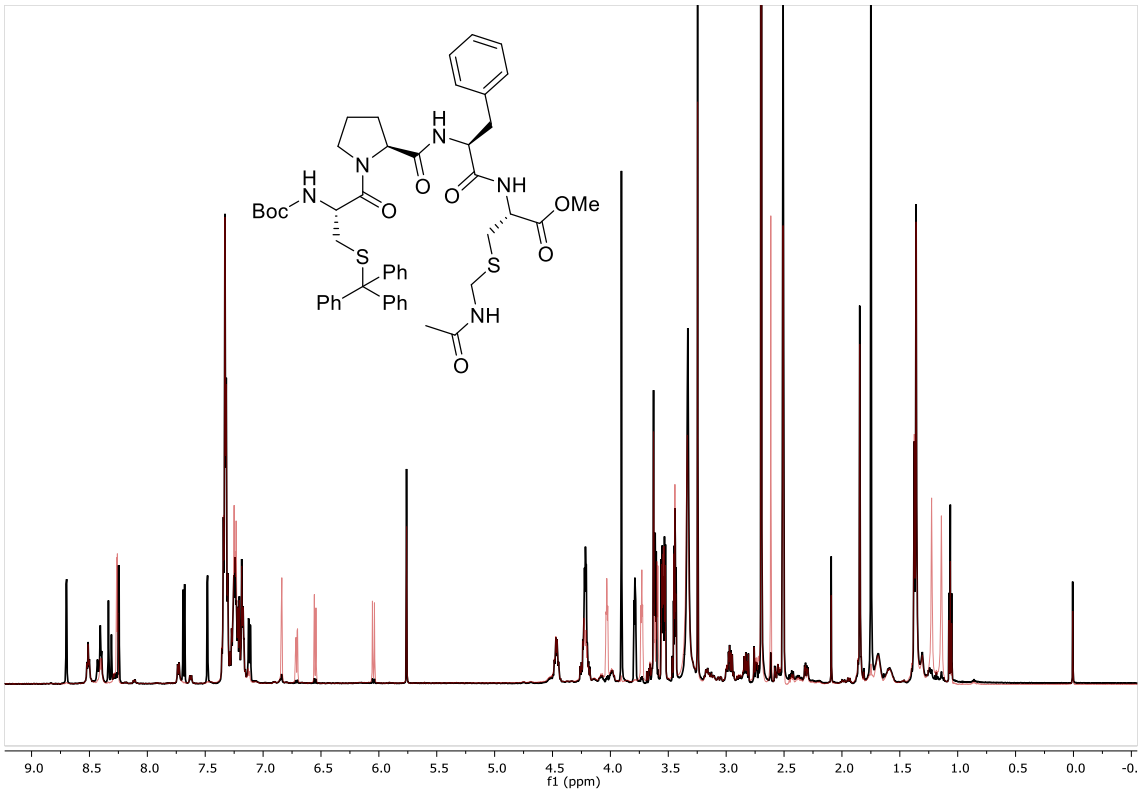

Scheme 106: ^{1}H-NMR (600 MHz) of Boc-Cys(trt)-Pro-Phe-Cys(Acm)-OMe and photoswitch **69** in the dark (black) and after irradiation with visible light (red) in DMSO-d6.

8.6 NMR-Spectra of Proline-based Peptides

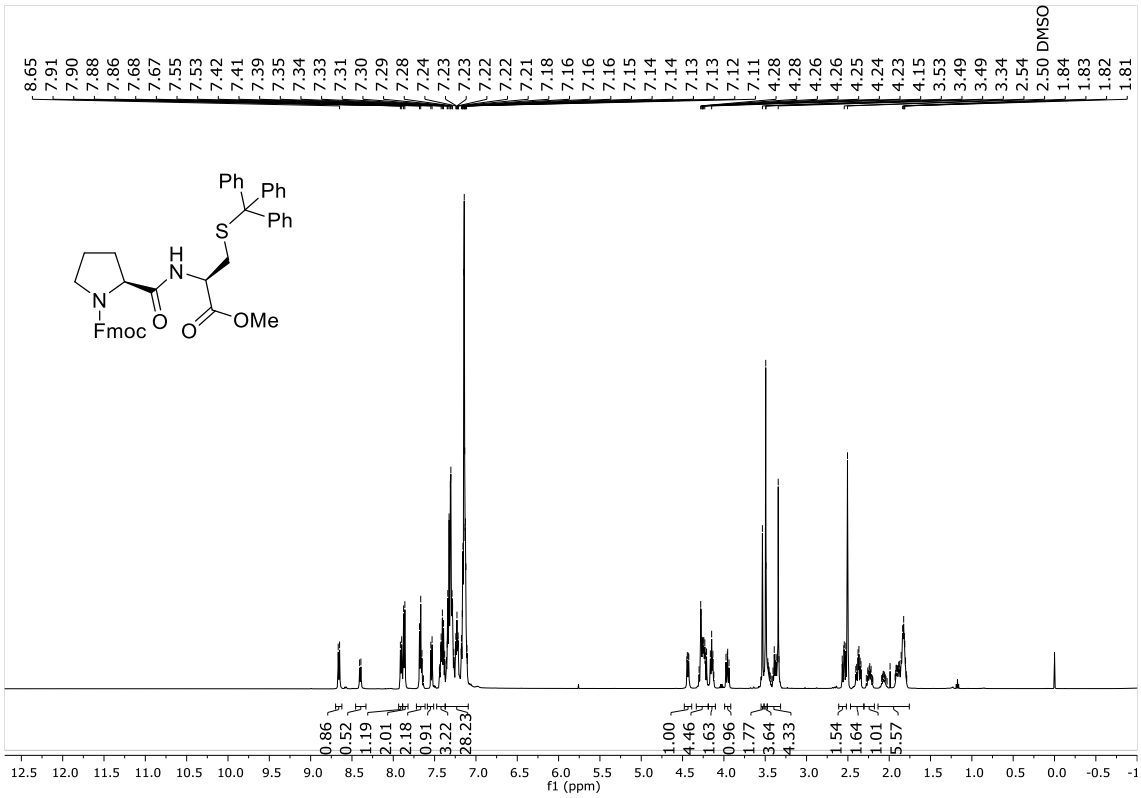

Scheme 107: ^{1}H-NMR of Fmoc-Cys(trt)-OMe in DMSO-d_6

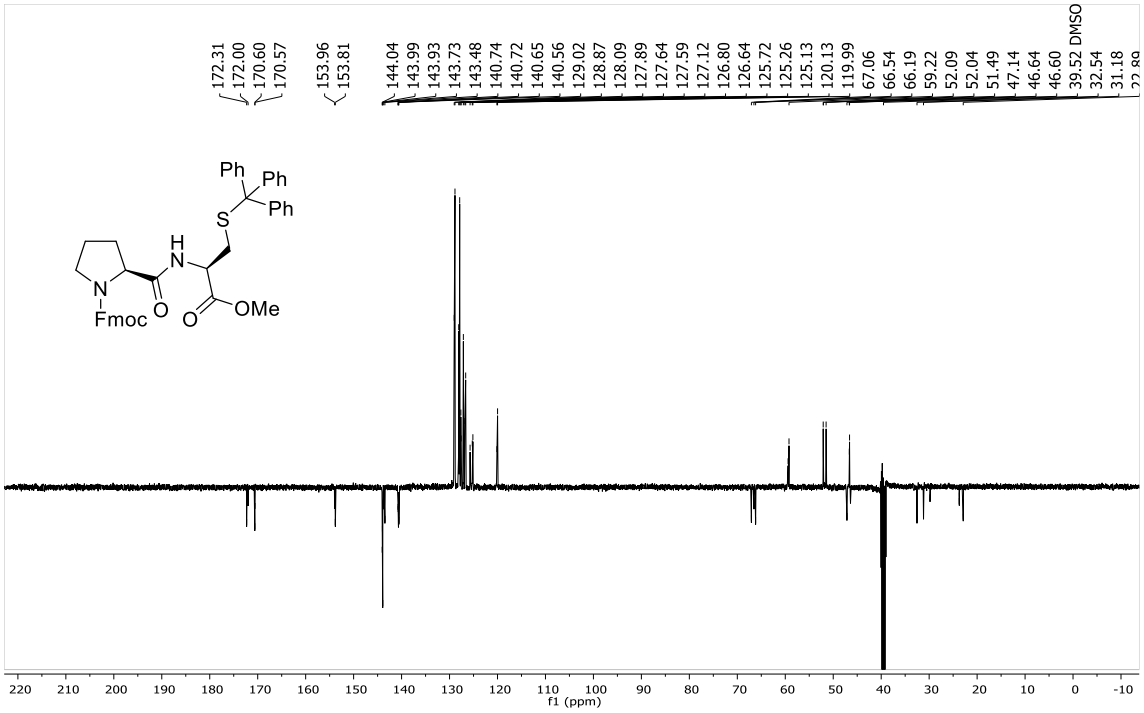

Scheme 108: ^{13}C-NMR of Fmoc-Cys(trt)-OMe in DMSO-d_6.

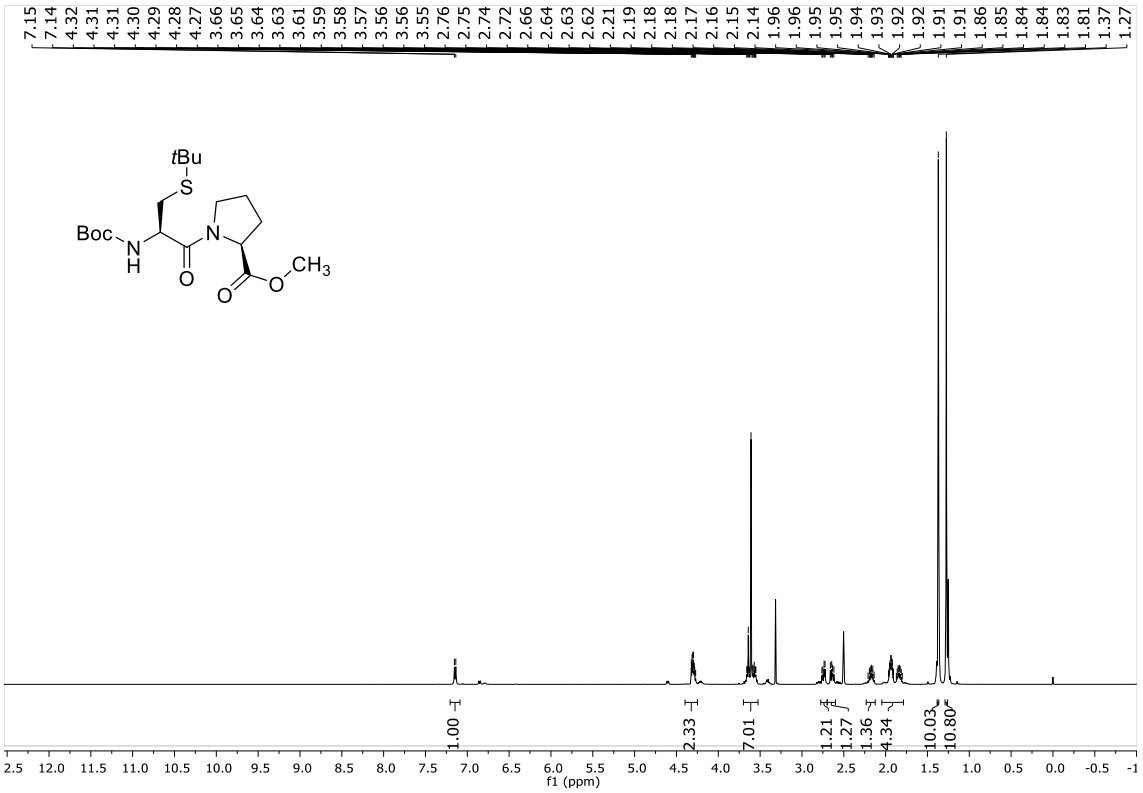

Scheme 109: ^{1}H-NMR of Boc-Cys(*t*Bu)-Pro-OMe in DMSO-d_6.

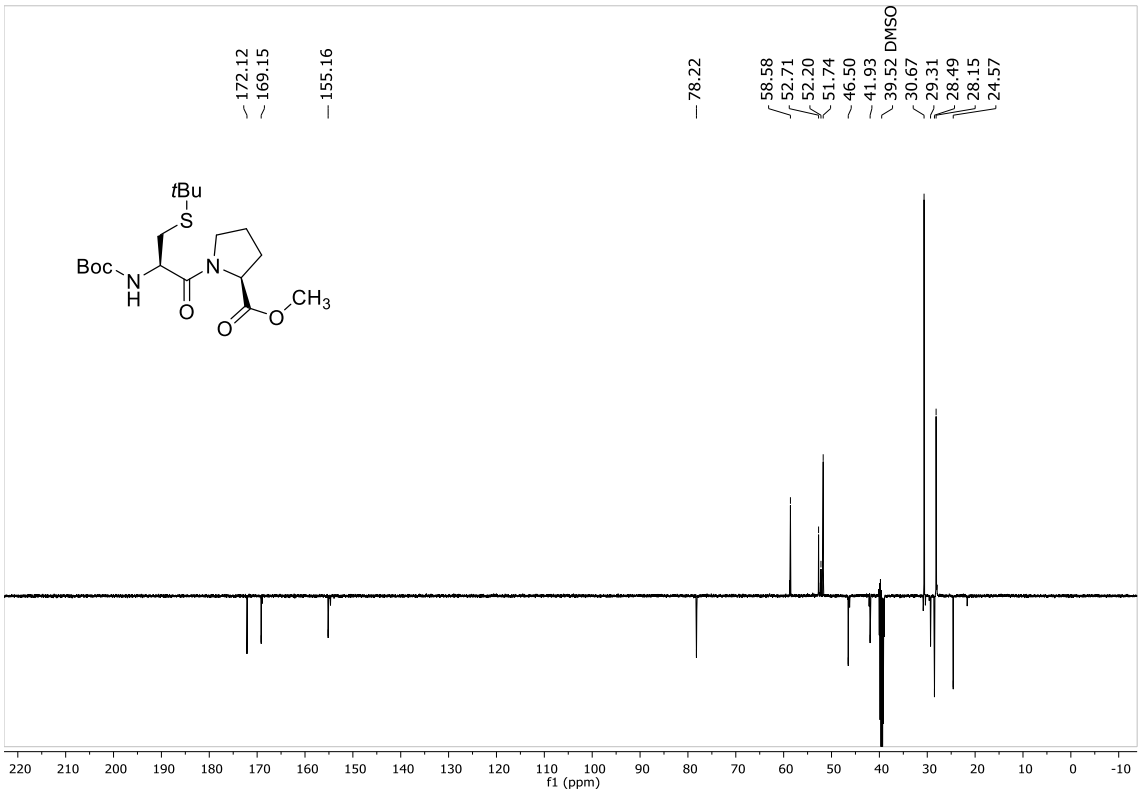

Scheme 110: ^{13}C-NMR of Boc-Cys(*t*Bu)-Pro-OMe in DMSO-d_6.

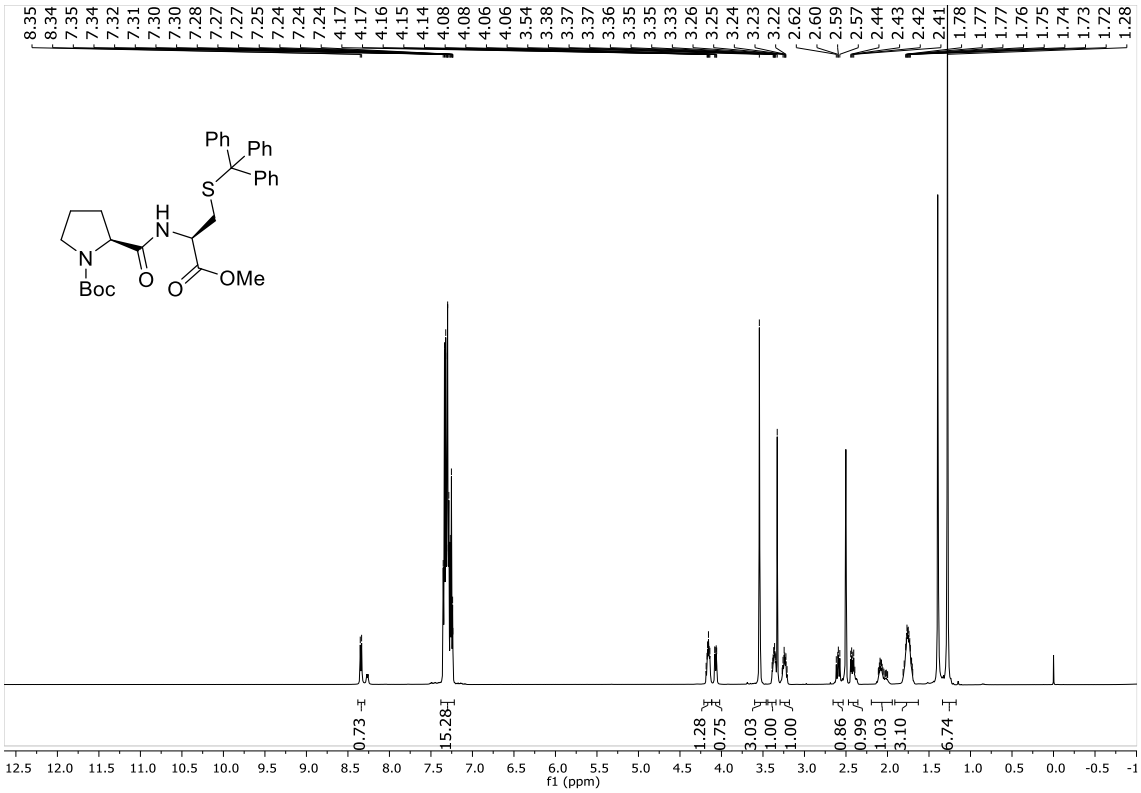

Scheme 111: ^{1}H-NMR of Boc-Pro-Cys(trt)-OMe in DMSO-d_6.

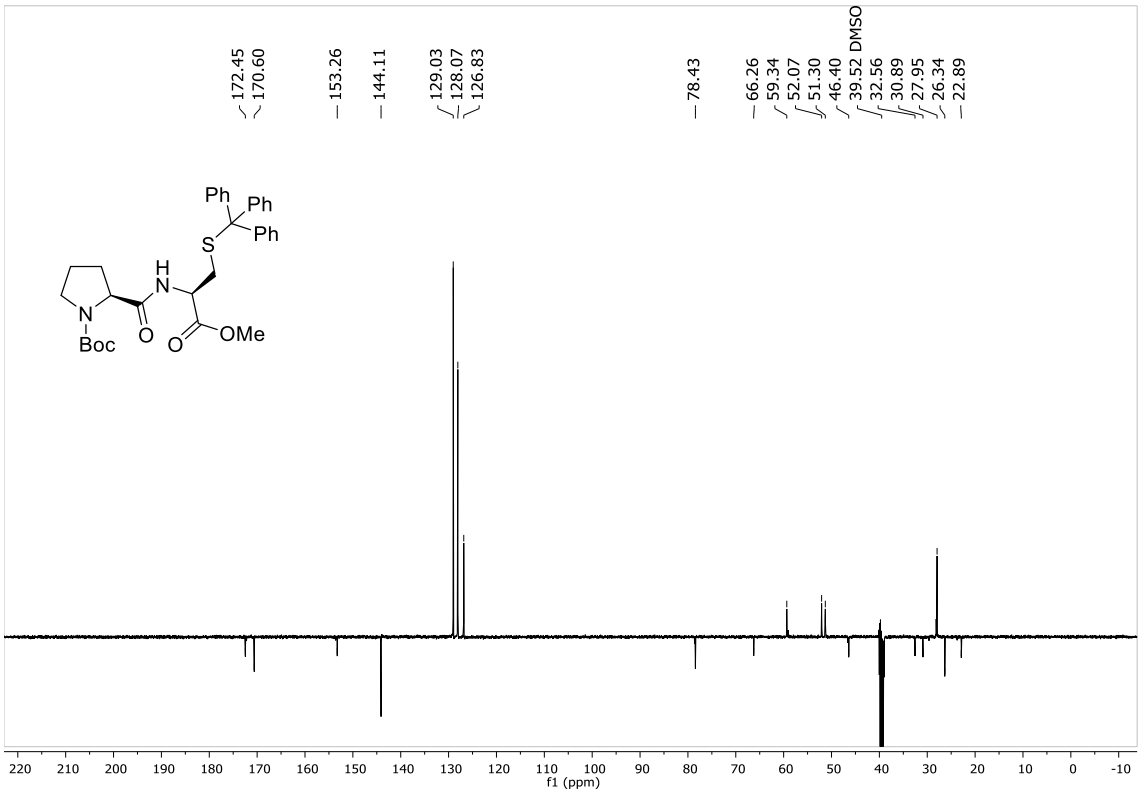

Scheme 112: ^{13}C-NMR of Boc-Pro-Cys(trt)-OMe in DMSO-d_6.

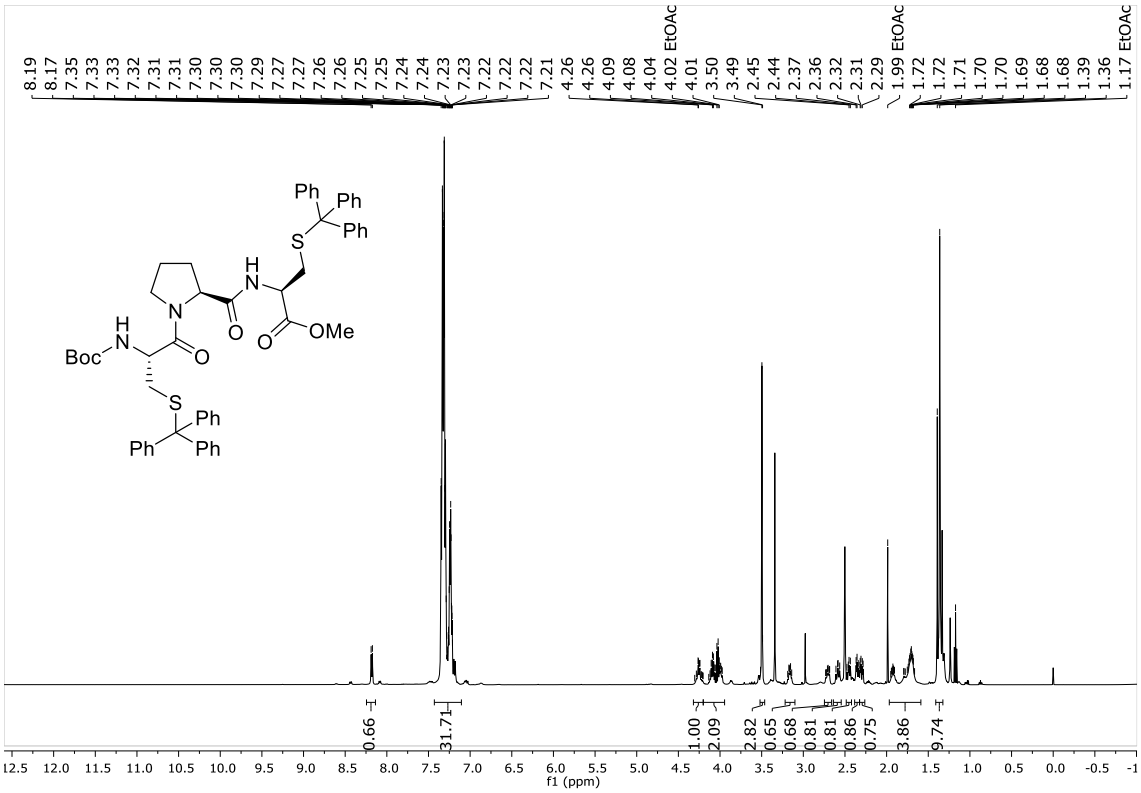

Scheme 113: ^{1}H-NMR of Boc-Cys(trt)-Pro-Cys(trt)-OMe in DMSO-d_6.

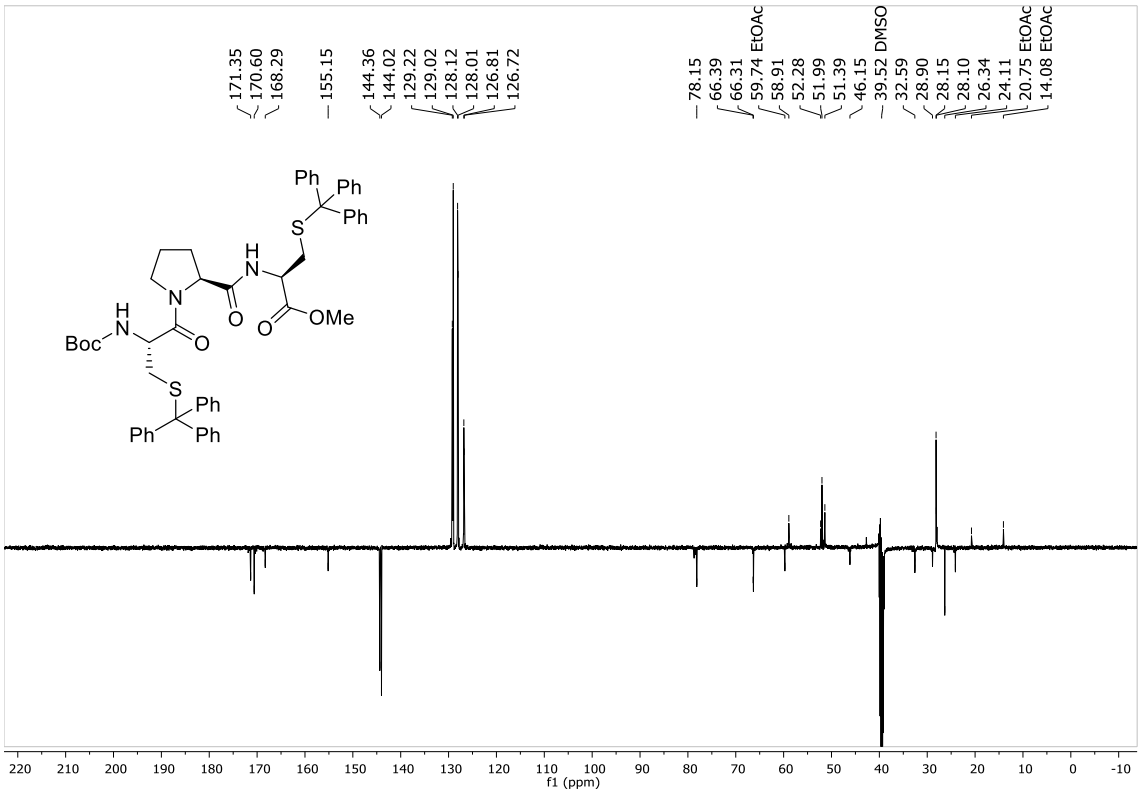

Scheme 114: ^{13}C-NMR of Boc-Cys(trt)-Pro-Cys(trt)-OMe in DMSO-d_6.

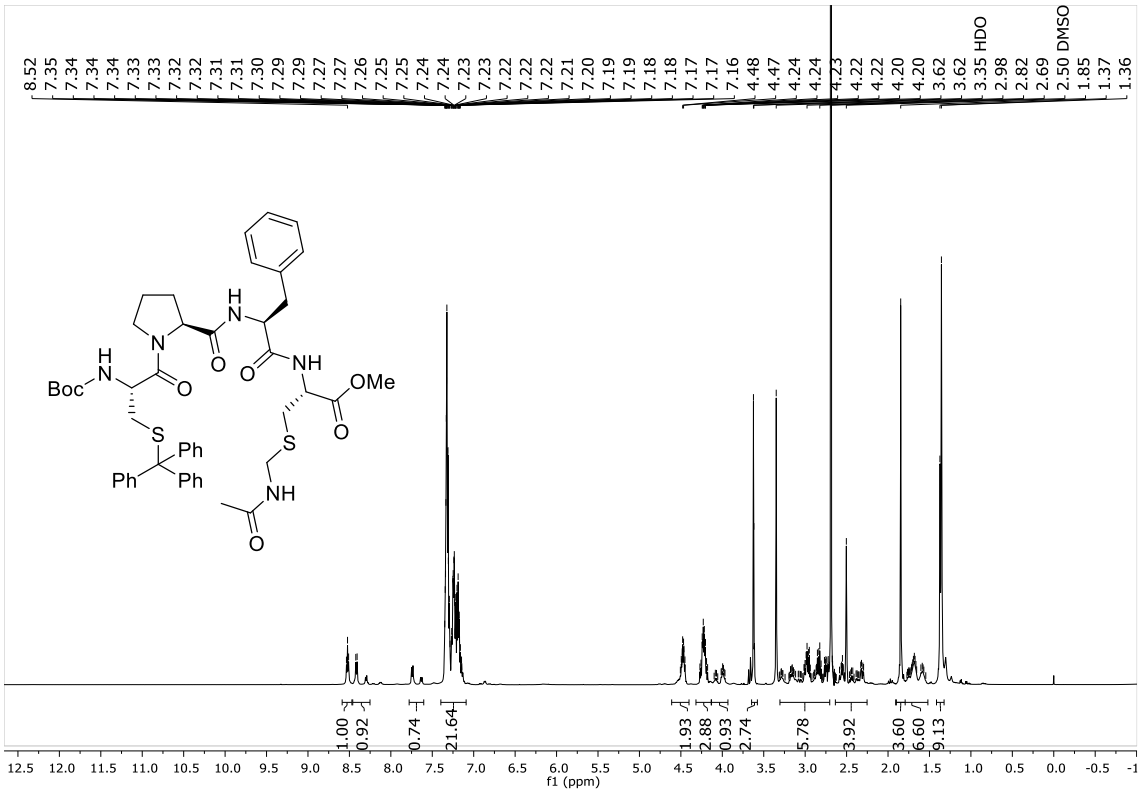

Scheme 115: ^{1}H-NMR of Boc-Cys(trt)-Pro-Phe-Cys(Acm)-OMe in DMSO-d_6.

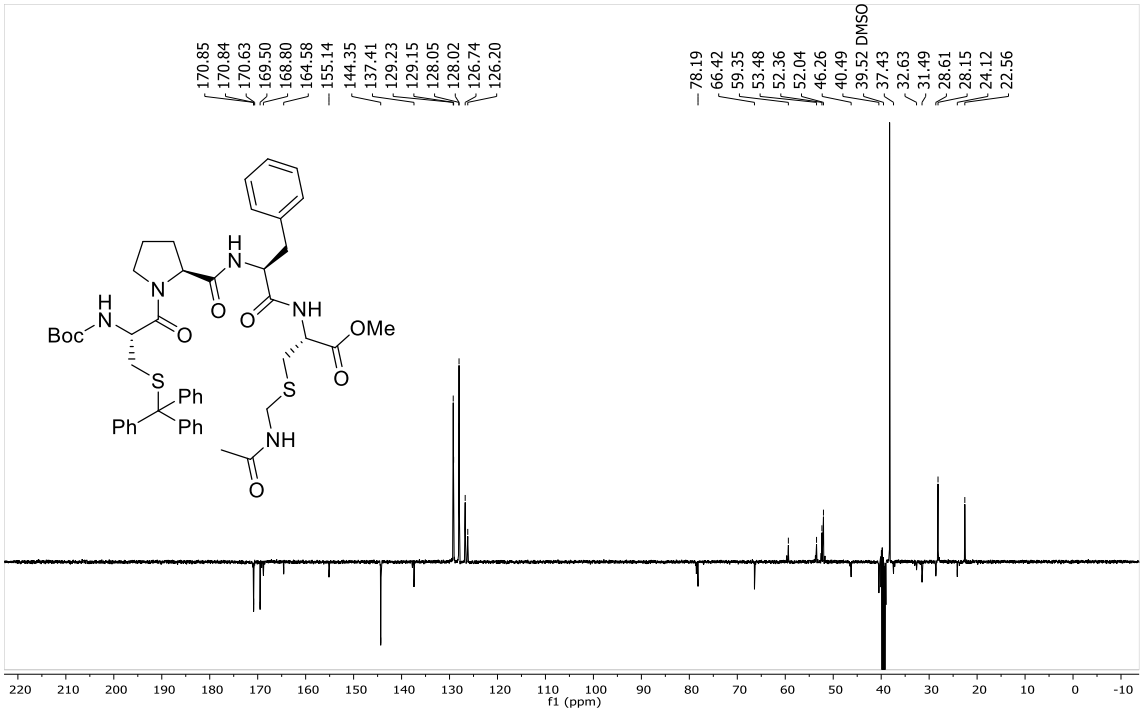

Scheme 116: ^{13}C-NMR of Boc-Cys(trt)-Pro-Phe-Cys(Acm)-OMe in DMSO-d_6.

9 Erklärung zur Dissertation

Hiermit versichere ich an Eides statt, dass ich die vorliegende Dissertation selbstständig und ohne die Benutzung anderer als der angegebenen Hilfsmittel und Literatur angefertigt habe. Alle Stellen, die wörtlich oder sinngemäß aus veröffentlichten und nicht veröffentlichten Werken dem Wortlaut oder dem Sinn nach entnommen wurden, sind als solche kenntlich gemacht. Ich versichere an Eides statt, dass diese Dissertation noch keiner anderen Fakultät oder Universität zur Prüfung vorgelegen hat; dass sie - abgesehen von unten angegebenen Teilpublikationen und eingebundenen Artikeln und Manuskripten - noch nicht veröffentlicht worden ist sowie, dass ich eine Veröffentlichung der Dissertation vor Abschluss der Promotion nicht ohne Genehmigung des Promotionsausschusses vornehmen werde. Die Bestimmungen dieser Ordnung sind mir bekannt. Darüber hinaus erkläre ich hiermit, dass ich die Ordnung zur Sicherung guter wissenschaftlicher Praxis und zum Umgang mit wissenschaftlichem Fehlverhalten der Universität zu Köln gelesen und sie bei der Durchführung der Dissertation zugrundeliegenden Arbeiten und der schriftlich verfassten Dissertation beachtet habe und verpflichte mich hiermit, die dort genannten Vorgaben bei allen wissenschaftlichen Tätigkeiten zu beachten und umzusetzen. Ich versichere, dass die eingereichte elektronische Fassung der eingereichten Druckfassung vollständig entspricht.

Datum, Name und Unterschrift